Julia Wappel

Contributions to the Chemistry of Halide exchanged Olefin Metathesis Catalysts

Doctoral Thesis

Dissertation

zur Erlangung des akademischen Grades einer Doktorin der technischen Wissenschaften an der Technischen Universität Graz

Betreuung: Assoc. Prof. Dipl.-Ing. Dr. techn. Christian Slugovc

Institut für Chemische Technologie von Materialien

Graz, November 2012

ACKNOWLEDGMENT

CONTENT

ABSTRACT

Olefin metathesis is not just since the awarding of the Nobel Prize in 2005 a very versatile and often used reaction. Due to the simplification of normally time-consuming and highly sophisticated reaction pathways to easy and very economic syntheses, it has raised to a useful reaction for daily routine in laboratories. Metathesis enables an easy way of forming new C=C double bonds with employing a great variety of different reactions and a wide library of possible substrates. Especially the Ring Opening Metathesis Polymerization (ROMP), giving rise to highly functional tailor-made polymers, and the invention of air and moisture tolerant ruthenium based initiators has boosted the interest in olefin metathesis further.

This work deals on one hand with the synthesis of anionic ligand exchanged initiators and their application in various fields of olefin metathesis such as enantioselective metathesis or latent metathesis. The attempt to synthesize enantioselective initiators via the exchange of chlorides against chiral anionic acid based ligands and the influence of different parameters on this exchange are presented. In case of the latent initiators, N-, O- chelating pre-catalysts bearing 8-quinolinolate co-ligands were synthesized and tested for their application in ROMP, especially regarding their performance in the ROMP reaction of the monomer dicyclopentadiene (**DCPD**). Furthermore the performance of another type of latent initiators, namely a threefold chelating carbene initiator bearing a lactic acid moiety was investigated closer. The impact of various NHC ligands, especially of the so called **SIMes** (N, N'-bis[2,4,6 (trimethyl)phenyl]imidazolin-2-ylidene), **SIPr** (N, N'-bis[2,6-(diisopropyl)phenyl] imidazolin-2-ylidene) and **o-tol** ((N, N'-bis[2-di(*ortho*-tolyl] imidazolin-2-ylidene)) ligand on the configuration of the polymer, especially on the *cis* to *trans* ratio of the double bonds within the polymer chain, was investigated. Three different norbornene derived monomers comprising different steric and electronic features were applied within this study. In the course of this work, the limitations of ruthenium metathesis initiators caused by steric and electronic effects were addressed shortly. On the other hand this work deals with the performance of several new ruthenium based metathesis initiators regarding the ROM polymerization. Complex (1,3-di(2,5-di-isopropyl-phenyl)-2-imidazolydene)-dichloro-(3-phenyl-1*H*-inden-1-ylidene)(triisopropylphosphite)-ruthenium) was tested regarding its polymerization behavior of dimethyl-bicyclo[2.2.1]hept-5-ene-2,3-dicarboxylate (**Mon1**) and **DCPD** and compared to its commercially available congeners. In this study, particularly the influence of the NHC and the dissociative ligand on initiation and propagation are emphasized and the results of these impacts are discussed in more detail. In the end, a class of ruthenium initiators, bearing a new chelating moiety was examined in ROMP. Most striking, those initiators bearing a cis dichloro arrangement show very high metathesis

activity even at room temperature. Interestingly, within this initiator family very diverse metathesis reactvities have been observed and are commented.

ZUSAMMENFASSUNG

Olefin Metathese ist nicht erst seit der Verleihung des Nobel Preises 2005 eine sehr nützliche und oft verwendete Reaktion. Wegen der Vereinfachung von normalerweise zeitaufwendigen und sehr anspruchsvollen Reaktionswegen zu simplen und wirtschaftlichen Synthesen, hat sie sich zu einer sehr nützlichen Reaktion für die tägliche Laborroutine entwickelt. Metathese ermöglicht einen einfachen Weg neue C=C Doppelbindungen zu knüpfen, wobei eine Vielzahl von verschiedenen Reaktionen und eine Vielzahl von möglichen Substraten eingesetzt werden können. Speziell die Ring Öffnende Metathese Polymerisation (**ROMP**), welche die Möglichkeit zur Herstellung von hochfunktionellen maßgeschneiderten Polymeren bietet, und die Einführung von luft- und feuchtigkeitstoleranten auf Ruthenium basierenden Initiatoren hat das Interesse an der Olefin Metathese weiter verstärkt.

Diese Arbeit beschäftigt sich einerseits mit der Synthese von Initiatoren mit ausgetauschten anionischen Liganden und ihrer Anwendung in verschiedenen Bereichen der Olefin Metathese wie zum Beispiel in der enantioselektiven Metathese oder der latenten Metathese. Der Versuch, enantioselektive Initiatoren durch den Austausch der Chloride gegen auf chiralen anionischen Säure basierende Liganden herzustellen und der Einfluss verschiedener Parametern auf diesen Austausch werden präsentiert. Im Falle der latenten Initiatoren, wurden N-, O- chelatisierende Pre-Katalysatoren mit 8-chinolat Co-Liganden synthetisiert und ihre Performanz in ROMP, insbesondere hinsichtlich der Leistung in der ROMP Reaktion des Monomers Dicyclopentadien (**DCPD**), untersucht. Weiters wurde das Verhalten einer anderen Art von latenten Initiatoren, nämlich den dreifach chelatisierenden Carben Initiatoren welche eine Milchsäureeinheit besitzen, genauer untersucht. Der Einfluss von verschiedenen NHC Liganden, vor allem von den sogenannten **SIMes** ((N, N'-Bis[2,4,6(trimethyl)phenyl]imidazolin-2-yliden), **SIPr** (N, N'-Bis[2,6-(diisopropyl)phenyl] imidazolin-2-yliden) und **o-tol** ((N, N'-´Bis[2-di(*ortho*-tolyl] imidazolin-2-yliden)) Liganden auf die Konfiguration eines Polymers, bzw. genauer auf das *cis* zu *trans* Verhältnis der Doppelbindungen innerhalb der Polymerkette, wurden untersucht. Als Monomere wurden drei verschiedene Norbornenderivate mit unterschiedlichen sterischen und elektronischen Eigenschaften in dieser Studie verwendet. Im Zuge dieser Studie, werden die Grenzen von Ruthenium Metathese Initiatoren verursacht durch sterische und elektronische Effekte kurz diskutiert. Weiters beschäftigt sich diese Arbeit mit dem Verhalten von verschiedenen neuen, auf Ruthenium basierenden Metathese Initiatoren hinsichtlich der ROM Polymerisation. Komplex (1,3-di(2,5-di-isopropyl-phenyl)-2-imidazolyden)-dichloro-(3-phenyl-1*H*-inden-1-yliden)(triisopropylphosphit)-ruthenium) wurde hinstichlich seines Polymerisationsverhaltens von Dimethyl-bicyclo[2.2.1]hept-5-en-2,3-dicarboxylat (**Mon1**)

und **DCPD** getestet und mit kommerziell erhältlichen „Artgenossen" verglichen. In dieser Studie wurde besonders viel Wert auf den Einfluss des NHC Liganden und des dissoziativen Liganden auf die Initiierung und Propagierung gelegt und die Resultate dieser Effekte werden detaliert diskutiert. Zum Schluss wird eine neue Klasse von Ruthenium Initiatioren mit einer neuen chelatisierenden Einheit in der Ring Öffnenden Metathese Polymerisation untersucht. Bemerkenswerterweise besitzen diese Initiatoren mit einer *cis* Dichlor-Konfiguration eine sehr gute auch bei Raumtemperatur Metatheseaktivität. Innerhalb dieser Initiatorenfamilie wurden interessanterweise sehr unterschiedliche Metathese Reaktivitäten festgestellt welche nachfolgend diskutiert werden.

1 PREFACE

This work was accomplished within the EUMET project. EUMET is a project funded by the European Community's Seventh Framework Program (FP7/2007-2013). The project consists of six academic research centers and three industrial partners located around Europe:

Universities:

University of St Andrews, Scotland - Team leader: Prof. Steven P. Nolan
University of Salerno, Italy - Team leader: Prof. Luigi Cavallo
University of Warsaw, Poland - Team leader: Prof. Karol Grela
Leibniz University of Hannover, Germany - Team leader: Prof. Andreas Kirschning
Technical University of Graz, Austria - Team leader: Prof. Christian Slugovc
Ecole Nationale Supérieure de Chimie de Rennes, France - Team leader: Dr. Marc Mauduit

Industries:

Umicore, Germany - Team leader: Dr. Angelino Doppiu
Janssen Pharmaceutica, Belgium - Team leader: Dr. Andras Horvath
IFP Energies nouvelles, France - Team leader: Dr. Helene Olivier-Bourbigou

The project was divided into four work packages, namely Synthesis, Computational, Homogenous Catalysis and Heterogeneous Catalysis. Our group from the TU Graz was mainly involved in two (Synthesis and Homogeneous Catalysis) of these four work packages. Regarding the work package Homogeneous Catalysis our group was responsible for the testing of all synthesized complexes within the EUMET regarding the Ring Opening Metathesis Polymerization.

Some parts of this work have been made in cooperation with partners of other universities. Therefore, in those collaborations only the ROMP performance of the new complexes are investigated and discussed closer. All other characterizations were done by other academic partners.

2 INTRODUCTION

The word metathesis can be derived from the greek word "μετάθεσις", which means change of position.[1] Not just since the Nobel Prize was awarded to Yves Chauvin, Robert Grubbs and Richard Schrock in 2005, Olefin Metathesis has emerged as a very versatile tool for the transition metal catalyzed rearrangement of carbon-carbon double bonds. During the Nobel Prize awarding the reaction was described as follows:

The atoms let go of each other for a moment – the bonds are broken. All of a sudden, a new molecule approaches. A new bond, or… ? Everything happens at breakneck speed and the dancers are so exceedingly small… This makes the challenge of working out what really happens all the greater. That's what chemistry is all about – keeping up with the dancing molecules.[2]

Until know, metathesis has found its way into many different fields such as pharmaceuticals, foodstuffs, chemicals, biotechnology, polymer and paper industries. The broad applicability in oleo- and polymer chemistry but also in the synthesis of fine chemicals arises due to the large pool of different substrates which can be used in the various forms of olefin metathesis.

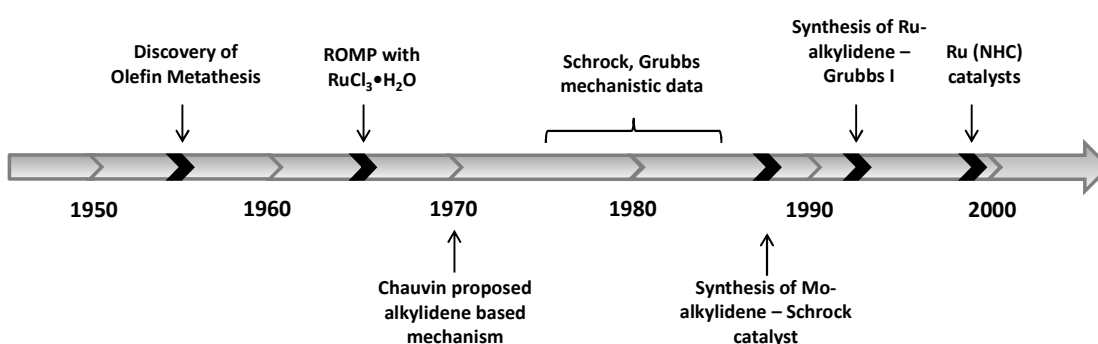## 2.1 The Story about Transition Metal Catalysts

Figure 1: Timeline of olefin metathesis; redrawn from reference 3 and 5

---

[1] N. Calderon, H. Y. Chem, K. W. Scott *Tetrahedron Lett.* **1967**, *34*, 3327.
[2] copy from: http://www.nobelprize.org/nobel_prizes/chemistry/laureates/2005/illpres/illpres.html.
[3] J. Hartwig, Organotransition Metal Chemistry, *University Science Books*, **2010**, 1020.

Olefin metathesis was discovered in the late 1950's and was primarily conducted with heterogeneous catalysts. These ill-defined catalysts mostly consist of metal halides or transition metal salts combined with main group alkylation agents deposited on solid supports.[4] Prominent examples therefore are WCl_6/Bu_4Sn, $WOCl_4/EtAlCl_2$, MoO_3/SiO_2 or Re_2O_7/Al_2O_3.[5] Due to low costs and easy operability, these kinds of complexes were applied in industrial applications such as the Shell Higher Olefin Process (SHOP) or the Phillips Triolefin Process.[6] Unfortunately these catalysts required harsh process conditions and Lewis acids as co-catalysts, making them incompatible with most functional groups. This lack of functional group tolerance restricts the implementation to aliphatic hydrocarbons only. An important step in the direction of more group tolerant catalysts was done by Hermann and co-workers with the discovery, that methyltrioxorhenium (MTO) is the actual active precursor of an $Re_2O_7/SnMe_4$ system and the subsequent synthesis of it.[7,8] In the 1970's the [2+2] cycloaddition mechanism was first proposed by Chauvin. This new insight into the olefin metathesis mechanism led to the formation of the first "well-defined" transition metal olefin metathesis catalysts. Well-defined catalysts are defined by two particular features, namely they can be characterized and the actual pre-catalyst itself has to be isolatable. The most prominent example among those, are doubtlessly the molybdenum based Schrock catalysts[9] and the ruthenium based 1st generation Grubbs catalyst.[10]

One of the most important inventions was without doubt the synthesis of the first four-coordinated olefin metathesis catalysts with the general formula $Me(NR_1)(CHR_2)(OR_3)_2$ where Me can either be tungsten (**I**) or molybdenum (**II**) as the central atom.[11] R_2 can either be an aryl system such as phenyl (**II**) or an alkyl system such as the adamentyl substituent shown in **III**.[9] Especially the molybdenum based catalyst protrudes by high and defined initiation and propagation rates and often allows living polymerization.[12] Nevertheless, those systems suffer from high sensitivity to oxygen and moister due to their 14- electron configuration and a limited functional group tolerance.[13] Hence, a total inert oxygen free

[4] N. Calderon, H. Yu. Chen,K. Y. Scott, Tetrahedron Letters 1967, 34, 3327-3329.

[5] T. M. Trnka, R.H. Grubbs, *Acc. Chem. Res.* **2001**, *34*, 18-29.

[6] J.C. Mol, *J. of Mol. Catal.A: Chem.* **2004**, *213*, 39-45.

[7] W. A. Herrmann, J.G. Kuchler, J.K. Felixberger, E. Herdtweck, W. Wagener, *Angew. Chem.* **1988**, *100*, 420-422.

[8] W. A. Herrmann, F.E. Kuhn, E.W. Fischer, W.R. Thiel, C. C. Romao, *Inorg. Chem.* **1992**, *31*, 4431-4432.

[9] J. H. Oskam, H.H. Fox, K. B. Yap, D. H. McConville, R. O'Dell, R. Lichtenstein, R.R. Schrock, *J. Organomet. Chem.* **1993**, *459*, 18-19.

[10] P. Schwab, R.H. Grubbs, J.W. Ziller, *J.Am.Soc,* **1996**, *118*, 100-110.

[11] R. R. Schrock, *Acc. Chem. Res.* **1990**, *23*, 158-165.

[12] R. R. Schrock, A. H. Hoveyda, *Angew. Chem.* **2003**, *115*, 4740-4782.

[13] C. Slugovc, *Macromol. Rapid Commun,* **2004**, *25*, 1283-1297.

atmosphere, dry and purified solvents and simple monomers had to be used when working with those initiators.
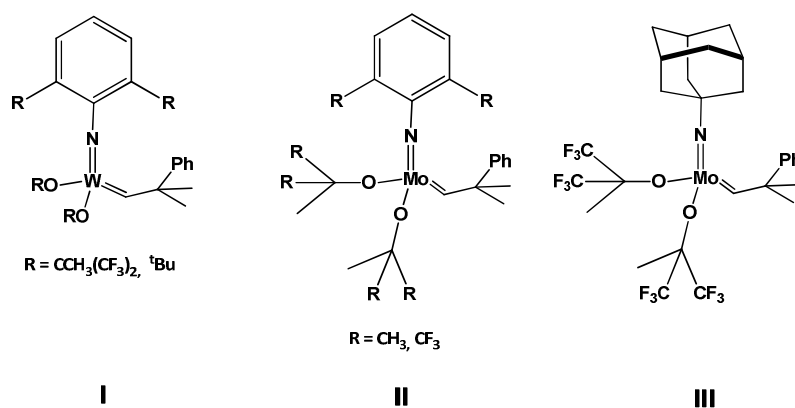
Figure 2: First well-defined tungsten and molybdenum complexes introduced by Schrock

Just a few years later, Grubbs et al. introduced the first well-defined ruthenium based alkylidene catalyst from the formula [(PCy$_3$)$_2$(Cl)$_2$Ru=CHPh]. This catalyst, commonly known as the first generation Grubbs catalyst (**G1**) exhibits an excellent moisture and oxygen tolerance and is also tolerant towards many functional groups, making them well suited for all kind of reactions in organic synthesis.[10] Basically, well-defined ruthenium catalysts consist of two neutral, two anionic and a carbene ligand. The first generation initiator exhibits a high initiation rate due to the easy dissociation of the phosphine ligand and a slow propagation caused by the high re-coordination tendency of the after the dissociation free phosphine ligand.
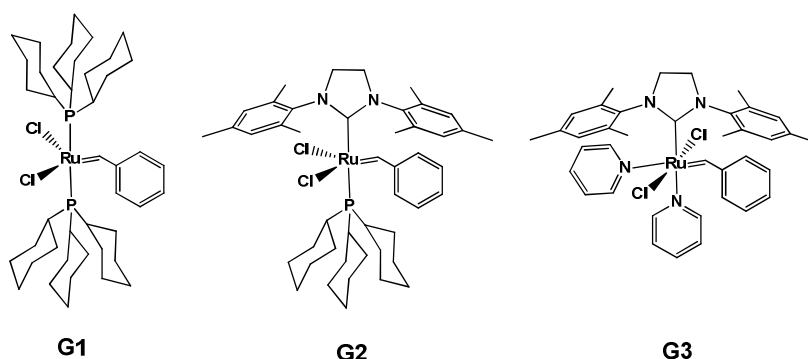
Figure 3: 1st to 3rd generation Grubbs catalysts

Substitution of one of the two phosphines of **G1** with a bulky N-heterocyclic carbene ligand namely (N, N'-bis[2,4,6-(trimethyl)phenyl]imidazolin-2-ylidene) led to the formation of the second generation catalysts **G2**.[14] The introduced NHC ligand has a stabilizing effect on the phosphine ligand causing a decreased initiation. Anyway, due to an increased affinity of the NHC substituted ruthenium center for π-acidic olefins relative to σ-donating phosphines, the second generation initiator shows an overall enhanced activity compared to **G1**. The next milestone in the development of ruthenium initiators was the development of a phosphine free initiator by the substitution of the remaining phosphine of **G2** against a pyridine. This step was done nearly contemporaneous by the groups of Grubbs and Slugovc. Grubbs introduced a 3-bromopyridine leading to the third generation Grubbs catalyst **G3** whereas Slugovc introduced an unsubstituted pyridine.[15,16] With these initiators, the first ruthenium initiators polymerizing in a living manner and hence enabling the synthesis of special and accurate polymers, caused by the lability and low re-coordination tendency of the pyridine to the ruthenium center, was established.

Table 1: Reaction tendency of different transition metals

Tungsten	Molybdenum	Ruthenium	
Acids	Acids	**Olefins**	
Alcohols, Water	Alcohols, Water	Acids	Increasing
Aldehydes	Aldehydes	Alcohols, Water	Reactvitiy
Ketones	**Olefins**	Aldehydes	
Olefins	Ketones	Ketones	
Esters, Amides	Esters, Amides	Esters, Amides	

Another system of the same reactivity as the Grubbs series is the indenylidene containing series **M1**-**M31** (analogues to **G1-G3**) from the German company Umicore. These catalysts possess a phenyl-indenylidene carbene, which lacks the carbene proton, instead of the benzylidene. Noteworthy, third generation **M31** possesses just one pyridine ligand instead of two as **G3**.[17] Also a big number of other indenylidene containing catalysts have been

---

[14] (a) J. Huang, E. D. Stevens, S.P. Nolan, J. L. Peterson, *J. Am. Chem. Soc.* **1999**, *121*, 2674. (b) M. Scholl, S. Ding, C. W. Lee, R.H. Grubbs, *Org. Lett*. **1999**, 1, *953.*

[15] C. Slugovc, S. Demel, F. Stelzer, *Macromol. Rapid Commun.* **2003**, *24*, 435-439.

[16] J.A. Love, J.P. Morgan, T.M. Trnka, R. H. Grubbs, *Angew. Chem.* **2002**, 114, *4207-4209.*

[17] D. Burtscher, C. Lexer, K. Mereiter, R. Winde, R. Karch, C. Slugovc, *J. of Polymer Science,* **2008**, *46*, 4630-4635.

investigated in the recent years and have shown that those initiators are highly active and extremely stable under ambient conditions.[18,19]

A further important step in the history of catalyst development was the introduction of the first isoproxystyrene ligand into a ruthenium initiator. The oxygen of the ether moiety of the carbene ligand can bind back to the ruthenium center, kicking out the dissociative ligand in place, leading to the first example of a chelating catalyst (**IV**).[20] By the substitution of the remaining phosphine ligand against a NHC, the second generation of this catalyst (**Hov**) was synthesized. This step was independently and almost simultaneously published by the groups of Hoveyda and Blechert.[21,22]

IV   **Hov**
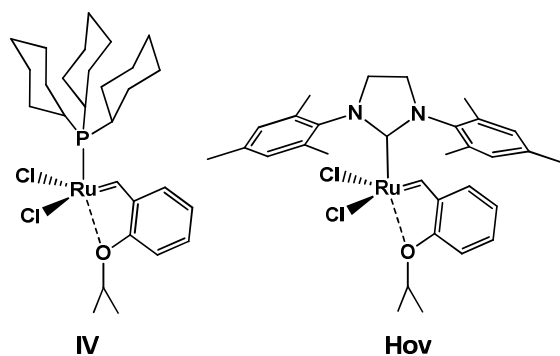
Figure 4: 1st and 2nd generation Hoveyda initiators

The 2nd generation Hoveyda catalyst possesses an enhanced activity in terms of initiation compared to the 2nd generation Grubbs catalysts. Furthermore it shows an increased thermal stability and displays an enhanced oxygen and moisture tolerance, which makes it also a popular starting material for further initiator synthesis. Nevertheless, living polymerization was so far not achieved with this kind of catalyst.

Until today a big library of many individual ruthenium based catalysts has been synthesized. The focus was therefore set on the different subjects such as supported catalysts, latent

[18] L. Jafarpour, H.-J. Schanz, E.D. Stefens, S. P.Nolan, *Organometallics* **1999**, *18*, 5416-5419.

[19] T. Opstal, F. Verpoort, *Angew. Chem., Int. Ed.* **2003**, *42*, 2876-2879.

[20] J. S. Kingsbury, J. P. A. Harrity, P. J. Jr. Bonitatebus, A. H. Hoveyda, *J. Am. Chem. Soc.* **1999**, *121*, 791.

[21] S. B. Garber, J. S. Kingsbury, B. L. Gray, A. H. Hoveyda, *J. Am. Chem. Soc.* **2000**, *122*, 8168-8179.

[22] S. Gessler, S. Randl, S. Blechert, *Tetrahedron Lett.* **2000**, *41*, 9973-9976.

catalysts, catalysts for enantioselective metathesis and so on. The majority of those initiators is summarized in reference 23.

2.2　Olefin Metathesis Reactions

The spectrum for the applications of olefin metathesis is broad. When using well-defined molybdenum or ruthenium initiators, many different reactions, namely Ring Closing Metathesis (RCM),[24] Cross Metathesis (CM),[25] Ring Opening Metathesis Polymerization (ROMP), enyene metathesis, Alternating Diene Metathesis (ADMET)[26], Ring Opening Cross Metathesis (ROCM), alkyne polymerization, Ring Rearrangement Metathesis (RRM)[27] and Ring Opening Metathesis (ROM), can be performed (c.f. Figure 5). These reactions do not only differ in their resulting reaction products, but also in the driving force for the reaction. In case of the RCM the driving force is the release of ethylene, an entropic effect where one product divides into two. The ROMP reaction on the other hand is driven by the release of ring-strain of the strained monomer.[28] CM, on the other hand, lacks both of these effects, the entropic and the ring-strain release, making it a reaction which proceeds more difficultly and especially makes it more difficult to predict the results.[29,30] Differences also lie in the main requirements for the applied catalysts for the different reactions. For RCM, a high turn-over number is the most important thing and initiation rates are not really reaction determining. On the other hand, for ROMP reactions, initiation and propagation rate influence the resulting polymer significantly.

[23] G. C. Vougioukalakis, R. H. Grubbs, *Chem. Rev.* **2010**, *11*0, 1746-1787.

[24] (a) H.-G. Schmalz, *Angew. Chem. Int. Ed. Eng.* **1995**, *34*, 1833-1836.(b) R.H. Grubbs, S. Chang, *Tetrahedron* **1998**, *54*, 4413-4450.(c) M. E. Maier, *Angew. Chem. Int. Ed.* **2000**, *39*, 2073 – 2077.

[25] (a) S. J. Connon, S. Blechert, *Angew. Chem. Int. Ed.* **200**3, *42*, 1900 – 1923.

[26] K. L. Opper, K. B. Wagener, *J. Polym. Sci. Part A: Polym. Chem.* **2011**, *49*, 821-831.

[27] H. Clavier, J. Broggi, S. P. Nolan, *Eur. J. Org. Chem.* **2010**, 937-943.

[28] K. B. Wiberg, *Angew. Chem. Int. Ed. Engl.* **1986**, *25*, 312.

[29] R. H. Grubbs *Handbook of Metathesis*; Wiley-VCH: Weinheim, Germany, 2003.

[30] A. K. Chatterjee, T.-L. Choi, D. P. Sanders, R. H. Grubbs, *J. Am. Chem. Soc.* **200**3, *125*, 11360-11370.
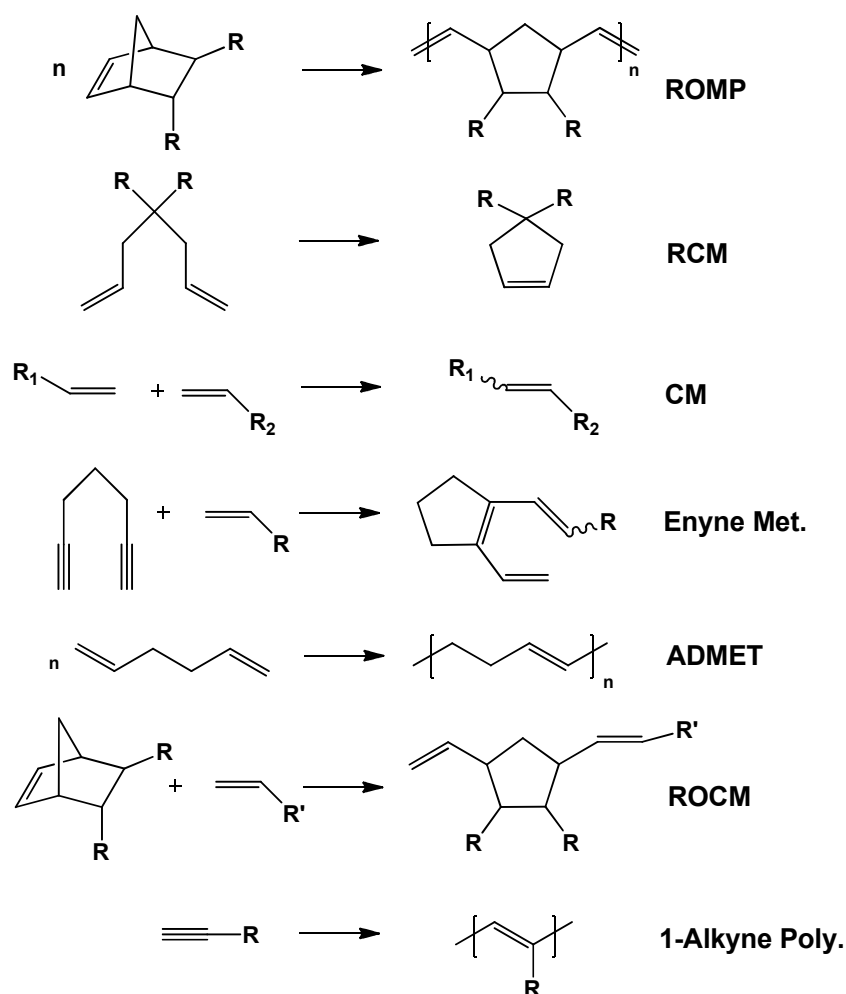
Figure 5: Overview of different metathesis reactions

2.2.1   Ring Opening Metathesis Polymerization

ROMP is a chain growth polymerization method which enables the synthesis of well-defined specialty polymers.[31,32] It is in general a three step reaction including initiation, propagation and termination. The general mechanism shown at the example of a norbornene is depicted in Figure 6. After the coordination of the monomer to the metal center, a [2+2]-cycloaddition affords a four-membered metalla-cyclobutane intermediate followed by a subsequent cyclorevision forming a new metal-alkylidene species. This circle is repeated until polymerization ceases, for example by full consumption of the monomer. In the end

---

[31] A. Leitgeb, J. Wappel, C. Slugovc, *Polymer* **2010**, *51*, 2927-2946.
[32] S. Sutthasupa, M. Shiotsuki, F. Sanda, *Polymer Journal* **2010**, *42*, 905-915.

the reaction is terminated via the addition of a terminating agent, such as ethylvinylether, leading an inactive Fischer Carbene. The termination step on one hand selectively removes the metal from the end of the polymer chain and on the other hand, gives the possibility to attach specific end-groups to the polymer chain.[33]
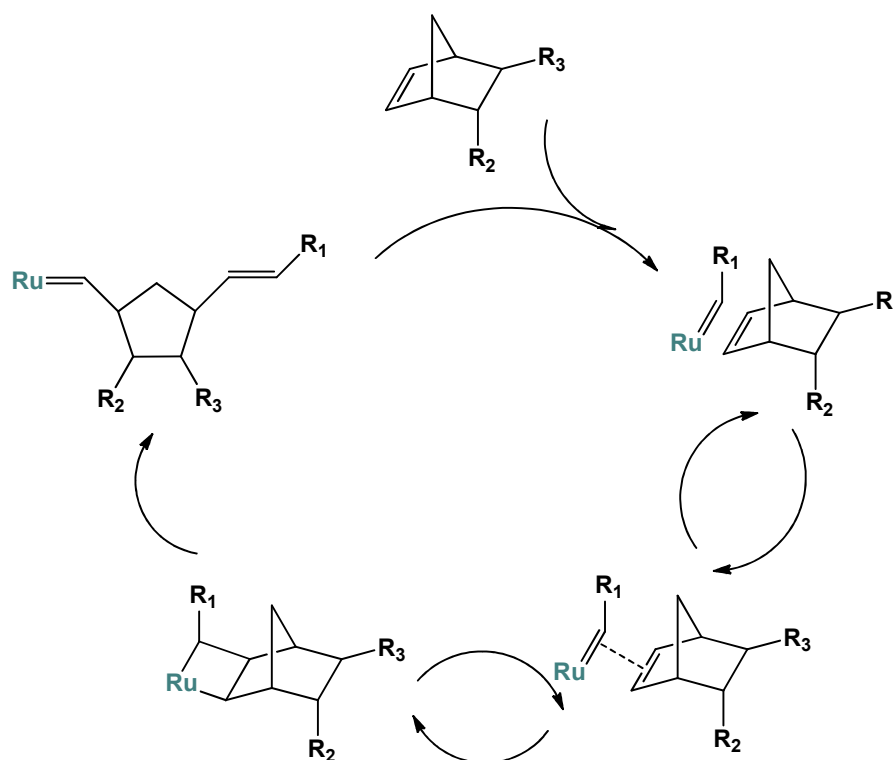
Figure 6: General ROMP mechanism shown at the example of a norbornene

The fact which distinguishes ROMP from many other polymerization methods is the possibility of living polymerization.[34] Living polymerization means, that the reaction proceeds without any side reactions, i.e. intermolecular or intramolecular (backbiting) chain transfer and yields polymers with narrow PDI's and predictable molecular weights.[35,36] With

---

[33] C. Lexer, R. Saf, C. Slugovc, *J. Polym. Sci. Part A: Polym. Chem.* **2009**, *47*, 299-305.

[34] (a) M. Szwarc, *Nature* **1956**, *178*, 1168-1169. (b) T.R. Darling, T. P. Davis, A. A. Gridnec, D. M. Haddleton, S. D. Ittel, *J. Polym. Sci. A: Polym. Chem.* **2000**, *38*, 1706-1708.

[35] C. W. Bielawski, R.H. Grubbs, *Prog. Polym. Sci.* **2007**, *32*, 1-29.

[36] A. M. Alb, P. Enohnyaket, J. F. Craymer, T. Eren, E. B. Coughlin, W. F. Reed, *Macromolecules* **2007**, *40*, 444-451.

this method, not only defined homopolymers, but also well-defined block- and graft-copolymers are accessible.

When conducting ROMP, especially for defined polymers, several things have to be considered. The reaction itself is not only determined by the initiator and the monomer used, but also by other parameters such as solvent and additives, temperature, monomer concentration etc. The influence of those parameters has been an intensive field of interest in the last years. A good overview is given in several reviews and papers dealing with this subject.[37]

2.2.1.1   ROMP in Industries

Apart of the specialty polymers, which are so far mostly made in field of research, ROMP is also applied in industrial scale. Vestenamer® is a polyoctenamer which was firstly produced by Degussa-Hüls AG. Depending on the *trans* content of the double bonds within the polymer, different Vestenamer® derivatives with distinct degrees of crystallinity are available. Vestenamer® 8012 exhibits a high *trans* content of around 80% and hence good thermoplasticity.[38] It is mainly applied for blending materials for other rubbers to improve the properties of those compounds. Vestenamer® 6213 on the other side exhibits a lower *trans* content (60%) and therefore lower crystallinity. Another commercially produced ROM polymer is a polynorbornene known under the trade name Norsorex®, which was firstly produced in France by CdF-Chimie, followed by Atofina, also in France and is nowadays made from Astrotech, Austria. Norsorex® has a high affinity to hydrocarbons and can absorb about 10 times its own weight. The main applications are protector systems for personal protective equipment due to its high damping features, feets for electronic equipment (microphones, loudspeakers, laptops, hard discs, reading heads for streamers etc.) due to its antivibration feature and tires and transmission belts because of its high friction.[39]

---

[37] (a) C. Slugovc, *Macromol. Rapid Commun.* **2004**, *25*, 1283-1297. (b) C. Slugovc, S. Demel, F. Stelzer, *Chem. Comm.* **2002**, 2572-2573.
[38] http://www.ilshinct.com/product/pdf//Vestenamer8012.pdf
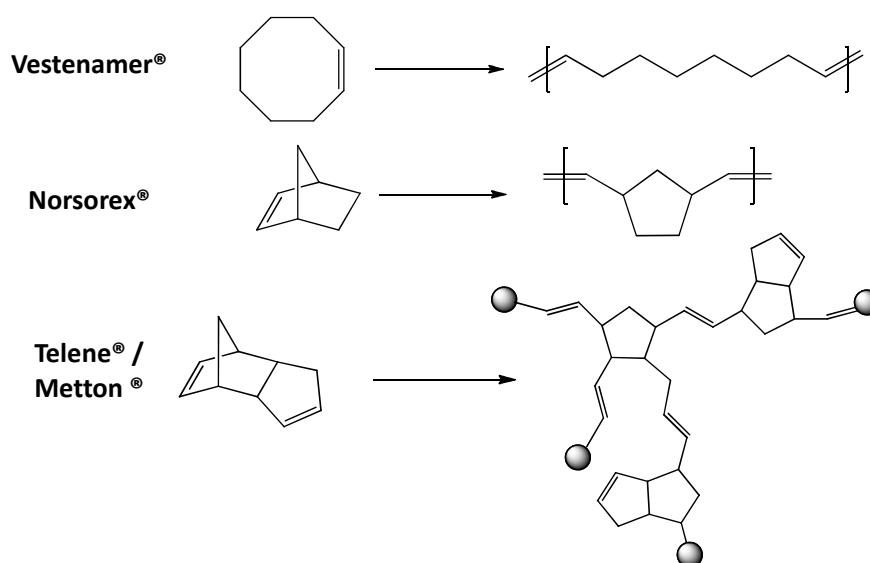[39] http://astrotech.at/index.php/norsorex.html

Figure 7: Commercial ROM polymers

The most interesting monomer used in industries is doubtless dicyclopentadiene (**DCPD**) leading to polydicyclopentadienes (**pDCPD**) with the trade names Metton® (Metton America, Inc. at La Porte and Teijin-Metton Co., Japan) or Telene® (Telene, France). Due to a second metathesis step of the second double bond in the monomer a cross-linked system is formed during one polymerization step. **DCPD** exhibits an outstanding rigidity and high impact strength. It is produced via a RIM (reaction injection molding) process, which means that two different streams, one containing the monomer, co-catalyst, additives, filler, retarder etc. and the other containing monomer, the catalyst, additives and filler first are mixed in a mixing chamber and then poured into a mold were the polymerization takes place right after a short induction period. In the Metton liquid molding resin (LMR) process, the catalyst/co-catalyst system is $WCl_6+WOCl_4/EtAlCl_2$ whereas in the Telene process, tetrakis(tridodecylammonium)octa-molybdate as the precatalyst and Et_2AlCl, propanol and $SiCl_4$ as the activating co-catalyst are used.[40] The main applications are highly engineered thermosets widely used for the production of body panels for truck, agricultural and earth moving equipment, cell covers for chlor-alkali plants, domestic waste water treatment units and large waste containers.[41] Furthermore, hydrogenated ROM polymers (Zeonex®) obtained from i.e. polynorbornene are manufactured in industrie. Zeonex® is an amorphous, colorless and transparent polymer with a high T_g and low moisture absorption making it suitable products for optical applications.[40]

---

[40] J. C. Mol, *J. Mol. Catal. A: Chem.* **2004**, *213*, 39-45.
[41] www.telene.com

2.3 Olefin Metathesis for Chiral Reactions

Since olefin metathesis is a very useful reaction often minimizing many reaction steps during organic synthesis, first attempts to apply this kind of reaction for enantionselective reactions, was done around 20 years ago. The synthesis of stereochemical pure components would be an important step in various fields of applications such as the production of drugs, biologically active compounds or agriculture chemicals. The main goal in this field would be the complete conversion of prochiral, racemic substrates into the desired enantiomeres. The first step in this direction was the synthesis of well-defined, enantiomerically pure chiral metathesis initiators to address tacticity control in ROMP.[42] Since then, a lot of research was done concerning this subject leading to several defined chiral olefin metathesis reactions, namely Asymmetric Ring Closing Metathesis (ARCM), Asymmetric Ring Opening Cross Metathesis (AROCM) and Asymmetric Cross Metathesis (ACM) and various craftily designed transition metal catalysts. Anyway, enantioselectiv metathesis reactions are still in their early stage of development and the "perfect" catalyst has not been synthesized yet. Currently, this reaction is mainly employed for chiral building blocks and fine chemicals. A desirable main aim would be the use of an enantioseletive conversion within natural product synthesis.

2.3.1 Development of Chiral Complexes

In the following chapter the development of well-defined molybdenum and ruthenium olefin metathesis catalysts for chiral metathesis reactions is described and their differences are discussed.

2.3.1.1 Molybdenum based Catalysts

The first reported example of an enantioselective molybdenum catalyst was biphenolate based catalyst **VI,** in which chirality was introduced via the bidentately bound diol. The initiator proofed to be highly active in the ARCM of 1,6-dienes, but failed in the enantioselective conversion of 1,7-dienes.[43] Following the attempt of the bidiolate complexes, soon after the groups around Schrock and Hoveyda synthesized catalysts bearing a binaphtolate ligand. In Figure 8 complex **VII** is depicted as a representative

---

[42] K.M Totland, T.J. Boyd, G. G. Lavoie, W.M. David, R.R. Schrock, *Macromolecules* **1996**, *29*, 6114-6125.

[43] J. B. Alexander, D. S. La, D. R. Cefalo, A. H. Hoveyda, R. R. Schrock, *J. Am. Chem. Soc*. **1998**, *12*0, 4041-4042.

example for a binaphtolate complex.[44] Unfortunately, these catalysts were just partially active in chiral metathesis reactions and could not reach their biphenolate congeners. Nevertheless, this system has the big advantage of easily accessible starting materials, compared to the biphenolate system. To circumvent those problem, catalyst from the type of **VIII** were made by partial hydrolyses of the napthol ligand, leading to initiators combining positive features of **VI** and **VII**. **VIII** shares structural features of both complexes **VI** and **VII**, e.g. it is easily prepared form commercially available starting materials and exhibits an unique selectivity profile.[45] Additionally, they can be used *in-situ*, allowing a more convenient handling compared to other molybdenum catalysts showing a distinctive sensitivity to oxygen and moisture.
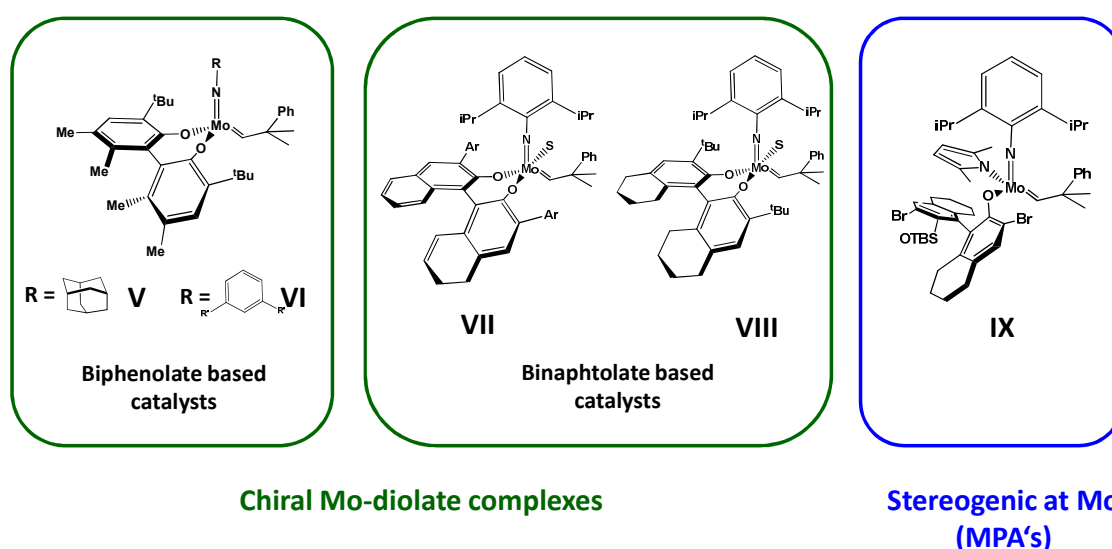

Chiral Mo-diolate complexes   **Stereogenic at Mo (MPA's)**

Figure 8: Representative example of enantioselective Mo catalysts; S=THF

But not only the oxygen based donor ligand has a pronounced effect on the enantioselectivity of a reaction, also the imido-system contributes significantly to the result. In general, this ligand has an important effect on the catalysts stability by shielding the sensitive metal center through the *ortho* subsitutents. If the normally used aryl-imido

---

[44] S. S. Zhu, D. R. Cefalo, D. S. La, J. Y. Jamieson, W. M. David, A. H. Hoveyda. R. R. Schrock, *J. Am. Chem. Soc.* **1999***, 121*, 8251-8259.

[45] (a) S. L. Aeilts, D. R. Cefalo, P. J. Bonitatebus, Jr., J. H. Houser, A. H. Hoveyda, R. R. Schrock, *Angew. Chem. Int. Ed.* **2001**, *40*, 1452-1456. (b) D. R. Cefalo, A. F. Kiely, M. Wuchrer, J. Y. Jamieson, R. R. Schrock, A. H. Hoveyda, J. *Am. Chem. Soc.* **2001**, *123*, 3139-3140.

complex is exchanged against an alkyl-imido complex (**V**, featuring a less bulky adamentyl group) better results can be obtained in some particular reactions.[46]

The third strategy followed to obtain molybdenum based catalysts for enantioselective metathesis was based on theoretical works of Eisenstein et al.[47] By the introduction of pyrrole and axially chiral alkoxides, both monodentate systems, instead of the up to that point used bidentate systems lead to catalysts which were stereogenic at the metal center (**IX** depicts one representative example).[48] The proposed mechanism implies that after every metathesis step, an inversion of the configuration at the metal center occurs. [49] These monoaryloxide-monopyrrolide based catalysts, short MAP's, are not only easily prepared, but also protrude by the possibility to be generated *in-situ* and subsequently used without any further purification steps.

In general, molybdenum based catalysts show good and promising results, especially for the use in natural product synthesis, for example in total synthesis of *Aspidosperma* alkaloid quebrachamine.[50]

2.3.1.2   Ruthenium based Catalysts

Regarding the ruthenium based catalysts two strategies to obtain enantioselective complexes have been followed: (**a**) catalysts which are chiral at the NHC and (**b**) catalysts which exhibit chiral anionic ligands. Catalysts which are chiral at the dissociative ligand or at the carbene are, due to the dissociation of those ligands off from the ruthenium, not very useful.

The chirality at the NHC brings the advantage along, that due to the strong binding of the NHC, this ligand does not dissociate from the ruthenium center during the catalytic cycle. Other than the dissociative or the carbene ligand it can therefore induce the chiral information during every metathetic cycle. The first pioneering report about the synthesis of a chiral molybdenum catalyst was published by the group of Grubbs in 2001.[51] This complex **X** was tested in the asymmetric ring closing metathesis of several trienes, yielding

---

[46] (a) T. S. Pilyugina, R. R. Schrock, P. Müller, A. H. Hoveyda, *Organometallics*, **2007**, *26*, 831-837. (b) W. C. Peter Tsang, J. A. Jernelius, G. A. Cotez, G. S. Weatherhead, R. R. Schrock, A. H. Hoveyda, *J. Am. Chem. Soc.* **2003**, *125*, 2591-2596.

[47] (a) X. Solans-Monfort, E. Clot, C. Copéret, O. Eisenstein, *J. Am. Chem. Soc.,* **2005**, *127*, 14015-14025. (b) A. Poater, X. Solans-Monfort, E. Clot, C. Copéret, O. Eisenstein, *J. Am. Chem. Soc.,* **2007**, *129*, 8207-8216.

[48] S. J. Meek, S. J. Malcolmson, B. Li, R. R. Schrock, A. H. Hoveyda, *J. Am. Chem. Soc.*, **200**9, *131*16407-16409.

[49] S. C. Marinescu, R. R. Schrock, B. Li, A. H. Hoveyda, *J. Am. Chem. Soc.,* **200**9, *131*, 58-59.

[50] A. H. Hoveyda, S. J. Malcolmson, S. J. Meek, A. R. Zhugralin, *Angew. Chem. Int. Ed.* **2010**, *49,* 34-44.

[51] T. J. Seiders, D. W. Ward, R. H. Grubbs, *Org. Lett.,* **2001**, *3,* 3225-3228.

more or less good results with moderate to good enatioselectivties depending on the substrate. Grubbs et al. took advantage of the so called "gearing effect", meaning that the *ortho* substituents within the aromatic rings are forced to reside opposite to the bulky groups of the NHC backbone. Hence, the chirality is transferred to the olefin's coordination sphere even though the stereocenters are remote from the metal. The enatioselctivity in these kind of catalysts could be improved by an *in-situ* exchange of the anionic chlorines against iodenes. Anyhow, this enantioselectivity increase was reflected at the expense of shorter lifetimes and the need of higher catalyst loadings. By varying the substitution pattern on the aryl ring of the NHC, selectivity and reactivity could be improved within this catalyst family (complex **XI** and **XI**I).[52]

---

[52] T. W. Funk, J. M. Berlin, R. H. Grubbs, *J. Am. Chem. Soc.,* **2006**, *128*, 1840-1846.

C$_2$ symmetric NHC's

R$_1$=^{i}Pr; R$_2$,R$_3$, R$_4$=H;   **X**

R$_1$=^{i}Pr; R$_2$=^{i}Pr; R$_3$,R$_4$=H;   **XI**

R$_1$=^{i}Pr; R$_2$=H; R$_3$=OMe, R$_4$=^{t}Bu;   **XII**

C$_1$ symmetric NHC's

R$_1$=^{i}Pr; R$_3$,R$_4$=H;   **XIII**

R$_1$=^{i}Pr; R$_3$=OMe, R$_4$=^{t}Bu;   **XIV**
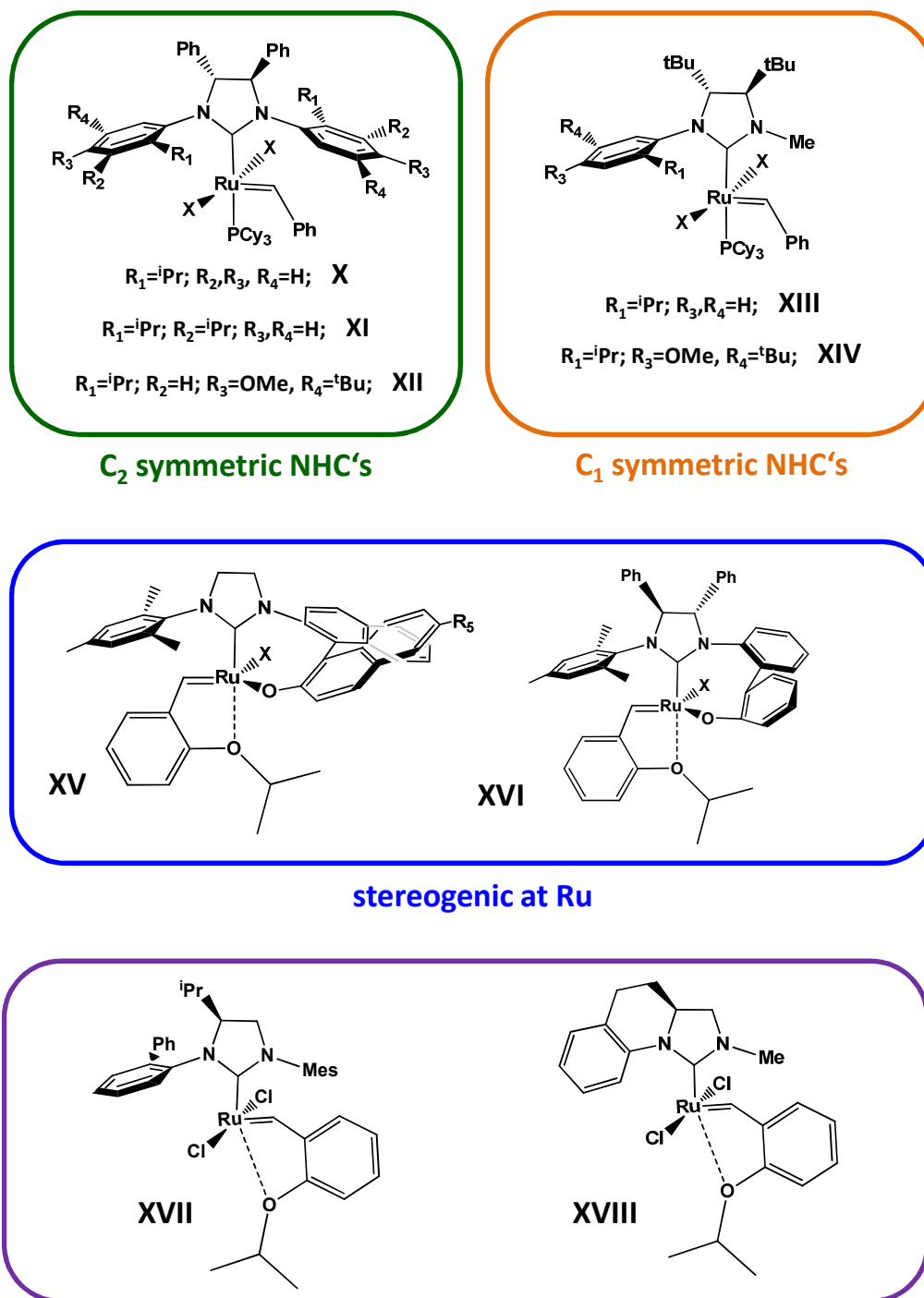
stereogenic at Ru

Figure 9: Enantioselective ruthenium based initiators

Another concept, established by Hoveyda in 2002, uses the same attempt of a "stereogenic-at-ruthenium" as was also applied in molybdenum catalysts. In these types of catalyst, a

bidentate NHC is introduced, whereby one chlorine is substituted against an alkoxid group, which is attached to the NHC.[53] Unfortunately, this space grabbing system causes a significant steric congestion, making the use of high catalyst loadings necessary. Furthermore the activity is dimished by a decrease of the Lewis acidity at the metal caused by the alkoxy ligand.[54] **XV** distinguishes itself also by means of a very pronounced stability, caused by the lack of backbone substitution of the NHC. Thus the mesityl group is not forced in the equatorial coordination sphere of the ruthenium which enables the adaption of the Hoveyda carbene system. Albeit the major drawback of this systems is a long and difficult synthesis. A further step in this direction was the implementation of complex **XVI** also published by the same group.[55] This system combines the features of the "stereogenic-at-ruthenium" from complex **XV** and the gearing effect of complex **X**-**XII**. Especially the iodine derivative of this complex yielded promising results in the AROCM of low strained oxa- and azabicycles. In 2007 a new concept for chiral ruthenium based catalysts was followed: with the introduction of bulky *tert*-butyl-groups the influence of the chiral backbone should be increased. Due to this increased steric demand one N-aryl substituent had to be downsized again, leading to the synthesis of complex **XIII,** a catalyst with an unsymmetrical N-heterocyclic carbene ligand. Tested in ARCM reactions, this C_1 symmetric catalyst showed increased reactivity in comparison to up to that point existing chiral ruthenium catalysts. [56] The latest invention of chiral catalysts was done by Blechert and co-workers. This complex class bears a monosubstituted backbone and monodentate NHC of C_1 symmetry (**XVII**).[57] Good to moderate enantioselectivities in ARCM and AROCM depending on the substrates used were obtained using this system. Additionally **XVII** protrudes with low catalyst loadings and an outstanding stability. Adopting this system the same group published one year later in 2011 complex **XVIII**. This bidentate NHC displays a linkage between the N-aryl and the NHC backbone, yielding a very rigid system. When employed in AROCM, **XVIII** gave excellent results still maintaining the good stability and low catalysts loadings of **XVII**.[58]

The second possibility to gain chiral initiators is the introduction of chiral anionic ligands. So far, just a very few examples regarding those kind of initiators have been reported. This attempts were followed mainly by the group of Fogg and co-workers. They adopted the concept of Schrocks molybdenum based complex **VII** and Hoveyda's ruthenium based complex **XV** and used biphenolate-derived ligands to introduce the chiral information.

[53] J. J. Van Veldhuizen, S. B. Garber, J. S. Kingsbury, A. H. Hoveyda, *J. Am. Chem. Soc.*, **200**2, *124*, 4954-4955.
[54] S. Kress, S. Blechert, *Chem. Soc. Rev.*, **2012**, *41*, 4389-4408.
[55] J. J. Van Veldhuizen, J. E. Campbell, R. E. Giudici, A. H. Hoveyda, *J. Am. Chem. Soc.*, **200**5, *127*, 6877-6882.
[56] P.-A. Fournier, S. K. Kollins, *Organometallics*, **2007**, *26*, 2945-2949.
[57] S. Tiede, A. Berger, D. Schlesiger, d. Rost, A. Lühl, S. Blechert*, Angew. Chem., Int. Ed.*, **2010**, *49*, 3972-3975.
[58] A. Kannenberg, D. Rost, S. Eibauer, S. Tiede, S. Blechert, *Angew. Chem., Int. Ed.,* **2011**, *50*, 3299-3302.

Starting from third generation Grubbs catalysts, they synthesized complex **XIV** bearing the bidentate "bino" ligand as the enantioselective main product. Additionally to the main product several minor products such as a η^3-enolate coordinated and a bipyridine derivative were obtained in small amounts.[59] The new complex **XIV** was tested in the AROCM of *endo*-norbornene-dicarbocylic anhydride with styrene yielding good conversions, but no enantiomeric excess could be detected and almost a racemic mixture of the two products was obtained.
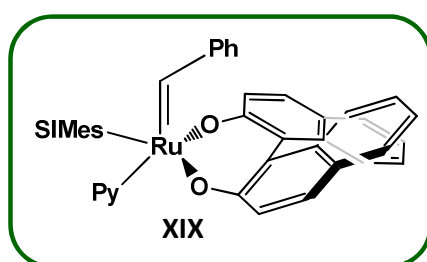

Figure 10: Chiral initiator through anionic ligands

2.3.2   Chiral Metathesis Reactions

In chiral metathesis reactions, a stereocenter is set into the emerging product even though when starting from prochiral meso compounds. As already described before, three different reactions accomplishing these requirements are known: ARCM, AROCM and ACM. Whilst the ARCM and the ARCOM are already well investigated reactions, ACM is still in its infancy. Herein, all three reactions are disclosed in more detail.

2.3.2.1   Asymmetric Ring Closing Metathesis (ARCM)

In general the ARCM describes the desymmetrization of prochiral trienes through transition metal catalysts. Apart from the standard benchmark reactions performed with all new developed chiral catalyst, this reaction has gained more and more interest within natural product synthesis. ARCM is able to promote the construction of small, medium as well as large carbon or heteroatom containing ring systems.

---

[59] (a) J. M. Blacquiere, R. McDonald, D. E. Fogg, *Angew. Chem., Int. Ed.* **2010**, *49*, 1-5. (b) J. M. Blacquiere, C. S. Higman, R. McDonald, D. E. Fogg, *J. Am. Chem. Soc.* **2011**, *133*, 14054-14062.

Since the first metathesis step is exclusively determined by the nature of the applied substrate (it takes place at the least congested double bond within the system) the propagating species is, depending on the substrate, predictable. As shown in Figure 11 the first metathesis step always occurs at the less crowded olefin, in this case the non-substituted double bond, leading to intermediate **C**. The crucial role of the catalyst is limited to the second metathesis step where ultimately the ring is closed (intermediate **D** > **A**).
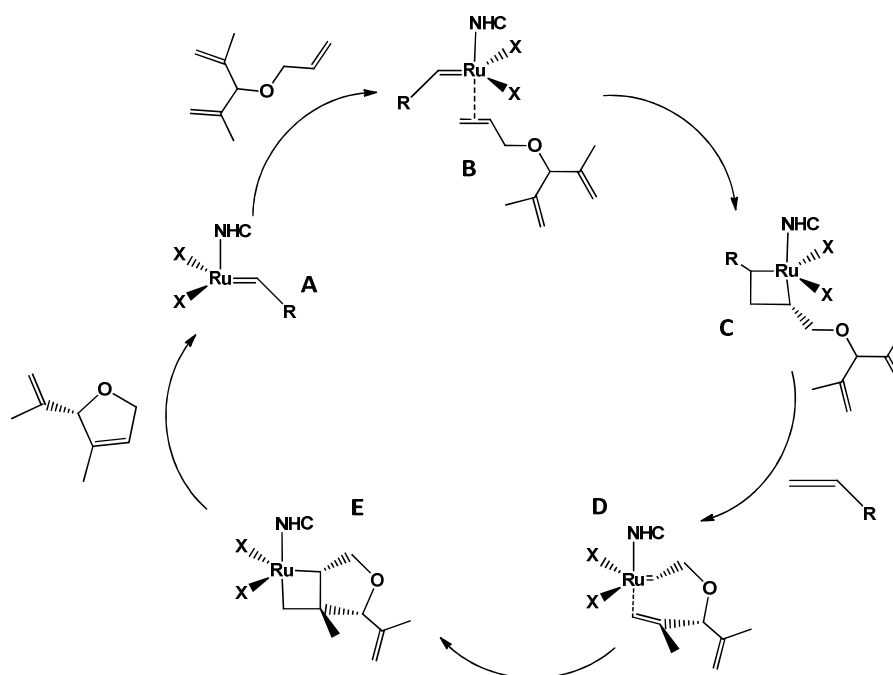

Figure 11: General mechanism for ARCM illustrated at the example of an Ru initiator; redrawn from reference 54;

In the following, two examples for different performances of chiral molybdenum and ruthenium complexes are shown. The first is the ARCM reaction of the standard benchmark substrate 4-allyloxy-3,5-dimethyl-2,5-heptadiene (**SI**) and the second one is the formation of a precursor (**SII**) which is subsequently hydrolyzed selectively to give the alkaloid quebrachamine.
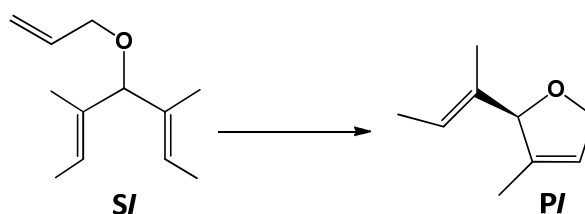
Figure 12: Benchmark reaction of S*I* to P*I*

Table 2: Comparison of molybdenum and ruthenium based initiators in the ARCM of S*I*

Catalyst	mol%	Temp. [°C]	Conv. [%]	ee%
VI	5	RT	32	94
VII	5	54	nr	94
X[a]	2.5	38	82	90
X	2	40	> 98	35
XI[a]	4	40	> 98	90

[a] iodine salts were added to the reaction to form the iodo-complexes

The ARCM of **S*II*** is a challenging reaction due to the hindered vinyl groups at a congested all-carbon quaternary center and the presence of a Lewis basic tertiary amine. In the beginning, none of the molybdenum based catalysts was able to perform well in this reaction, even though sub-stoichiometric amounts of catalyst of up to 50 % with respect to the substrate were used. It merits mentioning, that for example the ruthenium based catalyst **XVI** gave high yields at "lower" catalyst loadings, however enantioselectivity was disappointing. Only when complex **IX**, which is stereogenic at the molybdenum center, was applied, excellent conversions with satisfying enantioselectivity in short reaction times were accomplished. A mechanistic explanation for the success of this kind of initiator was given by Eisenstein and co-workers in reference 47b and 54.
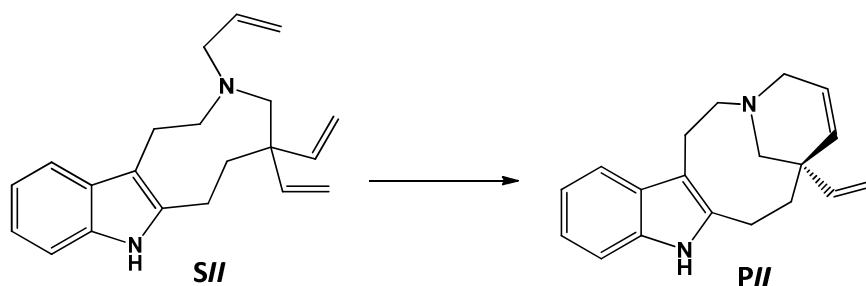

Figure 13: ARCM reaction of S*II* to the precursor for the quebrachamine synthesis P*II*

Table 3: Comparison of molybdenum and ruthenium based initiators in the ARCM of S/I

Catalyst	mol%	Temp. [°C]	Conv. [%]	ee%
VI	50		< 5	n.d.
XVI	15		> 98	< 5
IX[a]	1		> 98	96

[a] substituted with chlorines instead of bromines

2.3.2.2 Asymmetric Ring Opening Cross Metathesis (AROCM)

The most important facts about the AROCM were already summarized in several reviews.[54,60] The AROCM process can be rated to be a subsection of ACM reactions with the difference, that an additional metathesis step, namely the ring opening metathesis, occurs. As in this case two, instead of just one product as in ARCM reactions, are applied, the reaction is more complicated than the ARCM reaction and as further consequence more facts have to be considered.

In general, the AROCM reaction is a reaction occurring between two from each other independent cross-partners: olefin A (the *meso*-ring opened norbornene derivative) and olefin B (the cross partner, generally a terminal olefin). During an AROCM reaction several different products, namely the cross-product AB in *cis* and *trans* configuration and the homodimerization products AA and BB can be formed. The *cis* as well as the *trans* AB products are each formed in two different enantiomers. Overall, during one AROCM reaction eight different products can be formed. To predict or rather control the reaction somehow, certain points have to be considered.

If the norbornene derivative A is the more reactive olefin, the AROCM reaction is appropriately efficient. When the applied catalyst opens the norbornene, the ring closing-back-reaction is thermodynamically disfavored due to the released ring-strain. This leads to a favored reaction of the "metal-substrate A alkylidene" with the cross-partner B, which can additionally be enforced by an excess of olefin B. Nevertheless, if the norbornene is too reactive (i.e. an unsubstituted norbornene), the formation of an AA homodimer, or subsequently the build-up of oligomers or even polymers through the ring opening metathesis polymerization gets more likely. Here it merits mentioning, that in general, the oligomerization of A is more important to be suppressed than the homodimerization of B. If B dimerizes, only one product can be formed. On the other side, oligomers of A can still undergo a cross-metathesis reaction with B forming oligomeric-cross-products like AAB,

---

[60] D. S. La, E. S. Sattely, J. G. Ford, R. R. Schrock, A. H. Hoveyda, *J. Am. Chem. Soc.,* **2001**, *123*, 7767-7778.

AAAB etc. In case of dimerized B it can be separated from the other products via colu chromatography. Apart from the mentioned side reactions during the reaction, an additional cross-metathesis from an AROCM product AB with another olefin B can lead to a product of the form BAB. The possible side reactions are summarized in Figure 14.
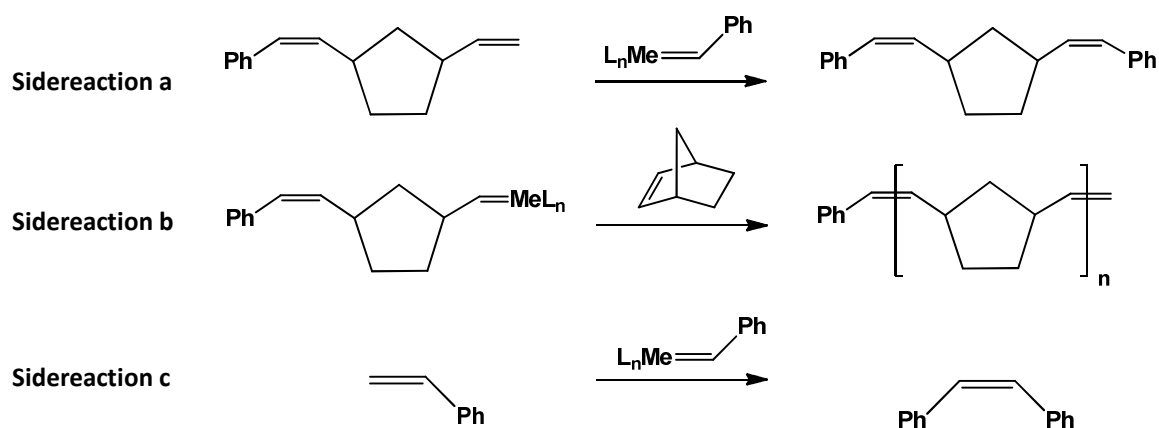

Figure 14: Possible side reactions of an AROCM reaction

If all side reactions are excluded, still two possible pathways leading to the desired AROCM products can occur.
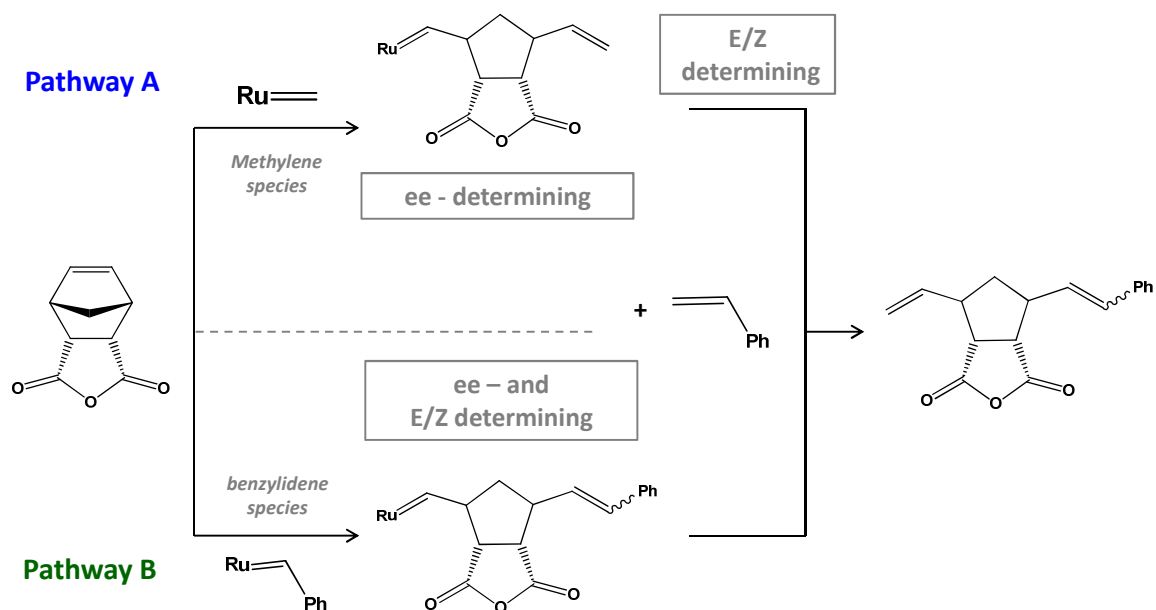
Figure 15: Possible reaction mechanism of AROCM depicted at the example of norbornenedicarboxylic acid anhydride and styrene; redrawn from reference 54;

In pathway A, a methylidene (formed via a previous metathesis step) species reacts with the norbornene monomer yielding a norbornene-alkylidene species. Here, the first step determines the enantioselectivity. The following metathesis step with styrene determines only the *cis* to *trans* ratio and leads to the desired AROCM product. Following this route, the ee values of the *cis* as well as of the *trans* species are the same. In contrast, in pathway B first a styrene reacts with the initiator and the subsequently formed benzylidene species can now react in the second metathesis step with the monomer. In this instance, this step determines enantioselectivity as well as the *cis/trans* ratio of the occurring AROCM product. Here, the *cis* and the *trans* species do not have necessarily the same ee values. This fact gives a hint, if the reaction proceeds either via pathway A or rather via pathway B. Still one has to keep in mind, that if both pathways happen concurrently and each route provides the opposite enantiomers, the overall enantioselectivity can be diminished.

The influence of the norbornene-derivative was well studied by the group of Hoveyda. Thereby it was demonstrated that due to high reactivity of molybdenum initiators, norbornenes which are substituted at position 7 pointing to the side of the double bond have to be used to circumvent oligomerization by means of enhanced steric. This restriction minimizes the availability of derivatives drastically and requires long and complicated synthesis routes. For this reaction, ruthenium based initiators outperform their molybdenum congeners considerably. Due to their somewhat lower reactivity and the

higher group tolerance a broad variety of several norbornene derivatives can be used. One of the most prominent ones, generally used as the standard benchmark monomer is the *exo*-norbornenedicarboxylic acid anhydride (**S1**). The main advantage of this monomer is its commercial availability and cheapness.
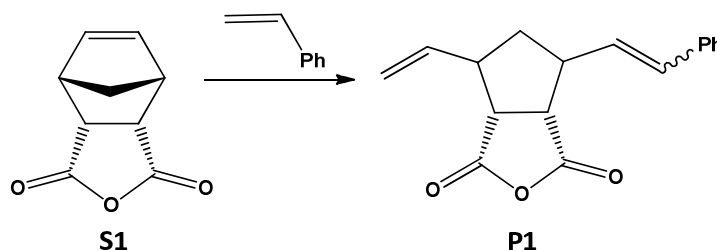
Scheme 1: Standard benchmark AROCM reaction of S1 to P1.

Table 4: AROCM data of several ruthenium initiators

Catalyst	mol%	Temp. [°C]	Conv. [%]	E/Z ratio	ee%
XII	1	40	96	1:1	80
XV	5	-	60	95:50	70
XVII	1	-10	>98	>30:1	93
XVIII	2.5	25	83	13:1	75

Table 4 compares the performance of a molybdenum based with several ruthenium based initiators in the AROCM of **S1** with styrene. Unfortunately the comparison of molybdenum and ruthenium metathesis initiators remains difficult because of the before mentioned high reactivity of the molybdenum initiators. In this case, almost exclusively 7-norbornene derivatives with a syn double bond are reported. These monomers cannot be ring openend by ruthenium initiators.

Another advantage of Ru initiators is their great tolerance to functional groups, making the use of several cross-partners such as allyl alcohols, homoallyl alcohols[61] and trimethylallylsilanes possible. Additionally Ru initiators can also provide the AROCM of oxabicycles leading to various pyrans which are versatile building blocks for the target

---

[61] J. Tornatzky, A. Kannenberg, S. Blechert, *Dalton Trans.*, **2012**, *41*, 8215-8225.

orientated synthesis. In comparison to norbornenes, these systems are less strained and give rise to different demands for the initiators.[62]

2.3.2.3   Asymmetric Cross Metathesis (ACM)

The Asymmetric Cross Metathesis (ACM) reaction is without a doubt the less explored reaction in the field of enantioselective synthesis. This reaction is due to many different reasons very difficult to control. Firstly, homodimerization of the two applied cross-partners should be suppressed. Secondly, secondary metathesis steps, where the resulting products are attacked should also not occur to ensure a selective formation of the desired product. Thirdly, E/Z selectivity should also be possible to control during the reaction. An ideal catalyst would react selectively with one of the two cross-partners leading to a well-defined propagating species. This species subsequently has to react selectively with the second applied cross-partner in a manner that the desired cross-product is formed. Unfortunately, this field, even though a very important one in the area of target orientated synthesis, is still one of the greatest challenges which has to be faced in metathesis synthesis.

---

[62] (a) D. Gl. Gillingham, A. H. Hoveyda, *Angew. Chem., Int. Ed.*, **2004**, *126*, 12288-12289. (b) G. A. Cortez, C. A. Baxter, R. R. Schrock, A. H. Hoveyda, *Org. Lett.*, **2007**, *9*, 2871-2874.

2.4 Latent Initiators for Olefin Metathesis Reactions

In general, latent olefin metathesis initiators are complexes featuring a certain characteristic which suppresses the metathesis reactivity under standard reaction conditions at room temperature. Nevertheless, these kinds of complexes can be triggered selectively by a certain stimuli and hence convicted in the best case into a highly metathesis active form. Until now, several activation mechanisms have been explored for metathesis initiators including heat, acid, light and chemical activation. Some pre-catalysts can only activated via one of the mentioned stimuli, others respond to more than one, meaning that they can for example be triggered either via heat or via the addition of acid. Latent systems have gained special interest in the context of ring-opening-metathesis polymerization for industry mostly due to the possibility of storing the initiator together with the monomer and the subsequent selective initiation when desired. This feature is interesting for RIM processes, ink jet printing or spin coating, especially when very reactive monomers such, as dicylcopentadiene (**DCPD**) are used.
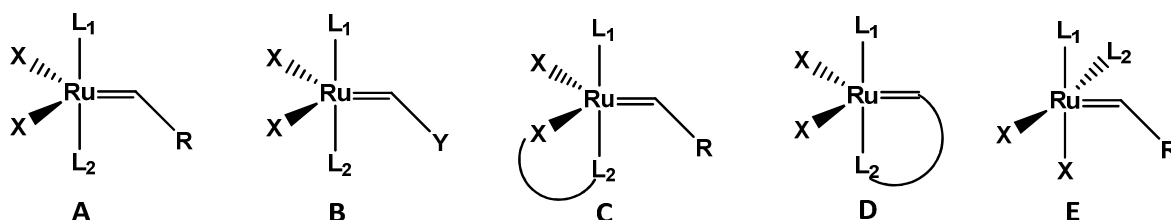
Figure 16: Different general approaches for latent olefin metathesis initiators

Different routes to realize latent systems have been used and are described in literature. Latency can either be introduced via a very unlabile L_2 ligand which does not dissociate easily from the ruthenium center (**A**) or via the introduction of a heteroatom leading to a so called Fischer carbene (**B**). A second often used approach is the implementation of chelating moieties. The chelation can be either between an anionic ligand and the dissociative ligand L_2 (**C**), or between the carbene ligand and L_2 (**D**). The advantage of the carbene/L_2 chelation is the fact that the chelating moiety moves further away from the ruthenium center with every metathesis step that happens and hence re-dissociates more difficultly. On the other

side, when the chelation is between an anionic ligand and L_2, L_2 stays next to the ruthenium center during the whole polymerization cycle making a re-dissociation more likely and hence hampers the metathesis reactivity. Another possibility for latent initiators was found, when initiators with a *cis* arrangement of the two anionic ligands were investigated more closely (**E**).

Latent initiators have already been applied in ill-defined metathesis systems. The main advantage of such ill-defined systems is that they are generally cheaper and readily commercially available. Nevertheless, their lack of initiation efficiency results often in broad molecular weight distribution of the polymers and makes the use of well-defined systems inevitable.

In the following, the several activation mechanisms and the appertaining well-defined metathesis initiators are elucidated more closely.

2.4.1   Thermally Triggered Metathesis Initiators

Heat activated initiators are probably the biggest group among latent initiators. Within this group different general forms such as catalysts with structure **A**, **B** and **D** have been applied. Generally in case of thermally triggerable initiators, the energetic barrier for the dissociation of the neutral ligand L_2 is too high to enable the activation at room temperature. Through a simple energy supply by means of heat, the barrier can be overcome, activation occurs and the catalyst becomes active. The best and probably easiest way to measure the activation temperature is the use of differential scanning calorimetry (DSC). Herein, the exothermic reaction occurring when polymerization starts can be measured and hence the activation temperature can be determined. Switching temperatures, depending on the pre-catalyst, can range from just a little bit over room temperature (30°C) to very high temperatures of over 100°C.

In Figure 17 several thermally switchable initiators invented in the last few years are presented. Complex **XX**, following concept **B**, was synthesized in 2000. Herein it was proven for the first time that Schrock carbenes are not necessarily totally inactive but can be triggered.[63]

---

[63] P. A. van der Schaaf, R. Kolly, H.-J. Kirner, F. Rime, A. Mühlebach, A. Hafner, *J. Organomet. Chem.*, **2000**, *606*, 65-74.

Even though none chelating examples of thermally switchable initiators do exist, most of them bear a chelating carbene/L_2 moiety with a heteroatom following various approaches. The group of Slugovc introduced a quinoline or quinoxaline ligand respectively (**XXI**) yielding complexes with a *cis* or a *trans* configuration. The *trans* initiators showed switching temperatures of up to 84°C. Furthermore it was demonstrated, that the activation temperature is not only influenced by the initiator itself, but also by the monomer applied for the reaction.[64]
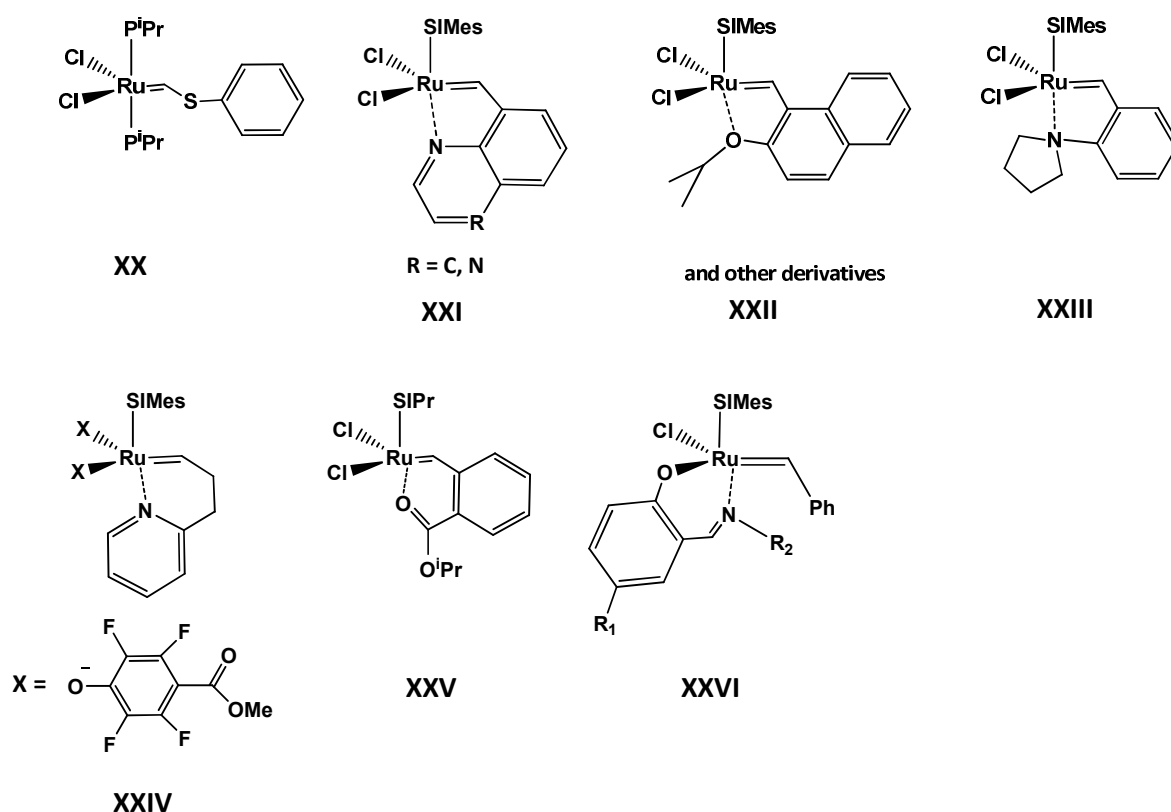
Figure 17: Several selected examples of thermally switchable metathesis initiators

In complex **XXIV** (and some other analogues) the influence of the anionic ligands on the latency of the new complexes was investigated. It was expected, that the electron withdrawing nature of the anionic -C_6F_4 group is expected to make the nitrogen-ruthenium

---

[64] X. Gstrein, D. Burtscher, A. Szadkowska, M. Barbasiewicz, F. Stelzer, K. Grela, C. Slugovc, *J. Polym. Sci: Part A: Polym. Chem.* **2007**, *45*, 3494-3500.

chelation stronger and hence the catalysts less active. Indeed, the synthesized catalysts were inactive at RT, but showed moderate activity at 55°C.[65] An interesting kind of latent initiators was introduced in a cooperating work of Slugovc and Grela using different naphthalene-based Hoveyda type initiators (**XXII** displays one example). Normally, the chelation via an ether moiety is not strong enough to prevent the metathesis reaction at room temperature - the highly established initiator **Hov** shows very good metathesis performance. Nevertheless, the introduction of an extended π-system which introduces aromaticity into the ring chelate strengthens the ruthenium oxygen bond and consequently decreases the activity of the complex.[66] In this coherernce it is worth mentioning, that not all applied initiators of this system are latent. Latency is introduced according to the Clars rule leading to different latent characteristics, depending on the ligand. Recently complex **XXV**, also invented by the group of Slugovc, was introduced as the first latent SIPr containing initiator. The extremely good stability of this latent initiator, caused by the strongly chelating carbene ligand, makes reactions at very high temperatures feasible. Thus this initiator is very useful for the conversion of challenging substrates for RCM reactions.[67]

Another big family of thermally switchable initiators are the so called "bis-NHC" complexes. The latency in these systems is introduced via the strong binding of the N-heterocyclic carbene to the metal center. In general, bis-NHC's show an increased stability of the catalysts at the cost of activity. In the last years, various bis-NHC systems have been developed by several groups leading to more or less metathesis active complexes.[68] Bis-NHC complexes, especially the one with electron poor NHC ligands such as complex **XIX**, proved to be particularly efficient for the transformation of sterically hindered substrates in RCM reactions. The group of Nolan introduced in 2010 mixed NHC complexes featuring one sterically small NHC and one larger SIMes NHC (**XXX**). These complexes were successfully used for RCM reactions at very low catalyst loadings of just 0.02 mol%.[69]

---

[65] Z. Yu, Y. Rogan, E. Khosravi, O. M. Musa, L. Hobson, A. S. Batsanov, *J. Organomet. Chem.* **2011**, *696*, 1591-1599.

[66] (a) M. Barbasiewicz, A. Szadkowka, A. Makal, K. Jarzembska, K. Woźniak, K. Grela, *Chem. Eur. J.* **2008**, *14*, 9330-9337.(b) A. Leitgeb, A. Szadkowska, M. Michalak, M. Barbasiewicz, K. Grela, C. Slugovc, *J. Polym. Sci. A: Polym. Chem*. **2011**, *49*, 3448-3454.

[67] A. Leitgeb, M. Abbas, R. C. Fischer, A. Poater, L. Cavallo, C. Slugovc, *Catal. Sci. Technol.*, **2012**, *2*, 1640-1643.

[68] (a) T. Weskamp, W. C. SChattenmann, M. Spiegler, W. A. Herrmann, *Angew. Chem.* **1998**, *110*, 2631-2633; *Angew. Chem. , Int. Ed.* **1998**, *37*, 2490-2493. (b) T. M. Trnka, J. P. Morgan, M. S. Sanford, R. E. Wilhelm, M. Scholl, T.-L. Choi, M. W. Day, R. H. Grubbs, *J. Am. Chem. Soc.* **2003**, *125*, 2546-2558. (c) T. Vorfalt, S. Leuthäusser, H. Plenio*, Angew. Chem.* **2009**, *121*, 5293-5296; *Angew. Chem., Int. Ed.* 2009, *48*, 5191-5194.

[69] X. Bantreil, R. A. M. Randall, A. M. Z. Slawin, S. P. Nolan, *Organometallics* **2010**, *29*, 3007-3011.
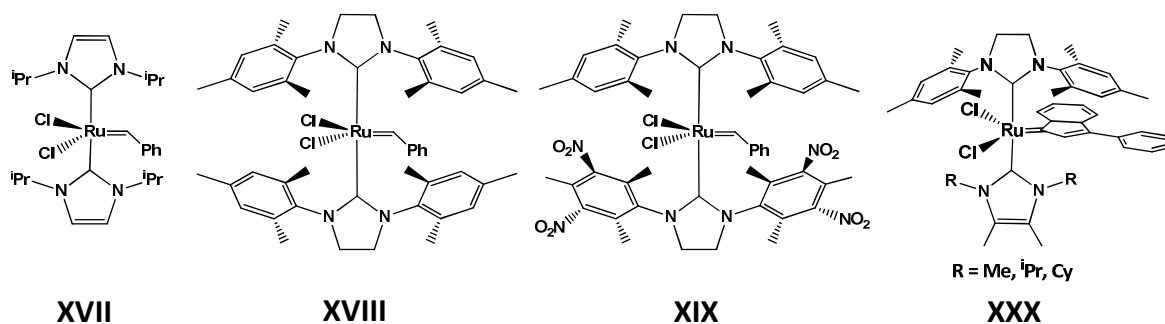
Figure 18: Bis-NHC complexes

Additionally to these only via heat activated complexes, complexes which can be activated via more than one trigger have been synthesized in the last years. An example for a heat and light activated initiator is complex **XXIII** synthesized by Lemcoff and co-workers.[70] **XXVI** on the other hand is a representative example for a combination of acid and heat triggerable complex.[71]

2.4.2 Acid Triggered Metathesis Initiators

One of the first reports regarding acid triggerable initiators was made in 1998. By the attempt, to prepare initiators with increased moister and oxygen stability, the octahedral 18 electron complex **XXXI** was synthesized. Due to its 18 electron configuration, at least one of the ligands has to dissociate from the ruthenium, which can be realized by the addition of hydrochloric acid. Nevertheless high amounts of acid from up to 20 mol% were used for **XXXI**.[72] Based on a report of Grubbs[73], Slugovc and group synthesized second generation tris(pyrazoylyl)borate complexes feature a similar structure to those of **XXXI** and investigated their metathesis activity. Interestingly, those initiators indeed showed latent behavior, but were in contrast to **XXXI** also easily activated by means of heat.[74] At this point it merits mentioning that the thermal activation of **XXXI** was not investigated in this report.

---

[70] C. E. Diesendruck, O. Iliashevksy, A. Ben-Asuly, I. Goldberg, G. N. Lemcoff, *Macromol. Symp.* **2010**, *293*, 33-38.

[71] B. Allaert, N. Dieltiens, N. Ledoux, C. Vercaemst, P. Van der Voort, C. V. Stevens, A. Linden, F. Verpoort, *J. Molec. Catal. A: Chem.* **2006**, *260*, 221-226.

[72] M. S. Sanford, L. M. Henling, R. H. Grubbs, Organometallic, **1998,** *17,* 5384-5389.

[73] M. S. Sanford, J. A. Love, R. H. Grubbs, *Organometallics* **200**1, *20*, 5314.

[74] D. Burscher, B. Perner, K. Mereiter, C. Slugovc, *J. Organomet. Chem.*, **2006**, *691*, 5423–5430.

Another concept for acid triggerable complexes is the general formula **C**, featuring two bidentate ligands. Very often the chelation occurs via N-, O- chelating ligands. The first reports of complexes with this kind of structure have been done by the group of Fröhlich in 2005.[75] They reported one initiator bearing two 2-pyridinecarboxylate ligands (**XXXII**). 5 years later in 2010, Grubbs and co-workers performed the same reaction and obtained two different derivatives, both exhibiting two 2-pyridinecarboxylate ligands. The two different derivatives were ascribed to pre-catalysts bearing the same ligands, but a different geometry of those around the ruthenium.[76] Both groups proved that upon the addition of acid, especially hydrochloric acid, the complexes can be converted into a metathesis active form. Performing NMR experiments, the group of Grubbs showed, that the catalysts gets activated via a re-substitution of the anionic ligands against chlorines forming the same active species as the applied starting material. Interestingly, one of the two derivatives shows an HCl dependency, whereas the other doesn't.

In this context it is also noteworthy that the activation can also be initiated via the addition of HCl releasing agents or Lewis-acids as the co-catalyst, whereas $AlCl_3$, CuCl or trialkylsilylchlorides have been applied.

XXXI   **XXXII**
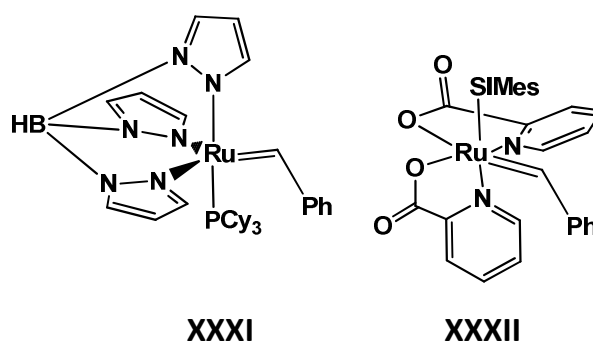
Figure 19: Acid triggerable metathesis initiators

[75] F. E. Hahn, M. Paas, R. Fröhlich, *J. Organomet. Chem,.* **2005**, *690*, 5816-5821.
[76] J. S. M. Samec, B. K. Keitz, R. H. Grubbs, *J. Organomet. Chem,.* **2010**, *695*, 1831-1837.

2.4.3 UV-light Triggered Metathesis Initiators

The very first publication about photo-induced metathesis was already published in 1975 by Dubois and Mc Nelis using ill-defined tungsten hexacarbonyl complexes.[77] The first reports on well-defined ruthenium systems initiating photocatalysed ROMP (PROMP) were made in 1995 by the group of Mühlenbach.[78] In their work, they introduced three different main types of photochemically triggerable precatalysts: η^6-arene sandwich complexes, half sandwich complexes and nitrile complexes. Both kinds of sandwich complexes were only activated by the means of UV-irradiation, whereas the nitrile complex showed also a slight tendency to thermal activation. Overall, polymers synthesized with these catalysts exhibit high molecular weights and broad molecular weight distributions. The proposed mechanism for the initiation proceeds through a gradual photodissociation of the arene ligand, followed by solvation of the photochemically excited molecule.

Sandwich complexes   **Half - sandwich complexes**   **Nitrile complexes**
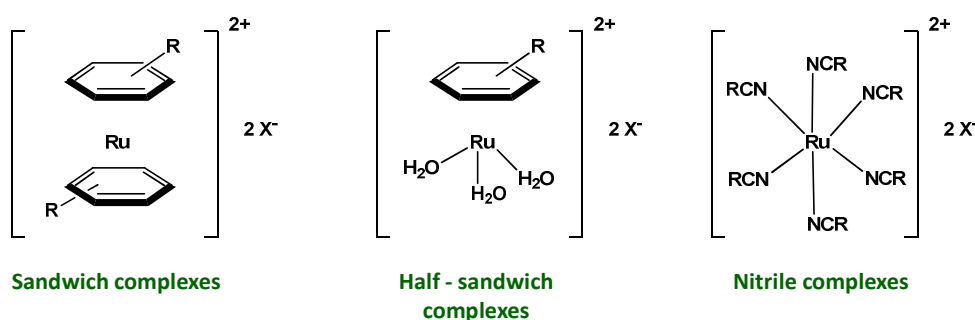
Figure 20: First examples of ruthenium based PROMP catalysts

Since then, several other systems have been invented, all of them possessing at least a half sandwich structure. For the aromatic system cymene was used very often.[79] A general drawback of all of these systems was the noticeable ROMP activity at elevated temperatures, even when they were not illuminated with light. Therefore, Buchmeiser

---

[77] (a) P. Krausz, F. Garnier, J.-E. Dubois, *J. Am. Chem. Soc.*, **1975**, *97*, 437-438; (b) A. Agapiou, E. J. Mc Nelis, *Organomet. Chem.*, **1975**, *6*, 187a.

[78] T. Karlen, A. Ludi, A. Mühlenbach, P. Bernhard, C. Pharisa, *J. Polym. Sci., Part A: Polym. Chem,* **1995**, *33*, 1665-1674.

[79] (a) A. Hafner, P. Van der Schaaf, *Angew. Chem., Int. Ed.,* **1997**, *36*, 2121-2124. (b) M. Picquet, C. Bruneau, P. H. Dixneuf, *Chem. Commun.* **1998**, *20*, 2249-2250.(c) J. Huang, E. D. Stevens, S. P. Nolan, J. L. Petersen, *J. Am. Chem. Soc.* **1999***, 121*, 2674-2678. (d) M. Scholl, S. Ding, C. W. Lee, R. H. Grubbs, *Org. Lett.* **1999**, *1*, 953-956.

emerged the concept of substituting the aromatic *p*-cymene against phenylisonitrile and the chloride ligands against trifluoroacetates.[80] Nevertheless when temperatures over 40°C were applied these systems also initiated the polymerization reaction. The breakthrough in this field came in 2008 with the invention of pre-catalysts **XXXIII**.[81]
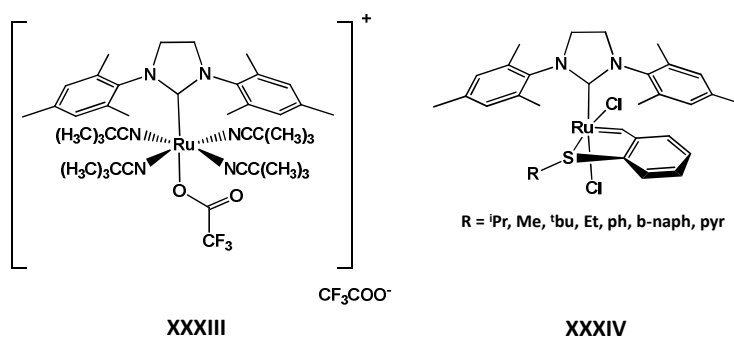

Figure 21: Thermally stable PROMP initiator

Another very interesting light induced complex was established by Lemcoff and his group. They synthesized a latent *cis* sulfur chelating complex (**XXXIV**), which isomerizes via UV light into its active *trans* isomer. Polymerization is subsequently initiated by this *trans* complex. By simple heating of the *trans* complex, the inactive *cis* isomer can be regenerated. This provides an effective "swicht-on – swicht-off" complex combining two different triggers.[82]

---

[80] Y. Zhang, D. Wang, P. Lönnecke, T. Scherzer, M R. Buchmeiser, *Macromol. Symp.* **2006**, *236*, 30-37.

[81] D. Wang, K. Wurst, W. Knolle, U. Decker. L. Prager, S. Naumov, M. R. Buchmeiser, *Angew. Chem., Int. Ed.*, **2008**, *47*, 3267-3270.

[82] A. Benz-Asuly, E. Tzur, C. E. Diesendruck, M. Sigalov, I. Goldberg, G. N. Lemcoff, *Organometallics* **2008**, *27*, 811-813. (b) T. Kost, M. Sigalov, I. Goldberg, A. Ben-Asuly, G. N. Lemcoff, *J. Organomet. Chem.* **2008**, *693*, 2200-2203. (c) C. E. Diesendruck, Y. Vidavsky, A. Ben-Asuly, G. N. Lemcoff, *J. Polym. Sci., Part A: Polym. Chem.* **2009**, *47*, 4209-4213; (d) C. E. Diesendruck, O. Iliashevxky, A. Ben-Asuly, I. Goldberg, G. N. Lemcoff, *Macromol. Symp.* **2010**, *293*, 33-38.(e) E. Tzur, A. Szadkowka, A. Ben-Asuly, A. Makal. I. Goldberg, K. Wozniak, K. Grela, G. N. Lemcoff, *Chem.-Eur. J.* **2010***, 16*, 8726-8737.

2.4.4 *Cis* Initiators

Cis complexes are already known since several years.[83] In general the thermodynamical *cis* product is known to exhibit a reduced activation in comparison with its kinetic *trans* isomer.[84] Several reports have proved this inactivity of *cis* complexes especially at room temperature.[64,82,85]

In 2011 Slugovc et al. elucidated the isomerization mechanism experimentally closer and reported a cationic intermediate which occurs during the isomerization of the inactive *cis* to the active *trans* species.[86] Their research was done by studying a *cis* dichloro complex bearing a chelating ester substituted benzylidene ligand. It was also proved, that the cationic intermediate is not the active species itself by simple exchanging the small chloride counterion of intermediate B against a bulky PF_6^- counterion. It showed, that this species was not active in olefin metathesis any more, and hence it could be assumed, that the re-coordination of the chlorine leading to the *trans* species is indispensable for the active catalyst.
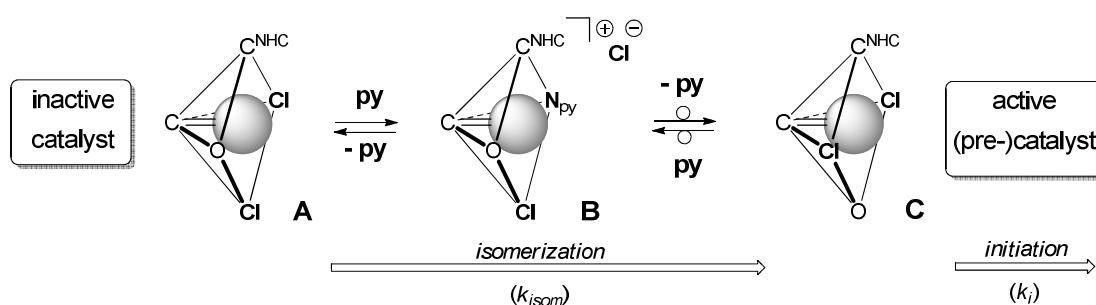
Figure 22: Proposed activation mechanism of *cis*-dihalide-species

[83] a) S. M**.** Hansen, F. Rominger,M. Metz, P. Hofmann, *Chem. Eur. J.* **1999**, *5*, 557-566. b) S. M. Hansen, M. A. O. Volland, F. Rominger, F. Eisenträger,P. Hofmann, *Angew. Chem. Int. Ed.* **1999**, *38*, 1273-1276. c) M. A. O. Volland, C. Adlhart, C. A. Kiener, P. Chen,P. Hofmann, *Chem. Eur. J.* **2001**, *21*, 4621-4632.

[84] (a) C. Lexer, D. Burtscher, B. Perner, E. Tzur, G. N Lemcoff, C. Slugovc*, J. Organomet. Chem.*, **2011**, *696*, 2466-2470. (b) X. Bantreil, T. E. Schmid, R. A. M. Randall, A. M. Z. Slawin, C. S. J. Cazin, *Chem. Commun.*, **2010**, *46*, 7115-7117.

[85]T. Ung, A. Hejl, R. H. Grubbs, *Organometallics*, 2004, *23*,5339. (b) M. Barbasiewicz, A. Szadkowska, R. Bujok, K.Grela, *Organometallics*, **2006**, *25*, 3599.

[86] M. Zirngast, E. Pump, A. Leigeb, J. H. Albering, C. Slugovc, *Chem. Commun,* **2011**, *47*, 2261–2263.

Just very recently the same group proposed a second possible mechanism for the *cis/trans* isomerization.[87] Studying the lability of the anionic ligands in *cis* dichloro-complexes via a chlorine exchange against iodenes, a high lability of the anionic ligand *trans* to the NHC, but a very low lability of the second anionic ligand *trans* to the chelating moiety was found. When the thermodynamic stability of the mixed *cis* complexes with one chlorine and one iodine was investigated closer, the formation of the dichloro-*trans*, the diiodo-*trans* and a mixed chloro/iodo *trans* species were observed. Regarding this results a second isomerization mechanism occurring via a bridged dimeric ruthenium species was proposed leading to the different *cis* and *trans* products.
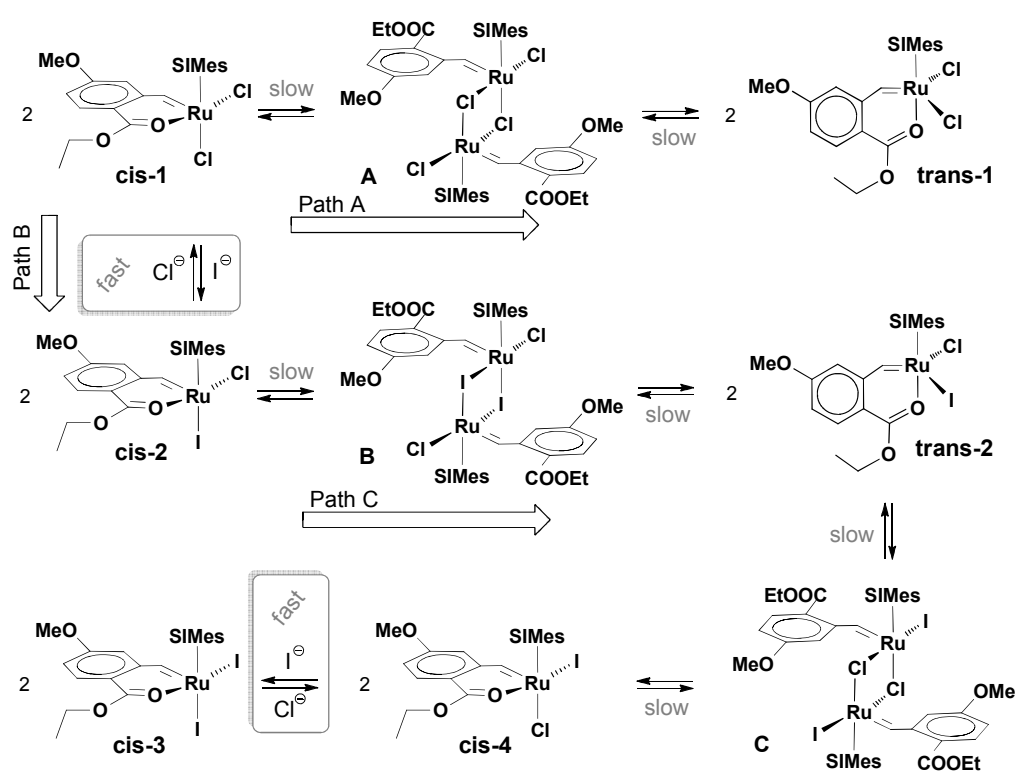
Figure 23: Proposed isomerization mechanism proceeding via a dimeric ruthenium species

Concluding, the results of Slugovc and several other groups have shown that the *cis* complexes are metathetically inactive and can therefore be considered to be latent. Other than thermally or acid switchable initiators, not a certain trigger leads to the formation of

[87] E. Pump, R. Fischer, C. Slugovc, *Organometallics,* dx.doi.org/10.1021/om300785t.

the active species, but a natural equilibrium which always happens between *cis* and *trans* catalysts especially in solution. By means of heat, this equilibrium can be shifted in the direction of the more active *trans* product.

3 ANIONIC LIGAND EXCHANGE

The following chapter including all subitems deals in some context with the exchange or the influence of the anionic ligands of olefin metathesis ruthenium initiators. Diverse forms of anionic ligands, such as chelating and none chelating substituents are addressed within this chapter. Generally the anionic ligands determine the assigned configuration of ruthenium complexes, defined by a *cis* or a *trans* orientation to each other. Metathesis initiators with these different orientations of the anionic ligands exhibit different characteristics, such as metathesis activity and lability of the ligands themselves. Hereinafter, only complexes with a *trans* orientation are discussed. Even though many results about the exchange and the influence of the anionic ligands have been published so far, they are still the less studied and above all the less understood ligands in ruthenium complexes.

3.1   Initiators with Chiral Anionic Ligands

Chiral anionic ligands have already been used as chiral substituents in ruthenium initiators for enantioselective metathesis reactions. Their main benefit is that they stay attached to the ruthenium center during the whole metathesis cycle. Nevertheless, they are in close distance to the ruthenium center and can therefore induce the chiral information. In the following, the synthesis of such chiral initiators via anionic ligands is addressed. As the starting complex the commercially available Hoveyda initiator (**Hov**) was used. **Hov** is beneficial due to its characteristic carbene proton at 16.56 ppm (CDCl$_3$) which makes the monitoring of the reactions very easy.

The first attempts to synthesize ruthenium initiators with chiral anionic ligands were done with a chiral amino acid, namely valine. As for anionic ligand exchanges the presence of a base is inevitable, the most efficient base was investigated. Therefore 1 eq of **Hov** was reacted with 15 eq valine and approximately 20 eq of several bases, namely Li$_2$CO$_3$, Na$_2$CO$_3$, K$_2$CO$_3$, Cs$_2$CO$_3$, Tl$_2$CO$_3$ and CU$_2$O in DCM and stirred overnight. The undissolved residues were filtered and ^{1}H NMR spectra were recorded. Li$_2$CO$_3$, Na$_2$CO$_3$, K$_2$CO$_3$, Cs$_2$CO$_3$ are all selected from the first group of the periodic table of the elements and therefore possess generally similar characteristics, but an increasing cationic radius. Additionally, Tl$_2$CO$_3$ and CU$_2$O were added in the series of experiments. From literature they are known to be suitable for anionic ligand exchange reactions.[59,88]
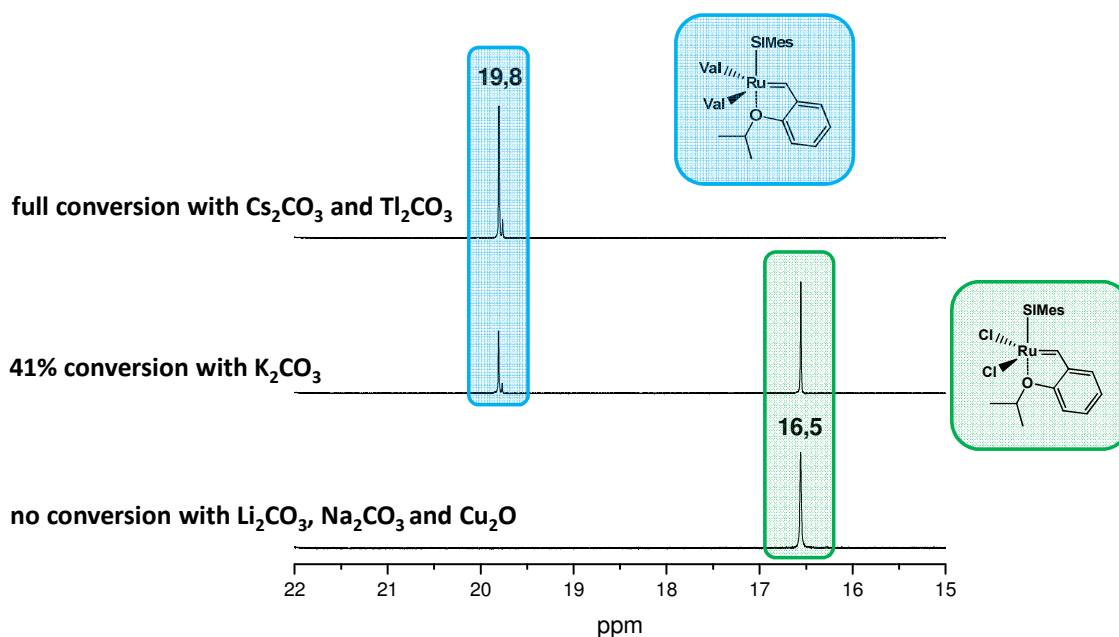
Figure 24: Evaluation of best reaction conditions

The best conversions were accomplished using Cs_2CO_3 and Tl_2CO_3. Even though Tl_2CO_3 gave good and fast conversions, it wasn't used for any further reactions due to its toxicity. From the experimental series it can be deduced that conversions mainly depend on the radius of the cationic species. The bigger the cation, the better is the converting, establishing a reactivity from Cs_2CO_3, Tl_2CO_3 > K_2CO_3 >> Li_2CO_3, Na_2CO_3, CU_2O. Surprisingly, CU_2O gave no conversion in the test reaction, even though it was used in some anionic ligand exchanges described in literature.[88] Silver salts were not used due to the ancillary reaction step of preparing the silver substrate salt, which is commonly done. *In situ* reactions with Ag_2O are not very usual.

With the best reaction conditions in hand, **Hov** was reacted with an excess of valine and an excess of Cs_2CO_3 in DCM at RT. The remaining undissolved Cs_2CO_3, valine and due to the chloride exchange formed CsCl were filtered and ^{1}H NMR spectra were recorded. Unfortunately, the reaction with valine as the anionic ligand always led to the formation of two different products, as can be deduced from the presence of two carbenes at 19.80 ppm and 19.76 ppm, respectively. The ratio of the two different species always accounted for

---

[88] J. S. M. Samec, R. H. Grubbs, *Chem. Commun.*, **2007**, *27*, 2826–2828.

1:0.2 independently of reaction time, temperature or other parameters were altered. Separation of the complexes via column chromatography or precipitation failed. Due to very bad resolved NMR spectra, an exact determination of the actual number of valines attached to the ruthenium or of structural assignments was hard to realize. Nevertheless, the large downfield shift in the proton NMR spectra from 16.56 ppm of starting material **Hov** to 19.80 ppm of the valine substituted initiator can be probably ascribed to a chelation of the carboxylic oxygen or the amino group to the ruthenium center.

Due to the apparent impossibility to obtain clean and defined valine substituted initiators, other substrates were used for the synthesis of chiral initiators. Therefore, enantiomerically pure, commercially available substrates lacking a nitrogen atom were investigated. Particularly, (*S*)-(-)-bromopropionic acid (**L1**) and an acetylated *L*-lactic acid (**L2**) were used as test substrates. The lactic acid was applied in its acetylated form, to avoid an interaction of the second free hydroxyl group in the molecule with the ruthenium center. The acetylation was done using acetyl chloride in acetic acid.
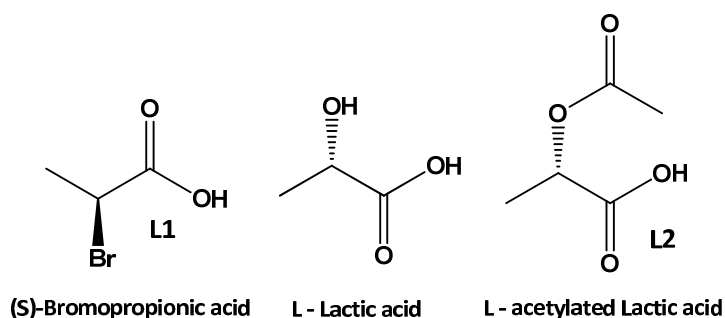
Figure 25: Anionic ligands for the synthesis of chiral initiators

Adopting the most efficient reaction conditions from the valine conversion, where an excess of base with respect to the acid was used, for **L1** and **L2** yielded almost no conversions and a high amount of decomposition product. Several repetitions or variation of the base did not lead to any improvements. Hence the influence of the acid and the base was investigated more detailed.

3.1.1   Acid/Base Influence

To evaluate if and to which extend acid or base influences a ruthenium initiator, polymerization test series with varying additives were performed. Within every single series a benchmark polymerization without any additives for a better comparison of the data, a polymerization using 100 eq of acid with respect to the initiator and a polymerization with 100 eq of acid and 150 eq of K_2CO_3 or Cs_2CO_3, respectively were done. Several test series with diverse initiators (**Hov** and **M31**), different acids, namely 2-chloro benzoic acid, acetic acid, trifluoroacetic acid and valine and two different monomers, namely *endo, exo*-dimethyl bicyclo[2.2.1]hept-5-ene-2,3-dicarboxylate (**Mon1**) and bicyclo-[2.2.1]hept-5-ene-2,3-diphenylketon (**Mon2**) were performed.

The results of these test series are shown in Figure 26. Generally bases seem to influence the polymerizations more than acids, no matter which base is applied. The greatest influence on the polymerization has the combination of acid and base together. Here it has to be pointed out, that it is not clarified if the acid and the base perform a halide exchange at the initiator, leading to a less active complex or, if both additives simply destroy the initiator yielding a none metathesis active decomposition product. In all cases, the addition of acid and base drops the conversion and increases the time until full conversion is reached, if full conversion is reached at all. M_n values either increase what simply indicates that a less metathesis active species is present in the reaction solution, or decrease evincing the decomposition of the initiator. One way or another, the presence of higher amounts of base in a reaction solution with a ruthenium complex is not beneficial for the desired reaction.

Interestingly these facts are not valid for the before used test reaction of **Hov** with valine and a base. In this case neither the conversion nor the molecular weight or the reaction time changed.
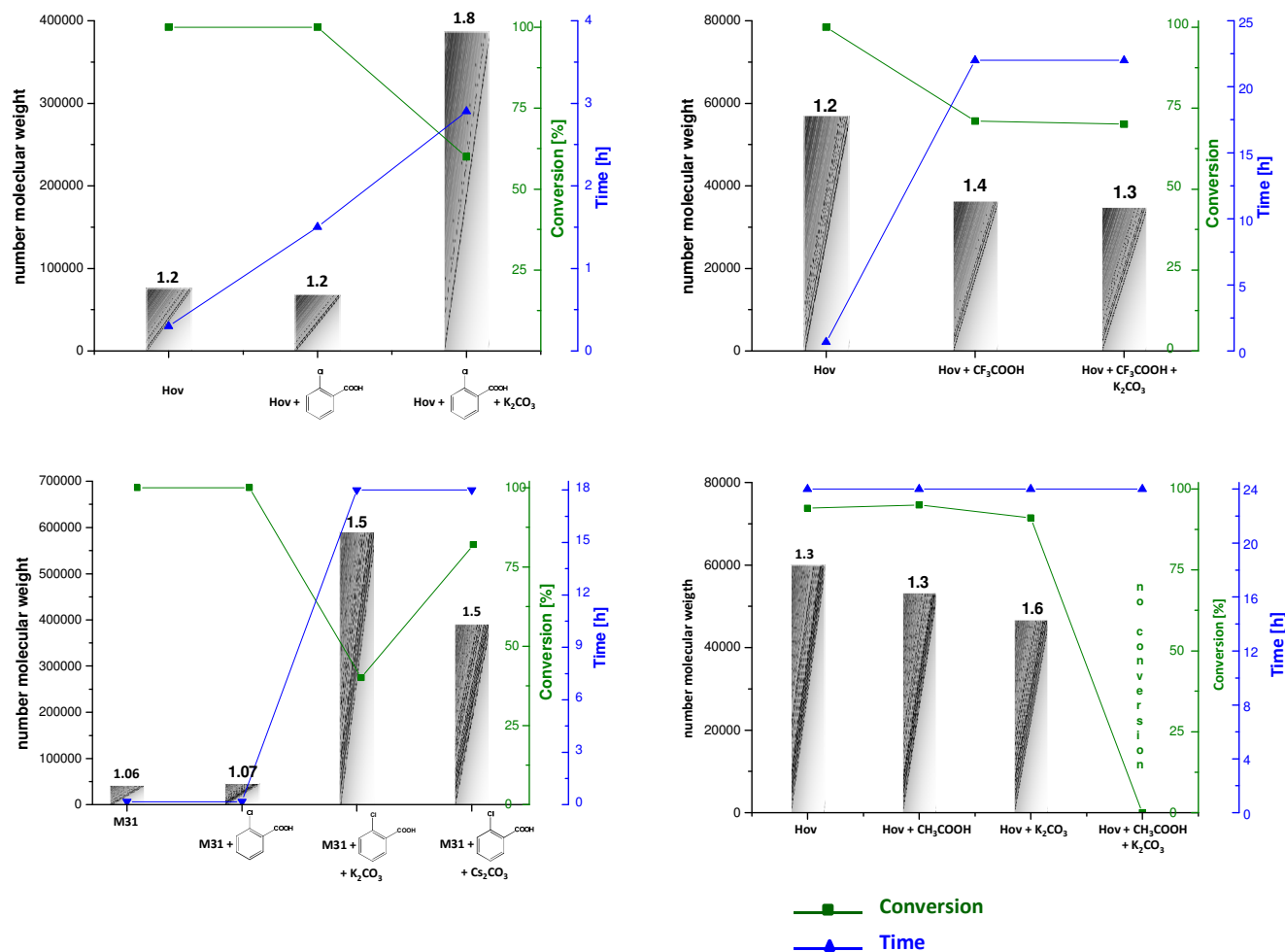
Figure 26: Influence of acid and base on the polymerization behavior of Hov and M31; Mon1 was used for the thirst three test series and Mon2 was used for the fourth series depicted in the bottom right corner

With the knowledge of the test polymerizations of chapter 3.1.1. in hand, the anionic ligand exchange using **L1** was performed with adapted reaction conditions. **Hov** was reacted for two hours with an excess of **L1** (10-20 eq) and a smaller amount of K_2CO_3 with respect to **L1** (1-10 eq) in DCM at room temperature. The reaction was accompanied by a color change from green to violet or brownish. As before, the undissolved residues were filtered and a proton NMR spectrum was recorded. This reaction conditions led to the formation of three new substituted complexes with their characteristic carbene peaks at 17.23 ppm, 16.96 ppm and 16.87 ppm (in $CDCl_3$), respectively in a ratio of 1:0.14:0.07. After a closer examination of the NMR spectrum, the carbene at 17.23 ppm was assigned to the disubstituted and the signals at 16.96 and 16.87 ppm to the monosubstituted complexes. In order to obtain a single complex, the reaction was repeated several times with small variations of the reaction parameters such as reaction time, temperature, solvent, ratio of K_2CO_3 etc. In the course of these reactions, the formation of two additional carbene peaks at 16.48 ppm and 16.40 ppm was observed. The complex with the carbene at 16.48 was assigned to the monobromo Hoveyda and the carbene at 16.40 ppm to the dibromo Hoveyda.[89]
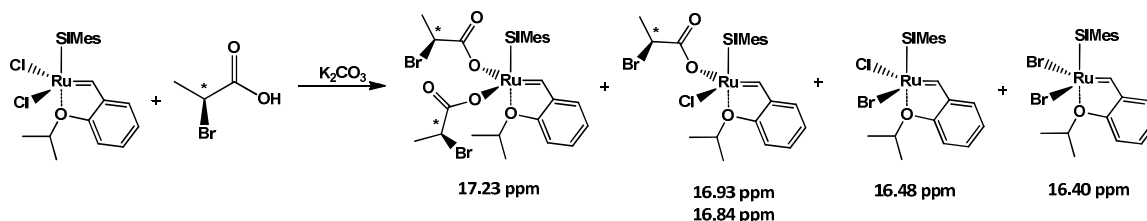
Scheme 2: Conversion of L1 with Hoveyda

---

[89] J. Wappel, C. A. Urbina-Blanco, M. Abbas. J. H. Albering, R. Saf, S. P. Nolan, C. Slugovc, *Beilstein J. Org. Chem.* **2010**, *6*, 1091-1098.

Table 5: Overview of anionic ligand exchange with L1 using different reaction parameters; samples are measured in CDCl$_3$

Base	Additives	Temp. [°C]	Time [h]	Hov (16.56) [%]	17.23 [%]	16.96 [%]	16.87 [%]	16.48 [%]	16.40 [%]
-	-	RT	4	100	-	-	-	-	-
K$_2$CO$_3$ (20 eq)[a]	-	RT	2	-	82[a]	12	6	-	-
K$_2$CO$_3$ (5 eq)[a]	-	RT	16	2	68	27	3	-	-
K$_2$CO$_3$ (2 eq)[a]	-	RT	2	8	46	40	6	-	-
K$_2$CO$_3$ (5 eq)[a]	-	40	1	7	60	33			
[a]	ext. H$_2$O	-	-	17	20	38	9	4	
[a]	3µL H$_2$O		120[c]	38				21	
Cs$_2$CO$_3$ (2 eq)[a,b]	-	RT	2.5	6	42	38	5	2	
[a,b]			216[c]	36	-	11	-	17	3
K$_2$CO$_3$ (3 eq)[d]		60	2	18	-	-	-	40	42

a) reactions are performed in DCM

b) if the carbenes do not devote fo 100 %, the missing percents belong to a decomposition product

c) product was left in the NMR tube and measured after a certain timeframe

d) reactions are performed in THF

The conclusions of all reactions using different reaction conditions can be summarized as follows:

- the ratio of di- to monosubstituted complexes cannot be influenced by the reaction time; longer reaction times do not significantly lead to higher ratios of disubsituted products;
- the ratio of K$_2$CO$_3$ does not influence the reaction dramatically; stoichiometric amounts of base are sufficient to achieve full conversion; still, the addition of base is crucial for the reaction; without base no conversion takes place;
- the ligands are not bound very tightly; the addition of a chloride source or the purification over aluminum oxide (Al$_2$O$_3$) leads to the re-formation of **Hov** complex;
- anionic ligand exchange does also occur amongst the initiators;[90]
- higher temperatures lead to an increase of bromosubstituted complexes; at 60°C solely the bromo products are formed;
- the addition or the extraction with water favor the formation of the mono- and the dibromo species, respectively;

---

[90] K. Tanaka, V. P. W. Böhm, D. Chadwick, M. Roeper, D. C. Braddock, *Organometallics* **2006**, *25*, 5696-5698.

- the acid substituted complexes are not very stable in solution and decompose quite rapidly;

The formation of the bromo substituted complexes was a surprising observation and was investigated closer in chapter 3.1.2.

Due to the unexpected and interfering side reaction of the anionic ligand exchange with **L1**, the adapted reaction conditions were used for the conversion of **Hov** (1 eq) with **L2** (10 eq) in the presence of K_2CO_3 (2 eq) in DCM at room temperature. The reaction proceeded without any unexpected side reactions but unfortunately did not reach completion. Nevertheless, again three different products with characteristic carbene peaks at 17.18 ppm, 16.95 ppm and 16.87 ppm, respectively were formed. At room temperature, the reaction seemed to be hampered and conversion of **Hov** was by far not complete. Therefore the reaction temperature was increased to 60°C and the solvent changed to dry and degased THF. As a result of the temperature increase, the reaction proceeded with full conversions always leading to the three mentioned complexes. The three complexes were assigned to belong to the disbustituted complex **1** (17.18 ppm) and the two monosubstituted complexes **2a** and **2b** (16.92 ppm and 16.87 ppm) in a ratio of 1:0.1:0.04. The true origin of these two different monosubstituted species is not proved yet but they possibly belong to a chelating (chelation can occur via the carbonyl oxygen of **L2**) and a non-chelating species.
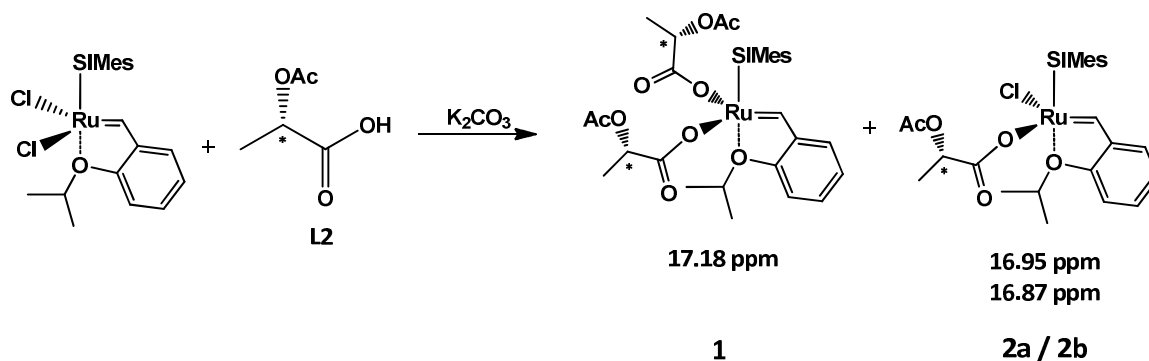
Scheme 3: Synthesis of L2 substituted complexes

Table 6: Overview of anionic ligand exchange with L2 using different reaction parameters; samples are measured in CDCl$_3$

Base	Temp. [°C]	Time [h]	Hov (16.56) [%]	17.19 [%]	16.96 [%]	16.88 [%]	10.5 [%]
K$_2$CO$_3$ (3 eq)[a]	RT	18	33	11	38	18	-
K$_2$CO$_3$ (3 eq)[b]	60	1	-	66	1	8	25
K$_2$CO$_3$ (1.8 eq)[b]	60	2	11	49	16	8	16

a) reactions are performed in DCM

b) reactions are performed in THF

Again several reaction conditions and purification methods were tested, leading to the following perceptions:
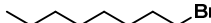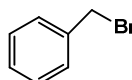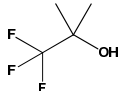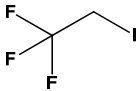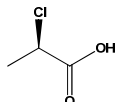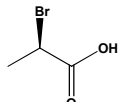
- reactions at RT do not lead to any decomposition products;
- reactions at RT do not yield full conversion;
- at RT the main products are the two mono-substituted initiators;
- reactions at 60°C forward the decomposition of the catalyst;
- at 60°C the main product is the di-substituted initiator;
- increasing amounts of acid and a reaction at 60°C yield more than 85 % of the disubstituted product;
- separation or purification of the three formed complexes via column chromatography was not possible due to similar R$_f$ values; the separation via other methods such as precipitation also failed;

As it was not possible to separate the di- and the monosubstituted complexes from each other, it was decided to investigate the ability of the complexes to perform an *in situ* chiral metathesis reaction (see chapter 3.1.3).

3.1.2 Halide Transfer in Ruthenium Complexes

Due to the unexpected observation of the transfer of a bromine from a substrate, namely the acid **L1**, to the ruthenium complex, this halide exchange reaction was investigated in more detail. Several halide containing substrates and solvents were reacted with an initiator, namely **Hov** or **I₂-Hov**, at elevated temperatures, either with an additional solvent as in case of the halide exchanges with substrates or neat as for the halide exchange with solvents. ^{1}H NMR spectra were recorded periodically or after a certain time period and the formation of the halide exchanged product was determined. NMR spectra were recorded in benzene d_6 and not in CDCl$_3$ to avoid a falsification of the results by a re-exchange of chlorides from chloroform to the complex. The conversion was determined by integrating the carbene peaks of the different complexes. The abbreviation **I₂-Hov** refers to a diiodo-Hoveyda catalyst. **Br-Hov** refers to a Hoveyda catalyst with mixed anionic ligands bearing on bromine and one chlorine ligand. **I-Hov** refers to **Hov** with one iodine and one chlorine.

Table 7: Halide transfer of bromine from several brominated or fluorinated substrates to Hov and from chlorinated substrates to I₂-Hov

Substrate	Time [h]	Solvent	Temperature [°C]	Cl₂-Hov [%]	Br-Hov [%]	Br₂-Hov [%]
	72	DCE	60	18	49	33
	24	THF	60	26	51	23
	48	THF	60	-	44	42

Substrate	Time [h]	Solvent	Temperature [°C]	Cl₂-Hov [%]	F-Hov or I-Hov [%]	Br₂-Hov or F₂-Hov [%]
	24	THF	60	100	no conversion	
	48	THF	50	100	no conversion	

Substrate	Time [h]	Solvent	Temperature [°C]	I₂-Hov [%]	I-Hov [%]	Cl₂-Hov [%]
	69	benzene	60	83	17	

Substrate	Time [h]	Solvent	Temperature [°C]	I₂-Hov [%]	I-Hov [%]	Br₂-Hov [%]
	24	benzene	60	60	34	6

The first complex in the table is always the complex from which the reaction was started

The halide transfer reactions (summarized in Table 7) showed that the substrate abstraction proceeds more smoothly when the sterically more bulky bromide is abstracted. Chlorines are more difficult to exchange. Therefore it is not very surprising, that the even smaller fluorine could unfortunately not be exchanged. Bizarrely in case of the conversion of 2,2,2-trifluoroethyl iodide neither the fluorine nor the iodine could be exchanged. The fact that the fluorine was not exchanged is not very surprising, but the fact that the iodine could not be exchanged is contrary to the before mentioned observations that bigger halides are exchanged more easily.

The halide exchanges done in halogenated solvents revealed the same picture than the ones performed with substrates. The bigger the halide, the faster is the exchange, no matter if the big halide is attached to the complex, or if it is in the solvent. The fastest exchange occurs if an exchange from the diiodo complex (**I$_2$-Hov**) to the bromo complex (**Br$_2$-Hov**) is performed. Reacting the same solvent, more exactly dibromomethane, with the diiodo- and the dichloro complexes at 90°C showed, that the exchange is about 30 folds faster with the bulky iodines.
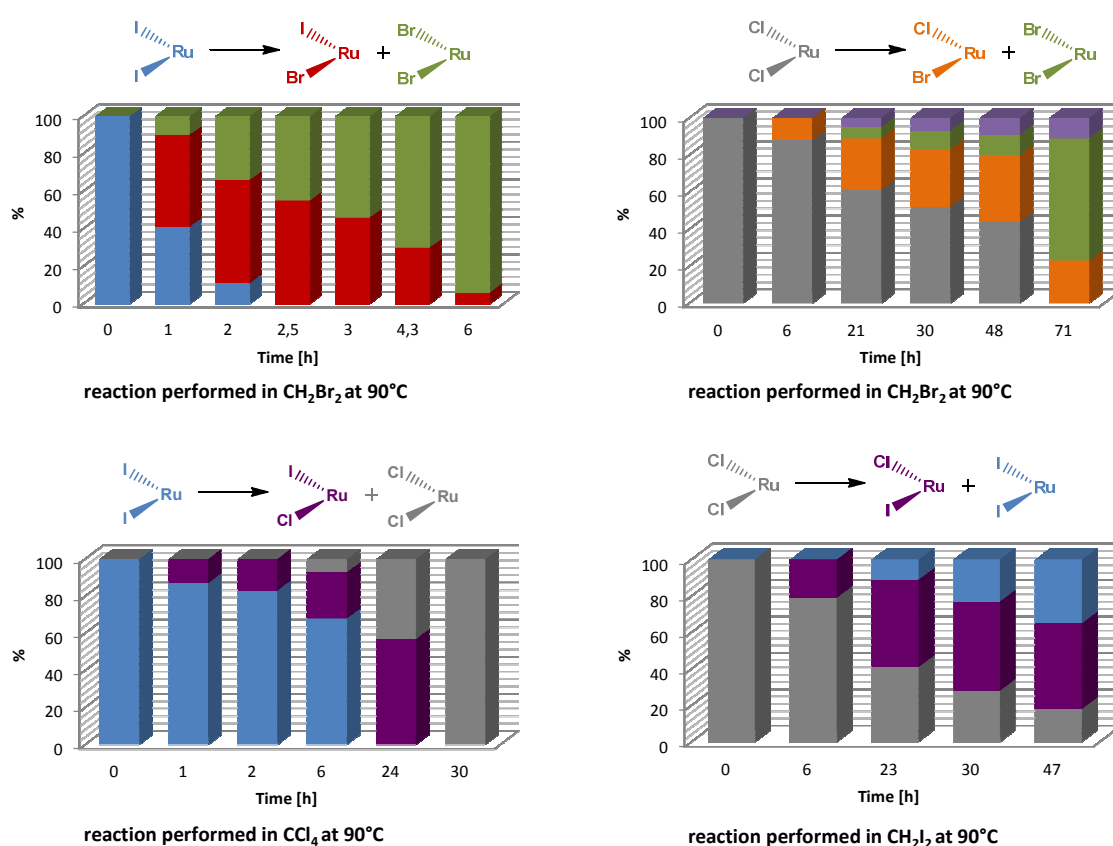
Figure 27: Halide transfer from solvents; the lila parts in the image on the right side of the top belong to a decomposition product

On the other hand, if the iodines in an **I$_2$-Hov** are exchanged against chlorines, the reaction is about 4 folds slower. Here it has to be pointed out, that this chlorine exchange was done

under different reaction conditions. Due to the fact, that DCM cannot be heated to 90°C, the reaction was performed using the four times halogenated carbon tetrachloride instead of the dihalogenated solvent. Several experiments have shown that higher halogenated solvents tend more to halide abstraction, lower halogenated ones. Nevertheless, the circumstance that bigger halides are more easily exchanged than smaller ones shows a more pronounced effect on the exchange than the fact of the solvent substitution. Summarized the reactivity trend of I>Br>Cl>F has been proofed with both reaction types performed.

After the reactivity tests, the question about the reaction mechanism arose. As proposed in several publications dealing with ATRP reactions using ruthenium based initiators such as **G1**, the reaction mechanism happens via a substrate radical and a Ru^{III} species bearing three halides. The hypothetical reaction pathway is shown in Scheme 4.[91] Though it merits mentioning that in many of those papers a second co-catalyst such as Al(O^{i}Pr)$_3$ was applied to initiate the ATRP reaction successfully.
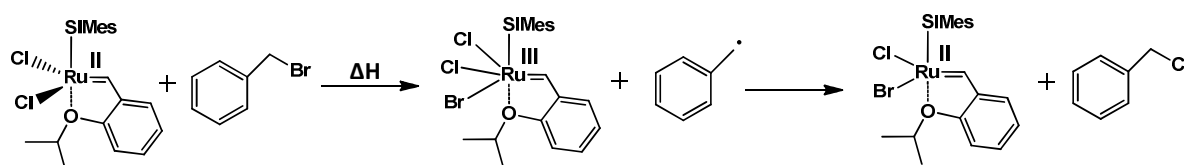
Scheme 4: Possible pathway for halide exchange

To clarify if in case of our halide exchange the same reaction mechanism occurs we performed two different experiments. Firstly we investigated if the addition of the stable radical TEMPO is able to suppress the halide exchange reaction. Unfortunately, this was not the case and halide exchange occurred again, even though to a bit smaller extend than without TEMPO. The second experiment was, to find an evidence for the presence of radicals using NMR technique. Again no hint for the presence of radicals could be found though. Hence, the exact mechanism of the halide exchange still remains unclear.

Another question under investigation was, if the reaction could be performed catalytically. Therefore in a NMR tube, **Hov** was reacted with 100 eq of benzylbromide and 100 eq of dichloroethane in benzene d$_6$ over five days. In this case, the halide exchange was not only monitored by the carbene signals of the complexes, but also by the signal of the CH$_2$ group of the benzylbromide (3.96 ppm) proportional to the newly formed benzylchloride (4.07 ppm). The idea was that dichloroethane acts as a chlorine sources, re-forming the dichloro complex **Hov**, which subsequently can undergo a new halide exchange until the whole benzylbromide is converted to benzylchloride. The reaction was monitored after 24 h, 48 h

---

[91] (a) T. Nishikawa, T. Ando, M. Kamigaito, M. Sawamoto, *Macromolecules* **1997**, *30*, 2244-2248. (b) T. Ando, M. Kamigaito, M. Sawamoto, *Tetrahedron* **1997**, *53*, 15445-15457.

and 144 h. After 24 hours, about 1 percent of the benzylbromide was converted to the corresponding chloride and all three complexes, namely **Hov**, **Cl/Br-Hov** and **Br₂-Hov** were present in the reaction solution. After 48 hours, 1.7 % of the benzylbromide were converted and no dichloro complex was visible in the spectra. After 144 hours exactly 2 % of the benzylbromide were converted to benzylchloride and solely **Br₂-Hov** could be detected. Hence the reaction was considered not to be catalytical.
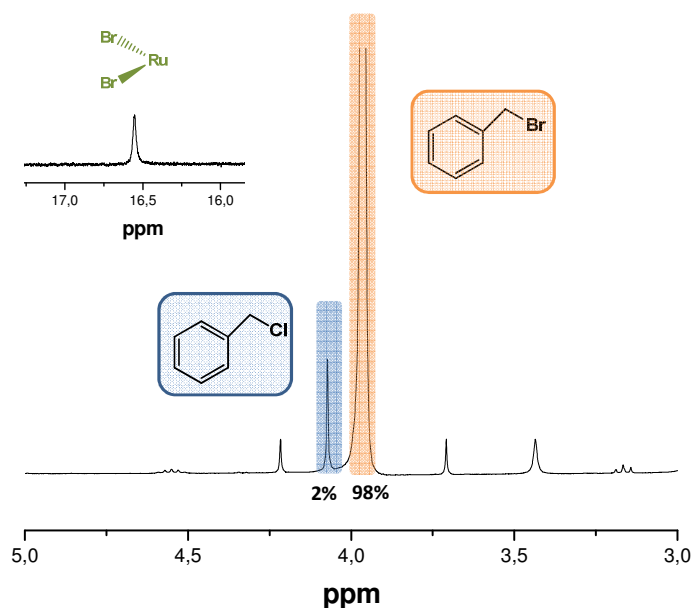
Figure 28: Halide exchange with benzylchloride

3.1.3   Chiral Test Reactions

In order to evaluate the ability of **1** and **2a/2b** to perform an enantioselective metathesis reaction, an Acyclic Ring Opening Cross Metathesis reaction (AROCM) was conducted. For the AROCM reaction, the selection of the two reactants is important, since both influence the outcome of the reaction significantly. The ring opened substrate of choice used for the benchmark reaction was the norbornene derivative *endo*-bicyclo[2.2.1]-2-heptene-5,6-dicarboxylic acid anhydride (**S1**), a strained bicyclic molecule. **S1** is a suitable candidate for an AROCM reaction because it is reactive enough to be opened by the ruthenium initiator, but it is not too reactive and subsequently can undergo the cross metathesis reaction with a convenient crosspartner.[54] More reactive substrates such as for example the unsubstituted norbornene, tend to form oligomers instead of the ring opened cross product. For the second reactant, namely the crosspartner, styrene (**S2**) was chosen. Via the ratio of the crosspartner to the ring opened substrate, the equilibrium of the reaction can be shifted to

the desired AROCM product. Noteworthy, the excess of **S2** leads to the formation of a styrene dimer (stilben) which has to be removed after the AROCM reaction is completed.
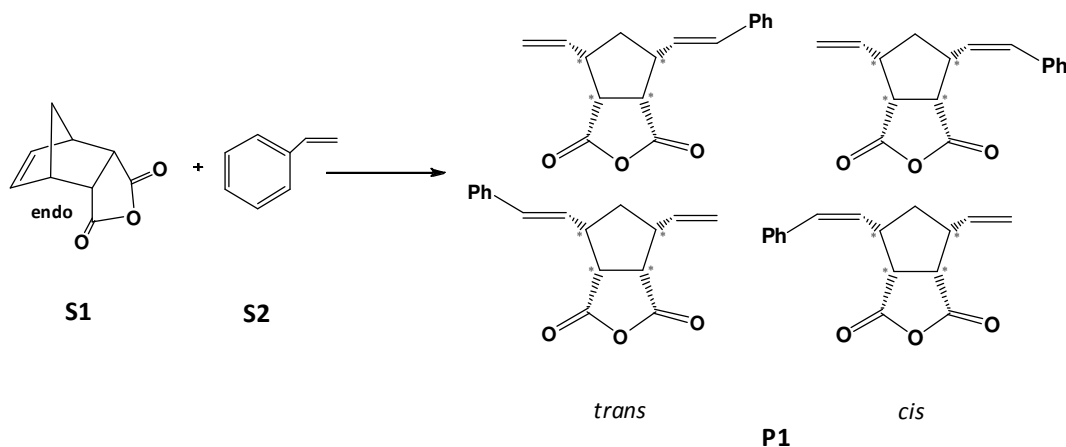
Scheme 5: AROCM reaction of S1 with S2

In the course of the AROCM reaction of **S1** with **S2**, several products can be formed. On the one hand, due to the cross metathesis reaction the formation of a *cis* as well as a *trans* species is possible. On the other hand, the sequence in which the substrates enter the catalytic cycle determines which of the two enantiomers is formed. All things considered, 4 different AROCM products can be formed within the reaction cycle. Hereinafter, the term **P1** refers to the general AROCM product. Closer definitions such as *cis* or *trans* are pointed out additionally.

The first reactions conducted were done with a reaction mixture containing racemic products for reference purpose. In the end, a ratio of **S1** to **S2** of 1:5, DCM as solvent, RT and an initiator concentration of 0.1 to 1 mol% with respect to **S1** have proved to give the best results. Importantly, **S1** and **S2** were mixed firstly in a Schlenk flask under a nitrogen atmosphere and the corresponding catalyst was added afterwards to avoid a previous polymerization of **S1** or dimerization of **S2**. The reaction progress was monitored using TLC. The TLCs were stained using $KMnO_4$. After complete conversion of **S1** (between 15 to 30 minutes), the reaction was quenched with an excess of ethylvinylether and purified via column chromatography to separate the *cis* and the *trans* product and to get rid of the stilben. The termination of the reaction has to occur timely, to avoid ongoing metathesis reactions with **P1** and hence the formation of oligomers. During the separation, stilben eluted first, followed by the *cis* product and finally by the *trans* product.

The *cis* and *trans* species were identified by their characteristic coupling constants from 15.70 Hz for the *trans* and 11.15 Hz for the *cis* fraction. Generally, *trans* double bonds

possess coupling constants from 12–18 Hz and *cis* double bonds from 6-12 Hz.[92] Overall, the reaction proceeded selectively and no oligomeric products according to the integrals of the proton NMR spectrum were formed.
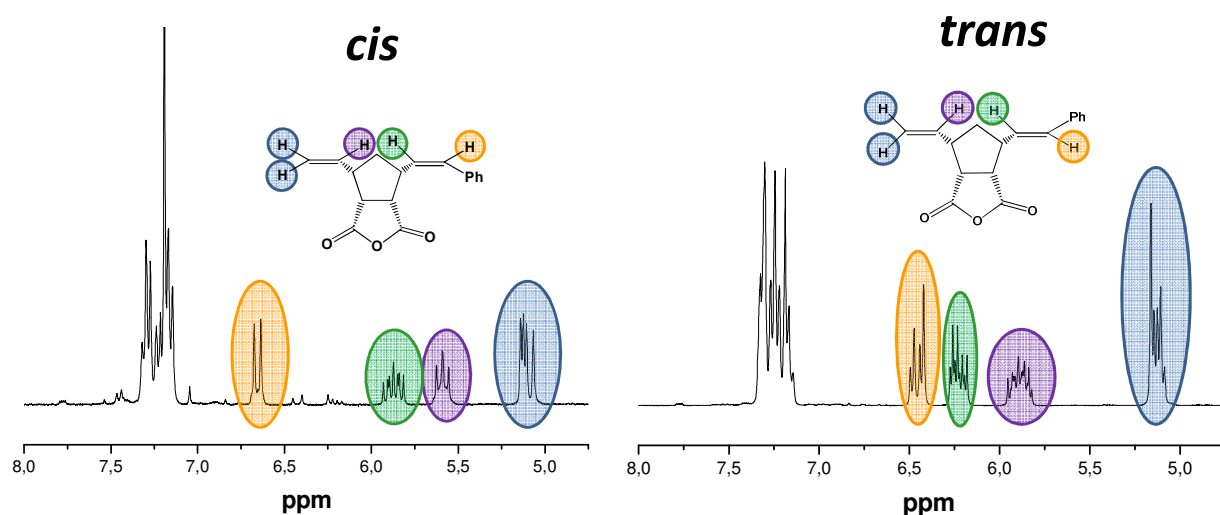
Figure 29: Olefinic region of the *cis* and the *trans* AROCM products

Generally more *trans* than *cis* product is formed during the reaction, but with a decreasing catalyst loading the share can be shifted towards the *cis* product.

Table 8: *Cis* to *trans* ratios in various AROCM reactions

Initiator	Conc. [mol%]	Temp. [°C]	Solvent	Time [h]	Conversion [%]	*cis* [%]	*trans* [%]
Hov	1	40	DCM	0.25	100	30	70
Hov	1	RT	DCM	0.25	100	30	70
G1	1	RT	DCM	5	65	10	90
M2	1	RT	DCM	2.5	100	40	60
Hov	0.1	RT	DCM	0.75	100	40	60
Hov	5	RT	DCM	0.17	100	20	80
1 + 2a/2b	1	RT	DCM	72	24	50	50
1 + 2a/2b	1	60	THF	17.5	39	40	60

[92] E. Breitmaier Vom NMR Spektrum zur Strukturformel organischer Verbindungen; Wiley-VCH, Weinheim, Germany, 2005.

The results summarized in Table 8 show, that the *cis* to *trans* ratio is influenced on one hand by the intiator used and on the other hand by the applied initiator concentration. Droping the initiator concentration of **Hov** from 5 mol% to 0.1 mol% declines the *trans* content from 80 % to 50 %. By changing the catalyst to the first generation initator **G1**, the *trans* content rises to 90 %. In both cases, the *trans* ratio is a function of the catalysts activity. The more active species is present in the reaction solution, the higher gets the *trans* content.
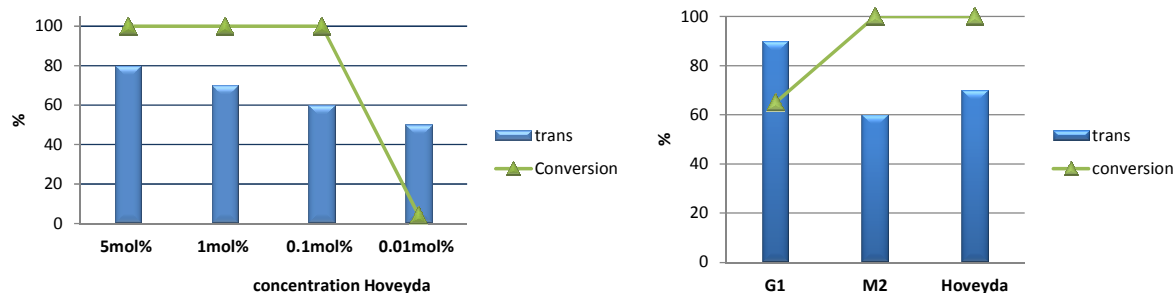
Figure 30: influence of initiator concentration and kind of initiator applied

Most conspicuous, when having a closer look at the first double bond signal in the NMR spectra (labeled in yellow in Figure 29) of the *cis* as well as of the *trans* product is the second small doublet apparent in this peak. For ongoing discussions of the addressed problem about the second unknown species, only the *trans* product is employed. Nevertheless, all information or results can be applied for the *cis* product, too.

The main peak at 6.52 ppm in Figure 31 belongs to the actual *endo-trans-***P1.** The second species at 6.55 ppm possesses the same coupling constant as the *endo-trans-***P1** of 15.70 Hz, indicating that it also comprises a *trans* species. The fact that these second species is present is also evident in all other double bond peaks, but not that obviously.
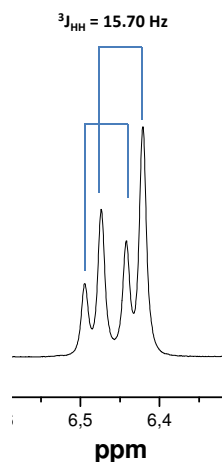
Figure 31: Magnification of ^{1}H NMR spectrum of the region of the double bond of *trans* P1

To get more information about the second unknown *trans* species, several theories about its origin were checked.

3.1.3.1 Norbornene-5,6-dicarboxylic acid

One possible explanation of the origination of the unknown product was, that due to the presence of water (noteworthy: the reaction has not been conducted in dry DCM) the anhydride is opened and the dicarboxylic acid is formed, leading to product **P2**.
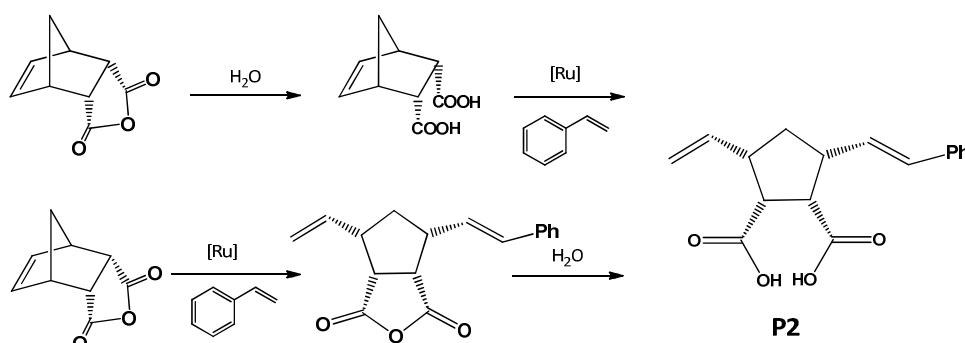
Scheme 6: Possible formation of P2

To prove this theory, three different experiments were done. Both, **S1** and an unseparated mixture of *cis* and *trans* **P1** were mixed with some water and NMR spectra were recorded. The reaction conditions were maintained the same as for the AROCM reactions (RT, DCM) to maintain a comparable environment.
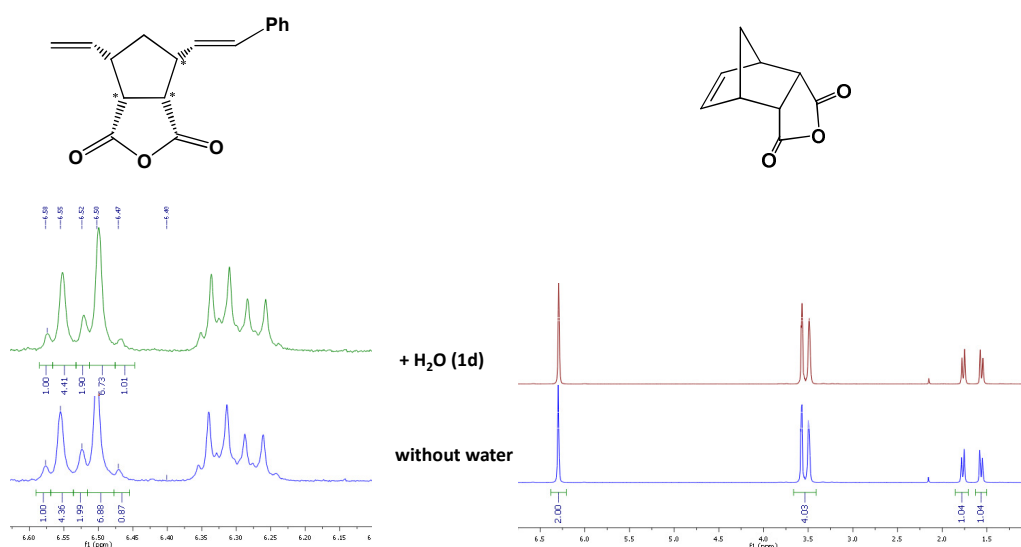
Figure 32: Reaction of water with crude P1 and S1

As can be seen from Figure 32, the presence of water at room temperature does not lead to the opening of the anhydride. This observation is in good accordance with the literature procedure for opening the anhydride which is conducted under refluxing conditions.[93] Additionally to these experiments, an AROCM of norbornene-5,6-dicarboxylic acid with styrene under standard reaction conditions was carried out. The NMR spectrum evinced, that the *trans* doublet of the AROCM product **P2** experiences an up-field shift compared to the peak of **P1**. The unidentified peak at 6.55 ppm was not found in this spectrum.

3.1.3.2   *exo* - Norbornene-5,6-dicarboxylic acid anhydride

The second theory about the origin of the second unknown *trans* species was, that somehow an isomerization of the *endo* to the *exo* product occurs. Therefore **S1** was converted to *exo*-bicyclo[2.2.1]-2-heptene-5,6-dicarboxylic acid anhydride (**S3**). **S3** was then applied for an AROCM reaction using the same reaction conditions as for **S1** leading to the AROCM product **P3**. The NMR spectra revealed, that the unknown doublet from **P1** is not the *trans* product of *exo*-**P3** (6.57 ppm), but most striking the unidentified signal at 16.55 ppm also appears to a small a extend in the spectra of crude **P3**.

---

[93] E. Groaz, D. Banti, M. North, *Eur. J. Org. Chem*., **2007**, 3727–3745.
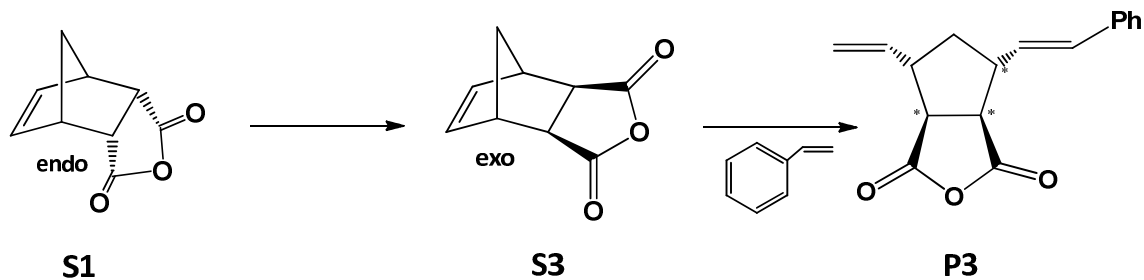
Figure 33: Isomerization of S1 to S3 with following AROCM to P3
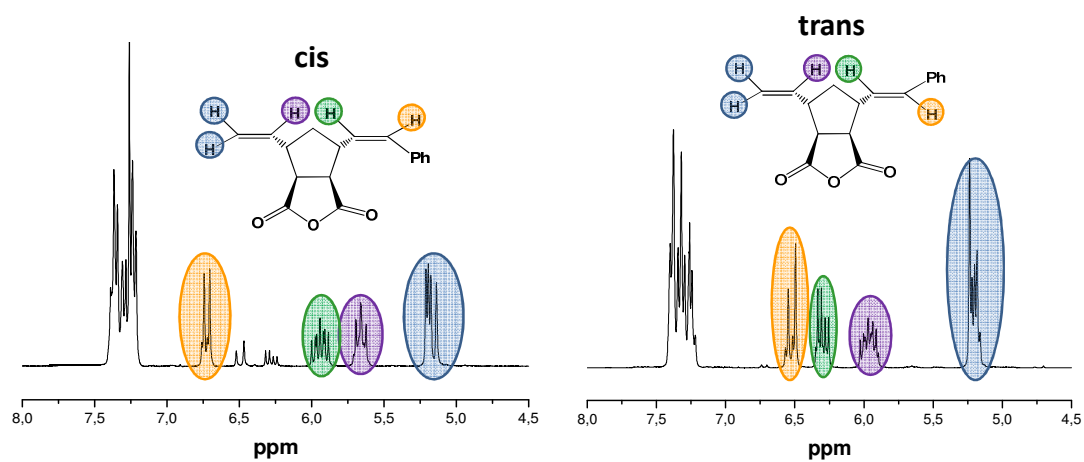
Figure 34: Olefinic region of the *cis* and the *trans exo* AROCM products

3.1.3.3   Other AROCM Products or Dimers

The third theory was, that the unknown peak originates either from the the diphenyl (**P4**) or divinyl (**P5**) product, respectively. Because in every spectra of **P1**, the aromatic peaks of the phenyl ring and the olefinic peaks of the double bond are in the expected ratio of five to five, **P4** and **P5** have to be present equimolarly in the reaction solution. Another possibility was that maybe a small amount of dimeric or trimeric products have been formed during the reaction.
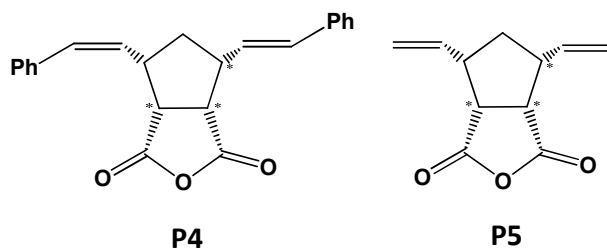
Figure 35: Product P4 and P5

As no information about the presence of **P4** or **P5** could be gained out of the NMR spectra, GC-MS measurements from the unseparated crude **P1** and from the purified *trans*-**P1** as well as from *cis*-**P1** were done.[94] *Cis*- and *trans*-**P1** were eluted sequencedly, whereas the *cis* fraction was eluted first. In contrast, the *endo* and the *exo* parts could not be separated from each other. In none of the measured samples the evidence of some dimers or trimers could be found. **P4** was only detected in the *trans*-**P1** spectra, but in too low amounts as this could cause the second unknown peak in the NMR spectra.
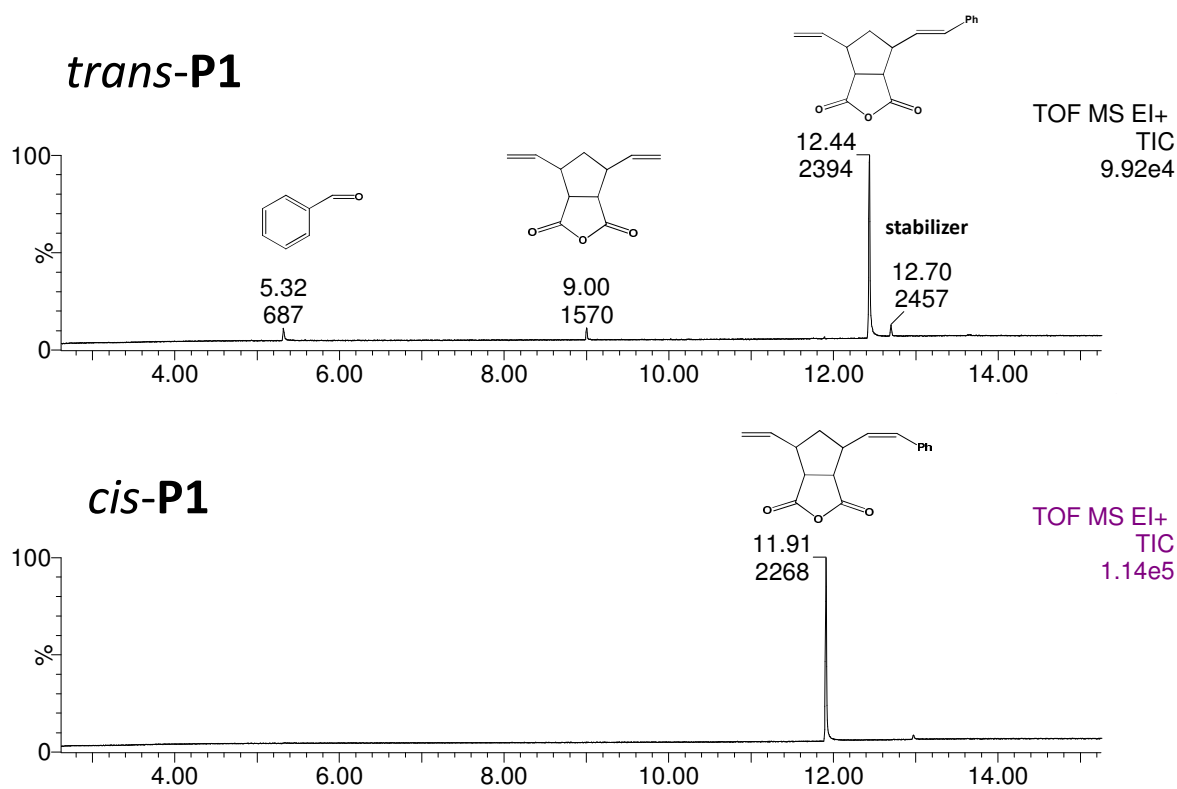
Figure 36: GC-MS spectra of *trans*-P1 and *cis*-P1

Even though, several possible products could be excluded, until now the second species with its doublet at 6.55 ppm still remains unidentified. Some other theories were established, but none of them could be either proofed or debunked and therefore are not addressed more closely.

Table 9: Ratio of *trans*-P1 to unknown product at 6.55 ppm in various AROCM reactions

Initiator	Conc. [mol%]	Time [h]	Conversion [%]	*trans*-P1 [%]	unknown species (6.55 ppm) [%]
Hov	5	0.17	100	67	33
Hov	1	0.25	100	71	29
Hov	0.1	0.75	100	83	17
Hov	0.01	72	4	86	14
M2	1	2.5	100	83	17
G1	1	5	65	88	12

reactions were all performed in DCM at room temperature

Table 9 summarizes the influence of the catalyst concentration and the applied catalyst on the occurrence of the unknown species. As discussed before regarding the *trans* content, again the reactivity of the used catalyst determines the amount of the unknown species. On the contrary to the *trans* content, in this case the share of the desired **P1** product drops with increasing amounts of **Hov** or with more active iniators. This means, that with the less active **G1** only 12 % of the unknown species are formed, whereas during the reaction with **Hov** under the same reaction conditions 29 % of this species are formed.
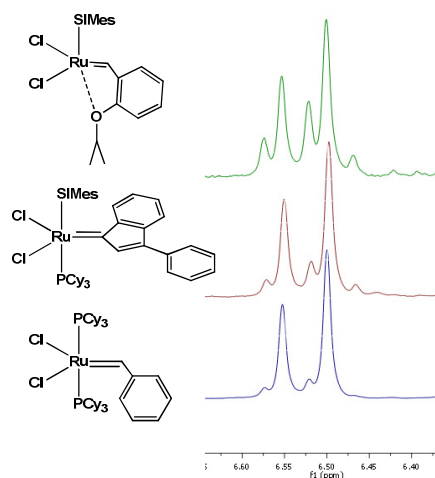
Figure 37: Influence of catalyst on the content of the unknown species

Even though the benchmark reactions with **Hov** yielded this additional unexpected product, the best reaction conditions found, were used for an AROCM reaction with the chiral initiators **1** and **2a/2b**.

The chiral initiator was synthesized as described in chapter 3.1. and due to its instability applied *in-situ* for the AROCM reaction. As a consequence a mixture of the disubstituted **1** with the monosubstituted **2a** and **2b** was applied for the reaction. Unfortunately **1** and **2a/2b** seem to be very inactive and conversions stayed very low (24 %) as room temperature reaction. Thus, the temperature was increased to 40°C and 60°C (in THF), enhancing the conversion up to 40 %. The *cis* and the *tran*s product were separated via column chromatography and NMR spectra were recorded. Interestingly, the before discussed unknown species was not formed during the AROCM reaction with **1** and **2a/2b**.

To finally find out, if the **1** and **2a/2b** exhibit some chiral induction, the purified *cis* and *trans* samples were analyzed via a chiral HPLC.[95] To allow comparison, the **Hov** samples were included in the test series. The enantiomerical excess was calculated according to the following equation:

Equation 1:

$$\text{ee (\%)} = \frac{|(R-S)|}{(R+S)} * 100$$

Table 10: ee% values of P1 made with Hov and 1 and 2a/2b

	Hov		1 and 2a/2b	
	cis-P1	*trans*-P1	*cis*-P1	*trans*-P1
ee [%]	2.6	2.8	3.9	4.8

As can be deduced from the measurements of **Hov**, small ee values can be ascribed to measuring errors and can therefore be neglected. Concluding, the acetylated lactic acid substituted chiral initiators **1** and **2a/2b** only yielded a racemic mixture of the two **P1** enantiomeres and hence are not suitable for chiral metathesis reactions.

---

[95] Chiral HPLC measurements were conducted at the Institute for Organic Chemistry at the TU-Graz by Norbert Klempier; samples were dissolved in isopropyl alcohol, eluant: n-Hep/iPA = 70:30, 0.75 mL/min, 30°C, 50 bar.

3.2 N-, O- Chelating Initiators – Quinlinolate Initiators

The following chapter deals with the synthesis of acid triggerable metathesis initiators. The concept followed was to introduce N-, O- chelating ligands to different known and commercially available ruthenium initiators, namely **M31**, **Hov** and **SIPr-Py** to obtain the mentioned acid triggerable metathesis initiators. For these studies, seven different hydroxyquinoline derivates were used. All of them resulted in the formation of new N-, O- chelating complexes, but just the compounds made with 5,7-dichloro-8-hydroxyquinoline and 5,7-dibromo-8-hydroxyquinoline, respectively were stable and could be easily purified. All closer investigations in the following chapter are done with pre-catalysts bearing one of these ligands.
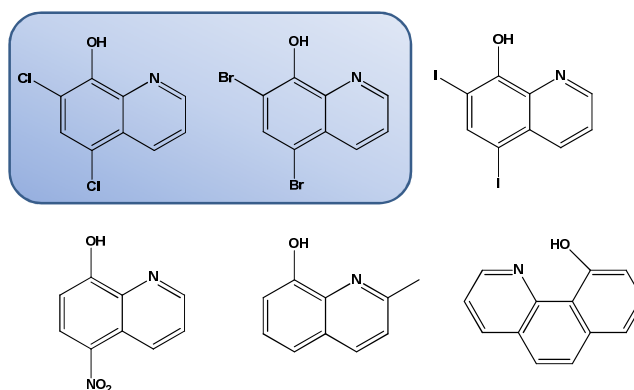
Figure 38: Applied 7-hydroxyquinolines for the complex synthesis

The initiators were characterized and tested regarding their metathesis activity. For the polymerization study, two different monomers namely **Mon1** and **DCPD** (Dicyclopentadiene) were used. **Mon1**, the standard benchmark monomer allows, due to the shielding of the double bonds in the polymer by the ester groups, a direct establishment of the initiation and the propagation rate and gives a good insight into the polymerization behavior of the applied initiator. If second metathesis reactions such as for example backbiting are neglected, molecular weight and the molecular weight distribution can be directly related to the ratio of initiator to monomer and hence to the carbene moieties participating in the metathesis reaction. In case of **Mon1** this omission is acceptable due to the before mentioned reason of the double bond shielding. **DCPD** is a very reactive monomer and yields polymers with high impact strength. Due to the second double bond in the tricyclic system of **DCPD** it is prone to form three dimensional cross-linked networks, if the metathesis initiators are on one hand active enough to crosslink the monomer and on the other hand latent

enough to allow an adequate mixing of the monomer and the initiator. Therefore **DCPD** is a very challenging monomer and gives good information about the initiator characteristic. For RCM studies the standard benchmark substrate **Dedam** (diethyldiallylmalonate) was used. **Dedam** is an easily ring-closed substrate due to the unsubstituted double bonds and gives a first impression of the ring-closing ability of the applied pre-catalysts.
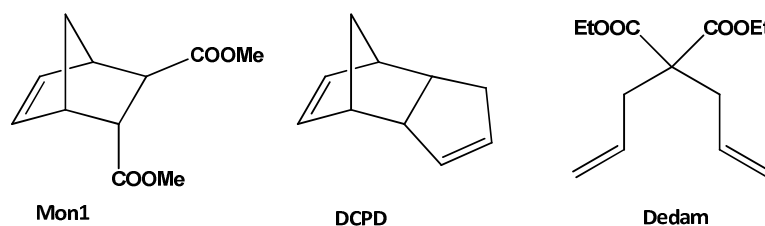
Figure 39: Used monomers and RCM substrate for metathesis reactions

3.2.1   Initiator Synthesis

Due to the knowledge of other anionic ligand exchanges (see the previous chapter) the most efficient reaction conditions were found very fast. The reactions were carried out in a Schlenk flask using dry and degased DCM. The general reaction procedure was to react the corresponding starting complex with an excess (5–25 eq) of the 5,7-dihalogenated-8-hydroxyquinoline and an excess of Cs_2CO_3 (10–25 eq) in DCM. In the course of the reaction a color change from either green to purple or from red-brown to purple occurred, making a visual monitoring of the reaction progress possible. The progression was additionally followed via TLC (CH/EE 5:1 or 10:1). In any case, the formation of at least two different derivatives could be observed via TLC. After complete conversion, the undissolved products were filtered and washed with cold DCM. The crude product was then separated via column chromatography, yielding 65 % to 90 % of the new products. Just in case of starting material **Hov** and **M31** reacting with the 5,7-dichloro-hydroxy-8-quinoline both formed isomers were formed in such amounts, that they could be isolated. In all other reactions, the second species was just formed as a minor isomer and hence could not be isolated or characterized. The reaction of **M31** with 5,7-dibromo-hydroxy-8-quinoline even yielded three different isomers. The isomers could be separated and characterized (see supporting information), but only the isomer bearing one quinolinolate ligand (**5**) was formed in satisfying quantities and was applied in the ongoing studies. The new formed initiators which were used for the structural and polymerization studies are depicted in Figure 40. Interestingly, in case of the indenylidene containing starting materials, the two derivatives formed were always a mono and a disubstituted initiator, in contrast to the two disubstituted initiators formed with **Hov**.

It seems that somehow the bulkier phenyl-indenylidene ligand hampers or even hinders the second quinolinolate ligand to coordinate to the ruthenium center.

Table 11: Yields of initiator synthesis

Initiator	Yield (Overall Yield)
3a	70.2 (90)
3b	19.8 (90)
4a	28 (83)
4b	57 (83)
5	n.d
6	52

Overall yield refers to the theoretical conversion of the starting material regarding the yield of both derivatives formed during the reaction;
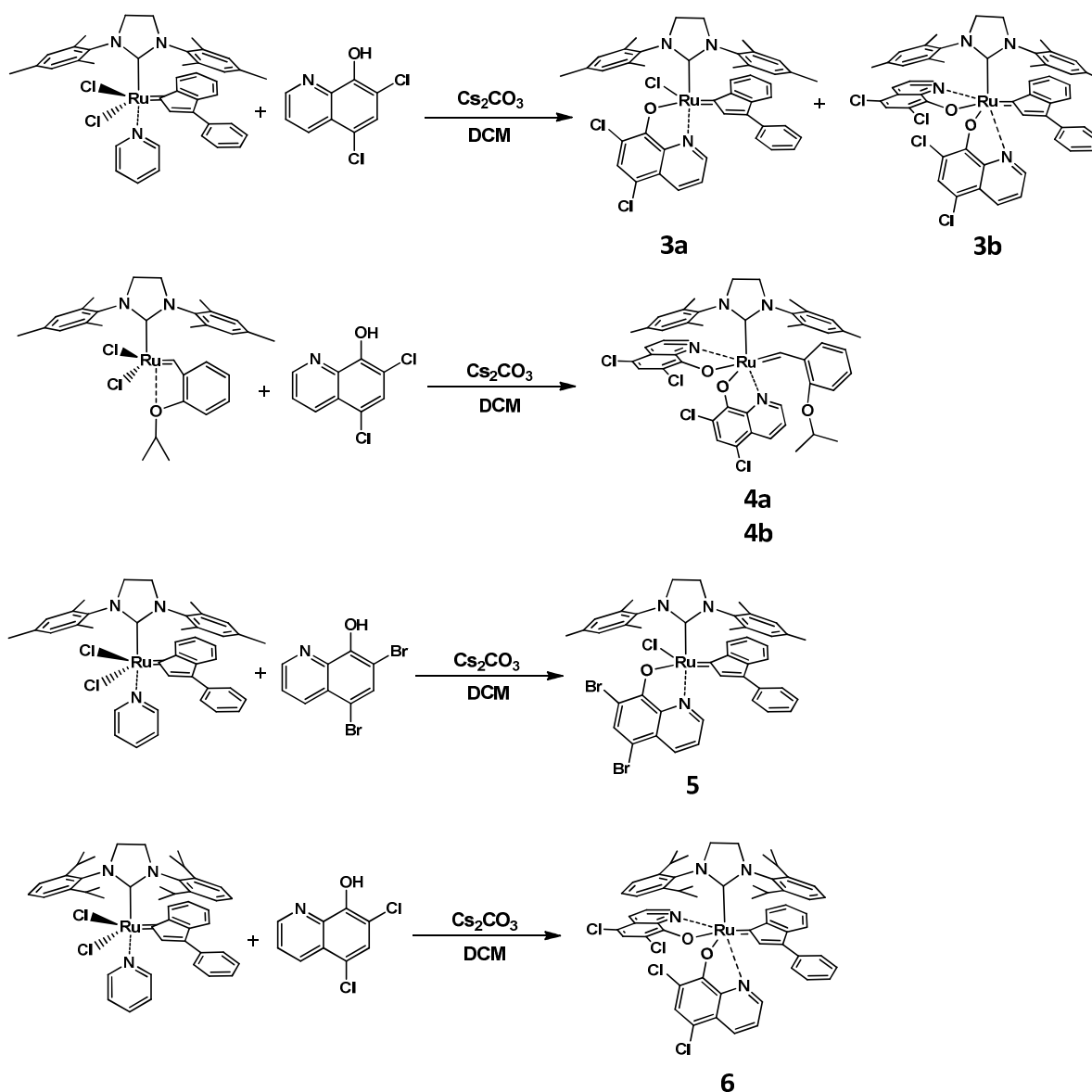
Figure 40: Synthesis of N-, O- chelating ruthenium metathesis initiators

For a clearer recognition of the different initiators during the ongoing discussion and in the several graphical representations, additionally to the ascribed numbers, a particular color was assigned to every initiator. **3a** = dark green; **3b** = bright green, **4a** = bright blue, **4b** = dark blue, **5** = orange, **6** = dark red

3.2.2 Initiator Characterization

All initiators were characterized using NMR techniques. **4a** and **4b** exhibit a characteristic carbene peak at 19.10 ppm (**4a**) and 18.24 ppm (**4b**), respectively. The signal of this alkylidene proton is shifted downfield compared to the mother complex **Hov** from 16.56 ppm to 19.10 ppm in **4a** and to 18.23 ppm in **4b**. Due to the indenylidene ligand in the other

compounds and hence the lack of the characteristic carbene proton, no specific peak can be assigned for them. All spectra were clearly interpretable and the desired product could be identified very easily.

The first thing which was observable when looking at the aromatic region of complex **3–6** was the number of quinolinolate ligands which are attached to the catalyst. As mentioned above, complex **3a** and **5** exhibit only one quinolinolate and one chlorine ligand, while complex **3b**, **4a**, **4b** and **6** possess two quinolinolate ligands. Generally ruthenium complexes can be assigned to have either a *cis* or a *trans* arrangement of the two halide ligands. The *cis/trans* geometry normally can be identified by the splitting of the NHC protons in the ^{1}H NMR spectra. In case of the disubstituted initiators this assignment cannot be made, due to the fact that these compounds are hexacoordinated to the ruthenium. Still the pattern of the protons of the NHC gives some information about the dynamic behavior of the compounds.

Complexes **4a** and **4b** reveal some interesting deviations from their starting compound **Hov**. **Hov** is a textbook example for an initiator with a *trans* configuration. The aromatic protons of the mesityl group, as well as the protons of the CH_2 group in the NHC appear in a perfect singlet, demonstrating a totally unhindered rotation of the NHC around the ruthenium bond as well as of the mesityl groups around the N-C bond. In case of **4a** and **4b** the aromatic protons of the mesityl group are split into two singlets, each with an intensity of two. Even more interesting is the sextet signal of the CH_2 groups of the imidazole. In a pentacoordinated sytem, this change of the singlet to a hextet would be indicative for a hindered rotation around the N-C bond. In our case, this conclusion can not be drawn so easily. From the crystal structure it is even more likely that the NHC is able to rotate in an unimpeded manner. Assuming that the rotation is unhindered every aromatic proton is in different vicinity due to the fact that the ruthenium is chiral. Most probably this fact leads to the splitting of the aromatic protons and the CH_2 groups even though the rotation is unhampered.
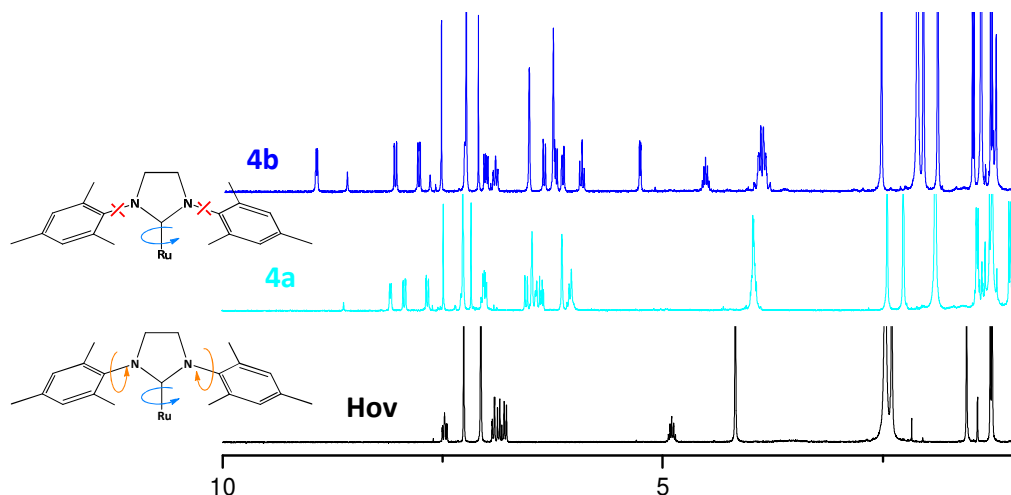
Figure 41: ^{1}H NMR spectra of Hov, 4a and 4b recorded in CDCl$_3$

In the aliphatic region the above described fact is also visible. The CH$_3$ groups of the mesityl also split from two to three singlets with an intensity of 6 protons, representing two CH$_3$ groups each. Most likely the hindered rotation of the mesityl groups is caused by a π-π interaction of the phenyl ring of the mesityl with the aromatic rings of the quinolinolate ligand. Although the π-π-stacking is not very pronounced it does exist. In **4b** the π-π-stacking is more distinct than in **4a**.
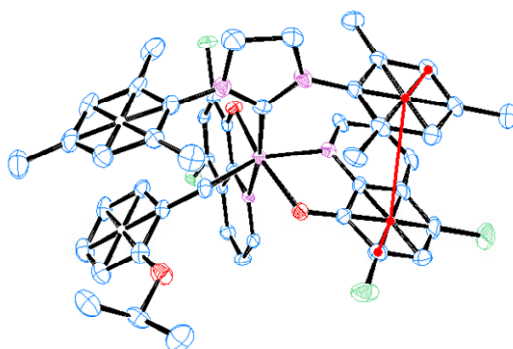
Figure 42: Schematic depiction of π-π-stacking in ruthenium complexes

Interestingly the indenylidene containing pre-catalysts bearing a SIMes NHC **3a**, **3b** and **5** reveal a contrary picture of a less hindered rotation of the NHC ligands in the quinolinolate complexes. While in starting material **M31** all four protons of the CH$_2$ at the indenylidene and all six CH$_3$ groups of the mesityl group are split up into single peaks, the quinolinolate catalysts possess just one signal for the CH$_2$ protons and three singlets with an intensity of six

for the CH$_3$ groups. Complex **6** shows no significant changes from its starting material **SIPr-Py** in the NMR spectra**.**
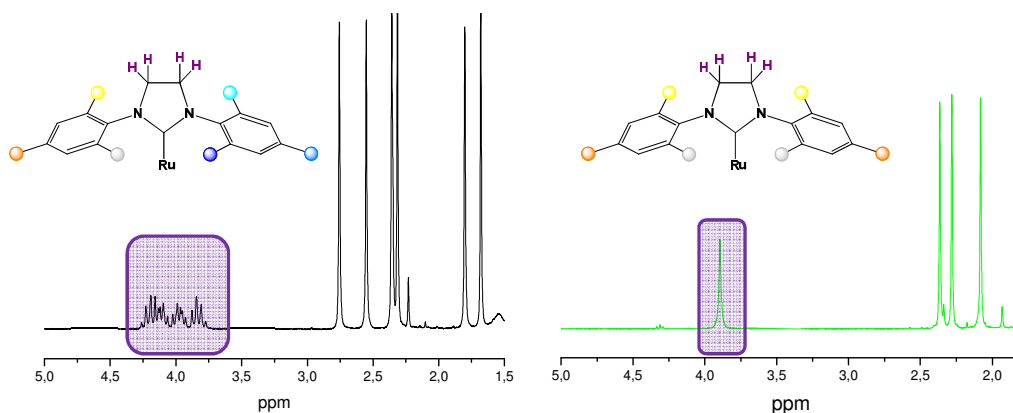
Figure 43: Comparison of aliphatic region of starting material M31 (left) and 3b (right) as a representative for the SIMes, indenylidene containing quinolinolate complexes; spectra are recorded in CDCl$_3$

Interestingly, even if complex **4a** and **4b** both exhibit two quinolinolate ligands, they possess a totally different NMR pattern (compare Figure 41). In the spectra of compound **4b** a full splitting of the aromatic peaks from 9 ppm to 5 ppm is apparent, whereas the aromatic region of **4a** is narrower and peaks overlap. The difference therefore probably is provoked by a distinct arrangement of the ligand sphere. Various coordination possibilities are depicted in Figure 44, comprising opened and closed carbene structures and the different coordination possibilities of the quinolinolate ligand itself. Due to the distinct downfield shift of the alkylidene proton for both derivatives the opened carbene form is the more likely one.
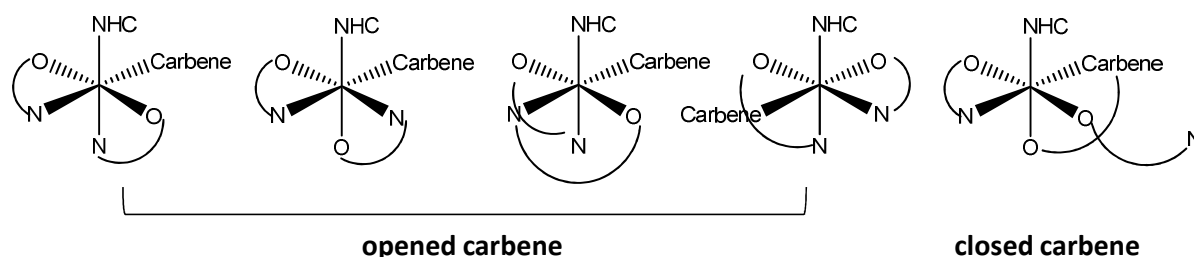
Figure 44: Different possible arrangements of quinolinolate ligands

To gain more insight into the structure of **4a** and **4b**, single crystals were grown and analyzed via single crystal X-ray analysis. The crystals were grown by slow diffusion of Et$_2$O in a saturated solution of DCM. The ORTEP diagrams of the two structures are shown in Figure

74

45 and Figure 46. The most conspicuous fact revealed by the X-ray is the different position of the two quinolinolate ligands to each other at the ruthenium center. The nitrogen atom of the first quinolinolate group is in both isomers arranged *trans* to the NHC ligand with the oxygen atom *cis* to the second quinolinolate ligand. In Isomer **4b**, the oxygen atom of the second quinolinolate co-ligand is arranged *trans* to the carbene, while in **4a** the nitrogen atom of the second quinolinolate occupies the *trans* position to the carbene. Summarizing the spectra with the less split aromatic region belongs to the initiator where the two oxygen of the quinolinolate ligands are *trans* to each other and *trans* to the carbene is a nitrogen. The initiator with the broad splitting of the spectra has an oxygen *trans* to the carbene. In contrast to other similar structures published recently by Grubbs, no isomerization of **4a** into **4b** or the other way round was observed after heating the complex to higher temperatures.[76]
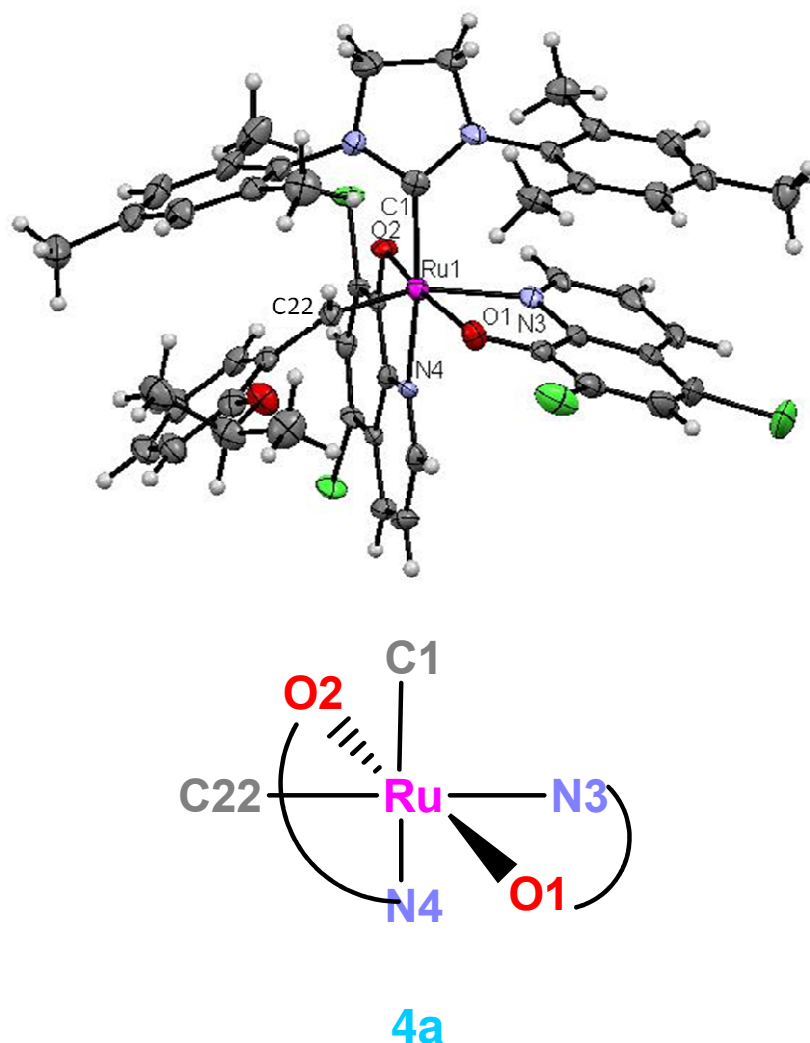
Figure 45: ORTEP diagram of 4a

4b
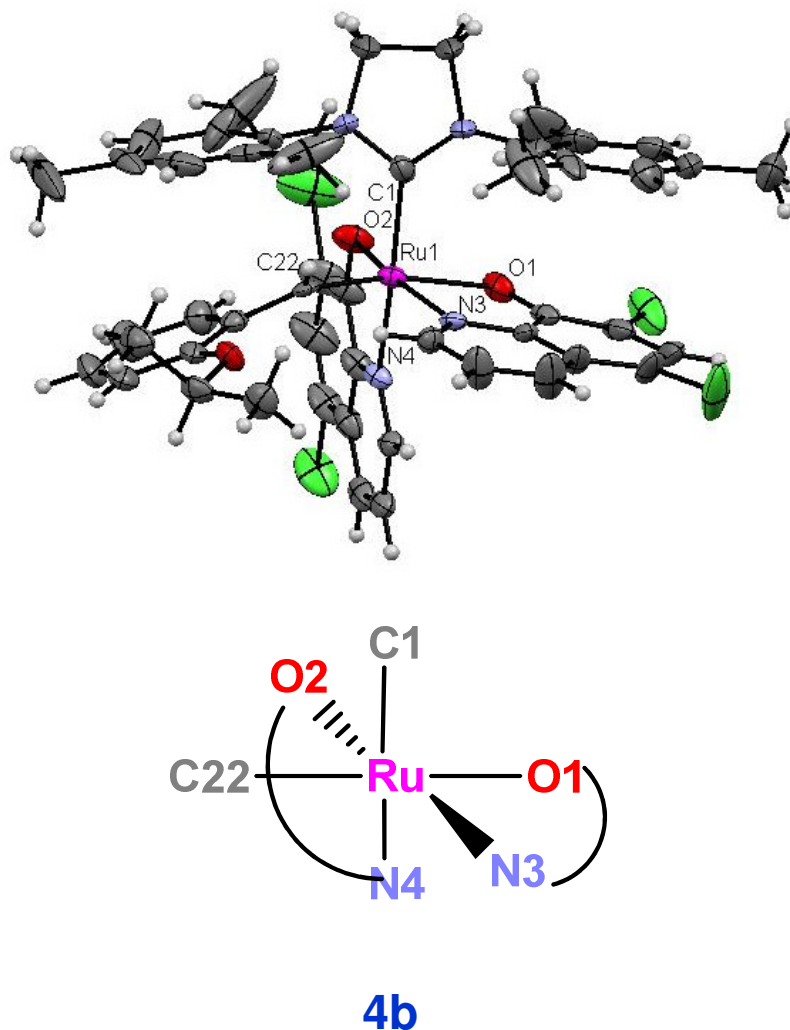
Figure 46: ORTEP diagram of 4b

Both initiators possess an octahedral fundamental structure. Bond lengths of both complexes possess roughly the same values. The O1 (see

Table 12 labeled in orange) in **4a** is shifted a little bit in direction to N4 compared to the N3 (labeled in orange) in **4b** which is indicated by a slightly increased C1-Ru-O1/N3 bond angle. As a consequence, the bond angle of the carbene carbon (C22) to N3/O1 (orange) is also different.

Percent Buried Volume %V_{bur}
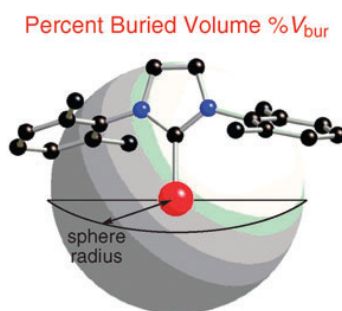
Figure 47: Depiction of the %V_{bur}; replicated from reference 97

The buried volume (%V_{bur}) gives information about how much space is occupied by an organometallic ligand (in our case the NHC) in the first coordination sphere of the metal and hence about the possibility for an olefin to approach the carbene. As both complexes exhibit a SIMes NHC and basically the same architecture, it is not very surprising that the buried volume of both initiators is basically the same (**4a**: %V_{bur}=30.5; **4b**: %V_{bur}=30.4).[96] Most striking, compared to other NHC ligands, it is about a few percent smaller (**Hov**: %V_{bur}=33.7; **M2**: %V_{bur}=32.8), a fact which could be beneficial for the metathesis reaction.[97]

Table 12: Selected bond lengths of 4a and 4b

Selected bond lengths			
4a		**4b**	
Ru-O1	**2.09**	**Ru-N3**	**2.08**
Ru-O2	2.04	Ru-O2	2.04
Ru-N3	**2.2**	**Ru-O1**	**2.17**
Ru-N4	2.11	Ru-N4	2.12
Ru-C22	1.89	Ru-C22	1.88
Ru-C1	2.05	Ru-C1	2.06

---
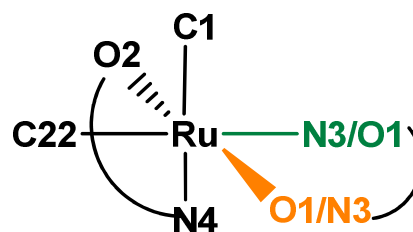
[96] Caculated by A. Poater, University of Salerno; https://www.molnac.unisa.it/OMtools/sambvca.php
[97] H. Clavier, S.P. Nolan, *Chem. Commun.* **2010**, *46*, 841–861.

Table 13: Selected bond angles of 4a and 4b

Selected bond angles			
4a		**4b**	
C1-Ru-N3	**102.3**	**C1-Ru-O1**	**97.2**
C1-Ru-O1	**95.9**	**C1-Ru-N3**	**96.6**
C1-Ru-O2	89.5	C1-Ru-O2	87.3
C1-Ru-N4	169.2	C1-Ru-N4	166.7
C1-Ru-C22	90.8	C1-Ru-C22	92.5
O1-Ru-O2	166.9	O2-Ru-N3	166.8
C(22)-Ru-N3	158.9	C(22)-Ru-O1	166.6

Comparing the results of **4a** and **4b** with its starting material **Hov**, the elongated Ru-C1 bond (1.98 Å) is remarkable.[98] It is probably caused by the more pronounced steric crowding of the **4a** and **4b** around the ruthenium center due to the quinolinolate ligands.

Based on the assignments of the crystal structures, we took the NMR spectra of **4a** and **4b** and compared it with the spectra of **3a**, **3b**, **5** and **6**. **3b** also shows a broad splitting of the aromatic peaks and possesses the same doublet appearing around 5.4 ppm which belongs to one of the two CH protons next to the nitrogen in the quinolinolate ligands. This signal can be easily identified by its coupling constant of around 4.5 Hz in contrast to the other aromatic doublets which have a coupling constant around 8.3 Hz in the quinolinolate and around 7.2 Hz in the indenylidene ligand. Thereof we assume, that the configuration of the two quinolinolate ligands around the ruthenium center in **3b** is the same than in **4b** with an oxygen in the *trans* position to the carbene. In **6**, the described signal is also shifted upfield to 5.9 ppm, which again suggests the assumption that the same geometry is apparent.

Due to the fact that **3a** and **5** exhibit only one quinolinolate ligand, geometric assignments by a simple comparison of the NMR spectra are difficult to make.

---

[98] S. B. Garber, J. S. Kingsbury, B. I. Gray, A. H. Hoveyda, *J. Am. Chem. Soc.* **2000**, *122*, 8168-8179.
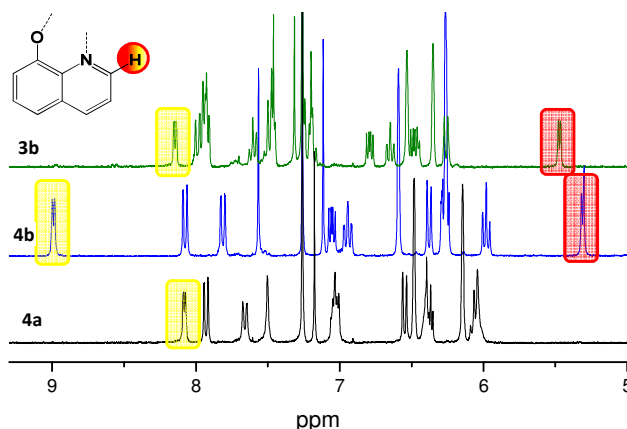
Figure 48: Structural comparison of 4a and 4b with the indenylidene derivative 3b; spectra are recorded in CDCl$_3$

3.2.2.1 UV-VIS Measurements

Very remarkable is the strong coloring of the pre-catalysts **3-6**, probably caused by the quinolinolate ligands. Even very low concentrated solutions exhibit a strong red color. The incorporation of the quinolinolate ligands into the ruthenium coordination sphere seems to cause changes in the electronic structure of the complex, which has important consequences on the light harvesting properties.[99] Therefore we became interested, if the optical properties of the initiators can be affiliated to, for example, the structure of the initiators. Thus, UV-VIS measurements at different concentrations were performed and the extinction coefficient was determined by rearranging the fundamental Beer-Lambert law.

Equation 2: Beer-Lambert law

$$E = \lg\left(\frac{I_0}{I_I}\right) = \varepsilon c d$$

Interestingly the UV-VIS spectra of the indenylidene derivatives **3a**, **3b** and **5** give a different, more precisely defined spectra than the Hoveyda derivatives **4a** and **4b** (see Figure 49). All three indenylidene containing catalysts exhibit a defined absorption maximum around 500 nm. **3b**, which possesses two quinolinolate ligands, holds a second maximum at 363 nm. According to Rochford et al. the transition observed around λ_{max} = 500 nm consists primarily of a HOMO to LUMO+3 transition with a significant contribution from a HOMO-2 to LUMO

[99] H. C. Zhao, J. P. Harney, Y-T. Huang, J-H. Yum, Md. K. Nazeeruddin, M. Grätzel, M-K. Tsai, J. Rochford *Inorg.Chem,.* **2012**, *51*, 1-3.

transition state. The transition state observed at λ_{max} = 363 nm is said to consist of HOMO-2 to LUMO+2 character.[99] Noteworthy, in case of the ruthenium complex investigated by them, the transition state at λ_{max} = 535 nm was the smaller and the one at λ_{max} = 393 nm the more pronounced one. The spectra of **4a** and **4b** are more difficult to interpret and do not show clearly defined absorption maxima. It seems, that they have also two absorption maxima around λ_{max} = 370 nm and λ_{max} = 460 nm. The maximum around 460 nm also belongs to the quinolinolate ligand and is as well described by Rochford and his group
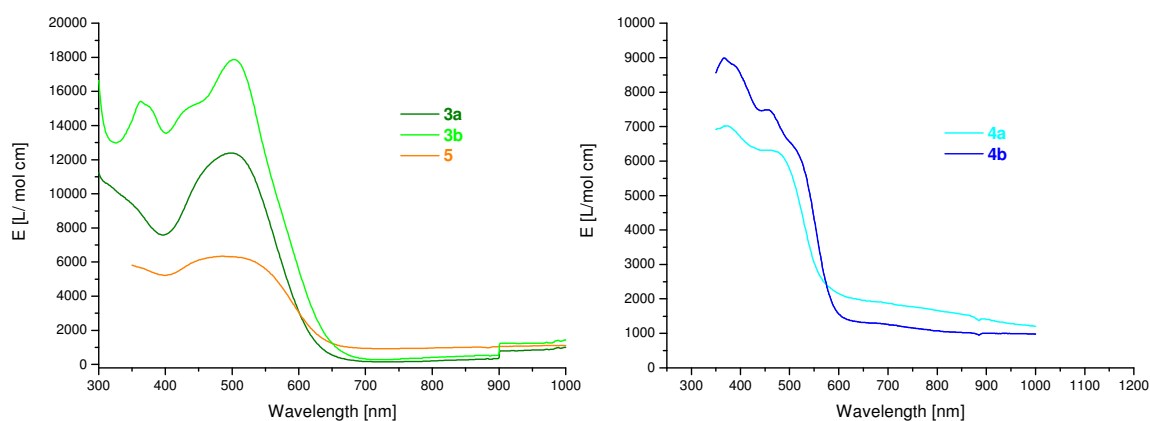
Figure 49: UV-VIS spectra of 3-5

Table 14: Extinction coefficients at adsorption maximum of 3-5

Initiator	Wavelength [nm]	ε [L/mol cm]
3a	500	$1.12 * 10^4$
3b	504	$1.78 * 10^4$
	363	$1.54 * 10^4$
4a	375	$7.02 * 10^3$
	462	$6.50 * 10^3$
4b	367	$8.97 * 10^3$
	456	$7.47 * 10^3$
5	483	$6.43 * 10^3$

3.2.3 Catalytic Activity

The catalytic activity of the new pre-catalysts was initially tested using **Mon1** as the benchmark monomer. The reactions were carried out under standard reaction conditions with an initiator to monomer ratio of 1:300, at room temperature in DCM. For these experiments a Schlenk flask was equipped with the initiators (**3**-**6**), a stirring bar, degassed solvent and the monomer. None of the initiators was able to convert the monomer to a polymer under the applied conditions. Also attempts to activate the pre-catalysts by means of heat or irradiation with UV-light failed. For the temperature activation the temperature was increased stepwise going from 40°C (in DCM) to 80°C (in toluene), with no hint of conversion in any polymerization. UV irradiation was done with a "G-Light: led visible light curing unit" over one hour. The wave spectrum of this lamp ranges from 390-550 nm which covers the absorption maxima of all of the complexes. Therefore, efforts to activate the initiators via acid have been made. Upon addition of HCl aq. complexes **3** to **6** became active and initiated the ROMP reaction of **Mon1**. The activation process is accompanied by a color change from deep red, to brownish to dark green in complex **3**-**5** and from brownish to red to yellow in **6**. The necessity of acid indicates that a protonation of an atom in the complex occurs, leading to the actual active species. The reaction progress of the polymerization reaction was monitored using thin-layer chromatography and stained with $KMnO_4$. After complete consumption of the monomer, the reaction was stopped with an excess of ethylvinylether, precipitated in vigorously stirred methanol and dried. Samples were collected for GPC analysis. Molecular weigths (M_n) and the corresponding polydispersity indices (PDI) were determined against a polystyrene standard.

Figure 50 and Table 15 summarize the results of the polymerization data. Generally it can be assumed, that except of **6**, the catalysts show a slow initiation and a, compared to the initiation, faster propagation. The high M_n values indicate that the activation process is relatively slow and the required protonation and ongoing formation of the active species is incomplete. In every case, the ratio k_i/k_p is < 1. PDI values are also relatively high and range between 1.8 and 2.4. Again the broad distribution is caused by the incomplete and prolonged initiation mechanism. **6,** on the other hand, exhibits pretty low molecular weights and narrower PDI's indicating an almost full activation by the acid. The PDI's are a little higher compared to the values of known living initiators such as **M31**, probably again caused by a retarded activation due to the protonation of the ligands. Interestingly the polydispersities of polymers made with **6** provide a bimodal distribution. This fact is already described in literature and is ascribed to a second metathesis active species formed during the reaction due to a fast partially decomposition of the initiator.[100]

---

[100] C. A. Urbina-Blanco, A. Leitgeb, C. Slugovc, X. Bantreil, H. Clavier, A. M. Z. Slawin, S. P. Nolan, *Chem. Eur. J.* **2011**, *17*, 5045-5053.

Table 15: Polymerization data of initiator 3-6

Temp. [°C]	Initiator	Activation	Time [h]	Conversion [%]	Isol. Yield [%]	M_n [kg/mol]	PDI
20	3 – 6	-	24	0	0	-	-
80	3 – 6	-	24	0	0	-	-
20	3 – 6	UV light	24	0	0	-	-
20	3a	HCl eth.	6.25	100	75	413	2.0
20	3b	HCl eth.	2	100	78	181	1.9
20	4a	HCl eth.	23	65	42	254	2.2
20	4b	HCl eth.	4	100	85	148	2.4
20	5	HCl eth.	24	76	23	278	2.1
20	6	HCl eth.	2.15	100	45	47.3	1.3
20	3a	HCl aqu.	3	95	80	392	2.0
20	3b	HCl aqu.	1.25	100	84	196	1.7
20	4a	HCl aqu.	23	44	20	296	1.8
20	4b	HCl aqu.	4.5	100	78	266	1.8
20	5	HCl aqu.	23	66	20	275	1.8
20	6	HCl aqu.	2	100	58	52.3	1.4
80	3a	HCl aqu.	2.25	100	84	411	2.1
80	3b	HCl aqu.	1	100	88	159	1.9
80	4a	HCl aqu.	24	77	46	132	2.3
80	4b	HCl aqu.	1	100	83	418	2.2
80	5	HCl aqu.	1.25	100	81	142	1.7
80	6	HCl aqu.	0.75	100	75	52.2	1.6
20[a]	3a + b	HCl eth.	3.5	100	77	173	1.9

[a] Pre-catalysts **3a** and **3b** were used together, without separating them with column chromatography. Purification was just done by filtration of the insoluble residues. Reaction conditions: [Mon1]:[I] = 1:300; [Mon1]=0.1 mol/L;DCM for room temperature polymerizations, toluene for 80°C polymerizations; 50 eq HCl relative to [Ru] in polymerization with etherical HCL; 2 trops of HCl aqu.
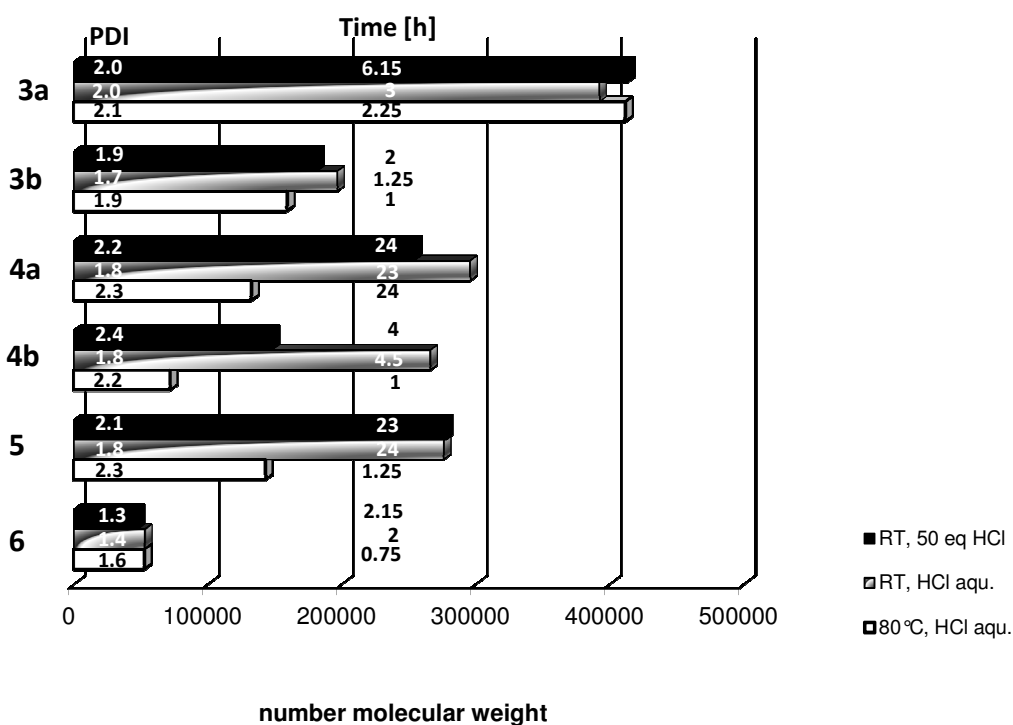
Figure 50: Polymerization data; reaction conditions: [Mon1]:[I] = 1:300; [Mon1]=0.1 mol/L; DCM for room temperature polymerizations, toluene for 80°C polymerizations; 50 eq HCl relative to [Ru] in polymerization with etherical HCL; 2 trops of HCl aqu.

Interestingly the results are not critically influenced whether etherical or aqueous HCl is used. The polymerization behavior is not dramatically affected by the presence of water in the reaction mixture. This suggests the assumption that the complexes are very stable against water, even during the activation step.

Additionally to the Schlenk polymerizations, kinetic measurements with **Mon1** were done. For these experiments, the procedure was conducted as follows: In an NMR tube, catalysts **3**-**6** (1 eq) were dissolved in degased $CDCl_3$. **Mon1** (50 eq) dissolved in $CDCl_3$ was added. An overall solvent concentration of 0.1 mol/L with respect to the monomer was used. Just before the first NMR spectrum was recorded, 25 eq of HCl in diethylether was added into the NMR tube and shacked to ensure a complete mixing. ^{1}H NMR spectra were recorded periodically until the reaction was complete or no further conversion of the monomers could be observed, to obtain conversion time plots. The results of the kinetic measurements are in very good accordance with the results of the solvent polymerization. As shown in Figure 51 the fastest conversions show the indenylidene derivatives possessing a dichloroquinolinolate ligand (**3a**, **3b** and **6**). **4b** shows slower, but still satisfying, conversion and reaches 100 % monomer consumption after around 4.5 hours. In contrast, **4a** and **5** initiate the polymerization of **Mon1** but do not reach more than 30 % conversion.

Initiator	$t_{1/2}$ [h]
3a	0.16
3b	0.16
4a	-
4b	1.78
5	-
6	0.27
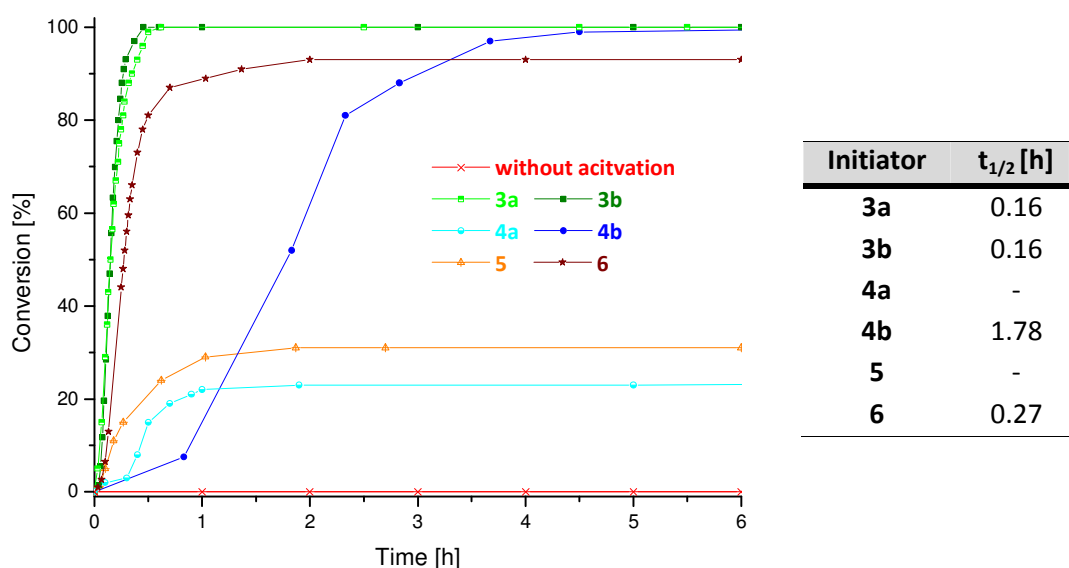
Figure 51: Kinetic plot of Mon1; [Mon1]:[HCl]:[I] = 50:25:1; [Mon1]=0.1 mol/L; CDCl₃

Even though the pre-catalysts are not critically influenced by the presence of water in the reaction mixture, oxygen seems to have a negative effect on the polymerization behavior. The Schlenk experiments of **4a** and **5**, which were performed under a nitrogen atmosphere, yield higher conversions than the kinetic experiments, which were performed under air.

3.2.3.1   Influence of Acid

To gain more detailed information about the influence of HCl, polymerization reactions with increasing HCl (in Et₂O) quantities were run under standard conditions using complex **3b, 4b** and **6**.

In every case an HCl rate-dependency is observable up to a certain extent. In the case of the indenylidene containing derivatives **3b** and **6**, polymerization activities increase with increasing HCl amounts, leading to faster conversion and lower molecular weights. Pre-catalyst **4b** in contrast, shows a minimum molecular weight and reaction time at 50 eq HCl with respect to ruthenium. When 100 eq HCl are used, both, reaction time and molecular weight rise, indicating a decomposition of **4b** due to the huge excess of acid. In every case the reaction times between 10 eq and 100 eq are decreased around 4 to 5 times.
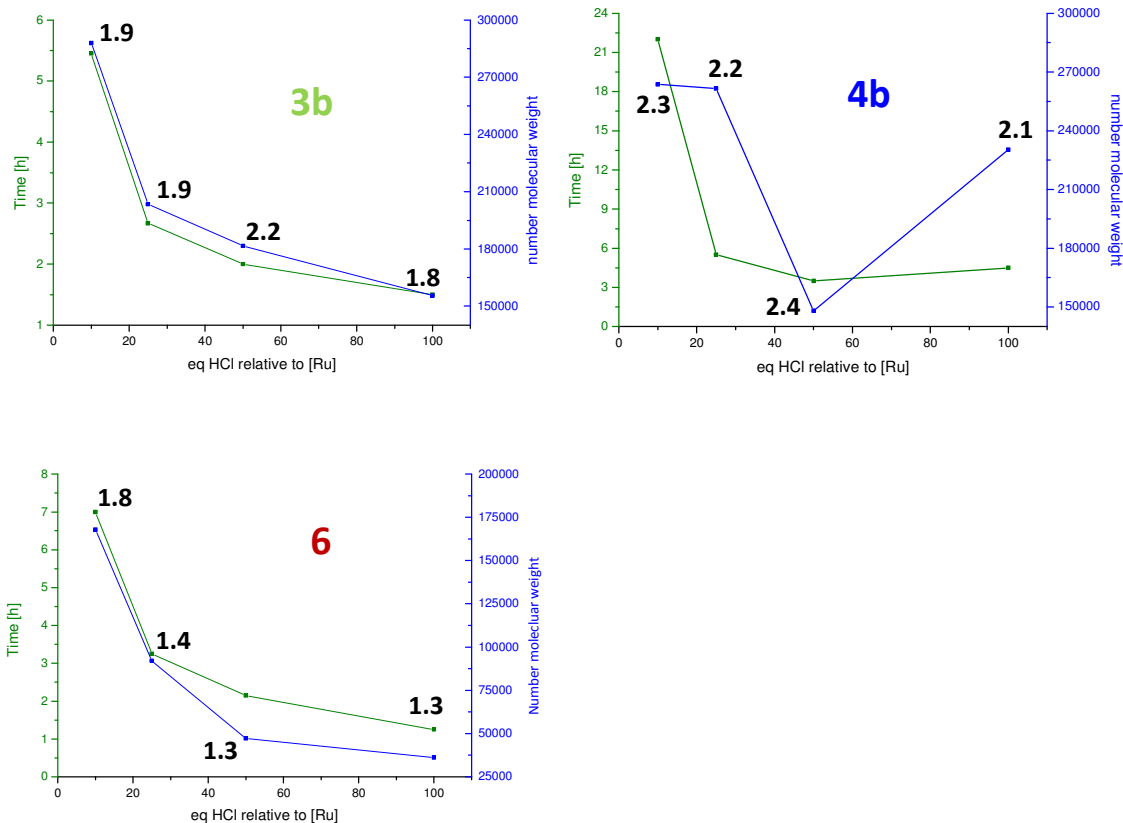
Figure 52: HCl dependency of 3b, 4b and 6 determined using Mon1 under standard reaction conditions (RT, [I]:[Mon1] = 300:1, DCM, 0.1 mol/L with respect to the monomer)

3.2.3.2 Controlled Polymerization

Due to the low molecular weights of polymers made with catalyst **6**, it was investigated if the initiator is capable of performing controlled polymerizations, even though, the PDI values are somehow too high for perfect controlled polymerizations. Therefore polymerizations with increasing ratios of **Mon1**, ranging from 150 to 900 equivalents were performed. All reactions were done under standard reaction conditions at RT using 50 equivalents of HCl in diethylether.
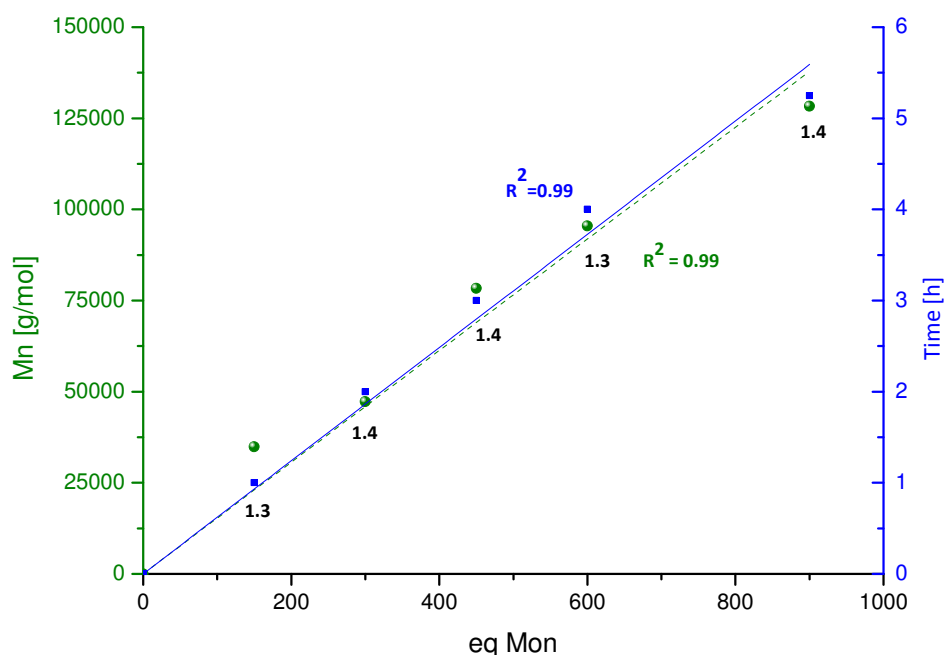
Figure 53: Controlled polymerization of Mon1 with 6; [Mon1]:[HCl]:[I] = 300:2:01; [Mon1]=0.1 mol/L; DCM

Plotting of the molecular weights versus the monomer units applied reveals a controlled polymerization behavior of **6**. Molecular weights increase in a linear manner resulting in a slope with a R^2 of 0.99. PDI values do not increase significantly with increasing monomer units, which is also indicative for controlled polymerizations. Most striking, even the reaction time increases linearly, a fact which not necessarily has to happen.

3.2.3.3   Acitve Species

To elucidate the activation mechanism of **3**-**6**, we tried to trap the active species of the pre-cataylsts. To do so, we mixed **6** with 5 eq of **Mon1** in degased $CDCl_3$ and activated it with 5 eq of etherical HCl in a NMR tube. After a view minutes, a carbene peak at 18.10 ppm appeared. To identify this carbene peak, the same experiment was repeated reacting **M31** with **Mon1**, leading to the same characteristic carbene peak at 18.10 ppm. We assume that, as proposed by Grubbs and co-workers, the hydrochloric acid protonates both quinolinolate ligands which are subsequently exchanged by chlorides forming the same active 14-electron species as the original starting complex **M31** does.[101] To strengthen this proof, a second monomer namely dimethyl bicyclo[2.2.1]hept-5-ene-2,3-phenylketone (**Mon2**) was added to the NMR tube, again leading to a new carbene at 18.30 ppm in both cases. Trapping the

---

[101] J. S. M. Samec, B. K. Keitz, R. H. Grubbs, *J. Organomet. Chem.* **2010**, *695*, 1831-1837.

active species with the SIMes analogues unfortunately failed. After comparing the polymerization data of **3**-**6** with the data of **6** it was obvious, that the small amount of initiator which is activated in the SIMes derivatives is too small to be detected via NMR spectroscopy.
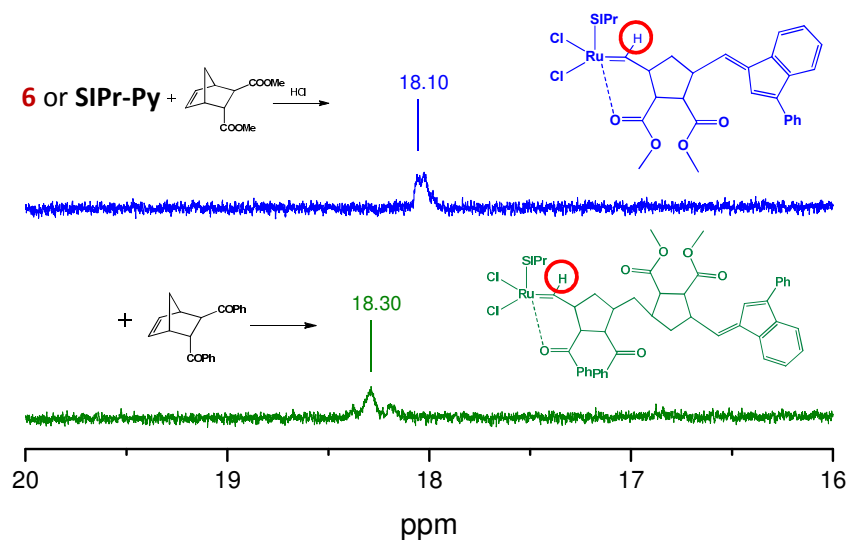
Figure 54: Active species of 6 and SIPr-Py; [Mon1/2]:[HCl]:[I] = 5:5:1; CDCl₃

Noteworthy, hydrochloric acid is the only acid which activates **3** to **6**. Initiation with other acids, for example acetyl chloride or trifluoroacetic acid, did not lead to any reaction. Also the addition of chloride containing salts, e.g. triethanolamine hydrochloride could not activate the metathesis reaction. A possibility to circumvent the use of hydrochloric acid is the application of HCl releasing reagents such as trimethylsilylchloride.

3.2.3.4   DFT Calculations

After the question about the actual active species was cleared up, the question about the detailed activation steps arose. The quinolinolate ligand can either be protonated at a nitrogen or at an oxygen atom. Another thing which still remained unclear was, which of the two quinolinolate ligands gets protonated first; the one *trans* to the carbene or the one *trans* to the SIMes. Lastly, the probably most interesting question which still remained unresolved was the question about why the two Hoveyda derivatives **4a** and **4b** exhibit such different polymerization activities. To shed light about the different behavior of complexes

4a and **4b** DFT calculations were envisaged.[102,103] In agreement with experiments, which indicated **4b** as the more stable isomer, calculations estimate that **4b** is 2.0 kcal/mol more stable than **4a**. To rationalize the different reactivity of **4a** and **4b** we compared the basicity of the 4 oxygen atoms by calculating the energy of the acid-base equilibrium shown in Equation 3,

Equation 3:

$$[Ru](CH_2Cl_2) + proton\ in\ water <=> [Ru]H+(CH_2Cl_2) + water$$

where [Ru] is **4a** or **4b**, [Ru]H^{+} is **4a** or **4b** with a protonated O atom. The energy of [Ru] and [Ru]H^{+} is calculated in DCM using the protocol described in the computational details sections, while for the aqueous solvation free energy of the proton we assumed the value of -262.2 kcal/mol from the literature[104] Equation 3 assumes that the protonated Ru species remains in the organic phase. The energetics of Equation 3 for the four O atoms of **4a** and **4b** are reported in Scheme 7.

---

[102] The optimized geometry of l is in perfect agreement with the X-ray structure (rmsd = 0.032 and 0.031 ement with the X-ray s and 0.9°nd 0.9031 e, where rmsd is calculated for distances and angles: sn-1 = [i=1→N (CV - EV)2/(N - 1)]1/2, where CV means calculated value, EV means experimental value (X-ray data), and N is the number of distances or angles taken into account.

[103] a) X. Sala, E. Plantalech, I. Romero, M. Rodríguez, A. Llobet, A. Poater, M. Duran, M. Solo, S. Jansat, M. Gó S., T. Parella, H. Stoeckli-Evans, J. Benet-Buchholz, *Chem. Eur. J.* **2006**, *12*, 2798-2807; b) J. Mola, M. Rodrb) Jz, M. Romero, A. Llobet, T. Parella, A. Poater, M. Duran, M. Solo, J. Benet-Buchholz, *Inorg. Chem.* **2006**, *45*, 10520-10529; c) A. Poater, L. Cavallo, *Inorg. Chem.* **2009**, 48, 4062hem.,; d) A. Poater, X. Ribas, A. Llobet, L. Cavallo, M. Solà, *J. Am. Chem. Soc.* **2008**, *130*, 17710-17717; e) C. Samojłowicz, M. Bieniek, A. Pazio, A. Makal, K. Wozniak, A. Poater, L. Cavallo, J. Wójcik, K. Zdanowski, K. Grela, Chem. Eur. J. 2011, 46, 12981-12993; f) J. Mola, I. Romero, M. Rodríguez, F. Bozoglian, A. Poater, M. Solào T. Parella, J. Benet-Buchholz, X. Fontrodona, A. Llobet, *Inorg. Chem.* **2007**, *46*, 10707-10716; g) A. Poater, F. Ragone, A. Correa, A. Szadkowska, M. Barbasiewicz, K. Grela, L. Cavallo, *Chem. Eur. J.* **2010**, *16*, 14354-14364.

[104] G.J. Tawa1, I.A. Topol1, S.K. Burt, R.A. Caldwell, A.A. Rashin, J. Chem. Phys. 1998, 109, 4852-4963.

(6.5)	(2.3)	(4.0)	(-5.3)
4a^{I}H$^+$	**4a^{II}H$^+$**	**4b^{I}H$^+$**	**4b^{II}H$^+$**
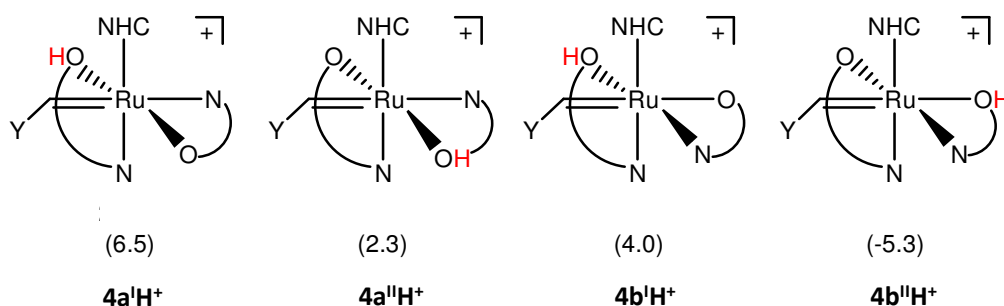
Scheme 7: Energetics of 4a and 4b protonation as in Equation 3, in kcal/mol

According to the numbers reported in Scheme 7, protonation of both O atoms of **4a**, leading to species **4a^{I}H+** and **4a^{II}H$^+$,** is unfavored, as well as protonation of the O atom of **4b** *cis* to the NHC ligand, leading to **4b^{I}H+**. The only O atom presenting a favorable protonation energy is the O atom *trans* to the Ru-alkylidene bond of **4b**, leading to **4b^{II}H+**. It is quite difficult to have an idea of the accuracy of the absolute protonation energies of Scheme 7, since they can vary with the computational protocol (i.e. functional, basis set and solvation model) and they also depend on experimental considerations, since Equation 3 is based on the assumption that all the Ru species are in the organic phase, while HCl is dissociated in aqueous phase. For this reason we do not stress further the absolute value of the protonation energies. However, the relative trend in the protonation energies is in agreement with the general idea that protonation of the O atom trans to the Ru-alkylidene bond should be favored, since this leads to a much softer –OH ligand *trans* to the Ru-alkylidene bond. Consistently, the protonated Ru-O distance increases by roughly 0.11 Å in **4a^{I}H$^+$**, **4a^{II}H$^+$**, and **4b^{I}H$^+$**, whereas it increases by 0.18 Å in **4b^{II}H$^+$**.

Having established a possible entry point to the activation of **4b** by HCl, we investigated the whole reaction pathway leading to the conversion of **4b** to a classical Hoveyda type complex. The activation pathwy is shown in Figure 55. After protonation of the O atom *trans* to the alkylidene ligand, a chloride anion could dissociate the Ru-OH bond through transition state **4b^{II}H$^+$ → 4b^{II}**, with displacement of the –OH group and coordination of the chloride *trans* to the alkylidene group. The next step corresponds to a rotation of the chloride ligand from the coordination position *trans* to alkylidene ligand to a coordination position *cis* to both the alkylidene and the SIMes ligands. This rearrangement requires dissociation of the quinoline N atom, and complete release of a neutral quinoline type ligand, leading to **4b^{III}**, 13.5 kcal/mol below **4b^{IV}**.

Protonation of the second O atom is calculated similarly to Equation 3, is disfavored by 7 kcal/mol. For this reason, it was searched for a transition state in which protonation of **4b^{III}** occurs by a HCl molecule through a concerted transition state in which the proton of HCl protonates the oxygen of the quinolinate while the chloride coordinates *trans* to the ylidene group. This concerted transition state costs only 1.5 kcal/mol and thus is favored over protonation followed by Cl$^-$ coordination. The final product is **4b^{IV}**, 17.0 kcal/mol below **4b**,

with the attacking Cl atom *trans* to the Ru-alkylidene bond. Of course, direct HCl attack to **4b** via a concerted transition state is not possible, since the Ru center of **4bI^V** has no vacant coordination position. Back to the second protonation step, **4b^{IV}** evolves to **4b^V** through a shift of the second Cl atom from the coordination position *trans* to the Ru-alkylidene bond to reach a geometry with a *trans* disposition of the two Ru-Cl bonds. Species **4b^V** corresponds to 14 e$^-$ species that can be formed by dissociation of the isopropoxy group from the classical Hoveyda catalyst **Hov**, which can be obtained by **4b^V** through coordination of the isopropoxy group. The overall energy balance for the transformation of **4b** to **Hov** is 33.1 kcal/mol downhill in energy.
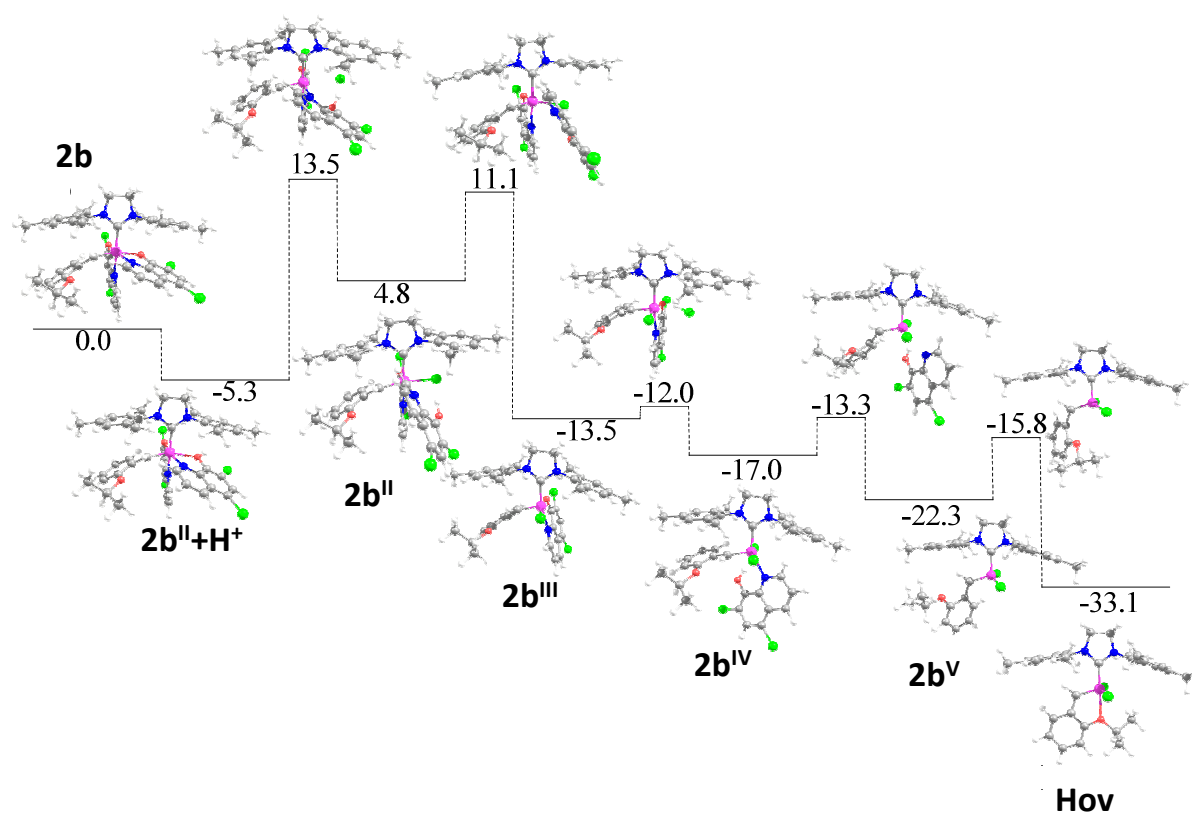
Figure 55: Reaction pathway of the transformation of 4b to Hov (in kcal/mol)

Similar energy profiles, corresponding to the transformation of **4a^{I}H$^+$**, **4a^{II}H$^+$**, and **4b^{I}H$^+$** into **Hov** are reported in Scheme 8, where also the protonation of the N atom of the quinolinate ligand has been explored.
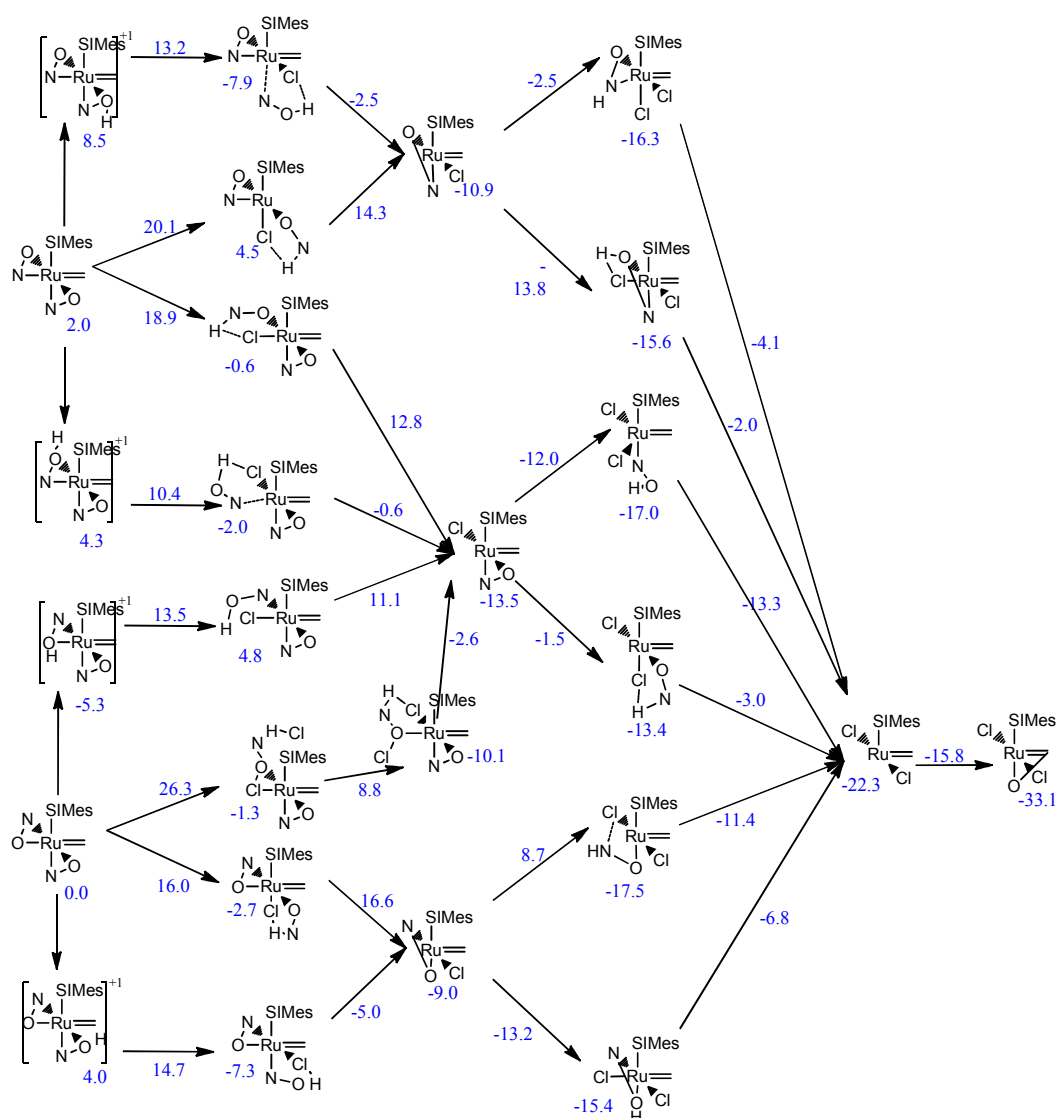
Scheme 8: Reaction pathways for 4a and 4b (in kcal/mol); the ligands have been simplified for the sake of clarity

3.2.4   DCPD

Due to the latent character and the retarded activation of the pre-catalysts, they may be suitable catalysts for the polymerization of very active strained monomers such as **DCPD**. Furthermore, **3-6** are very beneficial for the polymerization of **DCPD** due to their outstanding solubility in the neat monomer making a solvent free polymerization possible. **DCPD** is a cheap monomer which gains more and more attention for large scale applications. **pDCPD** is interesting due to its high impact strength and nowadays used for production of body panels for trucks, agricultural and earth moving equipment, cell covers for chlor-alkali plants, domestic waste water treatment units and large waste containers.[40,41] The main challenge of the polymerization of **DCPD** is to guarantee an adequate mixing of monomer and catalyst to obtain a homogenous reaction mixture and moreover a steadily polymerized product. **DCPD**

is also prone to undergo a Retro-Diels-Alder reaction at higher temperatures to the volatile cyclpentadiene, causing a mass loss during polymerization. Figure 56 shows the STA measurement of neat **DCPD**. The green curve represents the endothermic reaction of the Retro-Diels-Alder reaction. The blue curve depicts the mass loss during the reaction. The decomposition temperature is stated to be 69°C (determined from the DTA curve). At this point the overall mass loss accounts for 3 %.
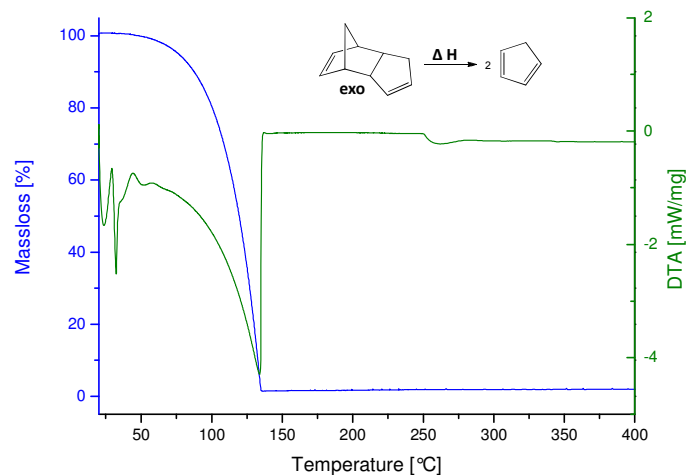
Figure 56: STA measurement of Retro Diels Alder reaction of DCPD; measurement was performed using a temperature program of 3 °C/min; the TGA is operated with a helium flow rate of 50 mL/min used in combination with a protetctive flow of 8 mL/min

The decomposition temperature is a crucial point for the polymerization of **DCPD**. Perfectly suited initiators for the ROM polymerization of **DCPD** are latent at room temperature, but can be triggered below this temperature.

Due to the second double bond present in the tricyclic system of **DCPD**, cross-linking occurs during polymerization, hence forming a three-dimensional network. The outstanding mechanical properties are owed to this cross-linked system.
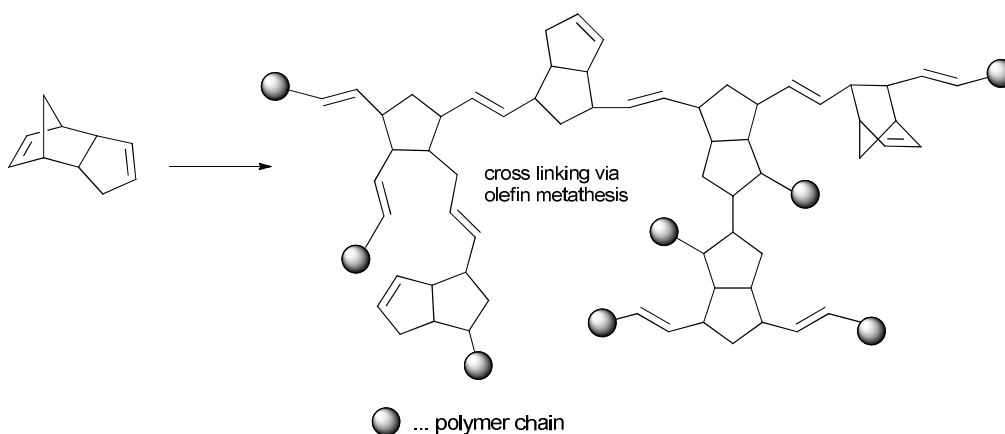
Scheme 9: Benchmark ROM polymerization of *endo/exo*-dicyclopentadiene

3.2.4.1   STA Measurements

To evaluate the qualification of pre-catalyst **3-6**, STA measurements were performed. The following procedure was observed: A weighted amount of pre-catalyst was dissolved directly in liquid **DCPD** so that an initiator amount of 100 ppm was maintained. 1 mL of the monomer/initiator mixture was transferred into a vial and 50 eq of HCl in diethylether were added. The reaction mixture was frozen immeditaly in liquid nitrogen to avoid an early polymerization. The STA measurement was performed using a heating rate of 3 °C/min and a constant helium gas flow of 50 mL/min. In an open system such as the STA system, the volatile cyclopentadiene is removed from the equilibrium by the gas stream.

In Figure 57 representative examples for a successful, a partly succesful and an unsuccessful **DCPD** polymerization are shown. **4a** and **5** totally fail the polymerization of **DCPD**. The monomer decomposes completely before any curing occurs. **3b** and **4b** on the other hand polymerize **DCPD** which can be seen by the exothermic peaks. **4b** requires more time to start the polymerization which causes a higher mass loss of the monomer. **3a** shows some curing, but the main part of the monomer decomposes before it can be polymerized. The exothermic peak of the polymerization merges into the endothermic peak of the monomer decompostion and hence is not visible.
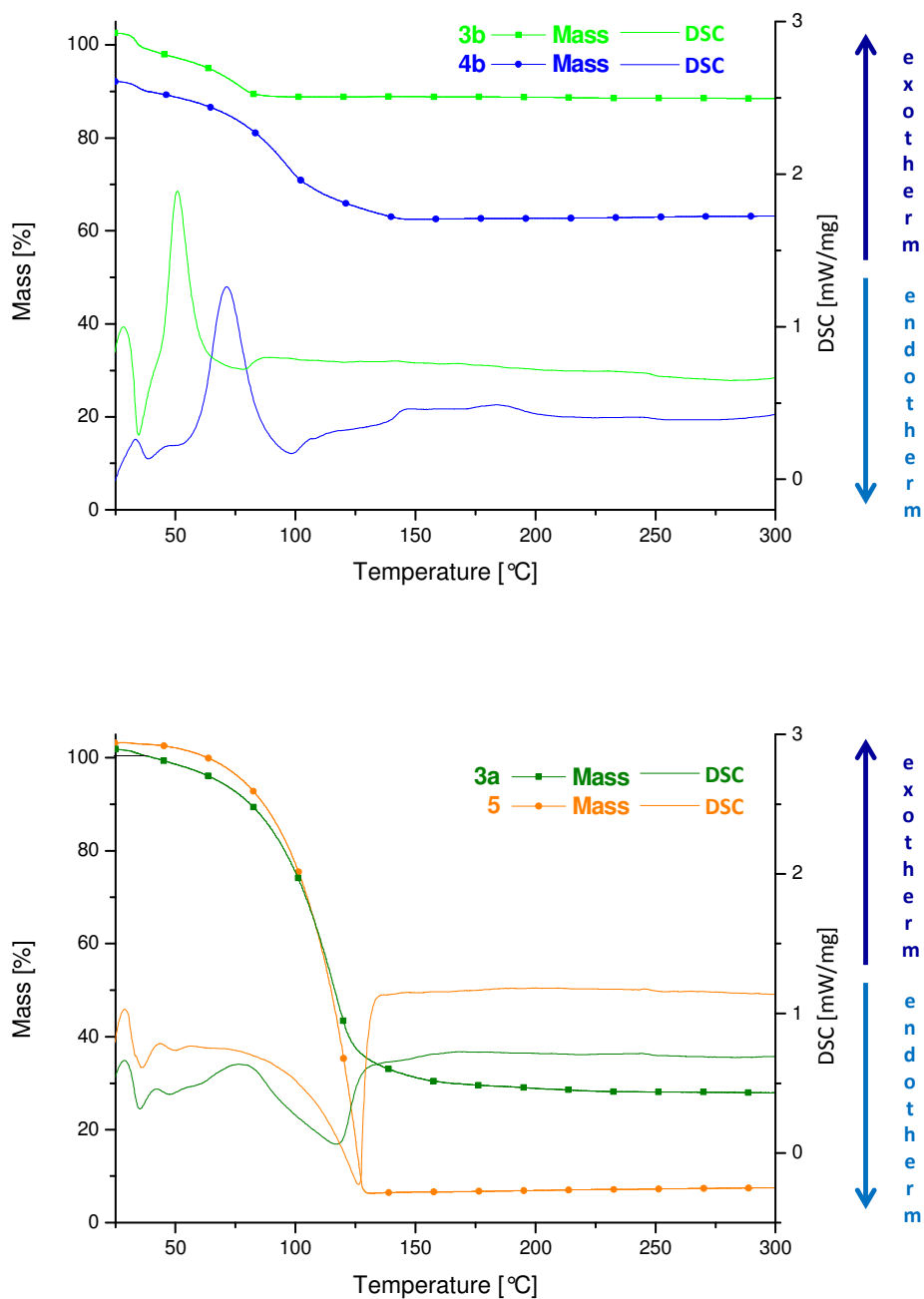
Figure 57: STA measurements of 3a, 3b, 4b and 4 with DCPD; 4a shows the same behavior as 5 and is therefore not displayed; reaction conditions: [I]:[DCPD]:[HCl]: 1:10.000:50; temperature program: 3 °C/min; the TGA is operated with a helium flow rate of 50 mL/min used in combination with a protetctive flow of 8 mL/min

Table 16: STA data with DCPD

Initiator	Onset [°C]	Peak max. [°C]	Mass loss [%]
3a	-	-	78
3b	45.4	50.8	11.5
4a	-	-	100
4b	59.8	71.3	27.5
5	-	-	100

3.2.4.2   Shoulder Test Bars – General Aspects

In general the mechanical properties of polymers are tested via tensile strength tests. The test specimen is subjected to a uniaxial tension until failure occurs. By doing so several parameters such as the Young's modulus (E), the ultimate tensile strength (R_m) and some others can be deduced. Shoulder test bars were selected as the specimen form of choice. The mold of the test samples is shown in Figure 58.

l_1 = 30 mm
l_2 = 65 mm
l_3 = 140 mm
r = 20 mm
h = 5 mm
b_1 = 8 mm
b_2 = 25 mm
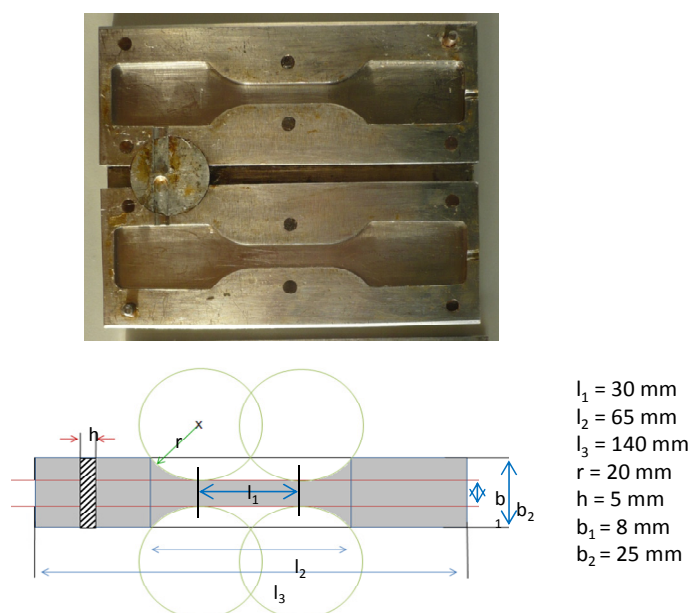
Figure 58: Shoulder test bar mold with the corresponding measures

The commonly used practice for the generation of shoulder test specimen is, to mix the initiator with melted **DPCD** and to pour this formulation into a pre-heated mold. It is essential that the initiator is completely dissolved in the monomer, making the use of some solvents unavoidable in some cases. If the initiator is not totally dissolved in the monomer, parts of it cannot participate in the reaction and therefore a non-reproducible, distorted

result will be received. The up warm of the mold in advance was necessary to ensure that the applied solvent evaporates before a curing of the sample takes place thus preventing that bubbles or cracks are formed within the sample. After a sufficient curing of the test specimen, they were taken out of the mold and curing was continued in the oven at around 70°C overnight. The specimens were inserted into the tensile test machine with a distance of 8 cm between the two clasps. The test was executed with a tractive rate of 1 mm/min.
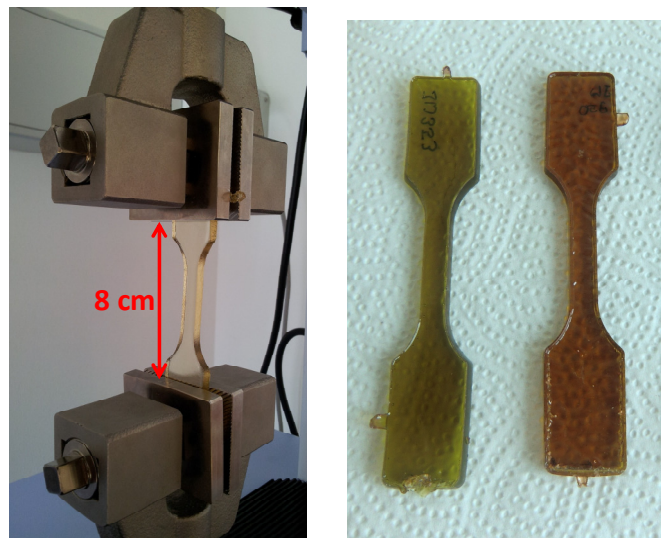
Figure 59: Setup for the tensile strength test (left); DCPD shoulder test bars (right)

The determination of the Young's modulus was made according to the following equation:

Equation 4: Calculation of the Young's modulus

$$E = \frac{\sigma}{\varepsilon} * 100 = \frac{F/A}{\Delta L/L} * 100$$

E   Young's Modulus [MPa]
σ   stress [MPa]
Ɛ   strain [%]
F   tensile force applied
A   cross sectional area: 35.2 [mm^2]
L   distance between clamps: 80 [mm]
ΔL   elongation

The values taken are from the slope within the linear part of a curve. For the actual stress in MPa, the tensile force applied had to be divided through the cross section area of 35.2 mm^2. For the strain in percentage the measured elongation had to be divided through the distance the test specimen was inserted between the two clamps.

The $R_{p\ 0.2}$ value determines the yield stress after 0.2 % deformation. It is taken from the intersection between a line, starting from 0.2 % deformation which is collateral with the linear part of the curve, and the curve itself.

The ultimate strength (R_m) is the stress determined from the maximum applied traction based on the sectional area of the test specimen. It can be directly assigned from the highest point at the Y-axis in the stress-strain-chart.
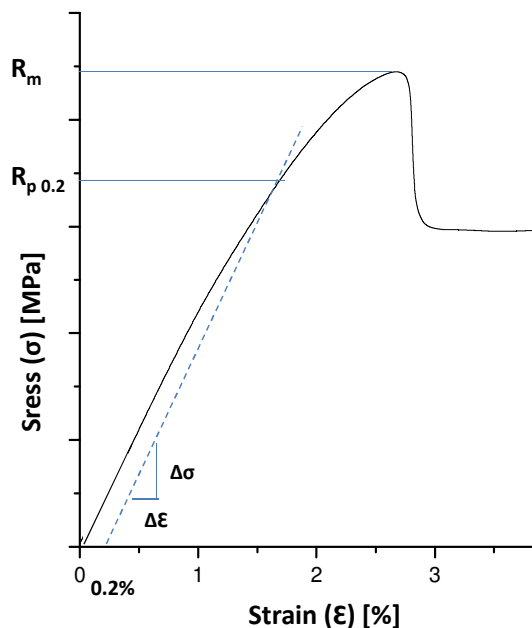
Figure 60: Graphical depiction of the characteristic data

3.2.4.3   Shoulder Test Bars made with 3-6

Due to the good solubility of complex **3** to **6,** they were directly mixed with neat **DCPD** without the addition of any solvent, until a homogenous solution was acquired. If necessary the solution was put shortly into an ultrasonic bath. Subsequently, 50 eq of hydrochloric acid were added and the reaction mixture was poured immediately into the pre-heated shoulder test mold. The test samples were cured in the oven at 70°C overnight. The best results were obtained when an initiator amount of 100 ppm was used. With initiator **4b**, also shoulder test bars with 50 ppm were made, resulting in a distinct decrease of the mechanical properties. Obviously initiator amounts below 100 ppm yield not enough active initiator to polymerize and cross-link the whole sample.
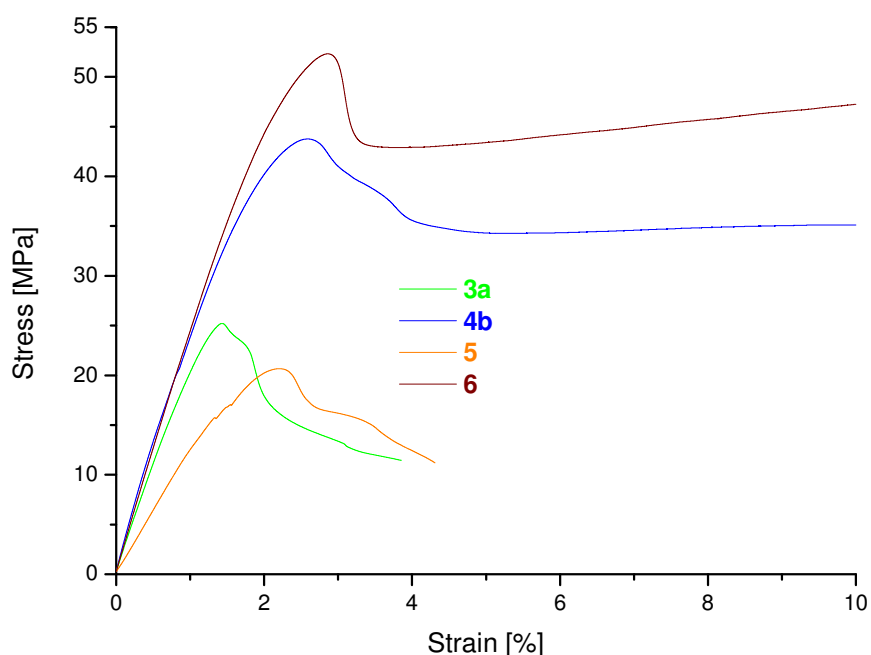
Figure 61: Tensile strength test of pDCPD; 100 ppm catalyst loading, 50 ppm HCl; measuring rate of 1 mm/min

Table 17: Tensile strength data of pDCPD

Initiator	Young's Modulus [MPa]	$R_{p\,0.2\%}$ [MPa]	R_m [MPa]
3a[a]	2137	24.4	25.2
3b[b]	-		-
4b[a]	2635	32.3	43.8
5[a]	1277	19.1	20.7
6[a]	2664	43.3	52.3
Comparative example[105]	1870 - 1980		$43.0 - 46.8$

[a] Values are taken from polymerizations with 100 ppm of the corresponding initiator and 50 ppm of HCl in diethylether

[b] no shoulder test bars could be obtained wit initiator **3b**

Matching the results of the polymerizations with **Mon1**, **6** is the best suited initiator for the preparation of **pDCPD** within this quinolinolate series. **5** and **3a** again exhibit the poorest polymerization performance leading to shoulder test bars with very low R_m values. Although, the test bars made with **3a** exhibit a satisfying Young's modulus, comparable with literature

---

[105] http://www.matweb.com/search/DataSheet.aspx?MatGUID=16d3d6b1e32c4c368fa1ddac6afb2b93&ckck=1

data. The Young's modulus of **4b** and **6** are even better than the comparative example taken from literature. The overall elongation ranges in every case between 1 % to 3 %. Concluding, the quinolinolate pre-catalysts are very useful initiators for the polymerization of **DCPD**, due to their pronounced latency and the outstanding solubility. The only drawback is the high amount of initiator required.

3.2.5   RCM

For the sake of completeness, RCM reactions were performed using the standard benchmark substrate **Dedam** (diethyldiallylmalonate). **Dedam** exhibits two unsubstituted double bonds, and hence is very easily ring closed. In contrast to the ROMP reaction, the driving force in the RCM is the release of ethylene during the metathesis reaction. The RCM experiments were performed in Schlenk flasks under nitrogen atmosphere. Catalysts **3**-**6** (1 eq) were dissolved in degased DCM and **Dedam** (100 eq) was added. The overall solvent concentration was fixed at 0.1 mol/L with respect to the substrate. 2 drops of HCl aqu. were added. The activation of the initiators was again observable by a color change of the reaction solution. Periodically samples were taken and directly put into an NMR tube. The tube was filled with CDCl$_3$ and ^{1}H NMR spectra were recorded. The procedure was repeated until the reaction was complete or no further conversion of the substrate could be observed. Conversions were plotted against reaction time to obtain the turn-over plots.
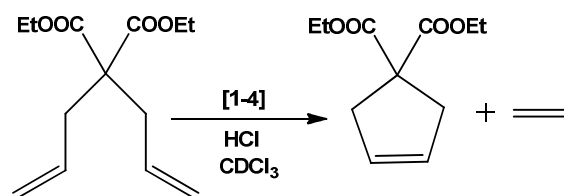
Figure 62: RCM of Dedam

The general trend, determined from the ROMP reactions, was also retained for the RCM reactions. The best performances show pre-catalyst **6** and **3b**. **4b** also yields nearly 100 % conversion, but in an unsatisfying time. None surprisingly, **3a**, **4a** and **5** are activated and start the reaction, but conversions stay very low. **3a** yields a maximum conversion of 52 %, **4a** and **5** of only 7 %.
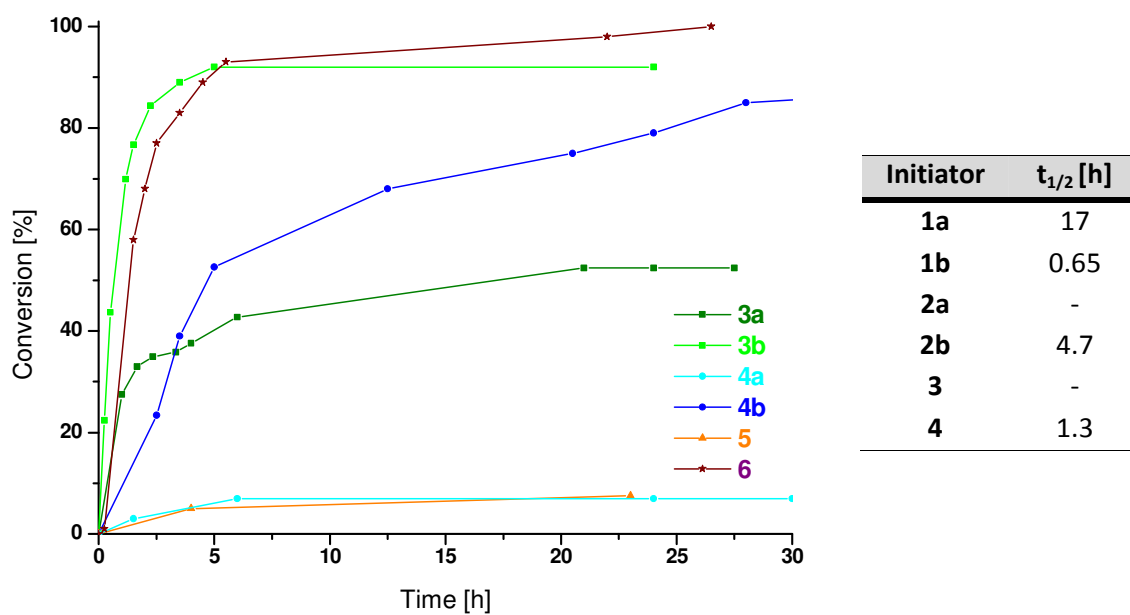
Figure 63: RCM of Dedam; [Dedam]:[I]= 100:1; 0.1 mol/L with respect to Dedam, RT, 2 drops of HCl aqu.

Initiator	$t_{1/2}$ [h]
1a	17
1b	0.65
2a	-
2b	4.7
3	-
4	1.3

3.3 Initiators with a Chelating Lactic Acid Carbene

The following studies evaluate the performance of three different ruthenium initiators **7–9** bearing a lactic acid containing carbene ligand. The initiators combine the characteristics of the Hoveyda ligand implicating a chelating ether moiety of the carbene with the characteristics of a tangling ligand which is coordinated to the ruthenium center over the anionic ligand. This means, that in case of **7–9** one and the same ligand is connected over three different positions to the ruthenium center. The remaining anionic ligand of the pre-catalysts is occupied by a chlorine in **7**, by a iodine in **8** or by a trifluoroacetate in case of **9** (see Figure 64). The initiators were synthesized by the working group of Karol Grela from the University of Warsaw who already investigated the performance of the pre-catalysts in RCM reactions using different substrates.[106,107] Their studies already revealed the latent character of these initiators at room- or lower temperatures. In this study, the efficiency of the pre-catalysts is tested using Ring Opening Metathesis Polymerization and compared to the commercially available second generation Hoveyda (**Hov**) initiator and to the third generation initiator **M31**.
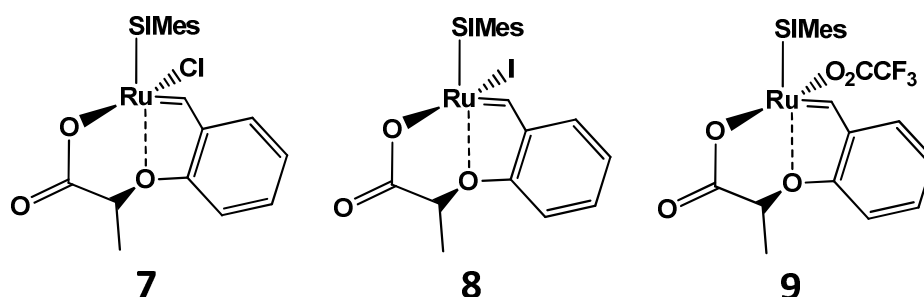
Figure 64: Initiators used in this study

For the ROMP Reaction the benchmark monomer **Mon1** was used.

3.3.1 Polymerization Reactions

The polymerization reactions of catalyst **7-9** are all performed under the same reaction conditions using Schlenk techniques. 100 mg (300 eq) of **Mon1** and the corresponding

---

[106] R. Garwin, A. Makal, K. Woźniak, M. Mauduit, K. Grela, *Angew. Chem.* **2007**, *119*, 7344-7347.

[107] M. Bieniek, R. Bujok, M. Cabaj, N. I. Lugan, G. Lavigne, D. Arlt, K. Grela, *J. Am. Chem. Soc.* **2006**, *128*, 13652-13653.

amount of initiator (1 eq) were dissolved under a nitrogen atmosphere in 4.8 mL of DCM to adjust a monomer concentration of 0.1 mol/L. The corresponding amount of acid (50 eq) was added to the monomer solution in one fast step. Polymerization progress was monitored using thin layer chromatography (TLC) and the monomer was visualized using the oxidizing reagents $KMnO_4$. After full conversion was determined, the reaction was quenched using a huge excess of ethylvinylether. The reaction volume was reduced to approximately 1 mL and added dropwise into cold vigorously stirred methanol. The resulting polymer was sampled, dried and analyzed via GPC.

7: X=Cl
8: X=I
9: X=CF$_3$COO$^-$
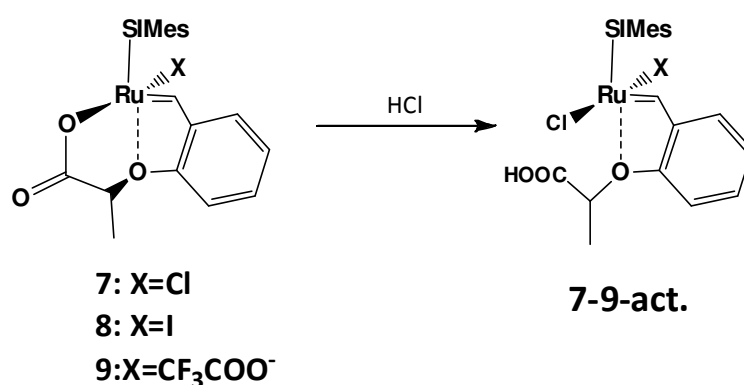
7-9-act.

Scheme 10: Activation of initiator 7-9 with HCl

According to the proposed reaction mechanism of the Grela group, the initial catalysts **7-9** are transferred to the metathesis active species **7-9-act** after the addition of acid. Therefore, the first reactions were performed using hydrochloric acid in diethyl ether to ensure good mixing of the polymerization solution and the acid and hence a fast activation. The results show that the polymerization characteristics especially of catalyst **7** and **8,** are similar to those of **Hov**, but the activation step seems not to be complete which is indicated by the higher molecular weights. Interestingly **8** shows the poorest polymerization behavior which can be caused by two possibilities: Either the more bulky iodine hinders the attack of the chlorine which is indicated by the higher PDI meaning that the activation and ongoing initiation step is retarded and occurs over a period of time, or the iodine solely hinders the attack of the olefin and thus delays the propagation. Most probably it is a combination of both effects. In any case, the activity decreases due to the iodine which is already well described in literature.[108] A second polymerization series using hydrochloric acid in water except of HCl in diethylether was also performed. The polymerization data (shown in Table 18) are in good agreement with the data of the diethylether serial.

---

[108] a) J. Wappel, C. A. Urbina-Blanco, M. Abbas, J. H. Albering, R. Saf, S. P. Nolan, C. Slugovc, *Beilstein J. Org. Chem.* **2010,** *6,* 1091–1098. b) E. L. Dias, S. T. Nguyen, R. H. Grubbs, *J. Am. Chem. Soc.* **1997**, *119*, 3887-3897.

Table 18: Polymerization data of 7-9 with Mon1 and 50 eq HCl

Initiator	Time [h]	Conversion [%]	isol. Yield [%]	M_n [g/mol]	PDI
Hov	1	100	49	76380	1.2
[a]7	1	100	91	142390	1.3
[a]8	6	100	63	203420	1.6
[a]9	1	100	92	143100	1.3
[b]7	1.5	100	84	145670	1.4
[b]8	5	100	77	117540	1.4
[b]9	1.5	100	74	134580	1.4
[c]7	1	100	71	156280	1.3

Reaction conditions: [I]:[Mon]=300; 0.01 mol/L, DCM, RT, 50 eq HCl
[a] hydrochloric acid in diethylether
[b] hydrochloric acid in water
[c] first the initiator was mixed with the acid, the monomer was added after 5min of mixing

Due to the somehow heightened PDI's it was investigated, if the moment of the acid addition plays a role for the polymerization behavior. If a retarded activation process caused by the chlorine substitution was the reason for this slightly increased PDI, a pre-reaction time of the initiator with the acid should lead to more narrow PDI values. Therefore another experiment using **7** was performed, whereby the initiator was mixed firstly with the acid and stirred for about 5 min. The polymerization finished after the same time-period and also PDI and molecular weight are in the same range as without this pre-reaction time.

As already shown with other initiators, the amount of acid can influence the polymerization performance of the initiators significantly. Therefore, the HCl dependency was investigated using pre-catalyst **7**. Polymerization reactions under standard conditions were run with increasing amounts (10 eq to 100 eq) of HCl. The results are depicted in Figure 65. Compared to the results of chapter 3.2.3.1, just a small decrease of the molecular weight occurs with increasing acid quantities. Nevertheless when the amount of HCl is increased from 10 eq to 50 eq a bigger amount of pre-catalyst gets activated. Raising the acid amount from 50 eq to 100 eq, the difference in the activation enhancement is negliable. This deviation can also be deduced to weighting errors, handling mistakes or imprecisions of the GPC analysis. Still here it has to be pointed out, that the amount of acid added for metathesis reactions is not irrelevant.
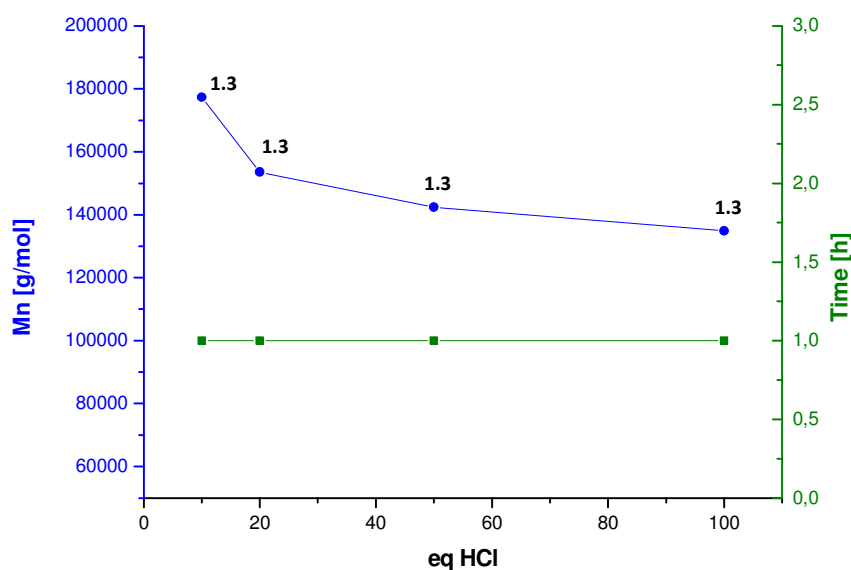
Figure 65: HCl dependency of 7 determined using Mon1 under standard reaction conditions (RT, [I]:[Mon1] = 300:1, DCM, 0.1 mol/L with respect to the monomer)

Due to the structure and the activation mechanism of these initiators, many different pre-catalysts bearing varying mixed anionic ligands can be prepared very easily. Hence, the attempt to activate pre-catalyst **7-9** via the addition of another acid, namely trifluoroacetic acid was done. Interestingly, only **7** was successfully activated and yielded 100 % conversion. The PDI again is comparable with the one of the hyrochlorid acid activated polymerization, although the polymer exhibits a lower molecular weight. **8** and **9** on the contrary were just minimally activated and yielded very low conversions of < 25 %. M_n and PDI values were not determined in this case.

Table 19: Polymerization data of 7-9 with [I]:[Mon1]=300; 50 eq CF$_3$COOH, 0.1 mol/L [Mon1], RT, DCM

Initiator	Time [h]	Conversion [%]	isol. Yield [%]	M_n [g/mol]	PDI
Hov[a]	1	100	49	76380	1.2
7	5	100	85	86400	1.4
8	22	39	-	-	-
9	22	15	-	-	-

[a] no CF$_3$COOH was added

As it is known from literature, latent initiators can often be triggered using different activation mechanisms. Therefore we had a closer look at the thermal properties of the

initiators. Standard polymerizations without acid, but at 80°C in toluene were performed revealing that a thermal activation of the pre-catalysts is also possible. Using heat, the initiators are less active than after acid activation. After about 22 hours at 80°C, none of the catalysts was capable to finish the reaction and no further progress could be detected via TLC. Therefore the reaction was stopped prematurely and conversions were determined using ^{1}H NMR spectroscopy. Again **7** is the most active catalyst within this family. The PDI is increased compared to the results of the acid activation, probably caused by a more difficult and therefore elongated activation mechanism. The relatively low molecular weight of the polymer is probably a result of the incomplete polymerization. Interestingly **8** outperforms **9** in this reaction and leads to a three-fold higher conversion.

Table 20: Polymerization data of 7-9 at 80°C with [I]:[Mon1]=300, toluene, 0.1 mol/L [Mon1]

Initiator	Time [h]	Conversion [%]	isol. Yield [%]	M_n [g/mol]	PDI
7	22.5	95	70	70950	1.7
[a]**8**	21.5	53	-	-	-
[a]**9**	21.5	14	-	-	-

[a] due to the low conversions M_n and PDI were not determined

Considering the acid activation mechanism, the anionic oxygen ligand is substituted against chlorine or another anion originating from the applied acid. Hence, the dissociation of the chelating ether moiety can proceed very easily. In case of the heat activation, two feasible activation pathways are possible which are illustrated in Scheme 11. Pathway A follows the normal metathesis route, but seems pretty unfavorable due to the hampered coordination of the olefin caused by the triple bonding of the carbene ligand to the ruthenium. Also the formed cyclic transition state after the first metathesis step seems doubtful. In contrast, pathway B and pathway C probably proceed via a bridged ruthenium dimer whereas a chlorine is transferred from one to another complex leading to an active species with two chlorines. This anionic ligand exchange was already observed several times in literature and is claimed to happen in solution constantly between all ruthenium species.[109] To investigate this activation mechanism closer, NMR experiments were performed. **7** was heated to 80°C in CDCl$_3$ overnight. The proton NMR spectra after 17 hours revealed, that there were 3 % of the dichloro species (δ = 16.74 ppm) present in the reaction solution. Continuing heating leads just to a very low increase of the dichloro species (5 % after 41 h). In another experiment a chloride source, namely benzyltriethylammonium chloride, was added to **7** to see, if a heightened chloride content results in the formation of the dichloro species. Interestingly, absolutely no conversion to the active dichloro complex could be observed in

[109] T. Kiyotaka, V. P. W. Böhm, D. Chadwick, M. Roeper, D. C. Braddock, *Organometallics* **2006**, *25*, 5696-5698.

this case. Concluding, it is so far not totally clear how or which active species is formed by heat activation, but it could be shown that at least a small amount of the same active species as in case of the acid activation is formed during the heating process. This indicates that pathway C at least participates partly in the formation of the active species and hence in the polymer formation. Anyhow, the relatively low molecular weight of the polymer (see Table 20) suggests, that the dichloro species is probably not the only active species participating in the reaction and that perhaps all mentioned pathways happen at the same time to a different extend.
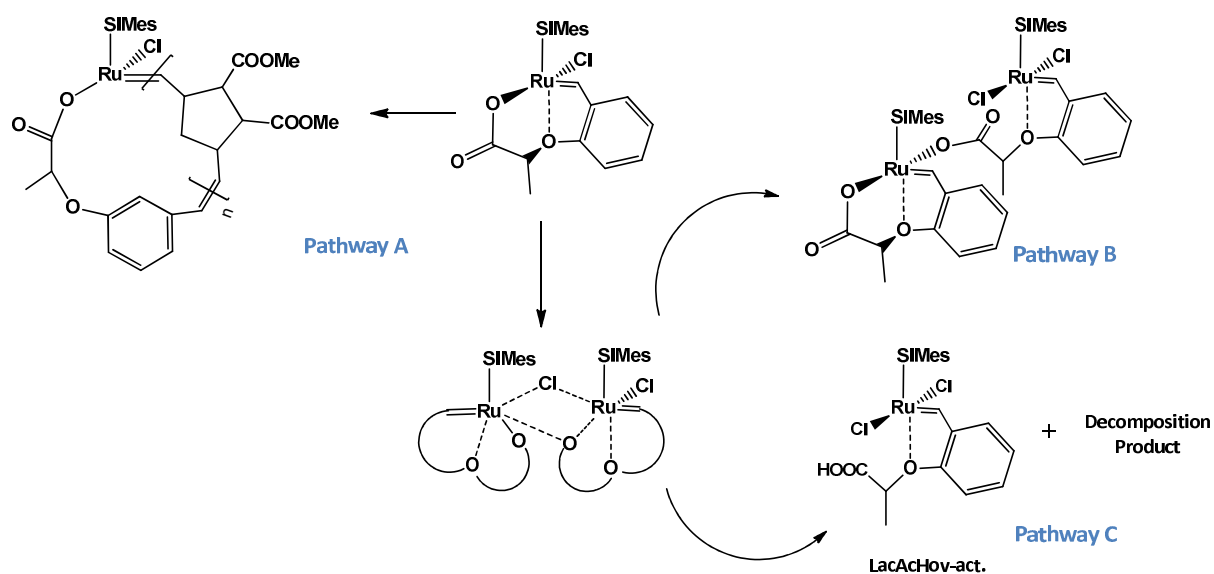
Scheme 11: Possible mechanism of of heat activation shown at the example of pre-catalyst 7

4 CIS AND TRANS CONFIGURATION IN POLYMERS

Within the following chapter the configuration of polymers and more important, the influence of the different initiator ligands is investigated more closely. The emphasis is set on the ratio of the *cis* and *trans* double bonds. Due to the fact, that the formed ROM polymers possess a double bond in the backbone of the polymer after every repeating unit, different polymer configurations are possible.
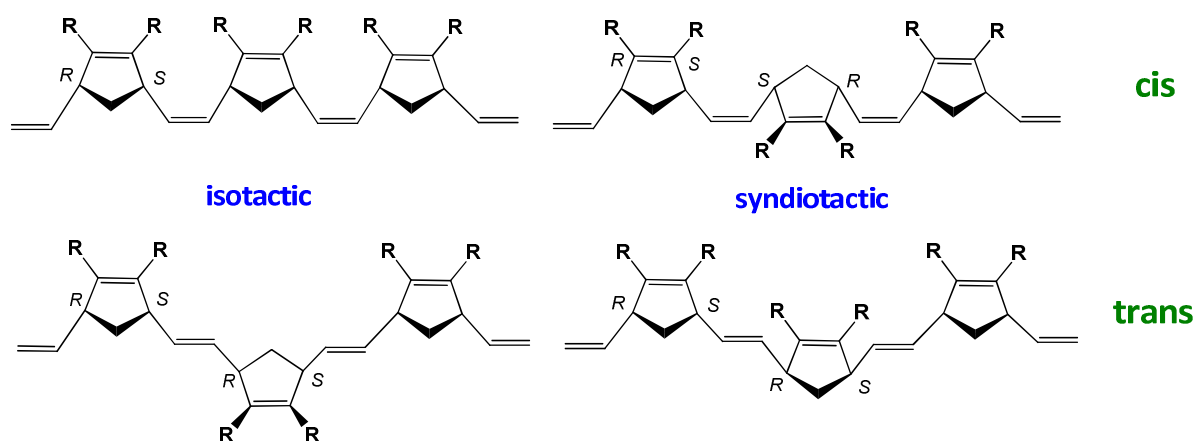
Figure 66: Possible configurations within a polymer

The first and foremost differentiation comes from the *cis* or *trans* configuration of the double bonds within the polymer chain. The second differentiation arises from the fact, that the allylic bridging carbons are chiral. Inside of one cyclopentenyl ring, the diad always consists of two stereo centers with an opposite chirality. Hence, depending on the repeating units, the polymer can be either isotactic, which means that the sequence of the chiral centers is always (-RS-RS-), or can be syndiotactic, indicating a racemic dyad of (-RS-SR-). Due to the symmetry in 2,3-disubstituted norbornadienes no head to tail arrangement can occur and therefore, only four different configurations in a polymer made from 2,3-disubstituted norbornadienes are possible. Furthermore, the substituents R influence the course of the polymerization. If more bulky substituents are used, they are able to shield the double bonds from an attack of the metathesis initiator and hence, narrower PDI values are possible to obtain. Polymers made with monomers possessing smaller R substituents basically exhibit a higher PDI.
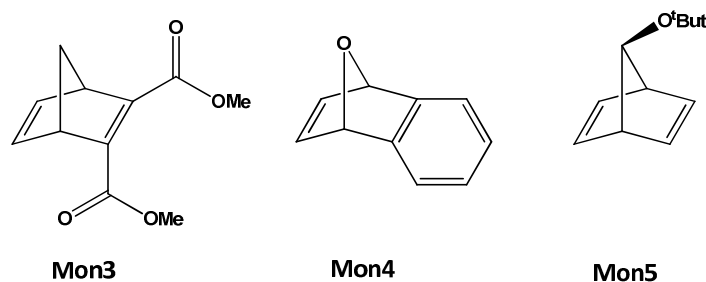
Figure 67: Monomers used for *cis/trans* studies

To cover all possible influences of the monomer on the configurations in the polymer, three different monomers, namely norbornadien-2,3-dicarboxylic acid dimethylester (**Mon3**), oxabenzonorbornadiene (**Mon4**), and 7-^{t}butyl-norbornadiene (**Mon5**) were used within this study. The corresponding polymers are consequently labeled with **poly3 – poly5**.

For the initial study, initiators with different ligands at all possible positions were used. All three catalyst generations (**M1**, **M2** and **M31**), chelating initiators (e.g. **Hov**), initiators with a *cis* configuration of the halides (**M22**) and initiators with different NHC's were applied. Most striking, within one polymer series, only the NHC seems to have an influence on the *cis/trans* ratio of the polymer. It should not go unmentioned, that the *cis/trans* ratio is also influenced significantly by the nature of the monomer. Differences are therefore also just discussed within one polymer series. In the following the influence of the NHC is investigated more closely.

4.1   Influence of Different NHC Ligands

The different initiators for the NHC study on the *cis/trans* ratio of **poly3–poly5** were mostly synthesized by our partners of the EUMET project. The **SIPr** NHC containing complexes were synthesized by the group of St. Andrews, the **o-tol** and **naphtyl** containing complexes by the Warsaw group and the **cyhexyl** NHC containing complex by our partners in Rennes. From the **SIPr** and the **o-tol** complexes, two different derivatives, namely the second and the third generation catalysts were applied. From the **naphtyl** and the **cyhexyl** complexes only the second generation initiator was used. In case of the **SIMes** containing catalysts additionally to 2nd and 3rd generation catalysts the chelating **Hov** was added in the group. The various NHC's differ mainly regarding the steric bulk of the substituents attached to the nitrogen in the imidazole ring. The **SIPr** NHC for example, is far more bulky than its *o-tol* analog. Furthermore, for a better comparison, the 1st generation complexes **M1** and **G1** were employed in the study.
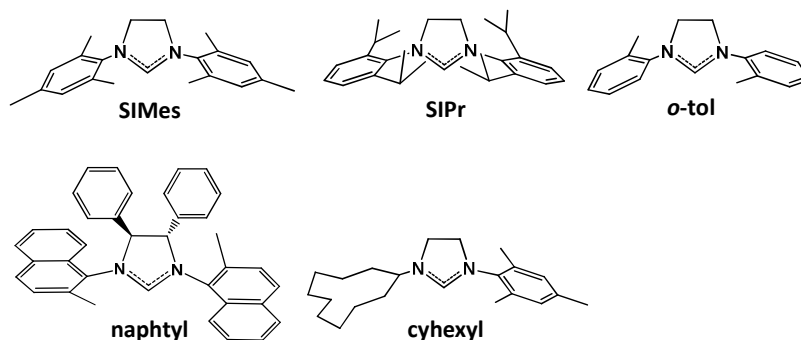
Figure 68: Used NHC's for *cis/trans* study

The polymerizations were made using standard reaction conditions with a monomer to initiator ratio of 100:1 in case of **Mon3** and **Mon4** and 300:1 in case of **Mon5**. All other reaction steps were maintained as described in ongoing chapters. Only the reference polymerizations with the first generation initiators were conducted at elevated temperatures due to the low activity of this initiator family. After a successful polymerization, ^{1}H NMR spectra, ^{13}C NMR spectra and in some cases IR spectra were recorded and the *cis/trans* ratio was determined. All NMR spectra were recorded in CDCl$_3$.

The *cis/trans* ratio in **poly3** can be either determined by the splitting of the olefinic double bonds in the backbone (*cis*: 5.53 ppm, *trans*: 5.41 ppm), or by the splitting of the C2 bridging atom (*cis*: 3.95 ppm, *trans*: 3.59 ppm) of the cyclopentenyl ring. The same splitting of the C2 carbon peak is observable in the ^{13}C spectra. The *trans* peak appears at 48.7 ppm and the *cis* at 44.4 ppm (for detailed information about the NMR spectra see the chapter 8.4.4 of the supporting information). **Mon3** exhibits similar properties as the standard benchmark monomer **Mon1**. PDI values of **poly3** are in comparable magnitudes to those of **poly1**. Polymers made with **SIPr** containing initiators also exhibit a bimodal distribution (chapter 3.2.3.). As can be seen from Figure 70, all of the initiators, except of the first generation initiators with a PCy$_3$ instead of a NHC, give **poly3** with raised *cis* contents. This fact was not very surprising, as first generation initiators are known to give polymers with a high *trans* content and second or third generation initiators with an increased *cis* content.[110,111] Noteworthy, the applied first generation initiator **G1** only yielded 11 % conversion, even when elevated temperatures and prolonged reaction times were used.

---

[110] J. G. Hamilton, U. Frenzel, F. J. Kohl, T. Weskamp, J. J. Rooney, W. A. Hermann, O. Nugken, *J. Organomet. Chem.*, **2000**, *606*, 8-12.
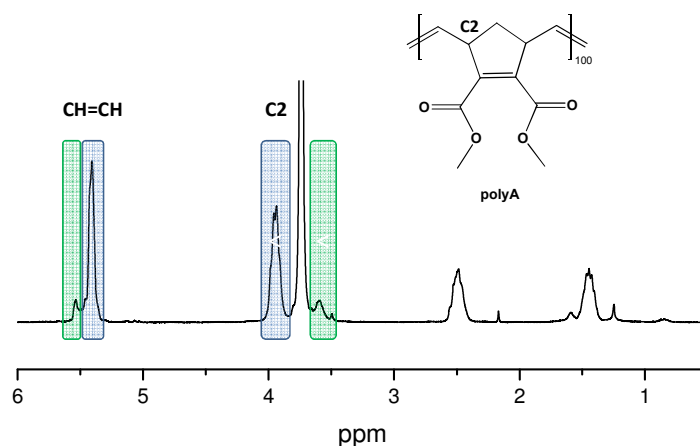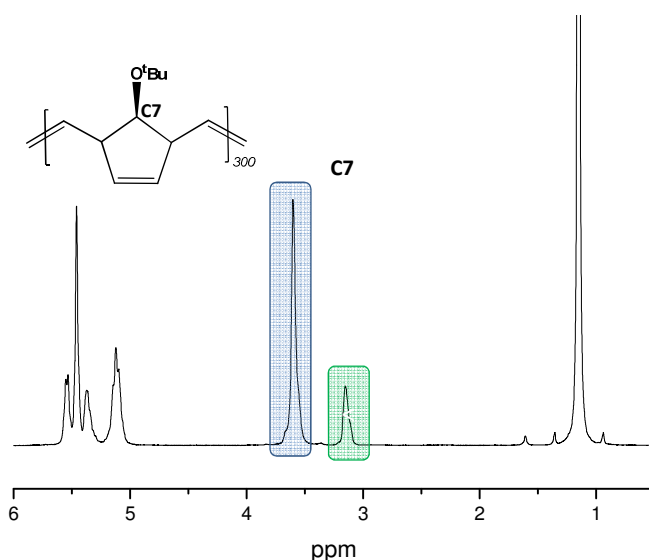
Figure 69: Proton NMR spectra of poly3 made with SIPr-Py; *cis* peaks are labeled in blue, *trans* peaks in green
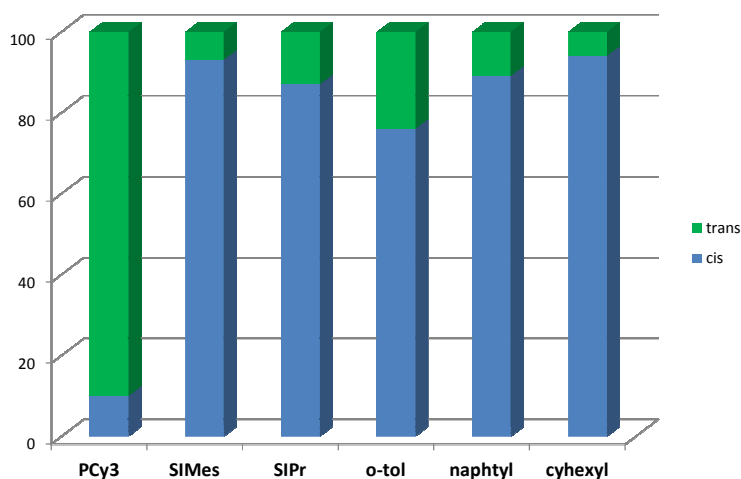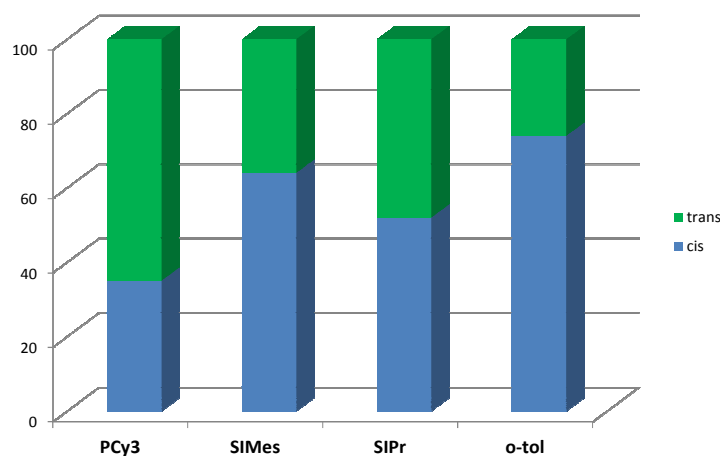

Figure 70: C*is* and *trans* ratio of poly3 of the various NHC's compared to reference initiators of the 1ˢᵗ generation; if two or more initiators with the same NHC were used within this series only small deviations were determined and therefore an average value of the *cis* and the *trans* ratio was taken

Interestingly, the **SIPr** and **naphtyl** initiators give polymers with a slightly increased *trans* content of the double bonds. In case of **poly3**, the highest amount of *trans* double bonds have polymers made with the **o-tol**, the smallest NHC tested. Within one initiator family (2ⁿᵈ and 3ʳᵈ generation catalysts with the same NHC) no considerable deviations in the *cis/trans* ratio are observable. Differences are just in a range of 1-2 %, which can be more likely traced back to integration errors during spectrum interpretation than to a different behavior of the catalysts themselves. This observation is also valid for the other polymers discussed later on.

For **poly4**, again the same peaks of the polymeric repeating units could be used for the determination of the *cis/trans* ratio. The *cis* peak of the double bond appears at 6.20 ppm or 6.16 ppm depending on the sample measured and of the C2 at 5.86 ppm or 5.79 ppm. The

110

trans peaks of the double bonds appear between 5.71 - 5.65 ppm and of the C2 between 6.09 – 6.02 ppm. Interestingly, the small upfield shift to 6.16, 6.09, 5.79 and 5.65 ppm only occurs, if the polymers are made with **SIPr** containing initiators.
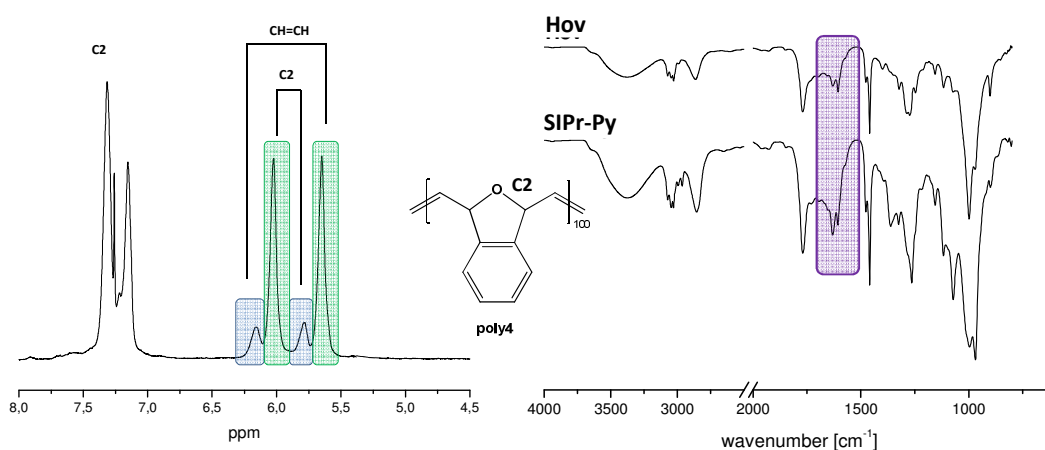
Figure 71: On the left side, proton NMR spectra of poly4 made with SIPr-Py; *cis* peaks are labeled in blue, *trans* peaks in green; on the right side, IR spectra of poly4 made with Hov and SIPr-Py. the double bonds (*trans* bond at 1630 cm^{-1}, *cis* bond at 1608 cm^{-1}) are marked in purple
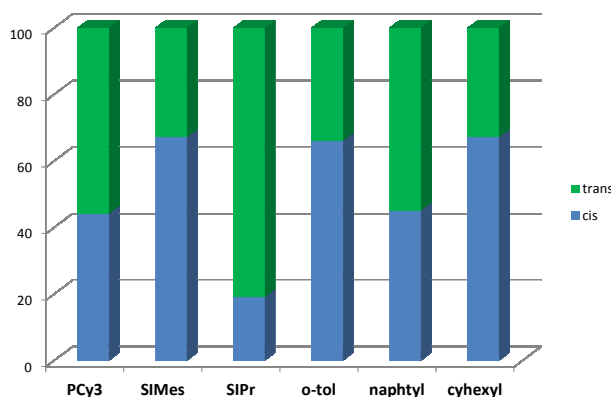
Figure 72: *Cis* and *trans* ratio of poly4 of various NHC's compared to 1st generation reference initiators; if two or more initiators with the same NHC were used within this series only small deviations were determined and therefore an average value of the *cis* and the *trans* ratio was taken

Here, the before realized trend is somehow obvious again. **Poly4** made with **SIMes** initiators gives polymers with the highest *cis* content of >60 %. Most striking, with **poly4**, the most bulky NHC namely **SIPr** and **naphtyl** give the highest *trans* contents. **SIPr** initiators even give polymers with a higher *trans* content than the first generation initiators. At this point the high PDI values of **poly4** should be mentioned. The increased PDI values indicate that a

second metathesis step occurs and hence the polymer chains are cut into small pieces. This is also indicated by the low molecular weight values obtained. To see, if the enormous differences in the *cis/trans* ratio are somehow caused by a backbiting of the initiator, polymerizations of **Mon4** in a NMR tube using once a **SIMes** and once **SIPr** initiator were done. NMR spectra were recorded periodically over some hours still continuing when the polymerization was already finished, to see, if the *cis/trans* ratio changes over time. The polymerization reactions were already finished when the first NMR spectra was recorded after approximately 2 minutes. After about 24 hours, still no change in the *cis/trans* ratio could be observed. Again, the reactions done with the **SIMes** complexes yielded polymers with a *cis* content of bigger 60 % and the one done with the **SIPr** complex polymers with a *cis* content of only <20 %. As a result, the differences in the polymer configuration could be excluded to originate from a secondary metathesis reaction.

Figure 71 shows the IR spectra of **poly4**, made with initiator **SIPr-Py** and **Hov**. The peaks at 1630 cm^{-1} and 1608 cm^{-1} display the *cis* and the *trans* double bond within the polymer. The distinct difference in the *cis/trans* ratio can be also deduced from the different size of the peaks. A closer investigation of the spectra was not done because the most important things were already seen from the NMR spectra.

Due to the reason, that the most pronounced differences always appear between **SIMes**, **SIPr** or **o-tol** containing complexes, for the reactions with **Mon5** only catalysts with those three NHC's were used. Noteworthy in case of the proton NMR spectrum, here the *cis/trans* differentiation was not done via the CH=CH or the C2. In this case the proton of the C7 carbon splits up and thus by integrating them, the configuration can be determined. Additionally to the *cis/trans* ratio and the tacticity of the polymer, the regioselectivity can be assigned. **Mon5** can be either polymerized from the *syn* or from the *anti* side of the monomer with respect to the substituent attached to the C7 carbon, depending on the reactivity of the particular double bonds. The different reactivties of the two double bonds in such diene systems can either depend on the position within the polycyclic system, as in the case of dicyclopentadiene (**DCPD**), or in case of structural similar double bonds as in **Mon5**, on steric constrains or electronic effects.[111] As the *syn* double bond is less accessible as the *anti* double bond, exclusively polymers made via an *anti* attack of the initiator were obtained. The regioselectivity could be determined only from the ^{13}C spectra, by a comparison of the different peaks of the C2 and the C7 atoms carbons, respectively. The peaks were assigned by comparison with published data.[112] The regioselectivity as well as the *cis/trans* ratio of the **SIMes** containing initiators are in good accordance with the in reference 112 published data of **poly5** made with **G3** (*trans* > 60 % and *anti* > 90 %).

---

[111] V. Amir-Ebrahimi, D. A. Corry, J. G. Hamilton, J. M. Thompson, J. J. Rooney, *Macromolecules* **2000**, *33*, 717-724.

[112] J. I. Kenneth, A. M. Kenwright, E. Khosravi, J. G. Hamilton, *Macromol. Chem. Phys*. **2001**, *20*2, 3624-3633.

Figure 73: Proton NMR spectra of poly5 made with M31; *cis* peaks are labeled in blue, *trans* peaks in green

Figure 74: *Cis* and *trans* ratio of poly5 of the various NHC's compared to reference initiators of the 1st generation; if two or more initiators with the same NHC were used within this series only small deviations were determined and therefore an average value of the *cis* and the *trans* ratio was taken

When the *cis/trans* ratio of the different NHC's are compared, the higher *trans* content in polymers made with **SIPr** complexes again is remarkable. Interstingly, ***o*-tol** gives polymers with even higher *cis* contents as their **SIMes** congeners which is the opposite observation as made in **poly3**, where the ***o*-tol** derivatives yielded polymers with the highest *trans* content.

Table 21: Summarized data of the influence of the NHC's on the *cis/trans* configuration of polymers

	poly3			poly4			poly5		
	cis	*trans*	*PDI*	*cis*	*trans*	*PDI*	*cis*	*trans*	*PDI*
1st Generation									
M1				44	56	2.7	35	65	n.d.
G1	10	90	n.d						
2nd + 3rd									
SIMes									
M31	94	6	1.2	67	33	2.9	64	36	n.d.
M2	91	9	2.2	67	33	3.9			
Hoveyda	93	7	1.2	68	32	3.7	65	35	5.17
SIPr									
SIPr PCy$_3$	85	15	1.2	20	80	n.d	52	48	
SIPr Py	88	12	1.2	18	82	2.6	51	49	2.76
o-tol									
o-tol-Py	74	26		66	34		75	25	2.04
o-tol-PCy$_3$	78	23	1.6	65	35	2.6	73	27	1.69
naphtyl									
naphtyl-PCy$_3$	89	11	1.6	45	55	3.2	n.d.	n.d.	
cyhexyl									
cyhexyl-PCy$_3$	94	6	1.9	67	33		n.d.	n.d.	

[**I**]:[**Mon3**] and [**Mon4**]=100; [**I**]:[**Mon5**]=300; RT, DCM, 0.1 mol/L with respect to the corresponding monomer

As discussed in the ongoing pages, the NHC seems to have a pronounced influence on the configuration of polymers. Most probably this influence is caused by steric factors. **SIPr** containing initiators always give polymers with higher *trans* contents no matter which monomer is applied. The second bulky NHC, the **naphtyl**, is in good accordance with those results. Again due to the bulkiness of the **naphtyl** groups in the NHC the *trans* content of the polymers is always increased compared to the smaller **SIMes** NHC polymers. Interestingly, for the ***o*-tol** containing initiator, the conclusion cannot be drawn that easily. Normally, considering the before discussed theory of "the bigger the NHC, the higher the *trans* content in the polymer" this initiators should always yield polymers with a heightened *cis* content. Unfortunately, this could only be proofed partly. In **poly4** *cis* contents are the same as with **SIMes** initiators and higher compared to the **SIPr** analogs. In **poly5**, ***o*-tol** initiators even yielded the highest *cis* content. Only in **poly3** the opposite observation was made. Here, polymers made with ***o*-tol** in fact exhibit the highest *trans* content.

4.2   None Polymerizable Monomers

In the course of the investigation of the influence of the NHC on the configuration of polymers, several other monomers namely 7-oxabicyclo[2.2.1]hepta-2,5-diene-2,3-dicarboxylic acid diethyl ester (**Mon6**), 1-methyl-7-oxabicyclo[2.2.1]hepta-2,5-diene-2,3-dicarboxylic acid dimethyl ester (**Mon7**) and 1,4-dimethyl-7-oxabicyclo[2.2.1]hepta-2,5-diene-2,3-dicarboxylic acid dimethyl ester (**Mon8**) were synthesized. 7-[t]butyl-bicyclo[2.2.1]hept-5-ene-2,3-diacetate (**Mon9**) in contrast was initially synthesized for an AROCM reaction.
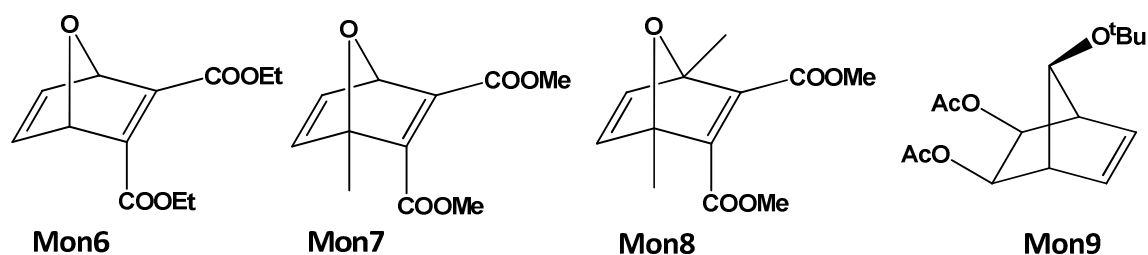
Figure 75: None polymerizable monomers

Mon6-**Mon8** were synthesized via a Diels-Alder reaction of the corresponding diene (furan, methylfuran or dimethylfuran) with the appropriate dienophile (diethylacetylenedicarboxylate and dimethylacetylenedicarboxylate) at elevated temperatures over several hours. Higher temperatures were necessary due to the lower reactivity of the heteroaromatic system of the furan compared to e.g. cyclopenatadiene. **Mon6** was stirred in toluene whereas the reactions of **Mon7** and **Mon8** were conducted neat. The reaction progress was followed via TLC. The diene was applied in excess and therefore, after full conversion of the dieneophile, the crude product was purified via column chromatography. [132,133]

Mon9 on the other side was prepared via a three step synthesis starting from the commercially available norbornadiene. The first step was a substitution of the C7 atom with a [t]butoxy group, followed by an oxidation of the *anti* double bond with KMnO$_4$ to give the norbornendiol. The last step was a simple esterification of the hydroxyl groups with acetyl anhydride in the presence of a base yielding only the *exo* norbornene. [131]

With all four monomers, polymerizations with the usually most active initiators namely **M31**, **SIPr-Py** and **Hov** were done. The reactions were performed using standard polymerization conditions at RT in DCM with an initiator to monomer ratio of 100:1. Interestingly, polymerizations with **Mon7**-**Mon9** did not yield any polymer. Even when elevated temperatures were used, no polymerization took place. Due to the finding that initiators with an *o-tol* NHC ligand exhibit an outstandingly good propagation rate we applied the third

generation derivative **o-tol-py** in this test series.[113] Again polymerizations using standard conditions were made with **Mon7** and **Mon8**. Unfortunately, once again no formation of polymer was observable.

Mon6 is not a totally unpolymerizable monomer, but only gives very low conversions ranging from 20 % to 30 %, even when the most active ruthenium initiators and elevated temperatures are used. Here, no very obvious reason for the occurring polymerization problems is recogniseable. The steric effects should be basically the same as in **Mon1**, which polymerizes well, or sometimes even too fast. Therefore one possible explanation are maybe electronic effects caused by the oxygen in the bicyclic ring. Another possible explanation could be remaining amounts of diethyl acetylenedicarboxylate from the preparation which reacts with the initiator leading to an inactive form.

The problems with polymerizing **Mon7** and **Mon8** probably origin from the enhanced steric bulk of the monomers due to the additional methyl group(s) at the bridging carbon. Somehow the methyl group(s) seem to block the coordination site at the ruthenium or maybe hamper the formation of the metallacyclobutane intermediate. In literature, only one paper about the polymerization of **Mon7** via olefin metathesis is published. There the monomer is polymerized using molybdenum based olefin metathesis initiators, which are known to be more active than their ruthenium analogs.[114]

To the best of our knowledge, no publication on the polymerization of **Mon9** with ruthenium initiators exists. **Mon9** is normally applied for the AROCM reaction of molybdenum initiators to circumvent, that the highly active Mo catalysts polymerize the monomer before performing the cross metathesis reaction.[115] Due to the fact that in **Mon9** only the *syn* double bond is present, it is more difficult to open it via a metathesis initiator. The polymerization reactions of **Mon5** already have shown, that with well-defined ruthenium initiators, only **poly5** in which the *trans* double bond is used for the metathesis reaction (see chapter 3.1.3.) are obtained.

---

[113] A. Leitgeb, PhD thesis "Contributions to the Advancement of Ruthenium Based Initiators for Olefin Metathesis", Graz 2012.

[114] M. M. Flook, V. W.L.Ng, R. R. Schrock, *J. Am. Chem. Soc.* **2011**, *133*, 1784-1786.

[115] D. S. La, E. S. Sattely, J. G Ford, R. R. Schrock, A. H. Hoveyda, *J. Am. Chem. Soc.* **2001**, *123*, 7767-7778.

5 SIPr – Phosphit Initiator

In this chapter, the ROMP performance of initiator **10** was evaluated. The initiator was synthesized from the Cazin group from the University of St. Andrews in Scotland. **10** contains a strong π-acidic triisoproylphosphite instead of the commonly used tricyclohexylphosphine as used in **M2**. This dissociative ligand was already introduced in complex **M22** containing a SIMes NHC, leading to a highly latent ruthenium initiator with a *cis* arrangement of the NHC and the phosphite.[116] **M22** exhibits an increase in stability. It is basically inactive at room temperature and can be turned on to a highly metathesis active form at elevated temperatures.[117] In contrast to **M22**, the combination of the sterically more demanding SIPr ligand with triisopropylphosphite yields a complex, with a *trans* arrangement of the NHC and the phosphite. This arrangement is the generally known arrangement for all established SIPr NHC containing complexes.[118] To the best of our knowledge, so far no *cis* SIPr initiator is established.

In the Cazin group, the RCM and cross metathesis performance of **10** was already investigated. It was shown, that **10** is a suitable initiator for these two metathesis reactions at low loadings. Herein we present the results of **10** in the ring opening metathesis polymerizations. The performance of **10** is compared to the performance of its architecturally familiar analogues **M2, SIPr-PCy₃** and **M22**. **Mon1** and **DCPD** were used to gain detailed information about its ROMP features.
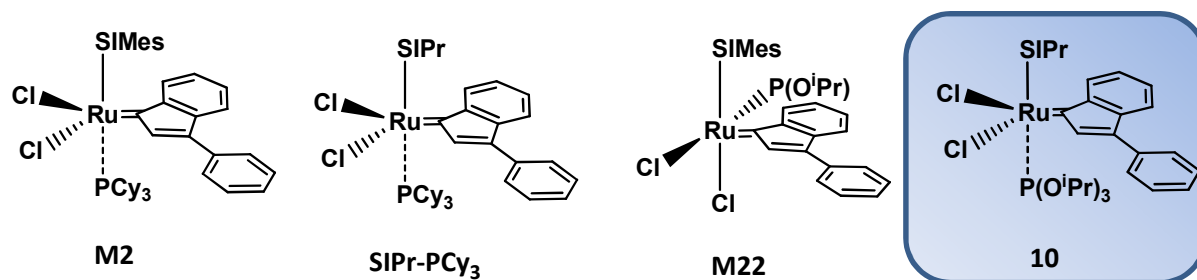
Figure 76: Reference initiators M2, SIPr-PCy₃ and M22 and its SIPr analog 10

[116] X. Bantreil, T. E. Schmid, R. A. M. Randall, A. M. Z. Slawin, C. S. J. Cazin, *Chem. Commun.* **2010**, *46*, 7115-7117.

[117] For detailed information of the ROMP data, see: A. Leitgeb, PhD thesis "Contributions to the Advancement of Ruthenium Based Initiators for Olefin Metathesis", Graz 2012.

[118] A. Leitgeb, M. Abbas, R. C. Fischer, A. Poater, L. Cavallo, C. Slugovc, *Catal. Sci. Technol.*, **2012**, *2*, 1640-1643.

5.1 Polymerization Reaction – Benchmark Polymerization

To get a first impression of the catalysts performance, the typical standard polymerization reaction using **Mon1** as the benchmark monomer at three different temperatures (RT, 40°C and 80°C) was done. A monomer to initiator ratio of 300 to 1 was used. Polymerizations were carried out using Schlenk techniques, dry and degased solvents and an inert nitrogen atmosphere. For room temperature and 40°C polymerizations DCM and for 80°C polymerization toluene were used as the solvents of choice. For the polymerizations at elevated temperatures, the monomer was added first and the solvent was allowed to warm to the desired reaction temperature before the corresponding initiator was added. For a better comparison **M2, SIPr-PCy₃** and **M22** were implied in the polymerization statistic. The polymerizations at the different temperatures using the mentioned related initiators were only conducted if the reaction was reasonable. All other reaction conditions and the general way of proceeding were maintained as usual and as described in previous chapters.

Table 22: Polymerization data of 10 compared to M2, M22 and SIPr-PCy₃

	Temperature [°C]	Time [h]	Conversion[b] [%]	isol. Yield [%]	M_n [g/mol]	PDI
M2	RT	4	100	78	300000	2.0
M22	RT	120	100	n.d[a]	n.d[a]	n.d[a]
SIPr-PCy₃	RT	2	100	n.d[a]	52000	1.3
10	RT	8	100	73	130000	1.6
M2	40	2	100	69	300000	1.7
M22	40	50	100	61	235000	2.0
SIPr-PCy₃	40	1	100	65	49000	1.2
10	40	3	100	81	81000	1.5
M2	80	1	100	62	109000	1.6
M22	80	1	100	91	105990	1.8
SIPr-PCy₃	80	n.d[a]	n.d[a]	n.d[a]	n.d[a]	n.d[a]
10	80	0.25	100	79	73000	1.3

Reaction conditions: [I]:[Mon1]=300; DCM for RT and 40°C polymerizations and toluene for 80°C polymerizations; 0.1 mol/L [Mon1]

[a] not determined

[b] 100 % conversion refers to full monomer conversion according to TLC

The results summarized in Table 22 show very clearly, that **10** is a sight more active than its SIMes analog **M22**. Even at room temperature it yields 100 % conversion in an acceptable time and with moderate molecular weights. The raised PDI is typical characteristic for

second generation initiators where the ligand dissociation is hampered due to the stabilization of the NHC ligand. Interestingly the PDI and also the M_n in case of the room temperature polymerization of **10** are significantly lower than the values of **M2**, indicating a higher initiation. The sterically more demanding SIPr ligand is held responsible for the enhanced dissociation of the phosphite ligand. The propagation rate on the other hand seems to be lower in **10** as in **M2**, which is also caused by steric hindrance induced by the more bulky SIPr NHC ligand. This fact is also apparent in the far longer reaction times of **10** compared to **M2** even though a higher percentage of the initiator is active. The effect of the decreasing propagation rate from SIMes to SIPr was already described in case of the 3rd generation initiators **M31** (bearing a SIMes and a pyridine ligand) and **SIPr-Py** (bearing a SIPr and a pyridine ligand). Here the initiation rate is basically the same, defined by the easily dissociated pyridine ligand. The propagation on the other side is considerably faster for the SIMes derivative. The reaction time for the benchmark reaction under standard conditions using **Mon1** with **M31** is 10 times faster as with **SIPr-Py**.[119] When the temperature is heightend slightly from RT to 40°C, both initiators experience a twofold increase of activity. Rising the temperature to 80°C boosts the activation of **10** dramatically and it outperforms **M2** in all points. The reaction time even decreases about four times compared to the one of **M2**.

Comparing **10** with its congener **SIPr-PCy₃**, the differences are even more conspicuous. Interestingly, even if **10** and **SIPr-PCy₃** should experience the same influences by the SIPr ligand, the phosphine derivative shows significant better polymerization efficiency. In both cases, initiation is accelerated by the room up taking NHC, whereas propagation is hampered due to the same reason. The difference in this case lies in the enhanced re-coordination affinity of the phosphite of **10** compared to the phosphine of **SIPr-PCy₃.** In Figure 77 the above discussed facts are summarized graphically. The thickness of the arrows sums up the tendency of the initiators for ligand dissociation, olefin coordination and re-coordination of the dissociative ligand.

---

[119] C. A. Urbina-Blanco, A. Leitgeb, C. Slugovc, X. Bantreil, H. Clavier, A. M. Z. Slawin, S. P. Nolan *Chem. Euro. J.* **2011**, *17*, 5045-5053.

the green arrow depicts the dissociation ability of the phosphine/phosphite

the blue arrow depicts the accessibility for olefin coordination

the red arrow depicts the recoordination tendency of the dissociative ligand
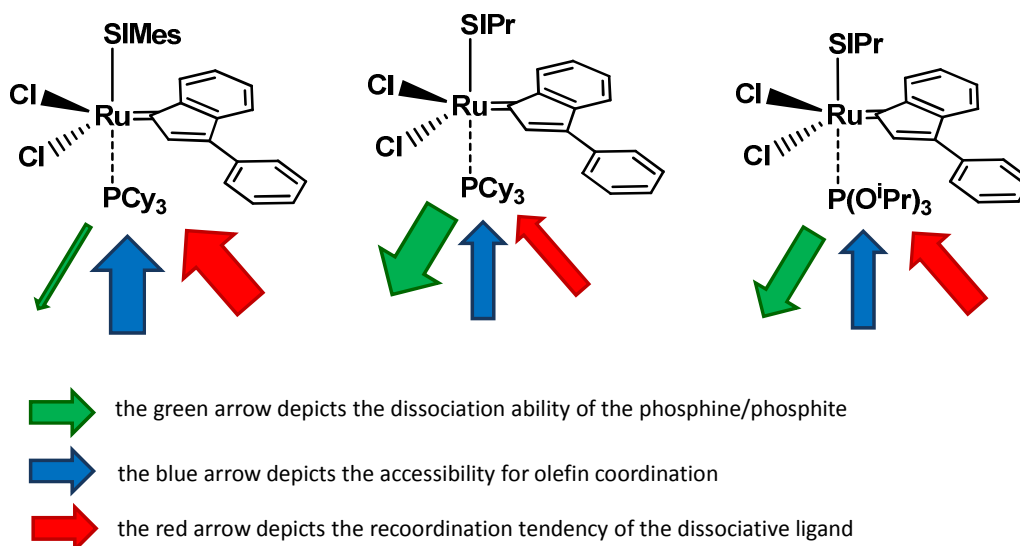
Figure 77: Charting of the initiation, propagation and re-coordination features of 10 and the reference initiators M2 and SIPr-PCy₃; the interaction of these three steps determines the molecular weight and the PDI

M22, as already mentioned previously, is inactive at room temperature. This fact is caused by the *cis* arrangement of the initiator, which is known to yield initiators with reduced activity. [120] At elevated temperatures **M22** becomes highly active and leads to comparable polymers with similar properties as those prepared with **10**. Interestingly, even if the molecular weights are in the same range, the PDI values of the polymers made with **M22** are heavily increased compared to those of **10**, which is probably explained by the before mentioned additional activation step.

---

[120] M. Zirngast, E. Pump, A. Leitgeb, J. H. Albering, C. Slugovc, *Chem. Commun.* **2011**, *47*, 2261-2263.
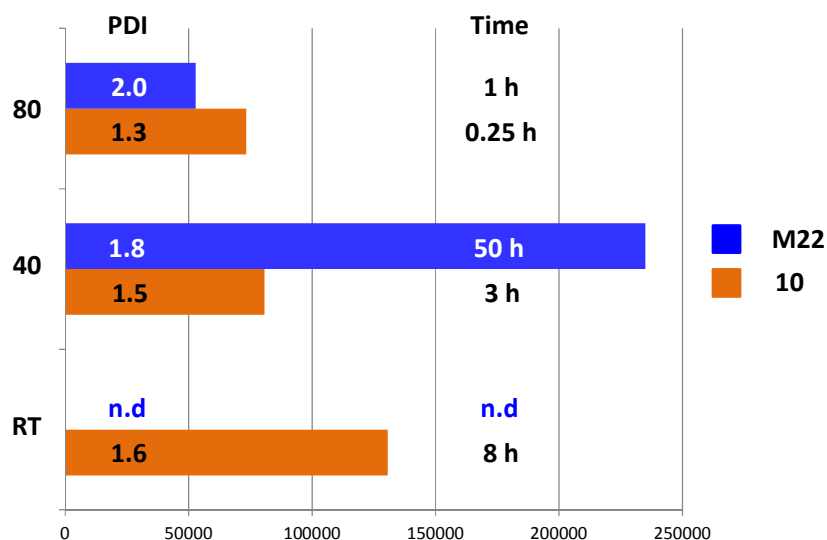
Figure 78: Polymerization data of 10 and M22; RT polymerization of M22 is not included due to an excessive reaction time and a too high M_n

Concluding, the SIPr NHC ligand in **10** leads to a strong increase of the activity especially at higher temperatures compared to its reference initiators possessing SIMes NHC's. Still, it shows enough latency at room temperature to be a suitable candidate for the highly active monomer **DCPD**.

5.1.1 Kinetic Measurements

For the kinetic plots, the reaction progress of the polymerization of **Mon2** was monitored using ^{1}H NMR spectroscopy. Conversions were determined by integrating the olefinic double bond peaks of the monomer and the polymer, respectively. The monomer to initiator ratio applied was 50:1 and the monomer concentration was fixed at 0.1 mol/L. The reaction was performed in degased $CDCl_3$.The results of the kinetic plot match the GPC data of the benchmark polymerization very well, whereas it has to be pointed out, that in these plots the influence of the propagation rate on the results is more pronounced than the influence of the initiation. Hence the above described hindered olefin coordination caused by the higher re-coordination tendency of the phosphite is displayed very clearly. While **SIPr-PCy₃** exhibits a half-life time of only 2.8 hours, **10** requires 13.2 h to reach the same conversion, although both initiators feature the same active species and the reaction difference only lies in the re-coordination of the dissociative ligand.
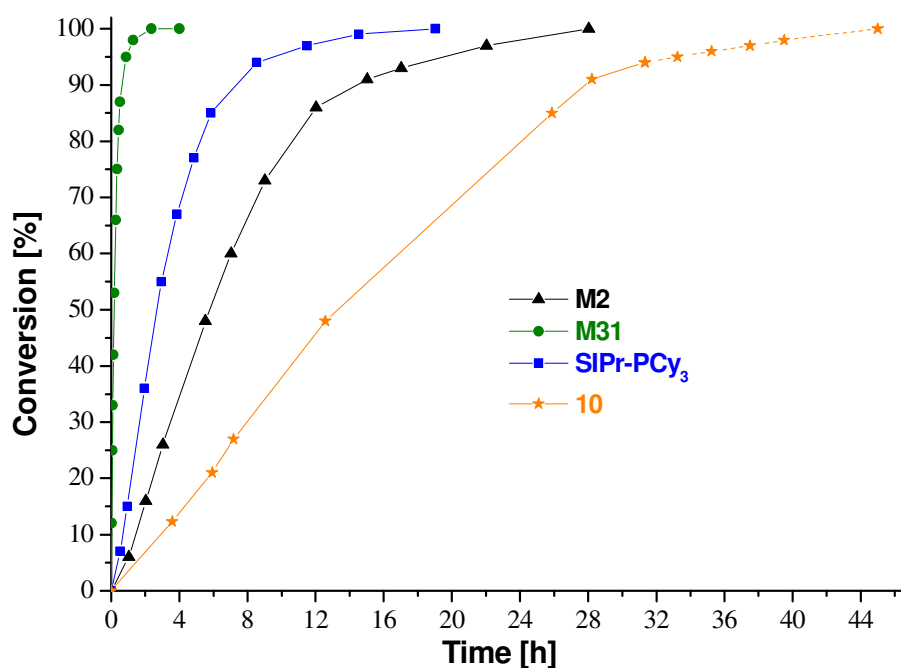
Figure 79: Kinetic plot with Mon2; the dashed line is extrapolated for a better comparison; [I]:[Mon2]=50; RT, 0.1 mol/L [Mon2], CDCl₃

Table 23: Half life times and times until full conversion

Initiator	$t_{1/2}$ [h]	t > 99% conv. [h]
M31	0.13	2.25
M2	5.8	28
SIPr-PCy₃	2.8	19
10	13.2	42

5.2 DCPD Shoulder Test Bars

For the **DCPD** tests, the general polymerization procedure to obtain **pDCPD** shoulder test bars was followed. 28 mL of tempered **DCPD** were mixed with the corresponding amount of initiator dissolved in 1680 µL toluene. Toluene was used, due to its higher boiling point to prevent a too fast evaporation of the solvent causing bubbles and holes in the polymer, which would alter the properties of the **pDCPD** negatively. The initiator/**DCPD** mixture was poured into a pre-heated mold and cured at 80°C overnight, to provide the initiator enough time not only to polymerize, but also to crosslink the polymer.

With **10,** shoulder test bars with 50 ppm, 30 ppm, 20 ppm and 10 ppm catalyst loading were made. The picture in Figure 80 clearly displays the different catalysts loadings visible at the

diminishing yellowish color, which also indicates a full initiation of the catalysts in every test series. If the initiator would not have fully initiated, the shoulder test bars would have kept some of their red starting color. At first instance, all of these shoulder test bars hardened very quickly and could be removed out of the mold after 5 to 20 minutes. Unfortunately, really stiff and suitable test specimen could only be obtained until a catalyst loading of 20 ppm. The test bars with 10 ppm initiator loading seem to be not really cross-linked and kept an elastic, rubbery texture. Therefore they were not included in the tensile strength test series.
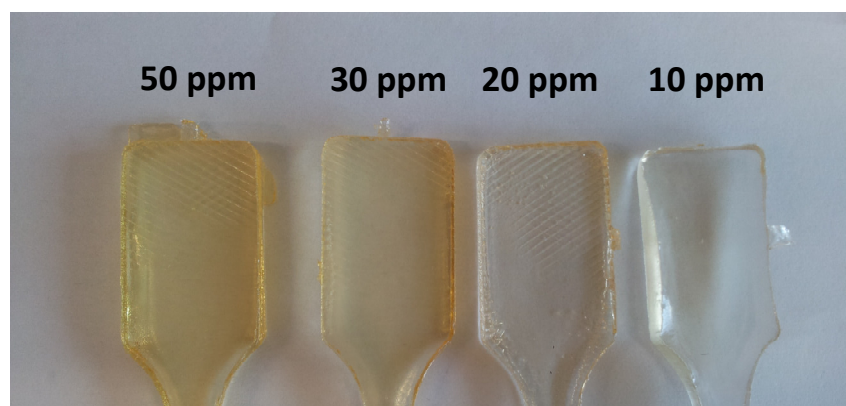
Figure 80: Shoulder test bars with decreasing initiator loading

Figure 81 and Table 24 illustrate the performance of **10** in the polymerization of **DCPD**. With 50 ppm and 30 ppm shoulder test bars with very good mechanical properties were obtained which are in good accordance with published literature values or yielded even better properties. The specimen made with 20 ppm catalyst loading display a significant decrease of the mechanical properties, indicating a less cross-linked system.

Table 24: Tensile strength data of 10; average values were calculated

Concentration [ppm]	Young's Modulus [GPa]	$R_{p\,0.2}$ [Mpa]	R_m [MPa]
50	2690	38,01	53,9
50	2690	47,6	54,3
50 – av.	2690	42,8	53,4
30	2385	42,85	48,4
30	2200	36,65	44,6
30 – av.	2570	49,05	53
20	2060	32,4	34
20	2000	31,2	32,5
20 – av.	2030	33,6	36,3
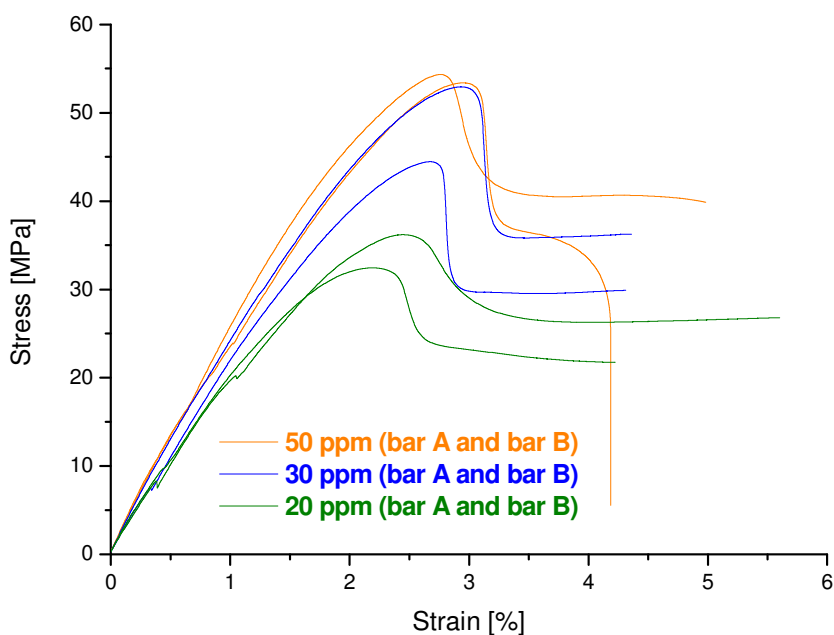
Figure 81: Tensile strength tests of initiator 10 at different loadings

In all cases after the ultimate strength (R_m) was reached, a plastic deformation occurred. After the ultimate strength was applied, elongation of the test bars continued until an undefined length was reached. This point always differs within one specimen series due to small imperfections such as bubbles or small cracks in the test bar. The tests were not always performed until the break of the test specimen occurred, due to the unimportance of this point in our case. Additionally to the above shown tests, the influence of the curing time was shortly investigated. Shoulder test bars with 20 ppm and 30 ppm were made which were not

allowed to cure overnight. The curing time was stopped, when the test bars had lost their characteristic smell of **DCPD** which is indicative for a total consumption of the monomer, but still no evidence for a total cross-linking of the sample. The tensile strength tests proved that the long curing times are necessary to achieve full setting of the samples. The Young's Modulus, the $R_{p\ 0,2}$, and the ultimate strength are always higher in the overnight cured sample (compare 30 ppm: $E_{overnight}$ = 2570 MPa to $E_{not\ overnight}$= 2170 MPa).

For a better estimation of the performance of **10** in the polymerization of **DCPD**, the data of the tensile strength tests were compared to the data of **M2** and **M22**. Figure 82 depicts clearly, that **10** outperforms its SIMes analog **M22.** Although, the maximal applied stress is in the same range when 25 ppm of **M22** and 30 ppm **10** are used, **10** shows a significantly higher Young's modulus even at lower ppm values. Regarding the Young's Modulus, **10** also outperforms **M2** at all loadings tested. Interestingly, polymers made with 20 ppm of **M2** exhibit the same ultimate tensile strength as the polymers made with 50 ppm **10** Summarizing, polymers made with catalyst **10** seem to be more cross-linked than the polymers made with **M2** and **M22**, respectively.
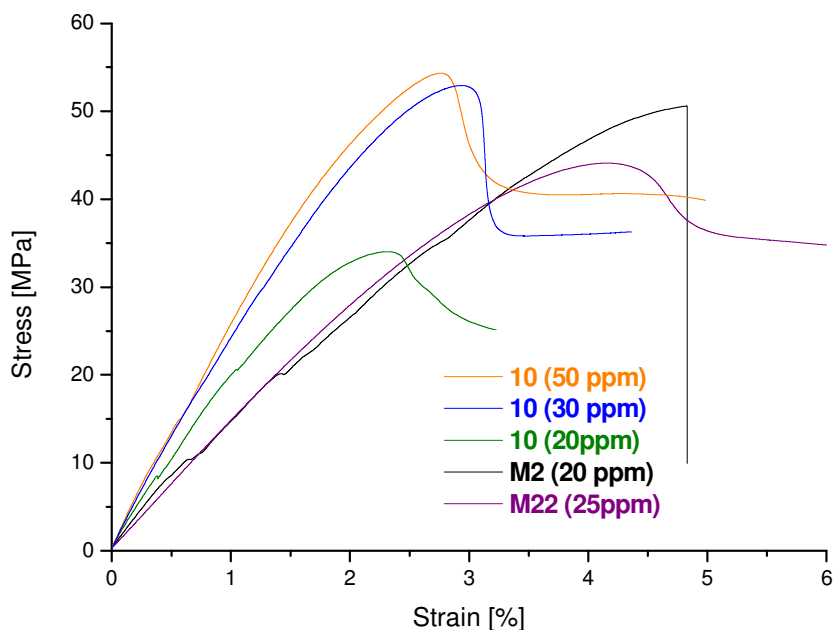
Figure 82 Comparison of tensile strength tests of M2, M22 and 10; for a clearer illustration just one curve is depicted

5.2.1   STA Measurements

To gain more information about the latency of **10**, STA measurements were done. 5 mL of **DCPD** were mixed with 100 µL DCM to hinder a solidification of the monomer. A stock solution of **10** was made, in order, that the overall amount of solvent in the reaction mixture was fixed at 160 µL. 60 µL of the stock solution were added to the monomer and mixed carefully. The STA measurements were conducted with a heat flow of 3 °C/min and a helium flow of 50 mL/min used in combination with a protetctive flow of 8 mL/min.

Two runs with 20 ppm and 40 ppm catalyst loading respectively were done and compared to **M2** (20 ppm). **M2** shows a distinct exothermic polymerization peak, whereas both polymerizations performed with **10** show only slight exothermic peaks. At a first glance this result is surprising because from the shoulder test bars it is known, that **10** is as capable to polymerize **DCPD** as **M2**. Looking at the STA samples more precisely, it can be noticed, that even at room temperature they cure faster than the samples of **M2**. A first possible explanation could be that **10** is at RT already more active than **M2** and therefore exhibits no well-defined activation temperature. Anyway **10** shows a temperature dependency which was already clearly displayed in the standard benchmark polymerizations. Therefore, due to the rising temperature, it experiences an activation increase, which becomes apparent in the small exothermic peak in the DSC plot. The mass loss, caused by the Retro Diels Alder reaction remains in an acceptable range.
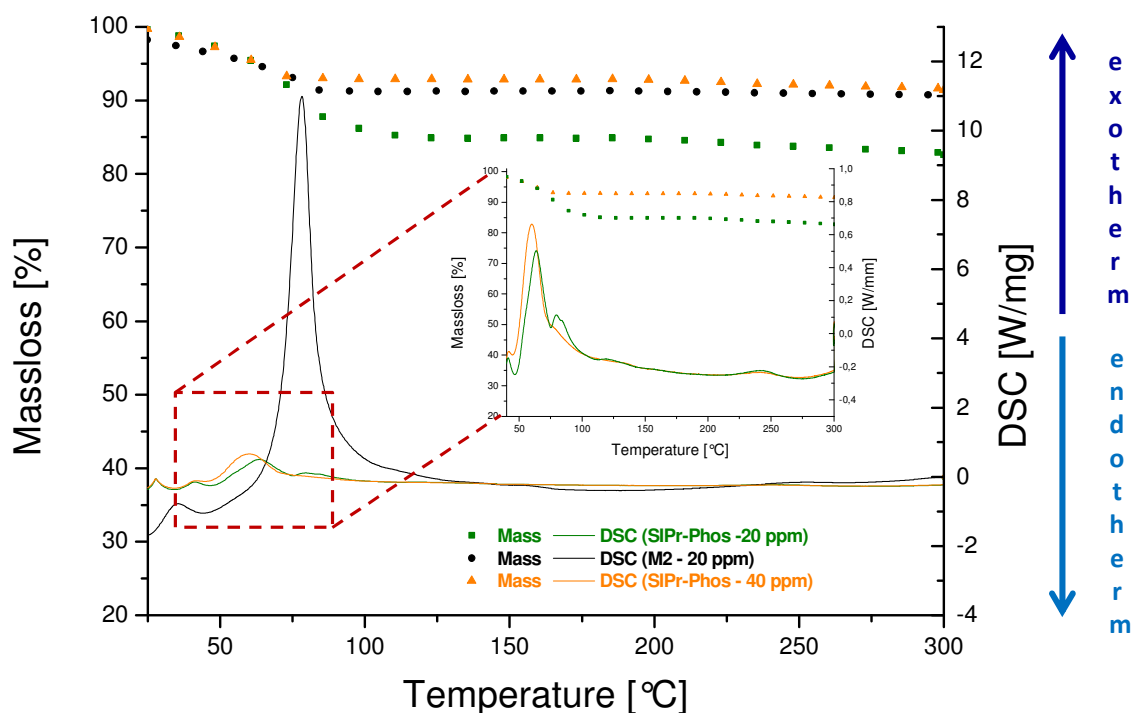
Figure 83: STA measurements of 10 and M2; the small graph in the interior is a magnification of the results of 10; [I]:[DCPD]=1:10.000; Temperature program: 3°C/min; the TGA is operated with a helium flow rate of 50 mL/min used in combination with a protetctive flow of 8 mL/min

Table 25: STA results of 10 compared to M2

Initiator	Concentration [ppm]	Onset [°C]	Peak max. [°C]	Mass loss [%]
M2	20	48.2	78.3	9
10	20	48.3	62.7	15
10	40	48.7	59.4	7

Another possible explanation of the missing exothermic peak is the humble propagation, which was already remarked in the benchmark polymerizations. Due to the low propagation rate, only a small amount of monomer is polymerized simultaneously and therefore the exothermic energy release occurs constantly, but is just very low. Therefore, an experiment to measure the exothermic reaction at room temperature was conducted as follows: 2 mL of **DCPD** were mixed with 50 µL of DCM. 50 ppm of the corresponding initiator, dissolved in another 50 µL of DCM, was added to the monomer. The reaction was performed in a Pasteur pipette. The pipette was put into a 25°C tempered oil bath and a temperature sensing element covered with aluminum foil was put into the **DCPD**/initiator mixture. The temperature over time was measured. Again in case of **10** no significant temperature

increase was observable, whereas **M2** shows a clear exothermic polymerization peak. This strengthens the second theory of the missing exothermic peak due to the hampered propagation of **10**.
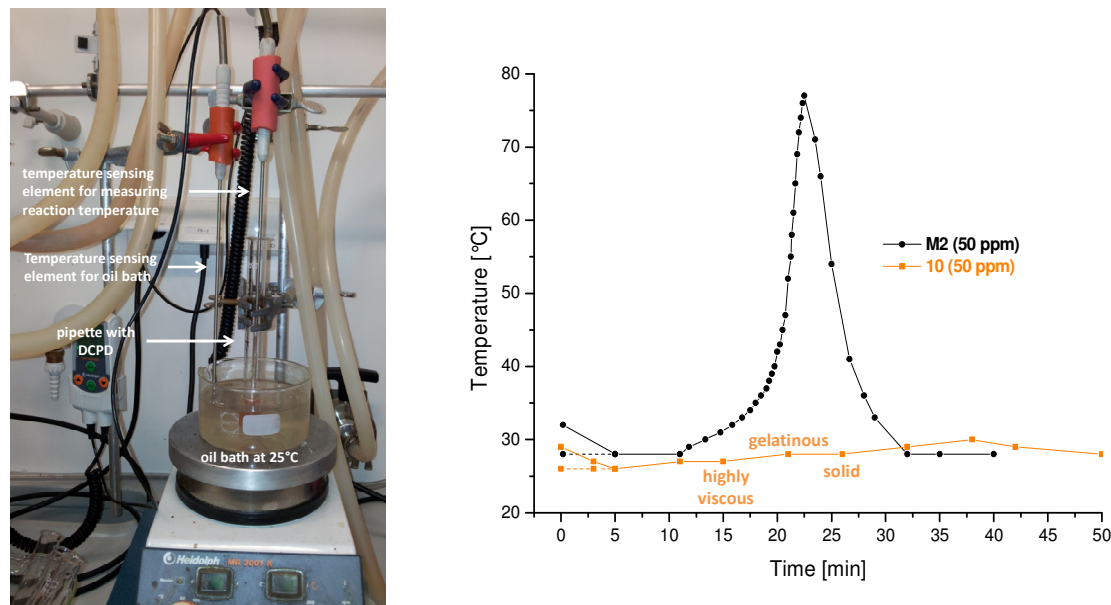
Figure 84: Left: illustration of the measuring equipment; right: polymerization temperature of DCPD; the higher temperatures at the beginning are due to the pre-heated DCPD, dashed lines were added for a better representation

5.2.2   Swelling Experiments

In order to support the cross-linking theory, swelling experiments were conducted. Swelling occurs in polymers which are cross-linked and therefore cannot be dissolved by the applied solvent. Thus, the solvent leads only to a volume and weight increase. When the solvent enters a cross-linked network, it moves the network junctions between the cross-linking points away from each other. On the other side, these junctions experience a stress, which is caused by the effort of the junctions to move back. This two facts lead to a swelling equilibrium, where the polymer does not accept any more solvent. The higher the polymer is cross-linked, the smaller are these junctions between two cross-linking points, and the less solvent the polymer can take up before the swelling equilibrium is reached. Therefore total weight or volume increase is an indirect indicator for the degree of crosslinking.
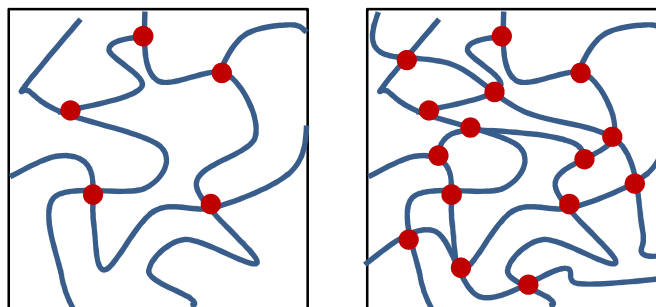
Figure 85: Schematic representation of low cross-linked polymer (left) and highly cross-linked polymer (right)

For the swelling experiments, approximately 1 g of the tested shoulder test bars was cut off and covered with toluene. The test samples were weighted periodically. Therefore, they were taken out of the toluene and the surface was dried carefully to remove the solvent on the outer surface. The weight increase is depicted as percent mass increase referred to the starting weight as 100 %.
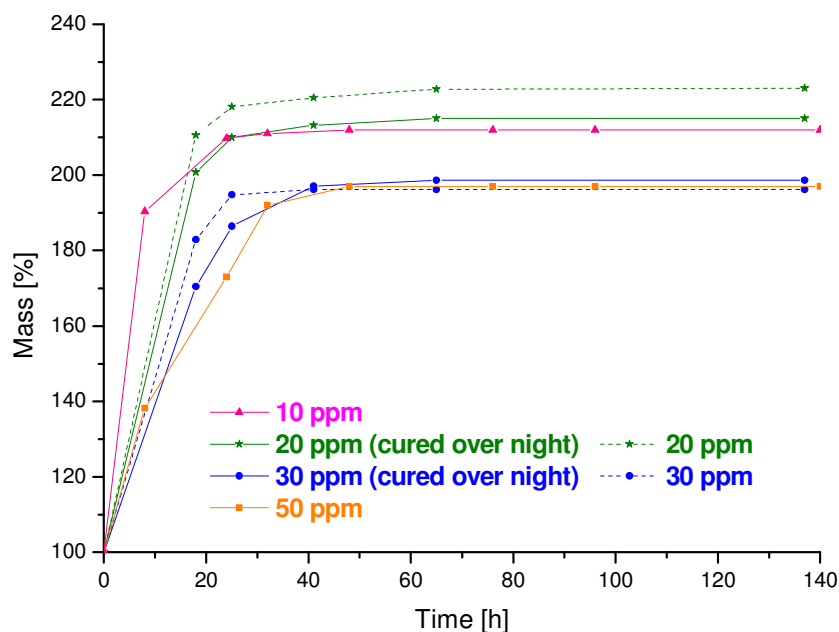
Figure 86: Weight increase of pDCPD samples made with 10 made with different catalyst loadings

As expected, samples with a higher amount of initiator show a significantly lower mass increase as samples made with lower amounts of initiator, indicating the higher cross-linking of these samples. The sample with 10 ppm catalyst loading nearly doubles its weight after just 8 hours, while the 50 ppm sample increases the weight just around 40 %. The swelling

equilibrium was reached in every case after approximately 24 hours. Comparing the curves of the 20 ppm and 30 ppm samples which were dried overnight with those which were just dried for some hours, it is evident, that the curing overnight is really necessary to reach the maximum cross-linking. The less cured samples swell faster as the cured ones. From these curves, it's also obvious, that the lower the catalyst loading, the more important is this additional curing time to achieve maximum cross-linking. Both samples with 30 ppm initiator reached in the end the same swelling equilibrium, whereas samples with 20 ppm reached different equilibriums. The curves also match the data of the tensile strength test very well. Samples with 50 ppm and 30 ppm catalyst loading show approximately the same mechanical properties and exhibit also the same swelling behavior indicating that both samples are cross-linked to the same extend.
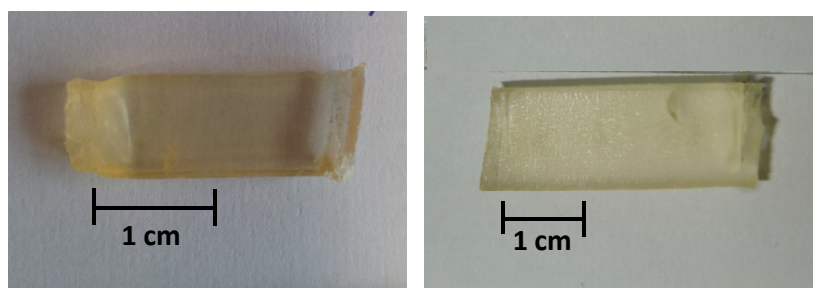
Figure 87: Sample (20 ppm cured overnight) before swelling (left) and after swelling (right)

Optically the samples did not change significantly. After 150 hours, the texture seems to be more brittle and bursting of the sample could be noticed in some cases.

6 *Cis* Initiators Chelating via a Halide Atom

Ongoing, the performance of the halide chelating initiators **11–18** was evaluated. **11–18** were synthesized by our EUMET partners from Warsaw by the group of Karol Grela.[121] The sensational feature of a halide atom, chelating to the ruthenium center was so far never described before. All initiators bear either a chelating iodine or bromine moiety, two chlorines for the anionic ligands and different aryl carbenes. Interestingly, within this halide-chelating family, all initiators show a *cis* arrangement of the two chlorines. As described before, normally *cis* catalysts are known to exhibit some latency at room temperature.
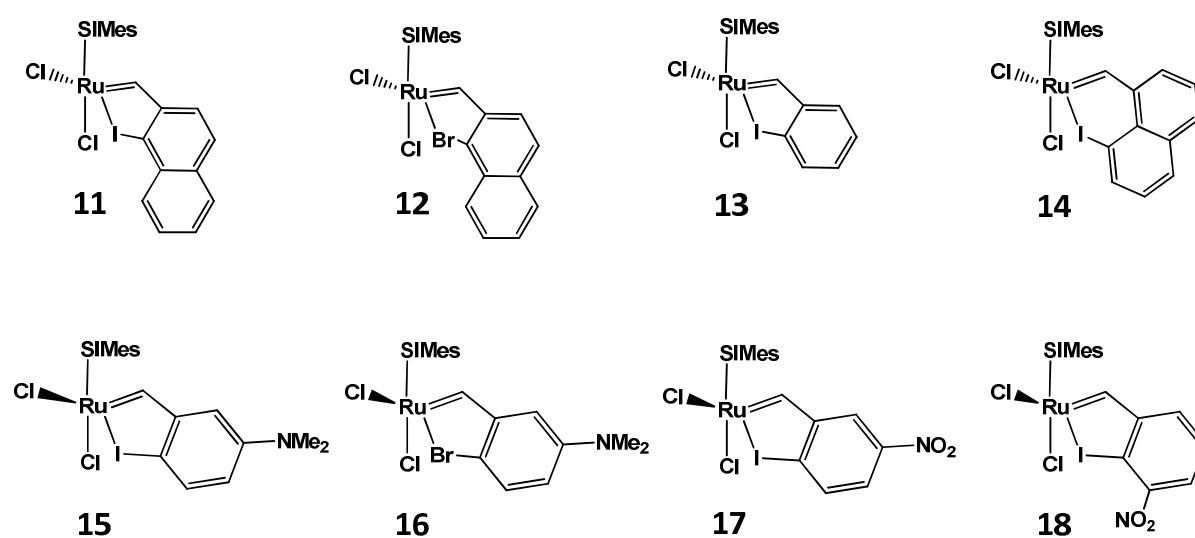
Figure 88: C*is* halide chelating initiators

6.1 Polymerization Evaluation

For a first estimation of the catalysts performance, the typical standard polymerization reaction using **Mon1** as the benchmark monomer at three different temperatures namely, RT, 40°C and 80°C, with a monomer to initiator ratio of 300 to 1 was done. Polymerizations were carried out using Schlenk techniques, dry and degased solvents and an inert nitrogen atmosphere. For room temperature and 40°C polymerizations DCM and for 80°C polymerization toluene were used as the solvents of choice. In all cases, firstly the monomer was dissolved in the corresponding solvent and the desired amount of solvent was added to preserve a solvent concentration of 0.1 mol/L. If necessary, the monomer solution was allowed to warm up to the desired temperature. Secondly, the corresponding pre-catalysts were for all reactions dissolved in DCM, due to their insolubility in toluene, and added in one

---

[121] M. Barbasiewicz, M. Michalak, K. Grela, *Chem. Eur. J.* **2012**, *00,* 0-0.

fast step. The amount of DCM in the toluene polymerizations never exceeded 200 µL. Progress determination and workup was done as usual when standard reaction conditions were used.
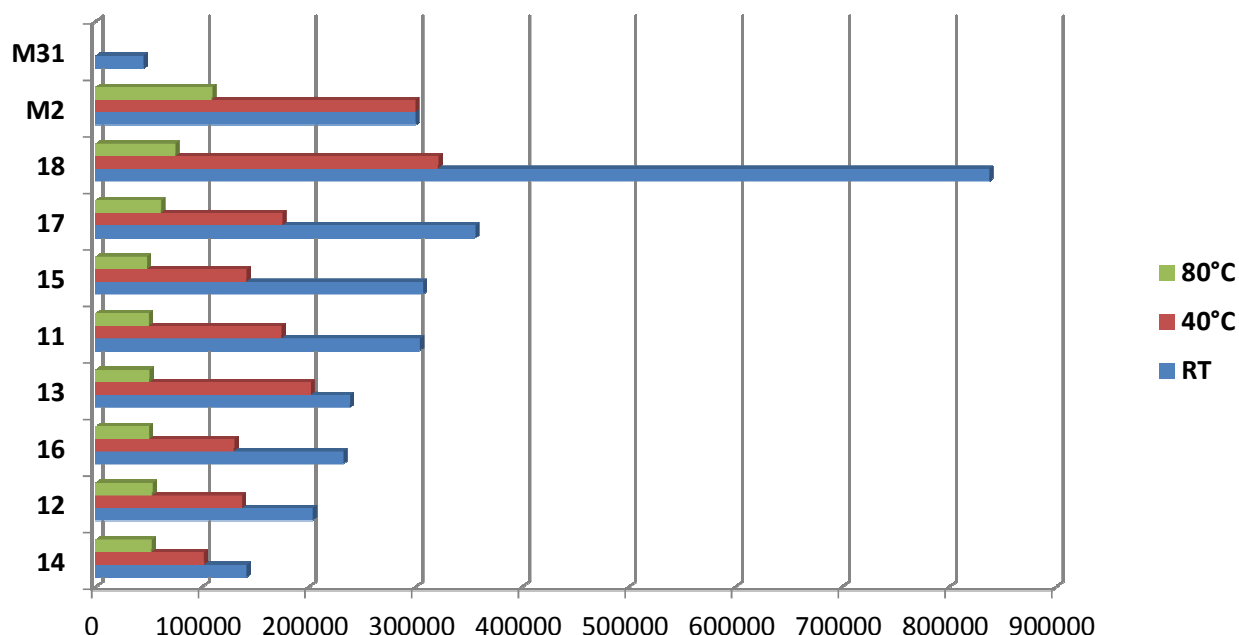
Figure 89: Polymerization data of 11 – 18 compared with M2 and M31; the initiators are sorted by their activity and not by number; due to the living polymerization and the full initiation behavior of M31, polymerizations at 40°C and 80°C were not included

The graphic clearly depicts a thermal activation of all pre-catalyst. With increasing temperature, the chain length, PDI values and polymerization time decrease (Figure 89 and Table 26). Increasing the temperature from RT to 40°C accelerates mainly the propagation rate which is indicated by the more or less similar PDI values, but significantly decreasing molecular weights of the made polymers. At 80°C, also the initiation is enhanced dramatically. All catalysts finish polymerization within 20 minutes and give polymers with very narrow PDI values ranging from 1.12 to 1.2. These values are comparable with the one of the living polymerizing initiator **M31**. Sole exception is complex **18** which yields polymers with a PDI of 1.4 at 80°C. Nevertheless, the activation increase of **18** is also worth mentioning since the molecular weight decreases from 837 000 g/mol to 74 000 g/mol, making it comparable with the commercially available **Hov** (under standard reaction conditions: M_n = 76 000 g/mol; PDI of 1.2)

Table 26: PDI and polymerization times of 11-18

	RT		40°C		80°C	
	PDI	Time [h]	PDI	Time [h]	PDI	Time [h]
11	1.82	3	1.55	0.92	1.2	0.33
12	1.59	1	1.46	0.67	1.16	0.33
13	1.75	2	1.53	0.92	1.2	0.33
14	1,35	0.67	1.32	0.3	1.12	0.25
15	1.67	1.58	1.66	1	1.2	0.33
16	1.54	1.25	1.57	0.3	1.15	0.25
17	1.69	2.08	1.78	1	1.16	0.33
18	2.27	6	2.0	2.5	1.4	0.33
M2	2	4	1.7	2	1.6	1
M31[a]	1.08	0.25	n.d.	n.d.	n.d.	n.d.

[a] 40°C and 80°C polymerizations with **M31** were not performed due to its perfect polymerization behavior at RT;

Reaction conditions: [I]:[Mon1]=300; DCM for RT and 40°C polymerization, toluene for 80°C polymerizations; 0.1 mol/L [Mon1];

To deduce the differences within this initiator family, the polymerization data of the RT polymerizations were examined closer. When looking at the structures, several different features of these catalysts which can in some way influence the polymerization behavior are evident. The first is the already in the introduction mentioned *cis* arrangement of the anionic ligands which normally leads to a more or less pronounced latency. As proposed, all *cis* complexes have to isomerize to the corresponding *trans* species which is the actual active species for the ROMP reaction.[120] Interestingly, none of the complexes, not even the at least active complex **18**, shows a mentionable latency, indicating a relatively fast isomerization. The second feature is the aromaticity of the via the chelation formed ring (according to Clare's rule).[122] Furthermore, the substitution of the phenyl or naphthyl rings by electron withdrawing or donating groups also influences the performance drastically, which was already shown in other examples for *trans* catalysts.[123] Additionally, the chelating halide, whether if it is an iodo or bromo substituent, can change the polymerization results. For an easier comparison of the complexes among themselves, they were divided into two separate groups, namely the "naphtyl" and the "benzyl" group.

The activity in the "naphtyl" group can be ordered as follows:

[122] A. Leitgeb, A. Szadkowska, M. Michalak, M. Barbasiewicz, K. Grela, C. Slugovc, *J. Poly. Sci. Part A: Polym. Chem.* **2011**, *49*, 3448-3454.
[123] A. Michrowka, R. Bujok, S. Harutyunyan, V. Sashuk, G. Dologonos, K. Grela, *J. Am. Chem. Soc.* **2004**, *126*, 9318-9325.
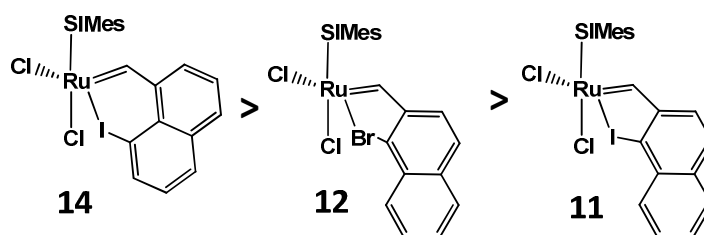
Figure 90: Activity ranking of naphtyl halochelating inititors

The first eye-catching fact is that obviously the bromo chelating complex **12** shows higher activity than its iodo analogue **11**. The iodine seems to be bound more tightly to the ruthenium center, and therefore shows a hampered dissociation attitude leading to a lowered activity. So far it is not clear, if this effect is already crucial in the starting *cis* complexes and somehow influences the *cis*/*trans* isomerization or if it determines the initiation in the formed *trans* complex. Interestingly, complex **14**, even if it bears a chelating iodo, still exhibits a higher metathesis activity as **12** with the bromo. One difference is that in **14**, the chelating ring with the ruthenium and the halide forms a six-membered ring, whereas the ring in **12** is only a five-membered ring. However, this fact was so far described in literature to yield slightly more latent initiators, which is just the contrary observation as in the discussed initiators.[124] Therefore another effect has to be considered when comparing complex **14** with **12**. According to the before mentioned Clar's rule, the more full aromatic rings in a polyhydrocarbon system can be formed, the less reactive is the system.[125] Figure 91 shows, that in **14**, the aromaticity of the chelating ring is smaller than the one in the chelating ring of **12**, leading to the higher activity of **14**.
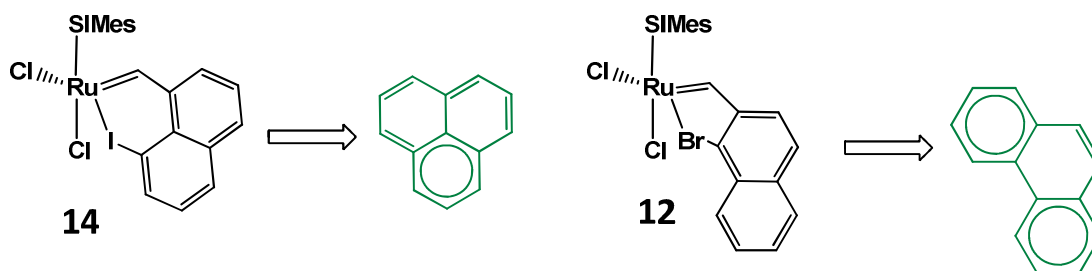
Figure 91: Aromaticity in the polyhydrocarbon system of complex 14 and 12

On the other hand, in the "benzyl" group, other effects influence the polymerization performance. The reactivity series is depicted in Figure 92. As discussed in the "naphtyl" group, complex **16** which chelates via bromine, shows the best ROMP performance and gives

[124] C. Slugovc, D. Burtscher, K. Mereiter, F. Stelzer, *Organometallics*, **2005**, *24*, 2255-2258.
[125] E. Clar, 1964, *Polycyclic Hydrocarbons.*

far better polymerization data as its iodine analogue **15**. When the series excluding complex **16** is considered, the influence of the substituents on the phenyl ring is apparent.
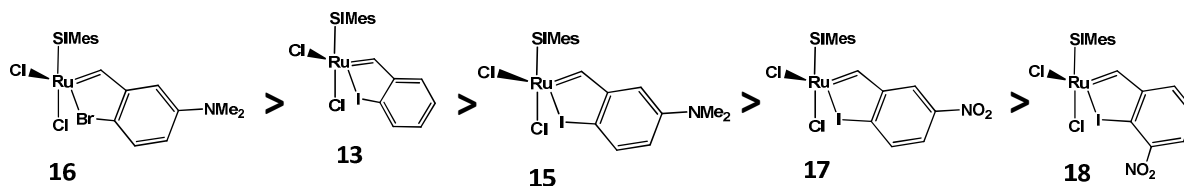
Figure 92: Reactivity series of the „benzyl" halochelating inititors

The nitro-group substituted initiators are the less active ones in this series. Interestingly, in the *cis* halochelates, the nitrogen-group seems to have the opposite influence on the catalysts performance than in *trans* catalysts. While in *trans* catalysts the metathesis activity is busted, it is strongly reduced in the *cis* complexes. A possible explanation for this observation probably once more is the isomerization to the corresponding *trans* complex. While in the, from the Grela group published *trans* **NO₂-Hov**, the nitrogen group withdraws electrons from the phenyl ring and thereby from the chelating oxygen which favors dissociation,[126] this same effect leads to a hindered dissociation of the anionic chlorines in the *cis* complex, which is a crucial step for the isomerization to the active *trans* species. Due to this suppressed isomerization, less of the active *trans* species is formed, and hence the metathesis reactivity stays low. Also worth mentioning is, that the position of the nitrogen-group has a very pronounced effect on the metathesis activity. While **17**, where the NO$_2$ is positioned *para* to the halide, still performs equally or just a little worse as **15**, the reactivity in **18**, where the NO$_2$ is positioned *ortho* to the iodine drops drastically.

Summarizing, the reactivity in all complexes is determined by the isomerization of the *cis* to the *trans* species, which is influenced by many different facts. Overall, complex **18** shows just a very low initiation and a low propagation. **11**, **15** and **17** otherwise show a polymerization behavior comparable with **M2**, but with a somehow higher propagation rate, which can be seen at the faster polymerization. The complexes **12**, **13**, **16** show even higher initiation and propagation rates. The best performance of all catalysts shows initiator **14** with a polymerization behavior comparable to **Hov**. From this data, the following activity order can be summarized: **14 > 12 > 16 > 13 > 11 > 15 > 17 > 18**.

---

[126](a) K. Grela, S. Hyrutyunyan, A. Michrowska, *Angew. Chem., Int. Ed.*, **2002**, *41*, 4038-4040. (b) A. Michrowska, R. BUjok, S. Harutyunyan, V. Sashuk, G. Dolgonos, K. Grela, *J. Am. Chem. Soc.*, **2004**, *126*, 9318-9325.

6.1.1 Controlled Polymerization

Due to the good performance of complex **11–18** at 80°C in toluene, we became interested if with this kind of *cis* complexes a controlled polymerization is feasible. Therefore, polymerizations with increasing chain length, ranging from 150 to 900 eq of **Mon1**, using initiator **14** were done. The polymerizations were conducted under standard reaction conditions at 80°C in toluene and for comparison reasons at RT in DCM.
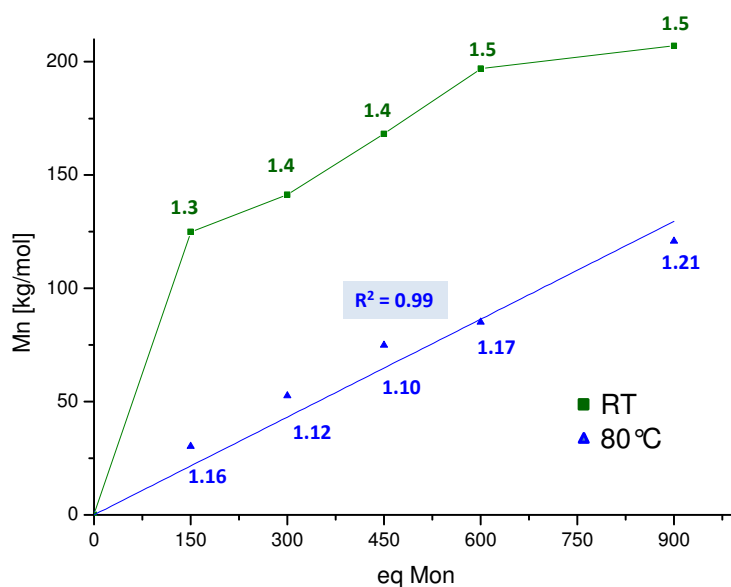
Figure 93: Controlled polymerization of Mon1 with 14; reaction conditions: [I]:[Mon1]=300; DCM for RT, toluene for 80°C polymerization, 0.1 mol/L [Mon1]

Plotting of the molecular weights versus the monomer units applied reveals a controlled polymerization behavior of **14** at 80°C and as expected, a non-controlled behavior at RT. Molecular weights from the 80°C polymerizations increase in a linear manner resulting in a slope with a R^2 of 0.99. PDI values do not increase significantly with increasing monomer units. For the RT polymerizations on the other side, the molecular weights do not increase linearly and PDI's which increase from 1.3 to 1.5. To the best of our knowledge, this is the first *cis* initiator which is capable of performing a ROMP polymerization in a controlled manner.

6.1.2   DCPD Polymerizations

To evaluate the performance of the halide containing intiators in the polymerization of **DCPD**, an experiment to measure the exothermic reaction at room temperature was conducted as follows: 2 mL of **DCPD**[127] were mixed with 50 µL of DCM. 50 ppm of the initiator **11**-**18**, dissolved in another 50 µL of DCM, was added to the monomer. The reaction was performed as described in chapter 5.2.1 and depicted in Figure 84. Noteworthy, the applied **DCPD** seems to hamper the polymerization reaction somehow, leading to slightly worse results. Nevertheless due to the high activity of the halide chelating initiators this fact was favourable because the reaction with other types of **DCPD** occurred too fast to perform the reaction successfully.
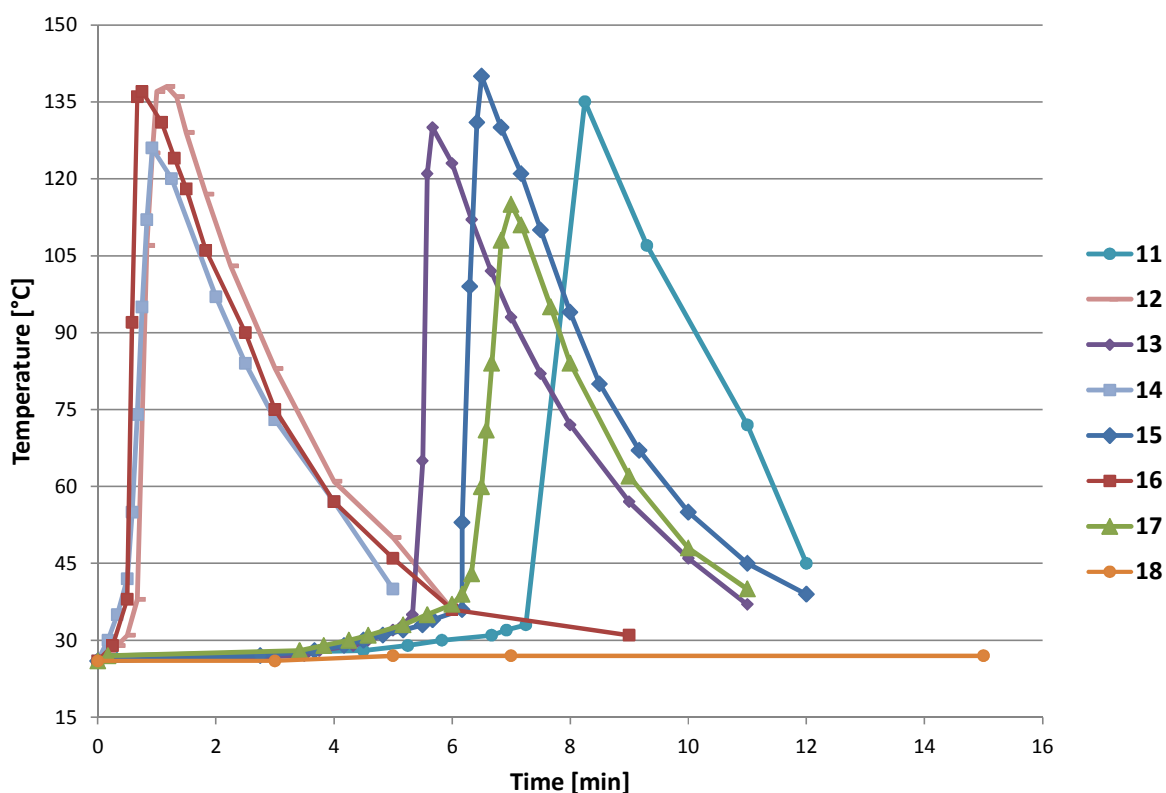
Figure 94: Exothermic polymerization of DCPD initiated with 11 – 18; 50 ppm of 11 – 18; 100 µL DCM

The results of the **DCPD** polymerization depicted in Figure 94 are in good accordance with the polmeriaztion data and the general reactivity order discussed earlier. The three best performing initiators **11**, **14** and **16** possess the lowest retardation time in the **DCPD** experiment indicating a high and fast initiation. In the solvent polymerization also these

---

[127] DCPD was purchased from Aldrich; Aldrich 454338, 100%, contains BHT as stabilizer.

three initiators yielded polymers with the narrowest PDI's and the fastest reaction times which is also indicative for a high and fast initiation.

7 CONCLUSION

Within this thesis, substantially two big topics have been discussed. The first one deals with the synthesis and characterization of initiators which are modified in some way at the anionic ligands leading to "chiral" or chelating initiators. In the second main part of the work, the evaluation of new initiators, synthesized by our partners of the EUMET project, has been executed by the means of ROMP. In both chapters, the standard benchmark reaction of **Mon1** to **poly1** was used as the main tool to receive an insight into the catalysts performance. This reaction allows an estimation of initiation, as well as propagation rate of the applied initiators by determining polymer characteristic features such as the number molecular weight and the polydispersity index. Additionally, values such as a re-coordination tendency of the dissociative ligand can be gauged by including the reaction time required for the polymerization.

In chapter 3.1 the attempt to prepare chiral initiators via variation of the anionic ligands and their evaluation in an achiral acyclic ring opening metathesis/cross metathesis reaction of norbornenedicarboxylic acid anhydride with styrene was made. Therefore, a brominated substrate **L1** and a halide free substrate **L2** were applied. It has shown that for this anionic ligand exchange Cs_2CO_3 or K_2CO_3 give the fastest and best results and that catalytic amounts of base are sufficient for a successful exchange of the ligands. During the synthesis of these chiral initiators using **L1** a halide abstraction side reaction was discovered. It was shown that this halide exchange between substrates or solvents and metathesis initiators bearing halogens as the anionic ligands occurs constantly at elevated temperatures. The reaction rates are differently depending mostly on the halides present in the reaction and in case of solvents, the grade of halogenation of the applied solvent. Recapitulating, the trend to perform this halide exchange increases from small, electronegative fluorines to big, less electronegative iodines (F < Cl < Br < I) and with enlarged halogenation grade (CH_3X < CH_2X_2 < CHX_3 < CX_4). When halogen free substrates such as **L2** were used for the anionic ligand exchange it has shown, that always three different complexes were formed, which could not be separated and were not very stable. The *in-situ* application of those initiators revealed, that they are not suitable catalysts for the chiral AROCM reaction.

The scope of chapter 3.2 was, to synthesize acid triggerable metathesis initiators. Therefore, the concept of N-, O- chelating initiators bearing 8-quinolinlate ligands was used. The initiators syntheses lead always to the formation of at least two different products, which were either the mono- and the disubstituted pre-catalysts (**3a** and **3b**) or, as in case of **4a** and **4b**, two disubstituted pre-catalysts. Unfortunately, the two isomers were not always isolatable. The catalysts protrude by their good stability under air and elevated temperatures and by their outstanding solubility in apolar solvents and substrates. Benchmark polymerization reactions with the 8-quinolinolate bearing initiators revealed a moderate metathesis activity leading to polymers comparable to those of **M2**. Most striking, SIPr bearing complex **6** performed a lot better and gives polymers comparable to those of

M31. Despite slightly elevated PDI's of around 1.3 it even showed a controlled polymerization behavior. By clarifying the structures of **4a** and **4b** via X-ray spectroscopy correlations of the metathesis activity with the geometric constitution could be made. Noteworthy, so far, hydrogen halides (especially HCl) are the only acids activating pre-catalyst **3**-**6**. It is also remarkable that **3**-**6** are absolutely not activated by the means of heat. Due to their good solubility in apolar substances, their polymerization performance of **DCPD** was evaluated. **pDCDD** shoulder test bars were made and characterized by means of tensile strength tests showing, that initiator **4b** and **6** ($\varepsilon \approx 2600$ MPa) outperform commercially available initiators such as **M2** and are in good accordance with literature examples. Using NMR techniques and DFT calculations, we also accomplished to identify the present active species and to elucidate the activation mechanism a little closer. During activation, most probably the quinolinolate ligands get protonated at the oxygen atoms and the quinolinolate substituents get re-substituted against the chlorides from the hydrochloric acid leading to the same active species than their starting materials.

Within the sub-chapter 3.3, the ROMP performance of twofold chelating ruthenium initiators **7–9** was evaluated. Those initiators show, in contrast to the quinolinolate complexes, thermal and acid activation. Still the activation with HCl gives the best results.

Summarizing the results of chapter 4 it was shown, that the NHC ligand severely affects the metathesis step. Especially the *cis/trans* ratio of polymers is heavily influenced by this ligand, most probably due to steric impacts. The most pronounced differences could be detected between the **SIMes**, **SIPr**, and the **o-tol** NHC. Basically, the sterically demanding **SIPr** produces the polymers with the lowest *cis* content within one series (**poly4**: 70% *cis* for **SIMes** and only 20% *cis* for **SIPr** complexes).

The evaluation of the, from the group of C. Cazin in St. Andrews made, initiator **10** in chapter 5 has strengthened the postulation of an initiation increase with and accompanied propagation decrease caused by the bulky SIPr initiator.[30] Additionally, most striking the highly pronounced effect of the re-coordination of the phosphit ligand could be proofed clearly. At 40°C, **SIPr-PCy$_3$** requires only one hour to complete the standard benchmark reaction with **Mon1**, whereas **10** takes 3 hours for the same reaction, even though both complexes possess except of the dissociative ligand the same structure. In the evaluation of the performance with **DCPD**, **10** proofed to be a very useful initiator due to its slight latency at RT and high activity at elevated temperatures. Shoulder test bars made with **10** outperform those made with **M2** and with **M22**.

In the last chapter 6, a new class of ruthenium complexes synthesized by our partners form Warsaw bearing a chelating halide moiety was evaluated regarding their performance in ROMP. Most striking, even if they possess a *cis* arrangement of the two chlorines which is normally known to lead to latent initiators, they show a considerable activity at RT. Within this family, a differentiation into two structural different groups, namely the "benzyl" and the "naphtyl" was made. The ROMP experiments revealed that basically bromine chelating initiators show a higher activity than iodine chelating initiators. Furthermore is the *cis/trans*

isomerization, which is the proposed mechanism to yield the actual active species, influenced by the aromaticity of the ring system ("naphtyl" group) and by the substituents at the phenyl ring ("benzyl" system). Overall, the halide chelating initiators of Warsaw are, especially at 80°C, highly active initiators which are even capable of performing metathesis polymerizations in a controlled manner as has been shown at the example of initiator **14**.

8 EXPERIMENTAL PART

8.1 Instruments and Chemicals

Thin layer chromatography (TLC) sheets purchased from Merck (silica gel 60 on aluminium) were utilized. Visualization was done by UV light irradiation or through oxidation with $KMnO_4$.

NMR spectra were recorded either on a Bruker Avanze 300 MHz spectrometer or on a Varian INOVA 500 MHz spectrometer operating at 499.803 MHz (^{1}H) and 125.687 MHz (^{13}C), respectively. Deuterated solvents were purchased from Cambridge Isotope Laboratories Inc. If not otherwise mentioned, NMR spectra were recorded in $CDCl_3$ with its characteristic peaks at 7.26 ppm (^{1}H) and 77.16 ppm (^{13}C). Peak referencing was done using the solvent peaks according to literature from Gottlieb.[128] The peaks are given in ppm relative to a $SIMe_4$ standard. Peaks are constituted with s (singlet), d (doublet), t (triplet), m (multiplet), h (heptet) and b (broad).

GPC measurements for determining the molecular weights and PDI values of the polymers were done in THF and if not possible in $CHCl_3$ using the following arrangement: a Merck Hitachi L6000 pump, separation columns of Polymer Standards Service (5 µm grade size) and a refractive index detector from Wyatt Technology, model Optilab (DSP Interferometric Refractometer). Calibration was done against a Polystyrene Standard purchased from Polymer Standard Service.

STA measurements were performed with a Netzsch Simultaneous Thermal Analyzer STA 449C (crucibles: aluminium from Netsch). A helium flow of 50 mL/min was used in combination with a protective flow of 8 mL/min.

XRD measurements for analysing crystals were done on a Bruker AXS Kappa APEX II diffractometer using MO Kα radiation. The structures were solved by direct methods using SHELXS and refined with SHELXL. The absorption correction was performed using the program SADABS.

Tensile strength tests were performed on a Shimadzu Autograph AGS-X, with a force measuring range from 10-100 kN. Clamping length of the samples was 80 mm and an initial tension of 10 N was applied. The area of the shoulder test bars was 35.2 mm^2. Measuring rate was fixed at 1 mm/min.

---

[128] H. E. Gottlieb, V. Kotylar, A. J. Nudelman, *Org.Chem.* **1997**, 62, 7512.

<u>Chirale HPLC</u> measurements were performed on Agilent 1100 HPLC using the following arrangement: Chiralpark Ad-H using an UV-VIS detector. The samples were measured in n-Heptan/iso Propanol 70:30 with a solvent stream of 0.75 mL/min.

<u>UV-VIS</u> spectra were recorded on a Cary 50 Bio UV-Visible Spectrometer.

The initiators **M1**, **M2**, **M20**, **M22**, **M23**, **M31** were obtained from Umicore AG and used as received. All other complexes were either prepared by our partners of the EUMET project (as mentioned in the corresponding chapters) or synthesized by ourselves. In this case, the synthesis is described in the following. Chemicals were purchased from commercially sources such as Sigma Aldrich, Alfa Aesar or ABCR and used without further purification.

8.2   Synthesis of Ru(II) Complexes

(SPY-5-31)-Dichloro-(κ^2 (C,O) – (isopropylbenzylidene) (1,3-bis (2,4,6 – trimethylphenyl) 4,5 – dihydroimidazol – 2 – ylidene) ruthenium – Hov
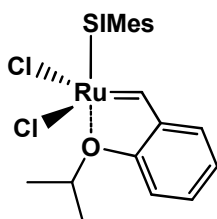
Complex **Hov** was prepared as published in: J. Wappel, C.A. Urbina-Blanco, M. Abbas, J.H. Albering, R. Saf, S. Nolan, C. Slugovc *Beilstein J. Org. Chem.* **2010**, *6*, 1091-1098.

(SPY-5-31)-Di-(2S)-2-acetoxylactat-(κ^2 (C,O) – (isopropylbenzylidene) (1,3-bis (2,4,6 – trimethylphenyl) 4,5 – dihydroimidazol – 2 – ylidene) ruthenium – **1** and (SPY-5-31)- (2S)-2-acetoxylactat-chloro-(κ^2 (C,O) – (isopropylbenzylidene) (1,3-bis (2,4,6 – trimethylphenyl) 4,5 – dihydroimidazol – 2 – ylidene) ruthenium – 2a/2b

Hov (12.0 mg, 0.0193 mmol, 1 eq) was dissolved in ca. 3 mL dry and degassed THF. (2*S*)-2-acetoxypropanoic acid **L2** (25.5 mg, 0.193 mmol, 10 eq) and K_2CO_3 (7.9 mg, 0.0572 mmol, 3 eq) were added. The reaction was performed in a Schlenk flask under a nitrogen atmosphere at 60°C and stirred for approximately one hour. The reaction progress was followed using ^{1}H NMR spectroscopy. The initiator was used *in situ* without further purification.
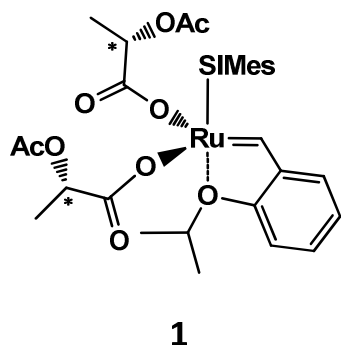
1: 17.18 (1H, s, RU-CH), 7.24 (m, 1H, CH^{ph}), 7.13 (s, 2H, CH^{mes}), 7.08 (s, 2H, CH^{mes}), 6.87 (t, 1H, CH^{ph}), 6.58 (1H, d J=8.30 HZ, CH^{ph}), 4.90 (m, 2H, CH^{L2}) 4.05 (s, 4H, CH$_2^{mes}$), 2.41, 2.37, 2.25 (s, 6H, CH$_3^{mes}$), 1.99, 1.91 (s, 3H, CH$_3^{L2}$). The missing signals could not be clearly assigned to **1** due to many in impurities.

1
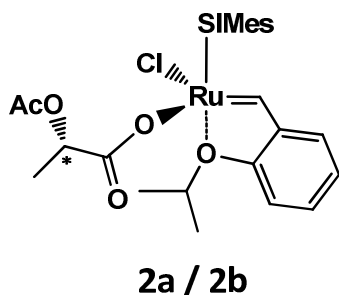
The peaks for **2a** and **2b** could not be assigned due to many impurities and the small amount present in the reaction mixture. The characteristic carbene peaks appear at 16.95 ppm and 16.86 ppm, respectively (recorded in CDCl$_3$).

2a / 2b

Di-(5,7-dichloro-8-quinolinolate − (isopropylbenzylidene) (1,3-bis (2,4,6 − trimethylphenyl) 4,5 − dihydroimidazol − 2 − ylidene) ruthenium − 3a and Chloro - 5,7-dichloro-8-quinolinolate − (isopropylbenzylidene) (1,3-bis (2,4,6 − trimethylphenyl) 4,5 − dihydroimidazol − 2 − ylidene) ruthenium - 3b

In a Schlenk flask **M31** (142 mg, 0.189 mmol, 1 eq) was dissolved in degassed DCM (≈ 18 mL). 5,7-Dichloro-8-hydroxyquinoline (810 mg, 3.785 mmol, 20 eq) and Cs$_2$CO$_3$ (1,24 g, 3.815 mmol, 20 eq) were added. The reaction mixture was stirred under a nitrogen atmosphere overnight. The insoluble residue was filtered over celite. According to a TLC (CH/EE 5:1) two derivatives were formed. The two catalysts were separated via column chromatography (CH/EE 10:1) and fully characterized by NMR. Yield = 90% (117 mg **3a** and 33 mg **3b**).

The same reaction using the same conditions was also performed using **M20** ((PPh$_3$)(H$_2$IMes)(Cl$_2$)Ru(3-phenyl-1H-inden-1-ylidene)) instead of **M31** as the starting material yielding the same products **3a** and **3b**. Yield = 73% (10,3 mg **3a** and 8,4 mg **3b**).
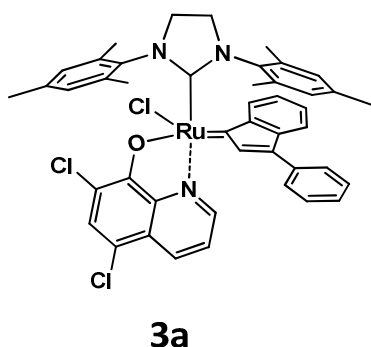
3a: **^{1}H-NMR** (δ, 20°C, CDCl$_3$, 75 MHz): 8.0 (d j= 8.1 Hz, 1H, CH$^{hq\ 3}$), 7.97 (d j= 4.8 Hz, 1H, CH$^{hq\ 1}$), 7.74 (d j= 8.1 Hz, CH), 7.30 (t, 2H, CH), 7.05 (s, 2H, CH), 7.23 (d, 2H, CH), 7.12 (d j= 7.14 Hz, 1H, CH), 7.03 (q, 1H, CH$^{hq\ 2}$), 6.44 (s, 3H CH), 6.23 (s, 2H, CH), 6.20 (d, 1H, CH), 3.87 (s, 4H, CH$_2$), 2, 32, 2.08, 1.92 (s, 18H, CH$_3^{mes\ 7,7',8,8',9,9'}$).

3a

^{13}C-NMR (δ, 20°C, CDCl$_3$, 300 MHz): Ru=C and Ru-C not observed, 167.2 (C$_q$), 164.6 (CH), 146.7 (CH), 143.8 (C$_q$), 143.2 (CH), 142.8 (CH), 141.8 (C$_q$), 129.1 (CH), 128.7 (CH), 128.0 (CH), 127.9 (CH), 127.6 (CH), 126.0 (C$_q$), 125.9 (CH), 125.7 (C$_q$), 121.8 (CH), 121.0 (CH), 118.9 (C$_q$), 118.5 (C$_q$), 117.6 (CH), 111.7 (C$_q$), 109.3 (C$_q$), 51.6 (2C, CH$_2$-N), 20.9, 18.1 (12C, CH$_3$).

3b
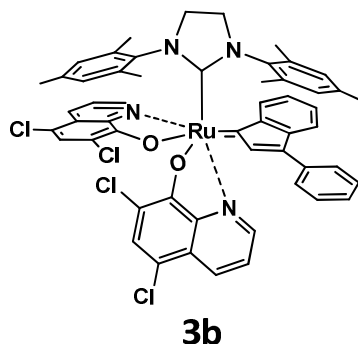
3b: **^{1}H-NMR** (δ, 20°C, CDCl$_3$, 300 MHz):8.15 (d j= 4.8 hZ, 1H, CH$^{hq\,1}$), 7.99 (dd j= 8.4, 1H, CH^{hq}), 7.9 (3H, CH^{hq}), 7.60 (1H, CH), 7.52 (1H, CH), 7.47 (1H, CH), 7.31 (s, 1H, CH), 7.24 (s, 1H, CH), 7.2 (t, 2H, CH^{ind}), 6.81 (q, 1H, CH^{hq}), 6.65 (t, 1H, CH^{ind}), 6.53 (s, 2H, CH^{mes}), 6.50 (q, 1H, CH^{hq})6.35 (s, 2H, CH^{mes}), 6.28 (d j=7.2 Hz, CH^{ind}), 5.48 (dd j=4.8 Hz, 1H, CH^{hq}), 3.89 (s, 4H, CH$_2$^{mes}), 2.36, 2.28, 2.08 (s, 18H, CH$_3$^{mes}).

^{13}C-NMR (δ, 20°C, CDCl$_3$, 75 MHz): Ru=C not observed, 204.3 (1C, C$_q$, Ru-C), 166.3 (C$_q$), 161.2 (C$_q$), 150.0 (CH), 145.8 (C$_q$), 145.1 (C$_q$), 143.1 (CH), 142.0 (C$_q$), 141.7 (CH), 140.4 (C$_q$), 137.9 (C$_q$), 137.5 (C$_q$), 137.3 (C$_q$), 136.8 (C$_q$), 136.4 (C$_q$), 136.3 (C$_q$), 136.4 (C$_q$), 136.3 (C$_q$), 136.2 (C$_q$), 133.3 (CH), 133.2 (CH), 130.0 (CH), 129.7 (CH), 129.6 (CH), 129.4 (CH), 129.3 (CH), 129.1 (CH), 128.5 (CH), 128.2 (CH), 128.1 (CH), 126.6 (CH), 126.0 (CH), 125.9 (C$_q$), 125.8 (CH), 125.4 (C$_q$), 120.9 (CH), 120.7 (CH), 120.1 (C$_q$), 118.5 (CH), 118.2 (C$_q$), 112.2 (C$_q$), 108.2 (C$_q$), 53.3 (2C, CH$_2$-N), 20.9, 20.3, 19.5 (18, CH$_3$).

Di-(5,7-dichloro-8-quinolinolate) – (isopropylbenzylidene) (1,3-bis (2,4,6 – trimethylphenyl) 4,5 – dihydroimidazol – 2 – ylidene) ruthenium – 4a and 4b

In a Schlenk flask, **Hov** (106 mg, 0.169 mmol, 1 eq) was dissolved in degassed DCM (≈18 mL). 5,7-Dichloro-8-hydroxyquinoline (707 mg, 3.303 mmol, 19 eq) and Cs$_2$CO$_3$ (150 mg, 0,461 mmol, 16 eq) were added. The reaction mixture was stirred under a nitrogen atmosphere overnight. The insoluble residue was filtered over celite. According to a TLC (CH/EE 5:1) two derivatives were formed. The products were separated via column chromatography (CH/EE 5:1) and fully characterized by NMR and crystal structure analysis. Yield = 83% (46.5 mg **4a** and 91 mg **4b**).
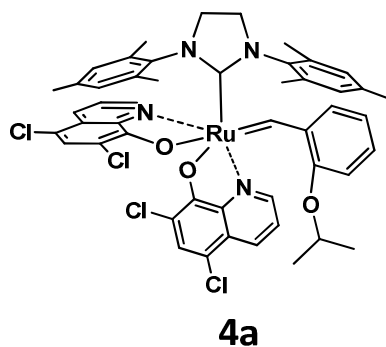
4a: **^{1}H-NMR** (δ, 20°C, CDCl$_3$, 300 MHz): 19.10 (s, 1H, Ru=CH), 8.09 (d J=4,04, 1H, CH^{hq}), 7.95 (d J=8,56; j=1,43, 1H, CH^{hq}), 7.68 (d J=8,43 j=1,30, 1H, CH^{ph}), 7.49 (s, 1H, CH^{hq}), 7.17 (s, 1H, CH^{hq}), 7.05 (m, 2H, CH^{hq}), 6.56 (d J=8,04, 1H, CH^{hq}), 6.48 (s, 2H, CH^{mes}), 6.43 6,39 (2H, CH^{ph}), 6.14 (s, 2H, CH^{mes}), 6.06 (2H, C$H^{hq + ph}$), 3.97 (?, 5H, CH_2 + C$H^{isoprop}$), 2.45 (s, 6H), 2.27 (s, 6H), 1.90 (s, 6H, C$H_3^{1, 1', 2, 2', 3, 3'}$), 1.43 (d, 3H, C$H_3^{isprop}$), 1.05 (d, 3H, C$H_3^{isoprop}$).

^{13}C-NMR (δ, 20°C, CDCl$_3$, 75 MHz): 338.6 (1C, Ru=CH), 227.6 (1C, Ru-C), 162.6, 161.3, 149.7, 149.4, 149.0, 144.2, 143.2, 142.4, 142.3, 138.1 (C$_q$), 136.9 (C$_q$), 136.6 (C$_q$), 135.8 (C$_q$), 132.3 (CH), 131.7 (CH), 129.3 (CH), 129.2 (CH), 128.7, 127.7 (CH), 126.2, 125.8, 125.7, 122.2 (CH), 121.6 (CH), 121.0 (CH), 119.5 (CH), 118.9, 112.0, 109.2, 76.2 (1C, CH^{isoprop}), 51.6 (2C, CH$_2$-N), 23.1 (1C, CH$_3^{isoprop}$), 21.5 (1C, CH$_3^{isoprop}$), 20.8, 18.8, 18.5 (2C, CH$_3^{mes\ 7,\ 7',\ 8,\ 8',\ 9,\ 9'}$).
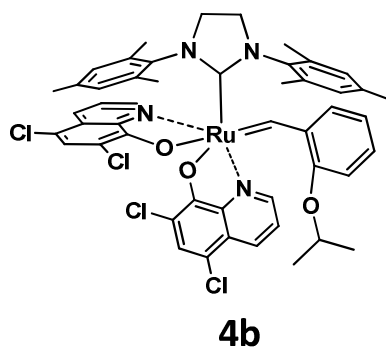
4b: **^{1}H-NMR** (δ, 20°C, CDCl$_3$, 300 MHz):18.23 (bs, 1H, Ru=CH), 9.00 (d j=4.67 Hz, 1H, CH^{hq}), 8.09 (d J=8.56 Hz, 1H, CH^{hq}), 7.83 (d J=8.30 Hz, 1H, CH^{hq}) 7.57 (s, 1H, CH^{hq}), 7.12 (s, 1H, CH^{hq}), 7.06 (q, 1H, CH^{hq}), 6.94 (t, 1h; CH^{ph}), 6.59 (s, 2H, CH^{mes}), 6.39 (d, 1H, CH^{ph}), 6.26 (s, 2H, CH^{mes}), (d, 1H, CH^{ph}), (t, 1H, Ch^{hq}), 5.98 (t, 1H, CH^{ph}), 5.32 (d j= 4.54 Hz, 1H, CH^{hq}), 4.54 (m, 1H, CH^{isoprop}), 3.92 (q, 4H, CH$_2^{mes}$), 2.57 (s, 6H), 2.04 (s, 6H), 1.91 (s, 6H, CH$_3^{mes}$), 1.53 (d, 3H, CH$_3^{isoprop}$), 1.31 (d, 3H, CH$_3^{isoprop}$).

^{13}C-NMR (δ, 20°C, CDCl$_3$, 75 MHz): 209.5 (1C, Ru-C), 166.4 (C$_q$), 160.9 (C$_q$), 147.7 (C$_q$), 146.7 (C$_q$), 147.1 (C$_q$), 146.7 (C$_q$), 164.5 (CH), 146.5 (CH), 144.9 (C$_q$), 141.2 (CH), 137.1 (C$_q$), 137.0 (C$_q$), 136.7 (C$_q$), 136.5 (C$_q$), 119.3 (C$_q$), 125.8 (C$_q$), 132.7 (CH), 132.2 (CH), 129.2 (CH), 129.1 (2C, CH), 129.0 (CH), 128.6 (CH), 127.9 (CH), 126.4 (C$_q$), 120.7 (CH), 120.1 (CH), 119.7 (CH), 118.0 (C$_q$), 111.3 (C$_q$), 110.5 (CH), 106.4 (C$_q$), 68.7 (1C, CH^{isoprop}), 51.7 (2C, CH$_2$), 22.7, 22.3 (2C, CH$_3^{isoprop}$), 20.9, 18.9, 18.1 (6C, CH$_3^{mes}$).

Di-(5,7-dibromo-8-quinolinolate)- (isopropylbenzylidene) (1,3-bis (2,4,6 − trimethylphenyl) 4,5 − dihydroimidazol − 2 − ylidene) ruthenium − 5

In a Schlenk flask, **M31** (160 mg, 0.214 mmol, 1 eq) was dissolved in degassed Et$_2$O. 5,7-Dibromo-8-hydroxquinoline (960 mg, 3.169 mmol, 15 eq) and Cs$_2$CO$_3$ (1 g, 3.077 mmol, 14 eq) were added. The reaction mixture was stirred under nitrogen atmosphere for 12 hours. The reaction progress was followed by TLC (CH/EE 5:1). The insoluble residue was filtered over celite. According to a TLC (CH/EE 5:1) three products were formed. The new formed

pre-catalysts were separated by column-chromatography (CH/EE 10:1). However, just the catalyst possessing one 8-quinolinolate could be isolated in workable amounts.
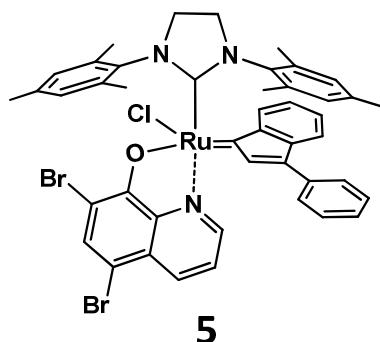
5: **^{1}H-NMR** (δ, 20°C, CDCl$_3$, 300 MHz): 7.97 (d J=8.52, 1H, CH), 7.90 (d J=4.26, 1H, CH), 7.81 (s, 1H, CH^{hq}), 7.71 (d J=8.33, 1H, CH), 7.57 (s), 7.53 (bs, 3H, CH), 7.34 (bs, 3H, CH), 7.11 (d J=7.00, 1H, CH), 7.03 (q, 1H, CH), 6.49 (bs), 6.42 (s, 3H, CH + CH^{mes}), 6.27 (s, 2H, CH^{mes}), 6.18 (1H, bs, CH), 3.89 (s, 4H, CH$_2$), 2.30 (s, 6H, CH$_3$), 2.15 (bs, 6H, CH$_3$), 1.93 (s, 6H, CH$_3$).

^{13}C-NMR (δ, 20°C, CDCl$_3$, 75 MHz): Ru=C not observed, 241.9 (Ru-C), 168.8, 144.5, 144.1, 143.7, 143.0, 137.8, 137.0, 136.9, 136.6, 135.6, 135.2, 134.2, 133.4, 129.2, 129.1, 128.2, 127.8, 127.6, 127.5, 125.9, 122.6, 121.6, 117.4, 108.7, 108.3, 98.2, 51.5 (2C, CH$_2^{mes}$), 21.0, 19.2 (18C, CH$_3^{mes}$).

Second formed derivative bearing two quinolinlate ligands:

^{1}H-NMR (δ, 20°C, CDCl$_3$, 300 MHz):9.05 (d J=8.14, 1H, CH), 8.83 (dd j=1.70 J=4.07, 1H, CH), 8.47 (dd j=1.42 J=8.70, 1H, CH), 8.20 (d J=8.61, 1H, CH), 7.75 (s+m, 5H, CH), 7.54 (m, 1H, CH), 7.46 (q, 1H, CH), 7.21 (s, 1H, CH), 7.16 (m, 3H, CH), 6.95 (t, 1H, CH), 7.76 (s, 3H, CH), 6.67 (m, 1H, CH), 6.51 (s, 2H, CH), 6.09 (d J=7.19, 1H, CH), 5.40 (s, 1H, CH), 4.05 (s, 4H, CH$_2$), 2.26 (s+, 6H, CH$_3$), 2.11 (bs, 6H, CH), 1.63 (s, 6H, CH$_3$).

Third formed derivative bearing two quinolinolate ligands:

^{1}H-NMR (δ, 20°C, CDCl$_3$, 300 MHz): 8.28 (d 4.92, 1H, CH), 7.96 (d J=8.33, 1H, CH), 7.88 (d, 89.2, 1H, CH), 7.83 (s, 1H, CH), 7.75 (m, 1H, CH), 7.58 (d 7.2, 1H, CH), 7.56 (s, 1H, CH), 7.51 (s, 1H, CH), 7.48 (d, 1H, CH), 7.16 (m, 2H, CH), 6.85 (q, 1H, CH), 6.65 (t, 1H, CH), 6.49 (s, 2H, CH), 6.47 (q, 1H, CH), 6.37 (s, 2H, CH), 6.27 (d J=7.3, 1H, CH), 5.35 (d, J=4.5, 1H, CH), 3.89 (m, 4H, CH$_2^{mes}$), 2.32, 2.30 (2s, 12H, CH$_3$), 2.06 (s, 6H, CH$_3$).

Di-(5,7-dichloro-8-quinolinolate) – (isopropylbenzylidene) (1,3-bis (2,4,6 – trimethylphenyl) 4,5 – dihydroimidazol – 2 – ylidene) ruthenium – 6

In a Schlenk flask, **SIPr-Py** (58 mg, 0,0697 mmol, 1 eq) was dissolved in degassed CH$_2$Cl$_2$ ($\approx$ 6 mL). 5,7-Dichloro-8-hydroxyquinoline (136 mg, 0,6355 mmol, 9 eq) and Cs$_2$CO$_3$ (300 mg, 0,9230 mmol, 13 eq) were added. The reaction mixture was stirred under nitrogen atmosphere overnight. The insoluble residue was filtered over celite. According to a TLC (CH/EE 5:1) two products were formed. The products were separated via column

chromatography (CH/EE 5:1). One derivative was just formed in very low amounts and not identified. The second derivative (**6**) was identified by NMR spectroscopy (^{1}H, COSY, ^{13}C and APT).

6
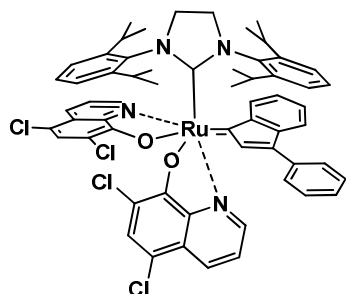
6: **^{1}H-NMR** (δ, 20°C, CDCl$_3$, 300 MHz): 8.03 (m, 3H, CH), 7.91 (s + d, 2H, CH), 7.67 (t, 1H, CH), 7.53 (t, 2H, CH), 7.41 (2s, 3H, CH), 7.30 (2s, 2H, CH), 7.21 (s, 1H, CH), 7.16 (m, 2H, CH), 6.79 (m, 2H, CH), 6.65 (m, 2H, CH), 6.47 (q, 1H, CH), 6.26 (m, 2H, CH), 5.9 (d, 1H J=4.51, CH^{hq}), 4.66, 4.17, 3.9, 3.76, 3.48 (8H, CH^{isop} + CH$_2$), 1.65, 1.34, 0.91, 0.61, 0.45 (s, 24H, CH$_3$9).

^{13}C-NMR (δ, 20°C, CDCl$_3$, 75 MHz): 286.2 (Ru=C), 206.6 (1C, Ru-C), 165.4 (1C, C$_q$), 162.0 (1C, C$_q$), 151.0 (1C, CH), 147.4, 146.4, 145.8, 145.6, 145.3, 145.2 (6C, C$_q$), 145.1 (1C, CH), 144.7 (1C, C$_q$), 144.0 (1C, CH), 141.2, 141.1, 139.3, 138.4, 137.0 (5C, C$_q$), 133.8, 132.6, 130.0, 129.8, 129.7, 128.9, 127.8, 127.7, 127.6, 126.0 (10C, CH), 125.8 (1C, C$_q$), 125.3 (1C, CH), 125.2 (1C, C$_q$), 124.8, 124.4, 124.3, 123.1, 121.5 (5C, CH), 120.4 (1C, C$_q$), 120.0, 117.9 (2C, CH), 117.7, 112.6, 108.4 (3C, C$_q$), 58.7, 55.9 (2C, CH$_2$), 29.7, 28.6, 28.5, 27.3, 26.9, 26.1, 25.6, 24.8, 24.6, 22.0, 21.9, 21.2 (12C, CH^{isop} + CH$_3$)

8.3   Monomer, Ligand and Substrate Synthesis
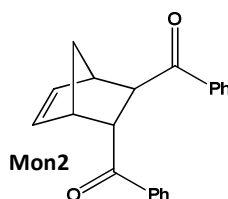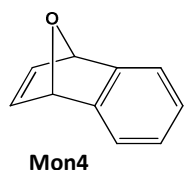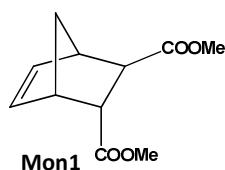
Mon1, **Mon4** and **Mon5** were prepared according to standard literature procedures and are therefore not discussed more detailed.[129]

Synthesis of (*2S*)-2-Acetoxypropionic acid – L2

Anionic ligand **L2** was prepared according to a literature procedure.[130] To a stirred solution of (*S*)-lactic acid (1,5 g, 16.6 mmol, 1 eq) in AcOH (4.8 mL) under a nitrogen atmosphere, acetyl chloride was added (2.6 ml, 33.3 mmol, 2 eq) slowly via a dropping funnel. The

[129] W. Kirmse, U. Mrotzeck, R. Siegfried, *Chem. Ber.* **199**1, *124*, 241-245.
[130] A. D. Hughes, D. A. Price, N. S. Simpkins, *J. Chem. Soc., Perkin Trans. 1*, **1999**, 1295–1304.

reaction mixture was stirred for 5 to 6 h before removing AcOH and acetyl chloride under reduced pressure.
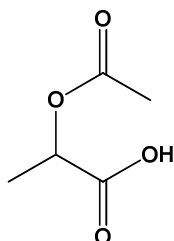
^{1}H-NMR (δ, 20°C, CDCl$_3$, 300 MHz): 11.42 (s, 1H, OH), 5.13 (q, 1H, CH), 2.13 (s, 3H, CH$_3$), 1.53 (d ^{3}J$_{HH}$=7.12, 3H, CH$_3$-CH).

^{13}C-NMR (δ, 20°C, CDCl$_3$, 75 MHz): 176.8 (1C, C$_q$, C-OH), 170.7 (1C, C$_q$, C-CH$_3$), 68.3 (1C, CH), 20.7 (1C, C-CH$_3$), 16.9 (1C, CH-CH$_3$).

Synthesis of Dimethyl bicyclo[2.2.1]hepta-2,5-diene-2,3-dicarboxylate – Mon3

In a round bottom flask, cyclopentadiene (2.05 g, 0.031 mol, 1.2 eq) was dissolved in degassed, dry DCM. Dimethylacetylenedicarboxylate (4.39, 0.026 mol, 1 eq) was added and the flask was closed with a drying tube. The reaction procedure was followed by TLC and NMR. After one day, the reaction did not reach full conversion. Another 0.34 eq (590 mg, 0.0089 mol) of cyclopentadiene were added. After another day, the solvent was removed by evacuation and the crude product was purified by column-chromatography and dried over vacuum. The product was characterized by ^{1}H and ^{13}C spectroscopy.
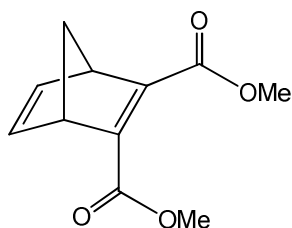
^{1}H-NMR (δ, 20°C, CDCl$_3$, 300 MHz): 6.88 (s, 2H, CH=CH^{3,4}, 3.90 (s, 2H, CH=CH^{1,2}), 3.75 (s, 6H, CH$_3^{8,9}$), 2.25, 2.08 (d, 2H, CH$_2^5$).

^{13}C-NMR (δ, 20°C, CDCl$_3$, 75MHz): 165.3 (2C, C^{6,7}), 152.3 (2C, C^{1,2}), 142.3 (2C, CH^{3,4}), 72.9 (1C, CH$_2^5$), 53.4, 51.9 (2C, CH$_3^{8,9}$).

Synthesis of 7-Butoxy-bicyclo[2.2.1]hepta-2,5-diene – Mon5

Mon5 was synthesized according to a literature procedure.[131] To a refluxing solution (≈ 80°C) of norbornadiene (10 g, 108.7 mmol, 2.5 eq) and CuBr (218 mg, 1.5 mmol, 0.035 eq) in benzene was added, in a nitrogen atmosphere, dropwise a solution of ^{t}butyl-perbenzoate in 10 mL benzene (8.4 g, 43.2 mmol, 1 eq) over a period of around 30 min. The reaction mixture immediately turned from yellowish to blue. After the addition was completed, the

---

[131] P. Story, *J.of Org. Chem.,* **1961**, *26*, 287-289.

reaction mixture was heated for another 30 min. The reaction progress was controlled via IR spectroscopy. The infrared indicated that not all of the perbenzoate had reacted (Figure 95). Therefore the mixture was heated for another 30 min. After this time, the infrared indicated that no ^{t}butyl-perbenzoate remained in the reaction mixture. The mixture is cooled to room temperature, transferred to a separator funnel and washed two times with saturated brine, to remove the copper salts, three times with 10 % NaOH solution to remove the benzoic acid and again one time with brine. The organic layer is then dried with Na_2SO_3 and the solvent is removed under reduced pressure. Vacuum distillation of the crude product yielded only 5 % of the desired product. The purified product was characterized using ^1H and ^{13}C NMR spectroscopy.
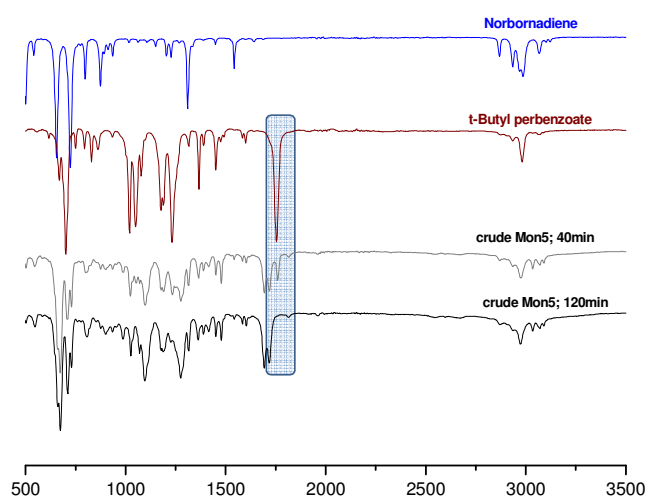
Figure 95: Reaction controll of Mon5; perbenzoate peak is labeled in blue

Table 27: Destillation protocol

Time [min]	Bath Temp. [°C]	Head Temp. [°C]	Observation
0	60	22	-
4	76	22	first condensate in column
10	96	29	destillate in whole column; first drops in collecting flask
12	101	35	destillate drops slowly in collecting flasks
15	120	30	head temperature sinks, dest. stops
23	135	25	last destillate drops
31	187	26	no more destillate
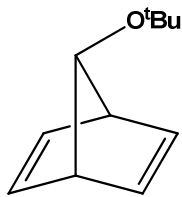
¹H-NMR (δ, 20°C, CDCl$_3$, 300 MHz): 6.65 (t, 2H, CH=CH), 6.59 (bt, 2H, CH=CH), 3.78 (s, 1H, CH-O), 3.4 (m, 2H, CH), 1.14 (s, 9H, CH$_3$).

¹³C-NMR (δ, 20°C, CDCl$_3$, 75 MHz): 139.9 (4C, CH=CH), 137.4 (1C, CH-O), 104.4 (1C, C$_q$), 55.5 (2C, CH), 28.3 (3C, CH$_3$).

Synthesis of Diethyl-7-oxabicyclo[2.2.1]hepta-2,5-diene-2,3-dicarboxylate – Mon6

Mon6 was synthesized according to a literature procedure.[132] In a round bottom flask, furan (1.5 g, 0.022 mol, 1.5 eq) is dissolved in degassed, dry toluene. Diethylacetylenedicarboxylate (2.5 g, 0.015 mol, 1 eq) was added and the reaction mixture was refluxed in an oil bath at 80°C for one day. The reaction procedure was followed by TLC and NMR. After one day, the reaction did not reach full conversion. Another 0.56 eq (600 mg, 0.00825 mol) of furan and one day later another 0.94 eq of furan were added. After 24 hours, the solvent was removed by evacuation and the crude product was purified by column-chromatography (CH/EE 5:1) and dried over vacuum. The product was characterized by ¹H and ¹³C NMR spectroscopy.
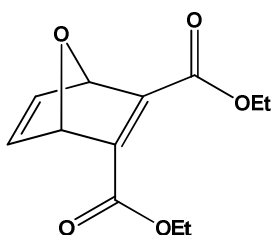
¹H-NMR (δ, 20°C, CDCl$_3$, 300 MHz): 6.88 (s, 2H, CH=CH^{3,4}, 3.90 (s, 2H, CH=CH^{1,2}), 3.75 (s, 6H, CH$_3$^{8,9}), 2.25, 2.08 (d, 2H, CH$_2$^{5}).

¹³C-NMR (δ, 20°C, CDCl$_3$, 75 MHz): 165.3 (2C, C^{6,7}), 152.3 (2C, C^{1,2}), 142.3 (2C, CH^{3,4}), 72.9 (1C, CH$_2$^{5}), 53.4, 51.9 (2C, CH$_3$^{8,9}).

Synthesis of 1-Methyl -7-oxabicyclo[2.2.1]hepta-2,5-diene-2,3-dicarboxylate – Mon7[133]

In a round bottom flask 2-methylfuran and diethylacetylenedicarboxylate were stirred overnight in toluene at 100°C. The solution was cooled to room temperature and the crude product purified by column-chromatography (CH/EE 1:1). The product was characterized by ¹H and ¹³C NMR spectroscopy.

---

[132] L. Delaude, A. Demonceau, A. F. Noels, *Macromolecules*, **1999**, *32*, 2091-2103.
[133] R. R. Burton, W. Tam, *Tetrahedron Lett.*, **2006**, *47*, 7185-7189.
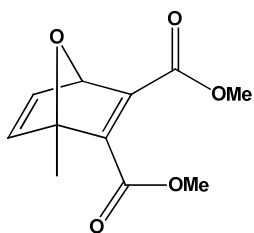
¹H-NMR (δ, 20°C, CDCl$_3$, 300 MHz): 7.17 (dd $^3J_{HH}$=5.08 $^4J_{HH}$f=1.74, 1H, =C*H*-CH), 6.96 (d $^3J_{HH}$=5.23, 1H, =C*H*-C$_q$), 5.58 (d $^3J_{HH}$=1.89, 1H, =CH-C*H*), 3.82, 3.75 (s, 6H, O-C*H$_3$*), 1.76 (s, 3H, C-C*H$_3$*).

¹³C-NMR (δ, 20°C, CDCl$_3$, 75 MHz): 165.0, 162.9 (2C, C$_q$, C^{7,8}), 156.6, 151.4 (2C, C$_q$, C^{4,5}), 146.1 (1C, CH, C^2), 144.7 (1C, CH, C^5), 94.0 (1C, C$_q$, C^3), 83.4 (1C, CH, C^6), 52.3 (2C, CH$_3$, C^{9,10}), 15.1 (1C, CH$_3$, C^{11}).

Synthesis of 1,4-Dimethyl-7-oxabicyclo[2.2.1]hepta-2,5-diene-2,3-dicarboxylate – Mon8

In a round bottom flask 2,5-dimethylfuran and diethylacetylenedicarboxylate were stirred at 100°C for about 4 hours. The solution was cooled to room temperature and the crude product purified by column-chromatography. The product was characterized by ¹H and ¹³C NMR spectroscopy.
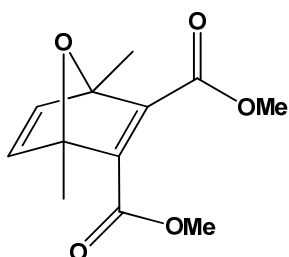
¹H-NMR (δ, 20°C, CDCl$_3$, 300 MHz): 6.94 (s, 2H, C*H*=C*H*), 3.79 (s, 6H, O-C*H$_3$*), 1.78 (s, 6H, C-C*H$_3$*).

¹³C-NMR (δ, 20°C, CDCl$_3$, 75 MHz): 164.5 (2C, *C*=O), 154.9 (2C, *C*=*C*), 147.4 (2C, *C*H=*C*H), 92.2 (2C, *C*H-*C*H), 52.3 (2C, *C*H$_3$-O), 15.5 (2C, *C*H$_3$-C).

Synthesis of *exo*7-^{t}butylbicyclo[2.2.1]hept-5-ene-2,3-diacetate – Mon9

Mon9 was synthesized via a three step synthesis:

<u>Step 1</u>, was the synthesis of **Mon5** and done as described above.
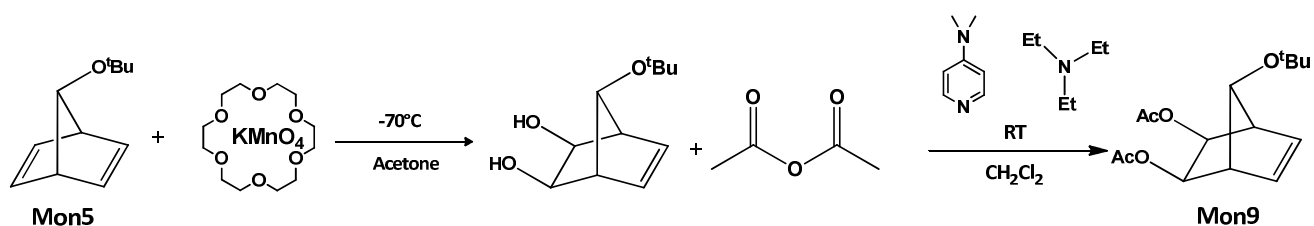
Scheme 12: Step 2 and step 3 of synthesis of Mon9

Step 2:

Step 2 was done according to a literature procedure.[134] 7-^{t}Butoxynorbornadiene (**Mon5**) (1 g, 6.1 mmol, 1 eq) was dissolved in acetone ($\approx$ 16mL) and cooled to -70°C. 18-Crown-6 (963 mg, 6.1 mmol, 1 eq) and KMnO$_4$ (1.61 g, 6.1 mmol, 1 eq) were added in a 1:3 benzene/acetone mixture (30 mL). The reaction mixture was stirred between -50°C and -70°C for four hours. The reaction progress was monitored using TLC (DCM/MeOH 10:1). After full conversion of **Mon5** the reaction solution was quenched by adding 23 mL of water containing 3.4 g of Na$_2$SO$_3$ and 900 mg of NaOH. After another hour of stirring at room temperature the pink reaction solution turned completely brown. The solution was filtered and the filtrate was washed twice with acetone. The solvent was removed under reduced pressure and the remaining aqueous solution was saturated with NaCl (better KCl) and extracted three times with DCM. The crude product was purified using column chromatography (DCM/MeOH 20:1, 10:1). The remaining brown solid contained the desired product and 18-crown-6. The still unclean monomer was dissolved in benzene (5mL) and cyclohexane (20mL) was added. The solution was cooled and the formed white crystals were filtered. The procedure was repeated three times yielding 200 mg of clean 2,3-dihydroxy-7-t-butoxynorbornene. Yield: m= 250 mg (21%)
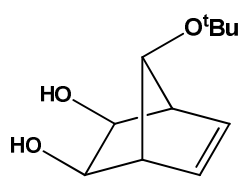
^{1}H-NMR (δ, 20°C, CDCl$_3$, 300 MHz): 6.01 (s, 2H, CH=CH), 4.40 (s, 1H, CH-O), 3.64 (d J=2.51, 2H, CH-OH), 2.82 (s, 2H, CH-OH), 2.75 (d J=1.47, 2H, CH-CH), 1.19 (s, 9H, CH$_3$).

^{13}C-NMR (δ, 20°C, CDCl$_3$, 75 MHz): 132.6 (2C, CH=CH), 85.0 (1C, CH-O), 74.1 (1C, C$_q$-CH$_3$), 67.2 (2C, CH-OH), 53.8 (2C, CH-CH), 28.5 (3C, CH$_3$).

Step 3:

Step 3 was done according to a literature procedure.[135] To a solution of 2,3-dihydroxy-7-butoxynorbornene (202 mg, 1.02 mmol, 1 eq) in 6 mL DCM were added DMAP (9.2 mg, 0.07 mmol, 0.07 eq) followed by Et$_3$N (252 mg, 2.5 mmol, 2.4 eq). Ac$_2$O was added stepwise (using a sampler) and the reaction mixture was allowed to stir for 3 hours at room temperature. The reaction progress was followed with TLC (CH/EE 5:1 or 2:1). After complete conversion of the starting material 6 mL of water were added to quench the reaction. The aqueous layer was extracted three times with Et$_2$O and the resulting organic layer was dried over Na$_2$SO$_3$ and concentrated in vacuo. The crude brown product was purified by column chromatography (pentan/Et$_2$O 2:1) yielding a white solid. Yield: m= 254 mg (88%)

[134] A. B. Cheikh, L. E. Craine, S. G. Recher, J. Zemlicka, *J. Org. Chem.* **1988**, *53*, 929-933.
[135] D. S. La, E. S. Sattely, J. Gair Ford, R. R. Schrock, A. Hoveyda, *J. Am. Chem. Soc.* **2001**, 123, 7767-7778.
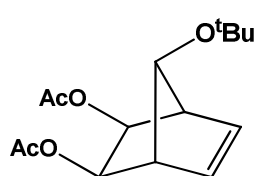
¹H-NMR (δ, 20°C, CDCl₃, 300 MHz): 6.11 (bs, 2H, C*H*=C*H*), 4.62 (s, 2H, C*H*-OAc), 4.49 (s, 1H, C*H*-O), 2.81 (q, 2H, C*H*- C*H*), 2.07 (s, 6H, CH₃^{ac}), 1.20 (s, 9H, CH₃$^{t-butyl}$).

¹³C-NMR (δ, 20°C, CDCl₃, 75 MHz): 170.2 (2C, C=O), 132.8 (2C, CH=CH), 85.5 (1C, *C*H-O), 74.2 (1C, C$_q$-CH₃), 68.7 (2C, *C*H-OAc), 51.3 (2C, CH-CH), 28.4 (3C, CH₃), 21.0 (2C, CH₃).

Synthesis of *exo*-bicyclo[2.2.1]hepta-2,5-diene-2,3-dicarboxylic anhydride – S3

Under a nitrogen atmosphere **S1** was put into a Schlenk and heated to 180°C. After 4 hours the liquid reaction product was cooled to room temperature. The *endo/exo* mixture was purified via column chromatography using CH/EE 5:1. The product was characterized by ¹H and ¹³C NMR spectroscopy.
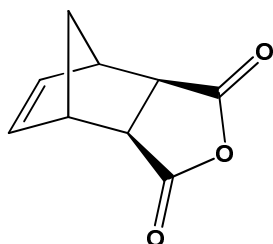
¹H-NMR (δ, 20°C, CDCl₃, 300 MHz): 6.33 (t, 2H, CH=CH), 3.46 (t, 2H, CH), 3.00 (d, 2H, CH), 1.68 (d, 1H, CH₂), 1.45 (d, 1H, CH₂).

¹³C-NMR (δ, 20°C, CDCl₃, 75 MHz): 172.7 (2C, C$_q$), 138.1 (2C, *C*H=*C*H), 48.9 (2C, CH), 47.0 (2C, CH), 44.3 (1C, CH₂).

8.4   Polymerization Reactions

8.4.1   Standard Benchmark Polymerization of Mon1

The standard benchmark reaction with **Mon1** was done according to Scheme 13.
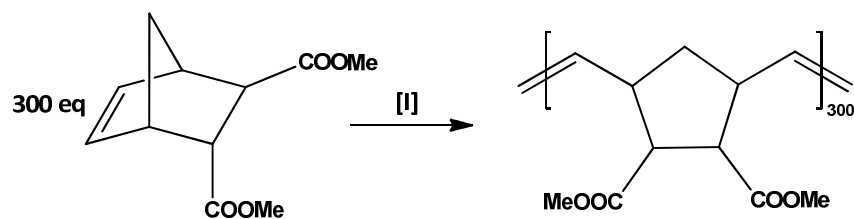
Scheme 13: Polymerization of Mon1

All polymerization reactions were carried out using Schlenk technique under an inert nitrogen atmosphere. The Schlenks were evacuated and subsequently flushed with nitrogen for at least three times before the reaction was performed. Generally 100 mg (0.475 mmol, 300 eq) of **Mon1** were dissolved in the corresponding amount of freshly degased DCM to obtain an overall monomer concentration of 0.1 mol/L (4.8 mL). A little bit more than the desired amount of the investigated catalyst was weighted into a small vial and dissolved in 200 µL DCM. The corresponding amount of the stock solution (containing 1 eq of the initiator) was added in one fast step to the monomer solution to start the reaction. The polymerization was monitored using TLC with a cyclohexane/ethylacetate mixture of 3+1 as the eluent. The TLC was stained with a $KMnO_4$ solution to visualize the monomer and the polymer. The monomer spot moves on the TLC with an r_f value of approximately 0.4, whereas the polymer spot does not move and stays on the start. After complete consumption of the monomer according to the TLC, the reaction was quenched with an excess of ethylvinylether (ca. 200 µL) and stirred for another 15 to 20 minutes. Then the polymer solution was concentrated under reduced pressure and precipitated in strongly stirred cold methanol (approximately 50 mL MeOH for 100 mg monomer). The precipitated polymer was collected and dried for ca. 24 hours on the vacuum line.

If this benchmark polymerization was conducted at elevated temperatures, the general reaction procedure was maintained the same. For the 80 °C polymerization, instead of DCM, toluene was used as the solvent. In case of all tempered polymerizations, the monomer solution was put into a preheated oil bath for about 5 minutes to allow the solvent to warm up to the desired temperature. Not until then, the initiator was added and all steps were conducted as described before.

In case of the acid triggerd polymerizations of chapter 3.2.3 and 3.3 again the general standard procedure was maintained. Only difference, in this case **Mon1** and the initiator were firstly mixed and afterwards the corresponding amount of the acid was added in one fast step to initiate the polymerization.

8.4.2 Controlled Polymerizations

The overall procedure was retained as described in chapter 8.4.1, no matter if the reactions were conducted at RT, elevated temperatures or were acid triggered. The overall amount of **Mon1** did never deceed 80 mg and did never exceed 150 mg. The various polymerizations were always performed at the same time to ensure the absolute same reaction conditions. The monomer for each reaction was always weighted separately into a vial and for the initiators stock solutions were made from which the corresponding amount was taken out.

8.4.3   Kinetic Measurements

The kinetic measurements were performed using proton NMR spectroscopy. In a NMR tube the monomer (50 eq) was dissolved in degassed $CDCl_3$ and the initiator (1 eq), also dissolved in $CDCl_3$, was added. An overall concentration of 0.1 mol/L with respect to the monomer was used. In case of the quinolinolate initiators of chapter 3.2.3, **Mon1** (ca. 18 mg) was used. Just before the first NMR spectrum was recorded, 25 eq of HCl in diethylether was added into the NMR tube and shacked to ensure a complete mixing. In case of chapter 5.1.1, **Mon2** instead of **Mon1** was used. In all cases, ^{1}H NMR spectra were recorded periodically (500 MHz) until the reaction was complete or no further conversion of the monomers could be observed. The conversion was determined by integrating the peaks of the double bond of the monomer (**Mon1**: 6.27 ppm and 6.07 ppm; **Mon2**: 6.44 ppm and 5.95 ppm) and of the polymer (**poly1**: 5.60 ppm – 5.10 ppm; **poly2**: 5.67 – 4.64 ppm).

8.4.4   Polymerization for *cis/trans* Determination

All polymerization reactions were carried out using Schlenk technique under an inert nitrogen atmosphere. The Schlenks were evacuated and subsequently flushed with nitrogen for at least three times before the reaction was performed. Generally a monomer to initiator ratio of 100 to 1 was maintained for **Mon3** and **Mon4** (approximately 50 mg monomer were used) and a ratio of 300 to 1 in case of **Mon5** (around 70 mg were used). The corresponding monomer was dissolved in an appropriate amount of freshly degased DCM to obtain an overall monomer concentration of 0.1 mol/L. A little bit more than the desired amount of the investigated catalyst was weighted into a small vial and dissolved in 200 µL DCM. The corresponding amount of the stock solution (containing 1 eq of the initiator) was added in one fast step to the monomer solution to start the reaction. The polymerization was monitored using TLC with a cyclohexane/ethylacetate mixture of 5+1 as the eluent. After complete conversion the reaction was quenched with an excess of ethylvinylether, stirred for another 15 minutes and precipitated in MeOH. The product was characterized by (^{1}H and ^{13}C)
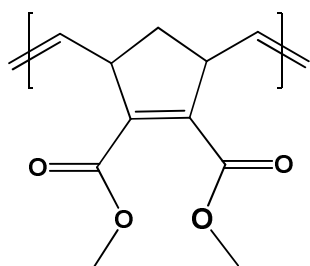
poly3: ^{1}**H-NMR** (δ, 20°C, $CDCl_3$, 300 MHz): 5.53-5.50 (trans) bzw. 5.40 (cis) (2H, C*H*=C*H*), 3.94 (cis) bzw. 3.59 (trans) (2H, C*H*-C=), 3.74 (s, 6H, C*H*$_3$), 2.48 (bs, 1H, C$_{H2}$), 1.44 (bs, 1H, C$_{H2}$).

^{13}**C-NMR** (δ, 20°C, $CDCl_3$, 75 MHz): 165.2 (2C, C=O), 142.4-142.2 (2C, C=C), 131.5-131.2 (2C, CH=CH), 52.07 (2C, CH_3), 48.6 bzw. 44.2 (2C, CH-C=), 38.8 bzw. 37.9 (1C, CH_2).
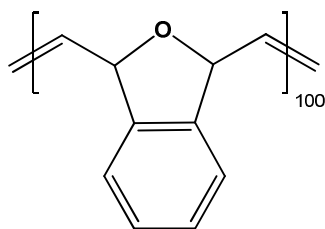
poly4: ^{1}**H-NMR** (δ, 20°C, CDCl$_3$, 300 MHz): 7.36 (bs, 2H, CH^{arom}), 7.21 (bs, 2H, CH^{arom}), 6.22 (cis) bzw. 5.69 (trans) (bs, 2H, CH=CH), 6.07 (trans) bzw. 5.86 (cis) (bs, 2H, CH).

^{13}**C-NMR** (δ, 20°C, CDCl$_3$, 75 MHz): 141.4-141.1 (2C, CH), 133.8-132.9 (2C, CH=CH), 128.3-128.2, 122.6-121.9 (4C, CH^{arom}), 84.1 (trans) bzw. 79.0 (cis) (2C, C$_q$).
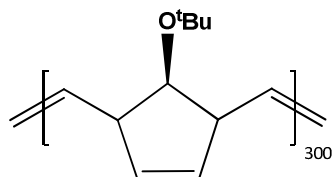
poly5: ^{1}**H-NMR** (δ, 20°C, CDCl$_3$, 300 MHz): 5.54 (trans) bzw. 5.46 (cis) (s, 2H, CH=CH), 5.36 (trans) bzw. 5.11(cis) (bs, 2H, CH=CH), 3.67, 3.60, 3.16 (s, 3H, CH-CH= und CH-O^{t}Bu), 1.15 (s, 9H, CH$_3$).

^{13}**C-NMR** (δ, 20°C, CDCl$_3$, 75 MHz): 132.7, 132.4, 131.8-131.4 (4C, CH=CH), 84.5-84.2 (1C, CH-CH), 73.6-73.4 (1C, C$_q$), 58.2 (trans) bzw. 53.8 (cis) (2C, CH-CH=), 29.2-29.1 (3C, CH$_3$).

8.5 AROCM Reactions

In a Schlenk flask, *endo*- norbornene-5,6-dicarboxylicanhydrid **S1** (1 eq) and styrene **S2** (5 eq) were dissolved DCM (0.07 molar with respect to **S1**). The investigated initiator (1 % for **1** and **2a/2b** and 0.1 mol% for **Hov** with respect to **S1**) was added. The reaction progress was monitored using TLC (CH/EE 2:1) and stained with KMnO$_4$ because the applied monomer is not visible under UV light. After full conversion, the reaction was stopped with an excess of ethylvinylether and stirred for another 15 minutes. The reaction mixture was concentrated in vacuo and separated via column chromatography (CH/EE 10:1). During the separation, stilben eluted first, followed by the *cis* product and finally by the *trans* product. The product was characterized by NMR spectroscopy (^{1}H, ^{13}C and HSQC).
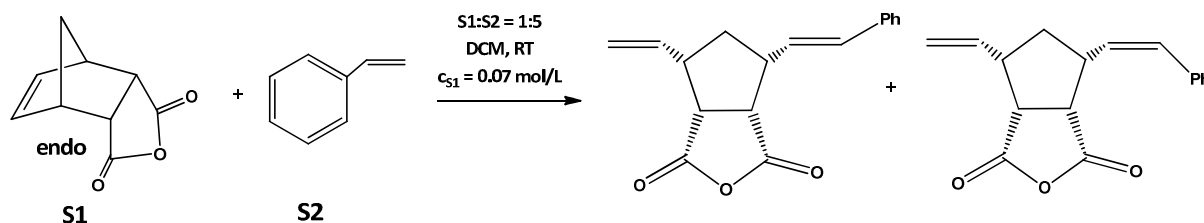
Scheme 14: AROCM reaction of S1 with S2
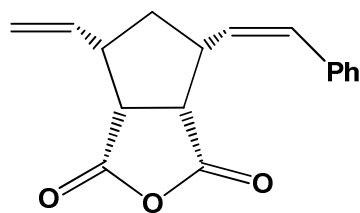
cis: **¹H-NMR** (δ, 20°C, CDCl₃, 300 MHz): 7.37 (t, 2H, CH^{arom}), 7.30 (d, 1H, CH^{arom}), 7.24 (t, 2H, CH^{arom}), 6.72 (d J=11.40 Hz, 1H, =CH-Ph), 5.94 (p, 1H, CH₂=CH), 5.66 (t, 1H, CH=CH), 5.18 (m, 2H, CH₂=CH), 3.46 (m, 3H, CH), 2.96 (m, 1H, CH), 2.05 (m, 1H, CH₂), 1.49 (q, 1H, CH₂).

¹³C-NMR (δ, 20°C, CDCl₃, 75 MHz): 170.67, 170.64 (C$_q$, 2C, C=O), 137.0, 134.9 (1C, CH=CH₂), 132.7 (1C, CH=CH-Ph), 128.6 (1C, CH=CH-Ph), 128.4, 127.4, 117.5 (CH_2=CH), 50.2, 49.7, 46.9, 41.2, 38.0 (1C, CH₂).
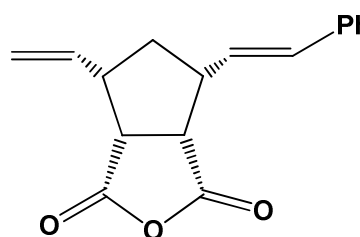
¹H-NMR (δ, 20°C, CDCl₃, 300 MHz): 7.40 - 7.20 (m, 5H, CH^{arom}), 6.52 (d J=15.60 Hz, 1H, =CH-Ph), 6.29 (q, 1H, CH=CH), 5.96 (m, 1H, CH₂=CH), 5.20 (q, 2H, CH_2=CH), 3.53 (m, 2H, CH), 3.16 (m, 1H, CH), 3.03 (m, 1H, CH), 2.12 (m, 1H, CH₂), 1.53 (o, 1H, CH₂).

¹³C-NMR (δ, 20°C, CDCl₃, 300 MHz): 170.83, 170.79,(C$_q$, 2C, C=O), 136.8, 134.9 (1C, CH=CH₂), 132.4 (1C, CH=CH-Ph), 128.7, 127.8, 126.6 (1C, CH=CH-Ph), 117.5 (CH_2=CH), 50.0, 49.5, 46.8, 46.3, 36.2 (1C, CH₂).

8.6 Sample Preparation for STA Measurements

Sample preparation for complexes 3-6: As **DCPD** is solid at RT it was liquified firstly in a preheated water bath. For the STA measurments, a defined reaction solution of the pre-catalysts (100 ppm relative to **DCPD**) and **DCPD** was prepared. Therefore, initiator **3–6** (between 1 to 2.5 mg) were weigthed into a vial and the corresponding amount of the liquified **DCPD** was added. If necessasary the mixture was put shortly into an ultra-sonic bath to ensure that the initiator is dissolved completely in the neat monomer. 1 mL of this mixture was taken out, put into another vial and 36.7 µL of 1 molar etherical HCl (25 eq relative to ruthenium) was added. To avoid polymerization before the measurment starts, the reaction solution was cooled with liquid nitrogen immediately after HCl was added. A weighted portion of the frozen pre-catalyst/**DCPD**/HCl mixture (around 15 mg) was put promptly into the STA (nitrogen flow rate of 50 mL/min) and measured with a temperature program of 3 °C/min. The TGA is operated with a helium flow rate of 50 mL/min used in combination with a protetctive flow of 8 mL/min.

Sample preparation for 10: To 5 mL of liquid **DCPD** 100 µL of DCM were added to prevent re-solidification of the monomer. **10** was weighted into a vial and dissolved in as much DCM to take out the corresponding amounts of initiator for the 20 ppm and the 40 ppm measurements in 60 µL. Without any additional treatment, a weighted portion of the mixture was put into the STA. All reaction parameters are the same as described above.

Sample preparation for M2 is described more detailed in A. Leitgeb, PhD thesis "Contributions to the Advancement of Ruthenium Based Initiators for Olefin Metathesis", Graz 2012.

9 APPENDIX

9.1 Abbreviations

ACM = Asymmetric Cross Metathesis

ARCM = Asymmetric Ring Closing Metathesis

AROCM = Asymmetric Ring Opening Cross Metathesis

ATRP = Atom Transfer Radical Polymerization

bs = Broad Singlet

CM = Cross Metathesis

d = Doublet

DCM = Dichlormethane

DCPD = Dicyclopentadiene

Dedam = Diethyldiallylmalonate

DSC = Differential Scanning Calorimetry

eq = Equivalents

GC-MS = Gas Chromatography with Mass Spectroscopy

GPC = Gel Permeations Chromatography

Hov = Hoveyda

HPLC = High Perfromance Liquid Chromatography

m = Multiplet

M$_n$ = Number Average Molecular Weight

Mon = Monomer

NHC = N-heterocylic carbene

NMR = Nuclear Magnetic Resonance

pDCPD = Poly(dicyclopentadiene)

PDI = Polydispersity Index

PROMP = Photoinduced Ring Opening Metathesis Polmerization

ppm = Parts Per Million

q = Quatruplet

RCM = Ring Closing Metathesis

RIM = Reaction Injection Molding

Rm = Ultimate Tensile Strength

ROMP = Ring Opening Metathesis Polymerization

RT = Room Temperature

SIMes = N, N'-bis[2,4,6-(trimethyl)phenyl]imidazolin-2-ylidene

SIPr = N, N'-bis[2,6-(diisopropyl)phenyl]imidazolin-2-ylidene

STA = Simultaneous Thermo Analysis

t = Triplet

TGA = Thermal Gravimetric Analysis

THF = Tetrahydrofuran

TLC = Thin Layer Chromatography

XRD = X-Ray Diffractometry

9.2 List of Figures

9.3   List of Schemes

9.4 List of Tables